

Assessing toxicity in *Daphnia magna*: an oxidative lipidomic approach

Thomas Andrew White

A thesis submitted to the
University of Birmingham for the degree of
DOCTOR OF PHILOSOPHY

School of Biosciences
University of Birmingham

September 2013

UNIVERSITY OF
BIRMINGHAM

University of Birmingham Research Archive

e-theses repository

This unpublished thesis/dissertation is copyright of the author and/or third parties. The intellectual property rights of the author or third parties in respect of this work are as defined by The Copyright Designs and Patents Act 1988 or as modified by any successor legislation.

Any use made of information contained in this thesis/dissertation must be in accordance with that legislation and must be properly acknowledged. Further distribution or reproduction in any format is prohibited without the permission of the copyright holder.

Abstract

Lipidomics, an under-utilised and rapidly developing field aims to identify the full complement of hydrophobic constituents in a cell, tissue or organism. Lipid peroxidation, a major consequence of oxidative stress, represents a mechanistically illuminating marker for numerous toxicants. Lipidomics offers the ideal technique to acquire a greater level of mechanistic detail compared to currently utilised methodologies. Here, I present a study into lipid peroxidation from simple *in vitro* models to complex *in vivo* systems utilising mass spectrometric techniques. Initially, oxidised products from a systematic range of phospholipids were induced and comprehensively annotated to allow the development of OxyLipidBlast. This is the first tool facilitating the identification of oxidised lipids and provides utility to numerous fields. Secondly I present the first annotated lipidome of the keystone ecotoxicological species *Daphnia magna* and the first annotated lipidome of algal species *Chlamydomonas reinhardtii* published in English. Subsequent oxidation *in vitro* of lipid extracts yielded perturbations, biologically relevant to the following *in vivo* exposures with well established toxicants and novel silver nanoparticles. Overall the work presented in this thesis enhances both eco and oxidative lipidomics. However, these studies also highlighted the limitations of shotgun lipidomics for ecotoxicology assessment.

This thesis is dedicated to Anthony White.

Acknowledgements

I would like to acknowledge the contributions of the following people to this thesis.

Professor Mark Viant for all the enthusiastic and encouraging meetings despite their tardiness. All the people at Cefas including Dr. Brett Lyons for financial support, encouragement and breaks to the seaside. Dr. Ulf Sommer for his instruction on the FT-ICR. Dr. Tobias Kind for his input to the oxidation experiments. Dr. Nadine Taylor for her culturing, exposure and extraction of *C. reinhardtii*. Dr. Isabella Römer, Dr. Ruth Merrifield, soon to be Dr. Mila Tejamaya and other members of the Lead group for their help with the alchemic science of nanoparticles.

In more personal terms my office mates in reverse chronological order for friendship and academic advice, Ralf, Martin, Rosie, Kate, Eva, Leanne, Alex, Andy, Nadine, Stefania, Anja, Lisa. All members of Mark's group during my studies, particularly Rob and Ralf for always being ready for a beer and considerable support. Greg for letting me win at babyfoot occasionally. Andy for never showing frustration with my persistent questions. Kate for being a big orange dot. Alex for all your help with nanoparticles and water fleas. Outside our lab. Chib (I miss your hiccups), Laura, Lauren and Farhat thank-you for making my lab time more bearable.

More personally. Dr. Kaat Brulez, I almost certainly would have quit without you to whinge to. Jon (BSc, PGCE), Leigh (A-levels), Tread (GCSEs), Simo (50m swimming certificate) and Baz (something boring about building supermarkets?), on our tin anniversary, I love you all but none of you are ever going to be more qualified than me. Rosie, this thesis wouldn't exist without you, when it got really tense toward the

end, your support and encouragement was pretty much the only thing holding me back from the abyss, thank-you.

I'll never forget how important you all have been to my work and to me.

Finally, this thesis marks the end of my formal education and four years of draining effort. More broadly, this thesis represents the support of my family both emotionally and financially throughout my entire life. I will never be able to appropriately express how much the encouragement to pursue whatever I wished and the reassurance that I can do anything I choose if I work hard enough has meant to me.

If...

List of contents

| | |
|--|----------|
| 1 - Introduction | 1 |
| 1.1 - Aquatic ecotoxicology..... | 1 |
| 1.1.1 - Model organisms for aquatic toxicology | 2 |
| 1.1.1.1 - <i>Daphnia magna</i> | 3 |
| 1.1.1.2 - <i>Chlamydomonas reinhardtii</i> | 6 |
| 1.1.2 - Aquatic contaminants | 8 |
| 1.1.2.1 - Nano-materials | 8 |
| 1.1.2.2 - Silver nanoparticles (AgNP) | 9 |
| 1.2 - Phospholipids..... | 11 |
| 1.2.1 - Phospholipid structure and nomenclature | 11 |
| 1.2.2 - Phospholipids in <i>D. magna</i> | 14 |
| 1.2.3 - Phospholipids in <i>C. reinhardtii</i> | 17 |
| 1.3 - Non-enzymatic toxic mediated lipid peroxidation | 17 |
| 1.4 - The emerging role of metabolomics in ecotoxicology | 19 |
| 1.4.1 - Environmental metabolomics | 19 |
| 1.4.2 - Lipidomics | 20 |
| 1.4.2.1 - Lipid extraction from biological tissue..... | 21 |
| 1.4.2.2 - Pre-analytical, chromatographic separation of lipids | 21 |
| 1.4.2.3 - Analytical platforms for lipidomic analysis | 22 |
| 1.4.2.4 - Statistical analyses in metabolomic studies..... | 25 |
| 1.4.2.5 - Identification of metabolites | 26 |

| | |
|--|-----------|
| 1.5 - Aim and objectives | 28 |
| 2 - Materials and methods..... | 29 |
| 2.1 - Chemicals | 29 |
| 2.2 - Culturing of <i>Daphnia magna</i> | 29 |
| 2.2.1 - OECD modified media preparation for culturing of <i>Daphnia magna</i> | 30 |
| 2.2.2 - Supplement preparation and regimen | 30 |
| 2.2.2.1 - Chlorella vulgaris..... | 30 |
| 2.2.2.2 - Baker's yeast..... | 32 |
| 2.2.2.3 - Marinure | 32 |
| 2.3 - Acute toxicity assessment | 32 |
| 2.3.1 - Exposures | 32 |
| 2.3.2 - EC ₅₀ calculation | 33 |
| 2.4 - General workflow to obtain, analyse and process shotgun lipidomic samples | 33 |
| 2.4.1 - Exposures | 34 |
| 2.4.2 - Metabolite extraction | 34 |
| 2.4.3 - Fourier transform ion cyclotron resonance mass spectrometry | 35 |
| 2.4.3.1 - Sample preparation for mass spectrometry..... | 35 |
| 2.4.3.2 - Acquisition of mass spectra..... | 36 |
| 2.4.4 - Processing mass spectral data to increase reliability and allow statistical analysis..... | 38 |

| | |
|--|----|
| 2.4.5 - Putative metabolite identification | 39 |
| 2.4.6 - Statistical analysis of lipidomic spectra | 40 |
| 2.4.6.1 - Univariate comparison of individual spectral feature intensities . | 40 |
| 2.4.6.2 - Multivariate comparison of spectral feature intensities | 40 |

3 - In vitro oxidation of lipid standards for creation of OxyLipidBlast database tool 41

| | |
|---|----|
| 3.1 - Introduction | 41 |
| 3.2 - Materials and methods | 43 |
| 3.2.1 - Molecular structure of PE lipid standards | 43 |
| 3.2.2 - Oxidation of PE species | 43 |
| 3.2.3 - Analysis of lipid species and oxidised products by FT-ICR and LTQ IT mass spectrometry. | 44 |
| 3.2.4 - Peak assignment..... | 45 |
| 3.2.5 - Creation of OxyLipidBlast conducted by Dr. Tobias Kind (UC Davis) | 45 |
| 3.2.6 - Validation of the OxyLipidBlast database | 46 |
| 3.3 - Results and discussion..... | 47 |
| 3.3.1 - Oxidation time-course | 55 |
| 3.3.2 - Annotation and interpretation of fragmentation patterns..... | 56 |
| 3.3.2.1 - Unmodified PE (positive ion mode) | 57 |
| 3.3.2.2 - Oxidised PE (positive ion mode) | 58 |
| 3.3.2.3 - Unmodified PE (negative ion mode)..... | 63 |

| | |
|---|----|
| 3.3.2.4 - Oxidised PE (negative ion mode) | 64 |
| 3.3.3 - Utilisation of OxyLipidBlast to identify oxidised products..... | 69 |
| 3.3.4 - Validation of the OxyLipidBlast database | 70 |
| 3.4 - Conclusions..... | 73 |

4 - Optimisation of mass spectrometric lipidomics and baseline

lipidome characterisation of *D. magna* and *C. reinhardtii*..... 75

| | |
|--|----|
| 4.1 - Introduction | 75 |
| 4.2 - Materials and methods | 76 |
| 4.2.1 - Optimising the preparation of samples for lipidomics analysis | 76 |
| 4.2.2 - Optimising the concentration of <i>D. magna</i> and <i>C. reinhardtii</i> extracts for mass spectrometric analysis in collaboration with Dr. Nadine Taylor (U of Birmingham) | 78 |
| 4.2.3 - Definitive identification of selected lipids to form a robust calibration list in collaboration with Dr. Nadine Taylor (U of Birmingham)..... | 79 |
| 4.2.4 - Annotation of baseline lipidomes of <i>D. magna</i> and <i>C. reinhardtii</i> .. | 80 |
| 4.3 - Results and discussion..... | 81 |
| 4.3.1 - Optimisation of the sample preparation methodology for mass spectrometric lipidomic analysis | 81 |
| 4.3.2 - Optimisation of the concentration of <i>D. magna</i> and <i>C. reinhardtii</i> extracts for mass spectrometric analysis..... | 83 |
| 4.3.3 - Creation of calibration list from identified lipids..... | 86 |
| 4.3.4 - Annotation of baseline lipidomes of <i>D. magna</i> and <i>C. reinhardtii</i> .. | 89 |

| | |
|--|------------|
| 4.4 - Conclusions..... | 110 |
| 5 - Oxidation of the <i>D. magna</i> and <i>C. reinhardtii</i> lipidomes by <i>in vitro</i> and <i>in vivo</i> stressors..... | 112 |
| 5.1 - Introduction | 112 |
| 5.2 - Materials and methods | 114 |
| 5.2.1 - In vitro oxidation of lipid extracts of <i>D. magna</i> and <i>C. reinhardtii</i> | 114 |
| 5.2.1.1 - Oxidation of <i>D. magna</i> and <i>C. reinhardtii</i> lipid extracts by exposure to air..... | 114 |
| 5.2.1.2 - Oxidation of <i>D. magna</i> lipid extracts by hydrogen peroxide and copper chloride..... | 115 |
| 5.2.1.3 - Putative annotation of potential oxidation..... | 115 |
| 5.2.2 - Assessing the acute toxicity of AgNO ₃ , and H ₂ O ₂ to <i>D. magna</i> and <i>C. reinhardtii</i> | 116 |
| 5.2.3 - In vivo exposure of <i>D. magna</i> and <i>C. reinhardtii</i> to oxidative stressors..... | 117 |
| 5.3 - Results and discussion..... | 118 |
| 5.3.1 - In vitro oxidation of <i>D. magna</i> and <i>C. reinhardtii</i> lipid extracts..... | 118 |
| 5.3.2 - Acute toxicity of AgNO ₃ and H ₂ O ₂ to <i>D. magna</i> and <i>C. reinhardtii</i> | 131 |
| 5.3.3 - Lipidomic responses of <i>D. magna</i> and <i>C. reinhardtii</i> to in vivo oxidative stressors..... | 134 |
| 5.4 - Conclusions..... | 144 |

| | |
|--|------------|
| 6 - Lipidomic analysis of silver nanoparticle toxicity in <i>D. magna</i> | |
| following extensive exposure optimisation..... | 146 |
| 6.1 - Introduction | 146 |
| 6.2 - Materials and methods | 148 |
| 6.2.1 - Acid washing of equipment..... | 148 |
| 6.2.2 - Silver nanoparticle preparation conducted by Dr. Isabella Römer and Mila Tejamaya (U of Birmingham) | 148 |
| 6.2.2.1 - Silver nanoparticle characterisation..... | 149 |
| 6.2.3 - Media dilution acute stress assessment..... | 149 |
| 6.2.4 - Media dilution chronic stress assessment | 150 |
| 6.2.5 - Acute toxicity conducted in collaboration with Alex Gavin (U of Birmingham) | 150 |
| 6.2.6 - Nanoparticle dissolution conducted in collaboration with Alex Gavin (U of Birmingham) | 151 |
| 6.2.6.1 - Ultracentrifugation separation of ionic and nano silver | 151 |
| 6.2.6.2 - Ultrafiltration separation of ionic and nano silver | 152 |
| 6.2.6.3 - Inductively coupled plasma mass spectrometry analysis of silver conducted by Dr Steve Baker (U of Birmingham)..... | 152 |
| 6.2.6.4 - Calculation of nano and ionic silver concentrations from ICP-MS results..... | 152 |
| 6.2.7 - Lipidomic analysis of <i>D. magna</i> exposed to PVP capped silver nanoparticles conducted in collaboration with Alex Gavin | 154 |
| 6.3 - Results and discussion..... | 155 |

| | |
|--|------------|
| 6.3.1 - Silver nanoparticle characterisation..... | 155 |
| 6.3.2 - Acute effects of diluting culture media on <i>D. magna</i> | 157 |
| 6.3.3 - Chronic effects of diluting culture media on <i>D. magna</i> | 157 |
| 6.3.4 - Acute toxicity of silver nanoparticles capped by citrate and PVP to <i>D. magna</i> | 158 |
| 6.3.5 - Dissolution of silver nanoparticles over the time-course of an acute exposure..... | 161 |
| 6.3.6 - Lipidomic perturbations caused by silver nanoparticles to <i>D. magna</i> | 164 |
| 6.4 - Conclusions..... | 173 |
| 7 - General conclusions and future work..... | 175 |
| 8 - References..... | 180 |
| A - Appendix | 197 |
| AI - Tables showing mass spectra from oxidised PE species | 197 |
| AI-I - Tables showing mass spectra of oxidised PE(14:0,0:0) in negative and positive ion mode..... | 197 |
| AI-II - Tables showing mass spectra of oxidised PE(18:1,0:0) in negative and positive ion mode..... | 198 |
| AI-III - Tables showing mass spectra of oxidised PE(14:0,14:0) in negative and positive ion mode..... | 199 |
| AI-IV - Tables showing mass spectra of oxidised PE(P-18,18:1) in negative and positive ion mode | 200 |

| | |
|---|------------|
| AI-V - Tables showing mass spectra of oxidised PE(18:1,18:1) in negative and positive ion mode..... | 201 |
| AI-VI - Tables showing mass spectra of oxidised PE(16:0,20:4) in negative and positive ion mode..... | 203 |
| All - Manually annotated fragmentation patterns from oxidised PE products | 205 |
| All-I - Fragmentation patterns from PE(14:0,0:0) and oxidised products thereof in negative ion mode | 205 |
| All-II - Fragmentation patterns from PE(14:0,0:0) and oxidised products thereof in positive ion mode..... | 206 |
| All-III - Fragmentation patterns from PE(18:1,0:0) and oxidised products thereof in negative ion mode | 206 |
| All-IV - Fragmentation patterns from PE(18:1,0:0) and oxidised products thereof in positive ion mode..... | 208 |
| All-V - Fragmentation patterns from PE(14:0,14:0) and oxidised products thereof in negative ion mode | 210 |
| All-VI - Fragmentation patterns from PE(14:0,14:0) and oxidised products thereof in positive ion mode..... | 211 |
| All-VII - Fragmentation patterns from PE(P18,18:1) and oxidised products thereof in negative ion mode | 214 |
| All-VIII - Fragmentation patterns from PE(P18,18:1) and oxidised products thereof in positive ion mode..... | 216 |
| All-IX - Fragmentation patterns from PE(16:0,18:1) and oxidised products thereof in negative ion mode | 218 |

| | |
|---|-----|
| All-X - Fragmentation patterns from PE(16:0,18:1) and oxidised products thereof in positive ion mode..... | 228 |
| All-XI - Fragmentation patterns from PE(18:1,18:1) and oxidised products thereof in negative ion mode | 233 |
| All-XII - Fragmentation patterns from PE(18:1,18:1) and oxidised products thereof in positive ion mode..... | 238 |
| All-XIII - Fragmentation patterns from PE(16:0,20:4) and oxidised products thereof in negative ion mode | 244 |
| All-XIV - Fragmentation patterns from PE(16:0,20:4) and oxidised products thereof in positive ion mode | 255 |
| AIII - Baseline lipidome of <i>D. magna</i> | 261 |
| AIV - Baseline lipidome of <i>C. reinhardtii</i> | 269 |

List of Figures

| | |
|---|----|
| Figure 1-1 Adult female <i>D. magna</i> chamber <14 days old with full brood (left) with parthenogenetic, female daughter <24 hrs old (right) (Barnett, 2014). | 4 |
| Figure 1-2 Life cycle of <i>Daphnia</i> (Ebert, 2005). | 6 |
| Figure 1-3 Scanning electron microscopy image of <i>Chlamydomonas reinhardtii</i> (Smith and Lefebvre, 1996). | 7 |
| Figure 1-4 Head-group structures of major phospholipid groups with LIPID MAPS identification codes. PE = glycerophosphatidylethanolamine, PG = glycerophosphatidylglycerol, PC = glycerophosphatidylcholine, PA = glycerophosphatidic acid, PI = glycerophosphatidylinositol, PS = glycerophosphatidylserine. | 13 |
| Figure 1-5 Structure of mono-unsaturated PE(16:0,18:1(9Z)), a representative glycerophosphatidylethanolamine | 14 |
| Figure 1-6 Bar chart modified from (Persson and Vrede, 2006). Shows composition of total fatty acids in <i>D. magna</i> , SFA are shown in blue, MUFA in red and PUFA in green. | 16 |
| Figure 1-7 Bar chart modified from (Bychek and Gushchina, 1999). Shows composition of total fatty acids in <i>D. magna</i> , SFA are shown in blue, MUFA in red and PUFA in green. | 16 |
| Figure 2-1 SIM-windows used during FT-ICR MS analysis. A typical post-processing spectrum from <i>D. magna</i> lipid extract is shown in red with SIM-windows shown in black. | 37 |
| Figure 3-1 FT-ICR mass spectrum of PE(16:0,18:1) and oxidised products. Hashed line at $m/z = 717.53$ denotes neutral mass of unmodified lipid. Named peaks indicate adducts of unmodified lipids, peak mass additions indicate oxygen modifications. Positive ion mode is shown above the x-axis and negative ion mode below. | 53 |
| Figure 3-2 Summary of oxidative modifications observed in PE molecules with varying chain chemistry. Relative intensities are represented by cones, single oxygen addition = blue, double oxygen addition = red, triple oxygen addition = green, quadruple oxygen addition = purple. Where cones are absent species was not observed with relative intensity above 1%. | 54 |

Figure 3-3 Intensities of oxidatively modified lipids relative to the unmodified lipid PE(16:0,18:1(9Z)) across a 96 hour period (n=1). Triangles (▲) represent single oxygen addition (M+O), circles (●) represent double oxygen addition (M+O₂), plus signs (+) represent triple oxygen addition (M+O₃) and crosses (×) represent quadruple oxygen addition (M+O₄). 56

Figure 3-4 Structure showing the major fragments of [PE(16:0,18:1)+Na]⁺. Arrows indicate observed fragments and *m/z* values..... 58

Figure 3-5 Structure showing the major fragments of [PE(16:0,18:1)+O+Na]⁺. Arrows indicate observed fragments and *m/z* values. Hydroxyl group position is for illustrative purposes only as not defined by MS² analysis. 60

Figure 3-6 Structure showing the major fragments of [PE(16:0,18:1)+O₂+Na]⁺. Arrows indicate observed fragments and *m/z* values. Peroxyl group position is for illustrative purposes only as not defined by MS² analysis..... 63

Figure 3-7 Structure showing the major fragments of [PE(16:0,18:1)-H]⁻. Arrows indicate observed fragments and *m/z* values..... 64

Figure 3-8 Structure showing the major fragments of [PE(16:0,18:1)+O-H]⁻. Arrows indicate observed fragments and *m/z* values. Hydroxyl group position is for illustrative purposes only as not defined by MS² analysis..... 66

Figure 3-9 Structure showing the major fragments of [PE(16:0,18:1)+O₂-H]⁻. Arrows indicate observed fragments and *m/z* values. Peroxyl group position is for illustrative purposes only as not defined by MS² analysis..... 68

Figure 4-1 Scatter plot showing correlation between mass spectral features and sample concentration of *D. magna* lipid extract. Points represent mean spectral features across concentration groups (n=8)..... 84

Figure 4-2 Scatter plot showing correlation between mass spectral features and sample concentration of *C. reinhardtii* lipid extract. Points represent mean spectral features across concentration groups (n=8)..... 85

| | |
|--|----|
| Figure 4-3 Representative mass spectrum of <i>D. magna</i> lipid extract. Spectra were collected in m/z range 70-2000. Inserts show zoomed regions containing peaks clusters (A) m/z 300-500, (B) m/z 700-900 (C) m/z 1000-1200. Relative intensity is normalised to peaks contained in zoomed regions. | 83 |
| Figure 4-4 Representative mass spectrum of <i>C. reinhardtii</i> lipid extract. Spectra were collected in m/z range 70-2000. Inserts show zoomed regions containing peaks clusters (A) m/z 300-500, (B) m/z 700-900 (C) m/z 1000-1200. Relative intensity is normalised to peaks contained in zoomed regions. | 84 |
| Figure 4-5 Histograms depicting mass error distributions of putatively annotated ion forms within the baseline lipidome of <i>D. magna</i> | 87 |
| Figure 4-6 Histograms depicting mass error distributions of putatively annotated ion forms within the baseline lipidome of <i>C. reinhardtii</i> | 88 |
| Figure 4-7 Chart showing specific [PA+Ac] ⁻ putative annotations of features observed in the basal <i>D. magna</i> lipidome. Species are separated along the x-axis by cumulative carbon chain length (sn1+sn2) and along the z-axis by saturation (number of double bonds). | 91 |
| Figure 4-8 Chart showing specific [PC+Ac] ⁻ putative annotations of features observed in the basal <i>D. magna</i> lipidome. Species are separated along the x-axis by cumulative carbon chain length (sn1+sn2) and along the z-axis by saturation (number of double bonds). | 92 |
| Figure 4-9 Chart showing specific [PE-H] ⁻ putative annotations of features observed in the basal <i>D. magna</i> lipidome. Species are separated along the x-axis by cumulative carbon chain length (sn1+sn2) and along the z-axis by saturation (number of double bonds). | 93 |
| Figure 4-10 Chart showing specific [PG-H] ⁻ putative annotations of features observed in the basal <i>D. magna</i> lipidome. Species are separated along the x-axis by cumulative carbon chain length (sn1+sn2) and along the z-axis by saturation (number of double bonds). | 94 |
| Figure 4-11 Chart showing specific [PI-H] ⁻ putative annotations of features observed in the basal <i>D. magna</i> lipidome. Species are separated along the x-axis by cumulative carbon chain length (sn1+sn2) and along the z-axis by saturation (number of double bonds). | 95 |

Figure 4-12 Chart showing specific [PS-H]- putative annotations of features observed in the basal *D. magna* lipidome. Species are separated along the x-axis by cumulative carbon chain length (sn1+sn2) and along the z-axis by saturation (number of double bonds). 96

Figure 4-13 Chart showing putatively annotated chain lengths in *D. magna* baseline lipidome. Phospholipid class is shown by colour and order, left to right: navy blue = PA, red =PC, green = PE, purple = PG, teal = PI and orange = PS..... 97

Figure 4-14 Chart showing putatively annotated double bond number in *D. magna* baseline lipidome. Phospholipid class is shown by colour and order, left to right: navy blue = PA, red =PC, green = PE, purple = PG, teal = PI and orange = PS..... 98

Figure 4-15 Chart showing putatively annotated chain lengths in *C. reinhardtii* baseline lipidome. Phospholipid class is shown by colour and order, left to right: navy blue = PA, red =PC, green = PE, purple = PG, teal = PI and orange = PS..... 100

Figure 4-16 Chart showing putatively annotated double bond number in *D. magna* baseline lipidome. Phospholipid class is shown by colour and order, left to right: navy blue = PA, red =PC, green = PE, purple = PG, teal = PI and orange = PS..... 101

Figure 5-1 Scores plot showing sample number vs. principal component 1 (PC1) for *in vitro* lipid extract exposures. Control samples are denoted by black circles, exposed samples are denoted by red squares. (A) H₂O₂ / CuCl₂ exposure to *D. magna* lipid extract. Significant separation between control and exposed is observed (P=5.29x10⁻³). (B) Air exposure to *D. magna* lipid extract. Significant separation between control and exposed is observed (P=3.86x10⁻⁹). (C) Air exposure to *C. reinhardtii* lipid extract. Significant separation between control and exposed is observed (P=2.56x10⁻⁹). 111

Figure 5-2 Exposed / control log₂ fold changes for *in vitro* exposed lipid extracts. Species with changes of more than 1 or less than -1 (i.e. an arbitrary two-fold change) are highlighted in blue and red respectively. (A) H₂O₂ / CuCl₂ exposure to *D. magna* lipid extract. (B) Air exposure to *D. magna* lipid extract. (C) Air exposure to *C. reinhardtii* lipid extract. 114

Figure 5-3 Log₂ fold changes (exposed / control) of unmodified (black), and potentially oxidatively modified (+O, blue) spectral features. (A) = *in vitro* H₂O₂ (*D. magna*). (B) = *in vitro* Air (*D. magna*). (C) = *in vitro* Air (*C. reinhardtii*). Spectral features which could be unmodified or modified are shown in red..... 116

Figure 5-4 Log₂ fold changes (exposed / control) of unmodified (black), and potentially oxidatively modified (+O₂, blue) spectral features. (A) = *in vitro* H₂O₂ (*D. magna*). (B) = *in vitro* Air (*D. magna*). (C) = *in vitro* Air (*C. reinhardtii*). Spectral features which could be unmodified or modified are shown in red..... 117

Figure 5-5 Scatter plots showing putatively annotated oxidation in H₂O₂ exposed *D. magna* lipid extracts. Exposed / control intensity log₂ fold changes of baseline lipidome matched spectral features (black), oxygen addition features (blue) and oxygen added features with an unmodified lipid annotation (red). (A) single oxygen addition. (B) double oxygen addition. 120

Figure 5-6 Scatter plots showing putatively annotated oxidation in air exposed *D. magna* lipid extracts. Exposed / control intensity log₂ fold changes of baseline lipidome matched spectral features (black), oxygen addition features (blue) and oxygen added features with an unmodified lipid annotation (red). (A) single oxygen addition. (B) double oxygen addition. 121

Figure 5-7 Scatter plots showing putatively annotated oxidation in air exposed *C. reinhardtii* lipid extracts. Exposed / control intensity log₂ fold changes of baseline lipidome matched spectral features (black), oxygen addition features (blue) and oxygen added features with an unmodified lipid annotation (red). (A) single oxygen addition. (B) double oxygen addition. 122

Figure 5-8 Concentration-response curves for immobilisation of *D. magna*. Blue diamonds (◊) indicate immobilisation at 24 hours, red circles (●) indicate immobilisation at 48 hours. EC₅₀s are indicated by squares. Vertical error bars represent standard error of the mean (SEM), horizontal error bars show 95% EC₅₀ confidence intervals. (A) AgNO₃ EC₅₀ = 1.49 µg/l (24hrs), 1.34 µg/l (48hrs). (B) H₂O₂ EC₅₀ = 9.44 mg/l (24hrs), 7.35 mg/l (48hrs). 125

Figure 5-9 Concentration-response curve for cell growth inhibition of *C. reinhardtii* exposed to AgNO₃.

72hour EC₅₀ is indicated by square with horizontal error bars representing 95% confidence interval and has a value of 73.17 µg l⁻¹. Vertical error bars represent standard error of the mean (SEM), horizontal error bars show 95% EC₅₀ confidence intervals. 125

Figure 5-10 Scores plot showing sample number vs. most significant principal component for *in vivo*

oxidative stress exposures. Control samples are denoted by black circles, low dose exposed samples are denoted by red down triangles and high dose exposed samples denoted by red up triangles. Vertical lines in A-C separate sample groups. (A) H₂O₂ exposure to *D. magna*. Significant separation between control and high dose is observed along PC2 (P=0.028). (B) CuSO₄ exposure to *D. magna*. Significant separation between control and high dose is observed along PC4 (P=0.019). (C) AgNO₃ exposure to *D. magna*. No significant separation observed, PC5 is shown as the most significant PC axis (P = 0.371) (D) AgNO₃ exposure to *C. reinhardtii* Significant separations seen along PC1 between low and high doses and PC5 between control and high dose (P= 0.033 and 0.0075 respectively)..... 127

Figure 5-11 High dose exposed / control log₂ fold changes for *in vivo* exposures. Species with

changes of more than 1 or less than -1 (i.e. a two-fold change) are highlighted in blue and red respectively. (A) H₂O₂ exposure to *D. magna*. (B) CuSO₄ exposure to *D. magna*. (C) AgNO₃ exposure to *D. magna*. (D) AgNO₃ exposure to *C. reinhardtii*..... 130

Figure 5-12 Scatter plots showing putatively annotated oxidation in H₂O₂ exposed *D. magna* lipid

extracts. Exposed / control intensity log₂ fold changes of baseline lipidome matched spectral features (black), oxygen addition features (blue) and oxygen added features with an unmodified lipid annotation (red). (A) single oxygen addition. (B) double oxygen addition. 132

Figure 5-13 Scatter plots showing putatively annotated oxidation in CuSO₄ exposed *D. magna* lipid

extracts. Exposed / control intensity log₂ fold changes of baseline lipidome matched spectral features (black), oxygen addition features (blue) and oxygen added features with

an unmodified lipid annotation (red). (A) single oxygen addition. (B) double oxygen addition. 133

Figure 5-14 Scatter plots showing putatively annotated oxidation in AgNO₃ exposed *D. magna* lipid extracts. Exposed / control intensity log₂ fold changes of baseline lipidome matched spectral features (black), oxygen addition features (blue) and oxygen added features with an unmodified lipid annotation (red). (A) single oxygen addition. (B) double oxygen addition. 134

Figure 5-15 Scatter plots showing putatively annotated oxidation in AgNO₃ exposed *C. reinhardtii* lipid extracts. Exposed / control intensity log₂ fold changes of baseline lipidome matched spectral features (black), oxygen addition features (blue) and oxygen added features with an unmodified lipid annotation (red). (A) single oxygen addition. (B) double oxygen addition. 135

Figure 6-1 Dose-response curves for immobilisation of *D. magna* exposed to (A) AgNP-cit and (B) AgNP-PVP. Blue diamonds (◊) indicate immobilisation at 24 h, blue crosses (X) represent pre-adjustment values for non-monotonically increasing immobilisation at 24 h, red circles (●) indicate immobilisation at 48 h. 24 h and 48 h EC₅₀s are indicated by squares. Vertical error bars represent standard error of the mean (SEM), horizontal error bars show 95 % EC₅₀ confidence intervals 135

Figure 6-2 Dissolution of silver nanoparticles across acute toxicity time course. Error bars show standard error of the mean (n=3). (A) Ultracentrifugation separation (B) Ultrafiltration separation. 135

Figure 6-3 PCA scores plots showing the most significant separation between exposure groups. Colour signifies toxicant, Black = control, Blue = AgNP-PVP, Red = silver ions. Letters signify concentration in toxicant groups H= High, M = Medium, L= Low, V = Very Low. Letters signify type in control groups, C = negative control, P = PVP, B = bulk silver. (A) PC3, (B) PC5. 137

Figure 6-4 Scatter plot showing log₂ fold changes of lipid species (high dose / control) versus *m/z*. Positive fold changes are shown in blue, negative fold changes are shown in red. (A) Ionic silver high dose, (B) AgNP-PVP high dose. 138

Figure 6-5 Log₂ fold changes (High dose ionic / negative control) of unmodified (black), and potentially oxidatively modified (blue) spectral features. Spectral features which could correspond to unmodified or oxidatively modified are shown in red. (A) shows +O modifications, (B) shows +O₂ modifications. 140

Figure 6-6 Log₂ fold changes (High dose AgNP-PVP / negative control) of unmodified (black), and potentially oxidatively modified (blue) spectral features. Spectral features which could correspond to unmodified or oxidatively modified are shown in red. (A) shows +O modifications, (B) shows +O₂ modifications. 141

Figure 6-7 Scatter plots showing putatively annotated oxidation in high dose ionic silver exposed *D. magna* lipid extracts. Exposed / control intensity log₂ fold changes of baseline lipidome matched spectral features (black), oxygen addition features (blue) and oxygen added features with an unmodified lipid annotation (red). (A) single oxygen addition. (B) double oxygen addition. 142

Figure 6-8 Scatter plots showing putatively annotated oxidation in high dose AgNP-PVP exposed *D. magna* lipid extracts. Exposed / control intensity log₂ fold changes of baseline lipidome matched spectral features (black), oxygen addition features (blue) and oxygen added features with an unmodified lipid annotation (red). (A) single oxygen addition. (B) double oxygen addition. 143

List of Tables

| | |
|---|----|
| Table 1-1 OECD recommended aquatic toxicity test species and endpoints. | 2 |
| Table 2-1 Composition of OECD modified media | 30 |
| Table 2-2 Composition of Bold's basal medium (BBM)..... | 31 |
| Table 2-3 Electrospray ionisation settings for shotgun lipidomics. | 36 |
| Table 2-4 Mass spectrometry settings | 37 |
| Table 3-1 Table detailing the PE standards used for oxidation, with chain chemistry, formula and neutral mass (Da). | 43 |
| Table 3-2 Mass spectrometry settings for data-dependant acquisition. | 44 |
| Table 3-3 Negative ion mode mass spectra from oxidised PE(16:0,18:1). M represents the unmodified lipid (PE(16:0,18:1))...... | 51 |
| Table 3-4 Positive ion mode mass spectra from oxidised PE(16:0,18:1). M represents the unmodified lipid (PE(16:0,18:1))...... | 52 |
| Table 3-5 Fragments of unmodified [PE(16:0,18:1)+Na] ⁺ and associated annotation..... | 58 |
| Table 3-6 Fragments of [PE(16:0,18:1)+O+Na] ⁺ and associated annotation. | 60 |
| Table 3-7 Fragments of [PE(16:0,18:1)+O ₂ +Na] ⁺ and associated annotation. | 62 |
| Table 3-8 Fragments of unmodified [PE(16:0,18:1)-H] ⁻ and associated annotation..... | 64 |
| Table 3-9 Fragments of [PE(16:0,18:1)+O-H] ⁻ and associated annotation..... | 66 |
| Table 3-10 Fragments of [PE(16:0,18:1)+O ₂ -H] ⁻ and associated annotation..... | 68 |
| Table 3-11 Table showing ability of OxyLipidBlast to annotate oxidised peaks. Numerical values represent reverse dot product scores which assess how well the theoretical spectrum matches the experimental one, scores run from 0 (no match) to 999 (perfect match)..... | 69 |

| | |
|--|-----|
| Table 3-12 Table showing the oxidised products identified by OxyLipidBlast. Numerical values represent the reverse dot product score which assesses how well the theoretical spectrum matches the experimental spectrum, 0 = no match, 1000 = perfect match..... | 72 |
| Table 4-1 Sample preparation differences. | 77 |
| Table 4-2 Table showing median RSD values from sample preparation optimisation analysis. Grey shading denotes lack of reliable sample spray from group D resulting in 3/7 analyses failing..... | 82 |
| Table 4-3 Identified species used as internal calibrants for <i>D. magna</i> lipidomic datasets. LipidBlast column shows the reverse dot product score indicating match success, NA indicates compound is not in the LipidBlast library and No ID indicates the compound is in the database but was not identified. | 88 |
| Table 4-4 Putatively annotated species used as internal calibrants for <i>C. reinhardtii</i> lipidomic datasets. | 89 |
| Table 4-5 Baseline lipidome peak lists retained following peak lists. Processed peak no. denotes spectral features remaining following processing filters. | 85 |
| Table 4-6 Summary of polar lipids annotated in baseline analysis of <i>D. magna</i> and <i>C. reinhardtii</i> . Features include lyso and plasmalogens. Lipid annotations are counted only once regardless of multiple ion forms..... | 85 |
| Table 5-1 Table showing the concentrations of oxidative stressors to which <i>D. magna</i> neonates were exposed. *NOAEL for CuSO ₄ communicated from Dr N. Taylor (University of Birmingham)..... | 109 |
| Table 5-2 Table showing significant group separation by principal scores of processed <i>in vitro</i> perturbed lipid extracts. * = P<0.05, *** = P<0.001. | 112 |
| Table 5-3 Table showing peak matrix size and univariate statistical results for <i>in vitro</i> oxidation studies. Peak number is the amount of spectral features which passed the filtering steps of processing. Spectral features with associated significant intensity changes between sample groups (FDR corrected P<0.05) are counted in the significantly changing column. | |

Unique peaks are those which are only observed in one sample group. Min and max fold changes are the highest and lowest intensity fold changes between sample groups

$\log_2(\text{exposed} / \text{control})$ 113

Table 5-4 Table showing significant group separation by principal scores of processed *in vivo* *D. magna* and *C. reinhardtii* exposed to oxidative stress. * = P(<0.05). 128

Table 5-5 Table showing peak matrix size and univariate statistical results for *in vitro* oxidation studies. 129

Table 6-1 Characterisation of AgNP-cit and AgNP-PVP in UP H₂O 148

Table 6-2 Acute toxicity of various media concentrations to *Daphnia magna* 149

Table 6-3 Chronic toxicity of various media concentrations to *Daphnia magna* 150

Table 6-4 EC₅₀ values for Ag⁺ (converted from AgNO₃), AgNPs-cit and AgNPs-PVP with 95 % confidence intervals at 24 and 48 h. 135

Table 6-5 Table showing significant group separation by principal scores of groups of *D. magna* exposed to varying concentrations of AgNP-PVP, AgNO₃, PVP or bulk silver. ** = P<0.005, *** = P<0.001 136

List of abbreviations

| | |
|-----------------------|--|
| 2D- HPTLC | Two-dimensional high performance thin layer chromatography |
| 4-HNE | 4-hydroxynonenal |
| AGC | Automatic gain control |
| AgNO ₃ | Silver nitrate |
| AgNP | Silver nanoparticles |
| AgNP-cit | Silver nanoparticles (citrate capped) |
| AgNP-PVP | Silver nanoparticles (PVP capped) |
| ANOVA | Analysis of variance |
| <i>C. reinhardtii</i> | <i>Chlamydomonas reinhardtii</i> |
| CHCl ₃ | Chloroform |
| CuSO ₄ | Copper sulfate |
| <i>D. magna</i> | <i>Daphnia magna</i> |
| DGDG | Digalactosyldiacylglycerol |
| DI | De-ionised |
| DIMS | Direct infusion mass spectrometry |
| DLS | Dynamic light scattering |
| DMSO | Dimethyl sulfoxide |
| EC ₅₀ | Concentration predicted to cause a given endpoint in 50% of a population |
| ESI | Electrospray ionisation |
| FA | Fatty acid |
| FAME | Fatty acyl methyl ester |
| FDR | False discovery rate |
| FFF | Field flow fractionation |
| FT-ICR | Fourier transform – ion cyclotron resonance |

| | |
|-------------------------------|--|
| glog | Generalised logarithm |
| H ₂ O | Water |
| H ₂ O ₂ | Hydrogen peroxide |
| HCl | Hydrochloric acid |
| HNO ₃ | Nitric acid |
| HR FT MS | High resolution Fourier transform mass spectrometer |
| ICP-MS | Inductively coupled plasma – mass spectrometry |
| LC | Liquid chromatography |
| LipidMAPS | Lipid metabolites and pathways strategy |
| LO | Lipid epoxide |
| LOH | Lipid hydroxide |
| LOOH | Lipid hydroperoxide |
| m/z | Mass to charge ratio |
| MALDI | Matrix assisted laser desorption ionisation |
| MDA | Malondialdehyde |
| MeOH | Methanol |
| MGDG | Monogalactosyldiacylglycerol |
| MS | Mass spectrometry |
| MS/MS | Tandem mass spectrometry |
| MTBE | Methyl-tert-butyl ether |
| MUFA | Mono-unsaturated fatty acid |
| NaOH | Sodium hydroxide |
| nESI | Nano-electrospray ionisation |
| NM | Nano-materials |
| OD | Optical density |
| OECD | Organisation for economic co-operation and development |

| | |
|-------|---|
| PA | Glycerophosphatidic acid |
| PC | Glycerophosphatidylcholine |
| PCA | Principal component analysis |
| PCR | Polymerase chain reaction |
| PE | Glycerophosphatidylethanolamine |
| PG | Glycerophosphatidylglycerol |
| PI | Glycerophosphatidylinositol |
| PL | Phospholipids |
| ppm | Parts per million |
| PQN | Probable quotient normalisation |
| PS | Glycerophosphatidylserine |
| PUFA | Poly-unsaturated fatty acid |
| PVP | Polyvinylpyrrolidone |
| ROS | Reactive oxygen species |
| RSD | Relative standard deviation |
| RT | Retention time |
| SFA | Saturated fatty acid |
| SNR | Signal-to-noise ratio |
| SPE | Solid phase extraction |
| SQDG | Sulfoquinovosylglycerol |
| TEM | Transition electron microscopy |
| TIC | Total ion chromatogram |
| TLC | Thin layer chromatography |
| TSK | Trimmed Spearman-Kärber |
| UP | Ultrapure |
| USEPA | United States Environmental Protection Agency |

1 - Introduction

1.1 - Aquatic ecotoxicology

Pollution of our natural environment is an unavoidable consequence of technological advances. Air, land and water can all become polluted, which can have far reaching effects such as species extinction. Ecotoxicology is the field of science which attempts to assess the impact toxicants may have on the environment. Aquatic toxicology has been a major component of ecotoxicology for over 40 years (Pritchard, 1993), focussing on the effect that sources such as industrial wastewater, domestic sewage and agricultural runoff will have on both freshwater and marine environments. Toxicity can be assessed by measuring any observable adverse effect in an organism. As evident from the Organisation for Economic Co-operation and Development (OECD) recommended tests discussed below, in its simplest form toxicity testing focuses on macro effects such as lethality and reproductive output. However, classic toxicology endpoints are being supplemented and replaced by higher throughput, mechanistically illuminating techniques, such as toxicogenomic methods. Comprising genomic, transcriptomic, proteomic and metabolomic (including lipidomic) assessment of toxicology, toxicogenomics allows assessment of perturbations across whole biological networks by comprehensive measurement of the full complement of DNA, RNA, proteins or metabolites in a xenobiotic exposed cell, tissue or organism (Garcia-Reyero and Perkins, 2011). This improves on classical toxicity endpoints which may only measure a phenotypic endpoint or a couple of relevant biomarkers allowing greater predictive

power from organism to population level and reducing the number of test animals (Snape et al., 2004).

1.1.1 - Model organisms for aquatic toxicology

The scope for aquatic toxicology testing is vast. Millions of relevant species could be exposed to thousands of existing and potential freshwater pollutants to assess multiple toxic endpoints (Breitholtz et al., 2006, Schwarzenbach et al., 2010). To avoid this impossible and unnecessary task the OECD has outlined batteries of tests on a reduced subset of organisms and endpoints to assess ecotoxicology. For aquatic systems these tests focus on representative species from three trophic levels: primary producers (algae); primary consumers (*Daphnia*) and secondary consumers (fish and amphibians) (Table 1-1).

Table 1-1 OECD recommended aquatic toxicity test species and endpoints.

| Trophic level | Recommended species | Toxic endpoints | OECD guideline |
|--------------------|--|---|----------------|
| Primary producer | <i>Anabaena flos-aquae</i> | Acute growth inhibition | 201 |
| | <i>Desmodesmus subspicatus</i> | | |
| | <i>Navicula pelliculosa</i> | | |
| | <i>Pseudokirchneriella subcapitata</i> | | |
| | <i>Synechococcus leopoliensis</i> | | |
| Primary consumer | <i>Daphnia magna</i> | Acute neonate immobilisation | 202 |
| | <i>Daphnia pulex</i> | Chronic reproductive success | 211 |
| Secondary consumer | <i>Cyprinodon variegatus</i> | Acute adult lethality | 203 |
| | <i>Cyprinus carpio</i> | Chronic adult lethality | 204 |
| | <i>Danio rerio</i> | Morphological and behavioural abnormalities | 210/212/215 |
| | <i>Lepomis macrochirus</i> | Chronic endocrine disruption | 229/230/234 |
| | <i>Oncorhynchus mykiss</i> | Acute embryo lethality | 236 |
| | <i>Oryzias latipes</i> | Thyroid development | 231 |
| | <i>Pimephales promelas</i> <i>Poecilia reticulata</i> | | |

1.1.1.1 - *Daphnia magna*

Known colloquially as water fleas, *Daphnia* are small crustaceans, in the milli size range, from the order Cladocera (Figure 1-1). Well recognised as a sentinel toxicological species, the response of *D. magna* has been reported over 20000 times to a range of over 2000 compounds according to the United States Environmental Protection Agency's (USEPA) ECOTOX database (USEPA, 2014). The life-cycle of *Daphnia* shown in Figure 1-2 allows adaptability to environmental changes both natural and anthropogenic. In the absence of stresses such as predation, starvation, short photoperiod or overcrowding, females reproduce parthenogenetically, creating genetically identical daughters, allowing colonies to expand rapidly in accommodating environments (Hobaek and Larsson, 1990). Under such stresses or chemical induction, production of male offspring and a switch to sexual reproduction can produce resting eggs, encased in ephippia, capable of surviving harsh environmental conditions and preserving the colony for many years (Doma, 1979, Carvalho and Hughes, 1983). Illustrating the capacity of this survival mechanism, a recent study recorded egg revival after ca. 700 years (Frisch et al., 2013).



Figure 1-1 Adult female *D. magna* chamber <14 days old with full brood (left) with parthenogenetic, female daughter <24 hrs old (right) (Barnett, 2014).

With near ubiquity in permanent bodies of fresh water (Tatarazako and Oda, 2007), *Daphnia* are crucial to many aquatic ecosystems acting as both a major food source for fish and, as the dominant herbivore in many lakes and ponds, moderating the water clarity by consumption of algae (Dodson and Hanazato, 1995). This environmental relevance, supplemented by ease of culture, short life-span, low cost and parthenogenetic reproduction has made *D. magna* an excellent choice for classic toxicity

testing. In recent years *D. magna* have also been utilised in novel toxicity assessments such as ecotoxicogenomics (Poynton et al., 2007, Soetaert et al., 2007), transcriptomics (Garcia-Reyero et al., 2012) and metabolomics (Taylor et al., 2010). This continued interest in *Daphnia* as a model species has been reflected by the published genome sequencing of *Daphnia pulex* (Colbourne et al., 2011) and the ongoing sequencing of *D. magna*. For biological relevance, importance in the literature and economic reasons we have chosen to use *D. magna* as our primary model organism for the work presented in this thesis.

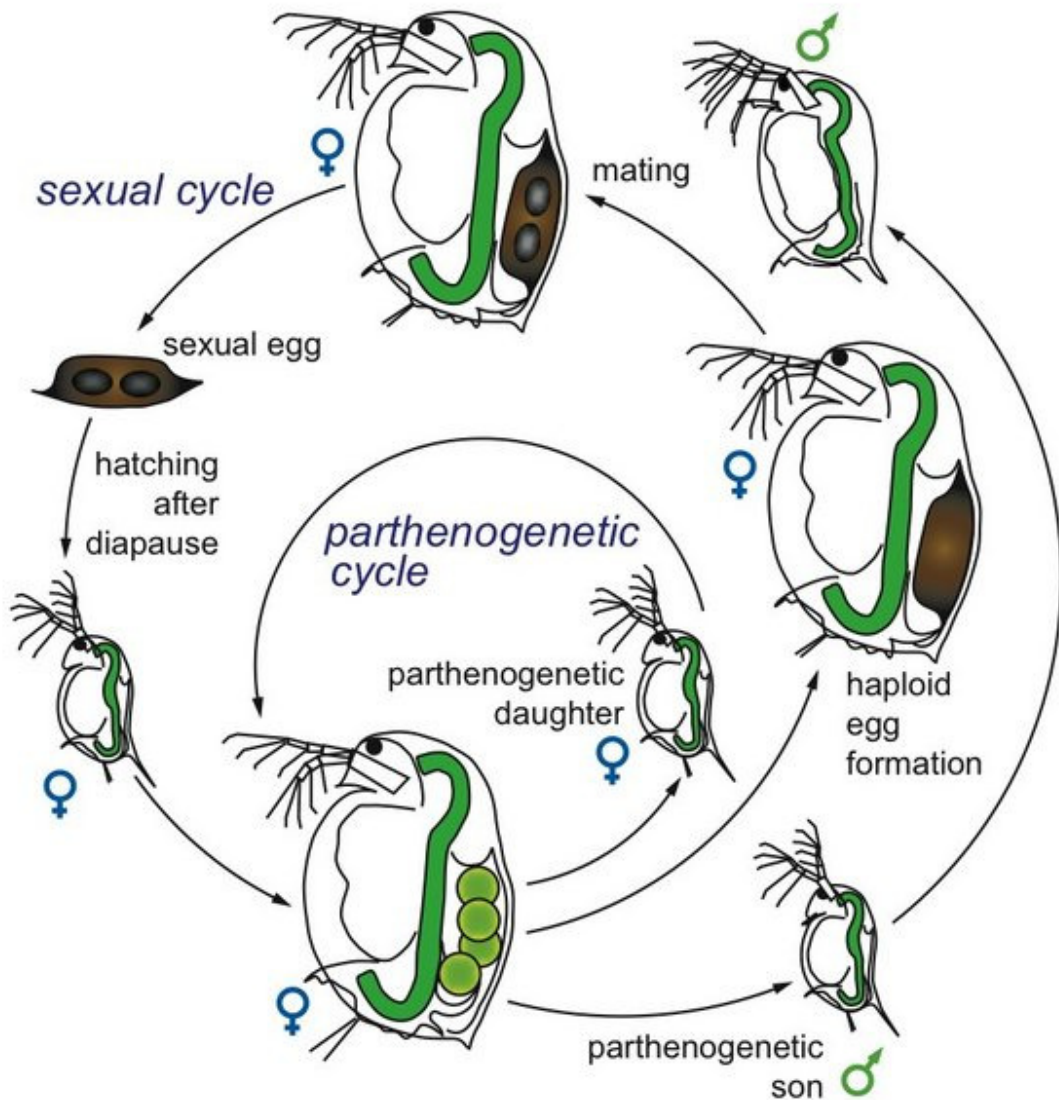


Figure 1-2 Life cycle of *Daphnia* showing parthenogenetic reproduction under favourable conditions and switch to sexual reproduction when stressed (Ebert, 2005).

1.1.1.2 - *Chlamydomonas reinhardtii*

A potential food source for *D. magna*, *Chlamydomonas reinhardtii* (Figure 1-3) is less established with regards to ecotoxicology testing, with only 781 reported responses to

144 chemicals (USEPA, 2014). However, it has been recognised as an important ecological species for the past century, reflected by the sequencing of its genome (Merchant et al., 2007). *C. reinhardtii*, the primary laboratory species of the genus *Chlamydomonas*, is a unicellular green alga averaging 10 µm throughout the cell cycle (Harris, 2001). The widespread use of *C. reinhardtii* is proliferated by ease of culture, as it grows rapidly with short generation time.

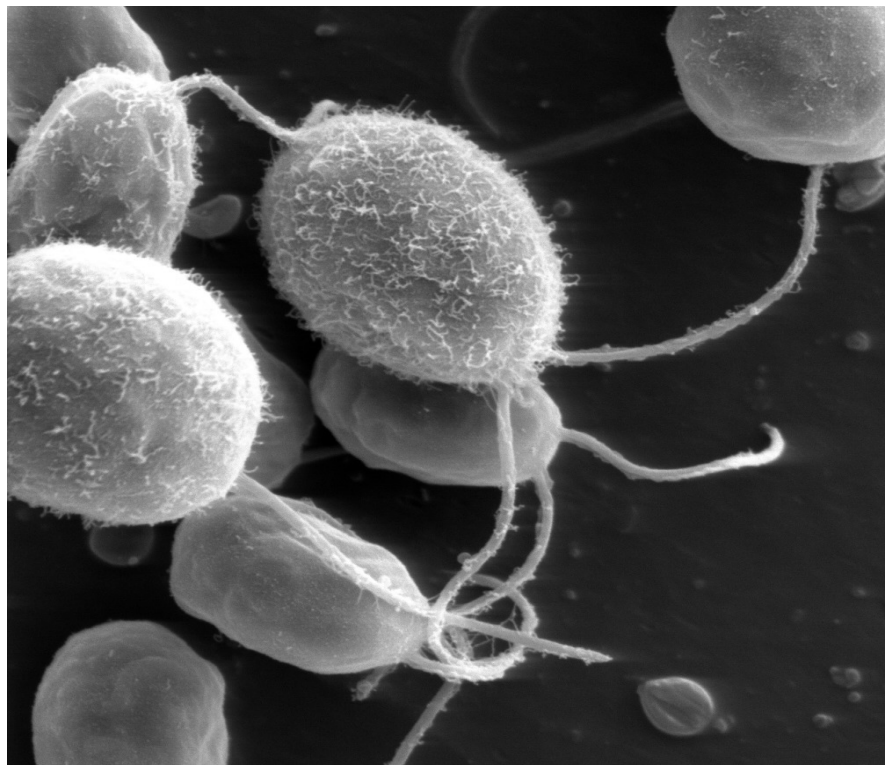


Figure 1-3 Scanning electron microscopy image of *Chlamydomonas reinhardtii* (Smith and Lefebvre, 1996).

Recently microalgae have shown potential utility in two major environmental industries, bioremediation and sustainable fuel generation. *C. reinhardtii*, have been proposed as tools for bioremediation as they have the ability to bind heavy metals with phytochlatin

(Scheidegger et al., 2011). Additionally *C. reinhardtii* has been proposed as a hydrogen generator and lipid source for biofuel, generating demand for a greater understanding of their lipid profile (Hu et al., 2008, Scoma et al., 2012).

As a primary producing food source for *D. magna* (McTeer et al., 2014), a heavy metal detoxification ability (Zheng et al., 2013) and a lipid rich, well reported biochemical profile (Valledor et al., 2013, Yang et al., 2013, Giroud et al., 1988), *C. reinhardtii* represents an excellent secondary model organism for the work presented in this thesis.

1.1.2 - Aquatic contaminants

The aquatic environment is subject to numerous contaminants many of which have been assessed for potential ecotoxicology. Recent high profile examples have included oil spills, including the Niger delta (Masters, 2013) and industrial waste, such as mining run-off containing heavy metals, particularly in developing nations (Ming, 2013). The exponential development of novel products containing nanomaterials has introduced the potential for functionally unknown aquatic pollutants which require rapid and comprehensive ecotoxicological assessment (Elsaesser and Howard, 2012).

1.1.2.1 - Nano-materials

Engineered nano-materials (NM) are a recent addition to environmental toxicology despite the fact that nano products such as colloidal silver medicines have been in use since the 1950s (Nowack et al., 2011). Defined as materials with a single dimension in the nano-range (1-100 nm) (Hosokawa, 2007, Klabunde and Richards, 2009), NMs can be divided into five main classes: carbonaceous, metal, metal oxide, nanopolymers and

quantum dots, based upon their molecular make-up. The huge surface area : mass ratio of these compound alters their functionality imbuing them with properties not observed from their bulk analogues (Colvin, 2003). These properties include increased tensile strength of carbon nanotubes, catalytic ability of metal oxides and increased anti bacterial activity of silver nanoparticles (AgNP). Elemental composition, size and surface properties (area, charge, coating) are intrinsic to the functional nature of the NM and are therefore key characteristics to be reported in all nano-literature, a practice which is far from universal (Reidy et al., 2013).

1.1.2.2 - Silver nanoparticles (AgNP)

AgNPs are produced in relatively small volume but are extremely widespread in terms of products and are contained in up to a third of commercial nano-items (Hendren et al., 2011, Fisher et al.). Anti-bacterial activity encourages AgNP use in products requiring freshness. Textiles used to create odour resistant garments are the primary use for nano-silver either surface coating or embedded within fibres (Reidy et al., 2013).

Washing nano-imbued clothes can release these AgNPs into effluent streams in a concentration-mediated manner (Benn and Westerhoff, 2008). It is likely that freshwater systems will act as terminal sinks for AgNPs following release into wastewater systems (Mueller and Nowack, 2008). Therefore knowledge of the impact AgNPs may have on the aquatic environment is crucial. At the onset of this study, very little literature existed which assessed the toxicology of AgNPs (Yoon et al., 2007). However, over the last four years, numerous publications have reported toxicity not only to aquatic organisms but specifically *D. magna* (Asghari et al., 2012, Hoheisel et al., 2012, Zhao and Wang,

2011). Generally these papers focus on classic toxicity endpoints immobilisation and reproductive output and compare AgNPs to silver ions (Ag^+). There is a consensus that AgNPs are less toxic than Ag^+ (Griffitt et al., 2012) and that nanotoxicity is particle size dependant, however, there remains much discussion as to whether AgNP toxicity is mediated by release of ions or not, and whether this dissolution occurs prior to, or following organism and cellular internalisation (Newton et al., 2013). A number of these studies exhibit insufficiencies in their experimental design, AgNPs are not always characterised fully and are often obtained from commercial sources where there may be a large spread of particle sizes including bulk particles ($> 100 \text{ nm}$) (Dhawan and Sharma, 2010). In addition to classic toxicity endpoints, some studies yielding mechanistic data have been completed. Numerous cellular effects have been reported in response to nanosilver exposure including disruption of cellular respiration, binding of RNA and DNA, disruption of both cellular and intracellular membranes and generation of reactive oxygen species (ROS) (Schluesener and Schluesener, 2013). Additionally lipid peroxidation, a down-stream effect of ROS generation, has been indicated as a toxic mechanism of action for AgNPs in numerous publications using targeted assays (Oukarroum et al., 2012, Gagne et al., 2012, McCarthy et al., 2013). Primarily composed of lipid species, cellular and intracellular membranes will be major targets for lipid peroxidation (Catala, 2012). Oxidative modifications to membrane lipids will have deleterious cellular effects increasing membrane permeability (Conte et al., 2013) and highlighting the cell to macrophages for apoptosis (Greenberg et al., 2008). Membrane function is crucial to cellular processes and as such phospholipids represent an excellent group of molecules within which to study lipid peroxidation.

1.2 - Phospholipids

The major constituent of cell membranes. phospholipids (PL) are present in all organisms (Vance and Vance, 2008). Amphipathic in nature, PLs exhibit structural variability around a glycerol backbone with two hydrophobic carbon chains and a phosphate containing 'head group' attached. Phospholipid bilayers such as those found in biological membranes are stabilised by hydrophilic polar head groups facing the aqueous media and the fatty chains forming a hydrophobic core (Tieleman and Marrink, 2006). Widely known as membrane constituents for a long period, in recent times other biological functions have come to light. The alteration of lipid membranes is a key step in apoptosis with glycerophosphatidylserine (PS) molecules translocating to the outer membrane which highlights the apoptotic cell to the macrophage for phagocytosis (Fadok et al., 2001). Additionally phospholipids act as precursors for platelet-activating factor (Honda et al., 2002), leukotrienes and prostaglandins (Pulfer and Murphy, 2003) as well as signalling molecules such as inositol triphosphate and diacylglycerols (Taylor, 2002).

1.2.1 - Phospholipid structure and nomenclature

Attached to the sn1 position of the glycerol backbone (see Figure 1-4) is a carbon chain, this can be bound via an ester, vinyl ether or ether bond to yield diacyl, plasmalogen or ether phospholipid respectively. In eukaryotic cells, the sn2 linked carbon chain is always bound as an ester (Pulfer and Murphy, 2003). The length and saturation of chains vary and are often organism specific, as general rules the sn1 chain exhibits

greater saturation and parity is usually even, although some odd chains have been identified (Bychek and Gushchina, 1999). Six major head groups are observed which are summarised in Figure 1-4.

The LIPID MAPS consortium has been leading the classification and annotation of lipid species for the past decade (Schmelzer et al., 2007, Fahy et al., 2009, Sud et al., 2007). The creation of the LIPID MAPS classification system has allowed comprehensive classification, naming and representation of lipids removing complexity of the previous systems. For example, 1-Palmitoyl-2-oleoyl-*sn*-glycero-3-phosphoethanolamine (Figure 1-5) was previously reported as POPE (Gullingsrud and Schulten, 2004), while this is an easily recognisable representation of a biologically abundant lipid, this system is ambiguous and difficult to extend to the vast range of lipids reported in lipidomic research. The LIPID MAPS naming policy follows the following structure: (*LC* (*a* : *b* (*cZ*, *dZ*....) , *e* : *f* (*gZ*, *hZ*....)), where *LC* is a short alphabetic code denoting lipid class (Figure 1-4), *a* and *b* are the number of carbons and double bonds respectively in the *sn*1 acyl chain (Figure 1-5), *c* and *d* denote double bond position and *e*-*h* are the corresponding values for the *sn*2 chain.

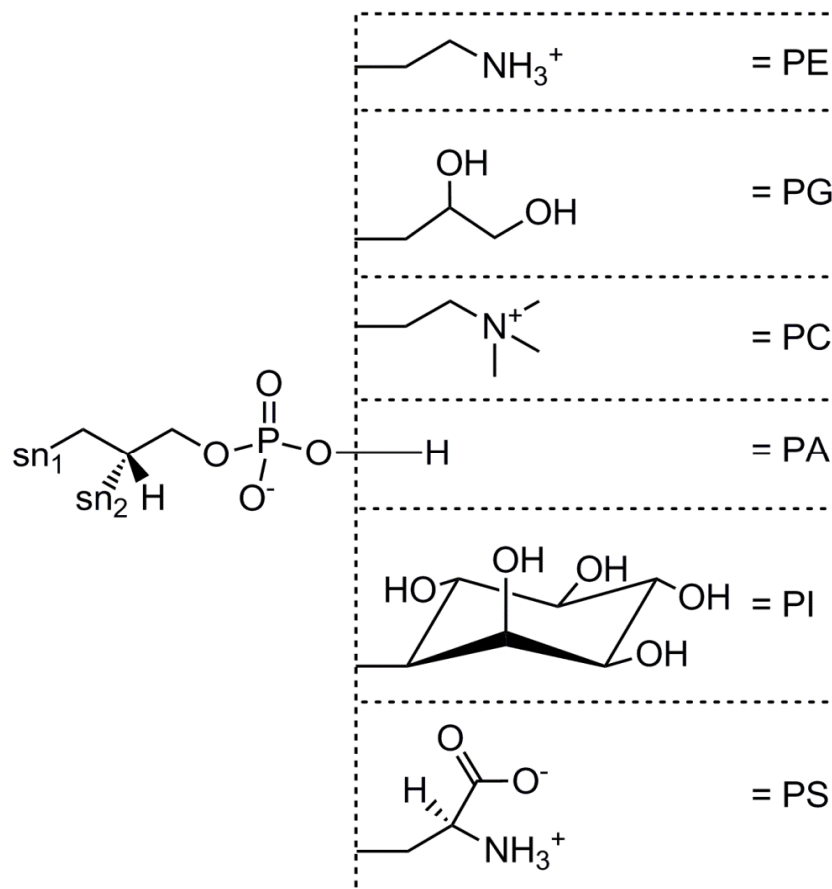


Figure 1-4 Head-group structures of major phospholipid groups with LIPID MAPS identification codes. PE = glycerophosphatidylethanolamine, PG = glycerophosphatidylglycerol, PC = glycerophosphatidylcholine, PA = glycerophosphatidic acid, PI = glycerophosphatidylinositol, PS = glycerophosphatidylserine.

Under this system POPE is renamed PE(16:0, 18:1(9Z)), a short and informative identifier which can easily be applied to all phospholipids and other lipid classes. Whilst this nomenclature is not yet universal it has been adopted by numerous scientific institutions including the Kyoto Encyclopedia of Genes and Genomes (KEGG) and will be used throughout this thesis.

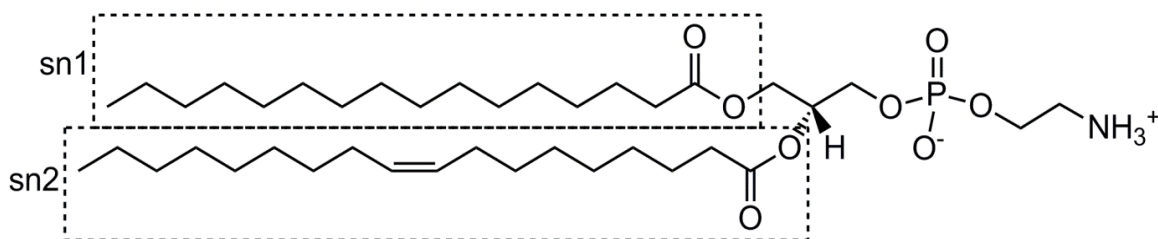


Figure 1-5 Structure of mono-unsaturated PE(16:0,18:1(9Z)), a representative glycerophosphatidylethanolamine

1.2.2 - Phospholipids in *D. magna*

There is a paucity of literature detailing the lipid make-up of *D. magna*. To my knowledge, only several studies exist, which have focussed on fatty acid content, particularly PUFAs. These are important dietary components in aquatic food webs with the suggestion that crustaceans cannot generate PUFAs such as 18:2 and 18:3. These studies used Fatty Acyl Methyl Ester (FAME) analysis to cleave and derivatise fatty acyl moieties from polar lipids e.g. PLs and glycerolipids (Masclaux et al., 2012, Bychek et al., 2005, Taipale et al., 2009). Persson et al, 2006 and Bychek et al, 2005 have published articles detailing the FA breakdown in adult *D. magna* (Figure 1-6; Figure 1-7). Whilst the ratio of saturated : monounsaturated : polyunsaturated fatty acids (SFA:MUFA:PUFA) is similar across the two studies (2.4:1.0:3.0 (Bychek et al., 2005)) vs 1.9:1.0:2.1 (Persson and Vrede, 2006)), the individual FA species are quite different, although 16:0 and 18:1 remain the most abundant SFA and MUFA respectively. The disparity in individual PUFA species abundance is likely related to diet due to the essential nature of PUFAs in *D. magna* but may also be related to genetic differences (Persson and Vrede, 2006).

Bychek et al, 2005, also identified the PL origins of these FA moieties using iodine visualised 2D-TLC compared to PL standards. These analyses identified five major PL species: PE,PC,PS,PG and PI in order of abundance. However, there has been no study detailing the composition of individual phospholipid species in *D. magna*. This thesis aims to contribute significantly to the lipid data available for *D. magna* by annotating the largest possible proportion of the lipidome.

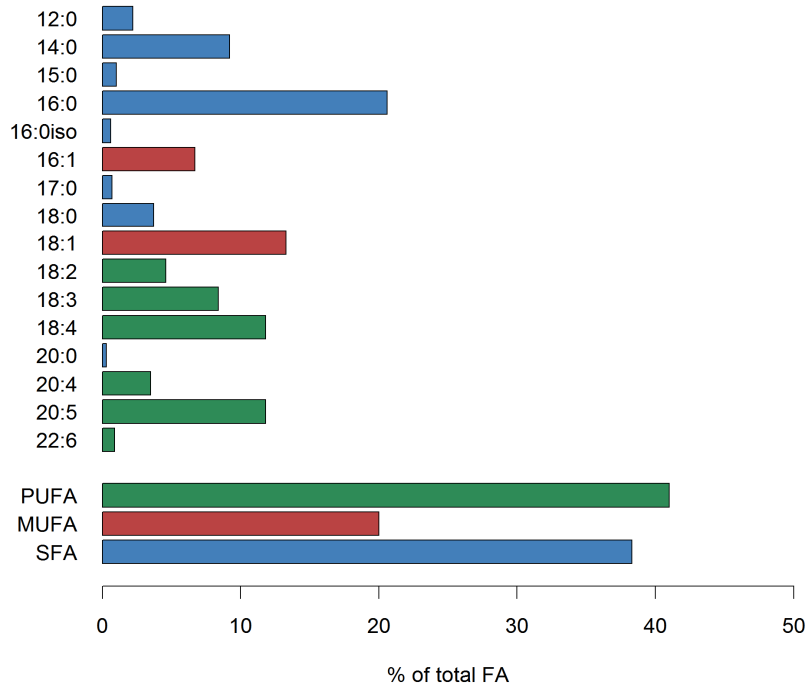


Figure 1-6 Bar chart modified from (Persson and Vrede, 2006). Shows composition of total fatty acids in *D. magna*, SFA are shown in blue, MUFA in red and PUFA in green.

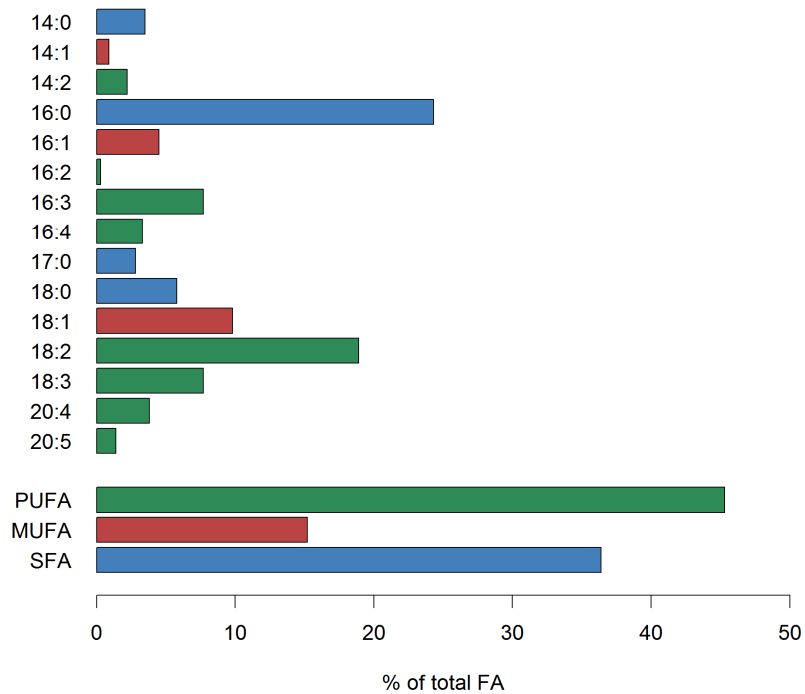


Figure 1-7 Bar chart modified from (Bychek and Gushchina, 1999). Shows composition of total fatty acids in *D. magna*, SFA are shown in blue, MUFA in red and PUFA in green.

1.2.3 - Phospholipids in *C. reinhardtii*

As mentioned above there has been a single lipidomic study published detailing the lipidome of *C. reinhardtii*, however, it is published in Chinese and as such is not discussed here. In general for *Chlamydomonas* species, the major classes of phospholipids observed are PG, PE and PI in order of abundance (Arisz et al., 2000). However, algal lipidomes contain other significant classes of polar lipids not observed in *D. magna* known as glycolipids. The first class of these galactosylglycerides are structurally similar to phospholipids, in that they contain fatty acyl chains at the sn1 and sn2 positions on a glycerol backbone. However, the phosphate containing head group is replaced by one or two galactose molecules to yield monogalactosyldiacylglycerol (MGDG) and digalactosyldiacylglycerol (DGDG) respectively. These neutral molecules can account for up to 40 % of thylakoid lipids (Guschina and Harwood, 2006). A third major glycolipid class is the sulfolipid, sulfoquinovosylgiacylglycerol (SQDG), which is MGDG with a sulfonic acid on the galactosyl head group and possessing a negative charge unlike the neutral galactosyl glycolipids. These lipids are generally highly unsaturated.

1.3 - Non-enzymatic toxic mediated lipid peroxidation

Non-enzymatic lipid peroxidation is a consequence of oxidative stress, a situation where, the concentration of reactive oxygen species has overwhelmed the cellular protective mechanisms such as antioxidants (Niki, 2008). This is a widely known mechanism of

action for a number of toxicants, including heavy metals, and is one of the major hypotheses for the toxicity of nanomaterials (Gagne et al., 2012, Vieira et al., 2009). The mechanism of non-enzymatic lipid peroxidation is well defined and maintained across *in vitro* and *in vivo* studies (Reis and Spickett, 2012). The sn1 and sn2 fatty acyl chains attached to the glycerol backbone in phospholipid species are the primary target for lipid peroxidation. Bisallylic hydrogen molecules (i.e. those bound adjacently to two double bonds along the fatty acyl chains) in PUFAs, and to a lesser extent allylic hydrogen molecules in MUFAs, are abstracted by ROS to form radical species due to their low C-H bond energies (Horton and Fairhurst, 1987). These lipid radical species react readily with molecular oxygen to yield lipid peroxy radicals and subsequently abstract a hydrogen atom to form a stable lipid hydroperoxide molecule (LOOH) (Horton and Fairhurst, 1987). The source of this stabilising hydrogen is often a second lipid molecule which will create a new lipid radical, creating a propagation cycle which can damage multiple lipids from a single radical initiator (Horton and Fairhurst, 1987). Termination occurs when two radicals react with each other, or anti-oxidant molecules intervene (Horton and Fairhurst, 1987). Lipid peroxide molecules can undergo further modifications to become, lipid hydroxides (LOH) and lipid epoxides (LO) which can follow reaction cascades down to terminal products such as aldehydes including 4-hydroxy nonenal (4-HNE), aldehydes including malondialdehyde (MDA) and conjugated dienes which have cleaved from phosphate head groups (Horton and Fairhurst, 1987). These secondary products have been widely used in the past in order to measure the occurrence of lipid peroxidation (Fan et al., 2012, Tang et al., 2011), however, as they are generic products they contain little information on the phospholipid species of origin.

In this thesis we attempt to develop MS methods capable of observing intact lipid hydroperoxides which both indicate the occurrence of lipid peroxidation and retain the structural information of the lipids undergoing modification which can lead to mechanistic insights.

The work presented within this thesis primarily involves the detection of non-enzymatic lipid peroxidation products with increasing complexity. Initially lipid peroxides are formed from individual lipid species, a very simple model, then oxidised products are formed from the lipid extracts of our model organisms (*D. magna* and *C. reinhardtii*). Finally we attempt to induce and observe lipid peroxidation *in vivo* with classic toxicants (copper sulfate (CuSO₄), silver nitrate (AgNO₃) & hydrogen peroxide (H₂O₂)) and novel AgNPs.

1.4 - The emerging role of metabolomics in ecotoxicology

1.4.1 - Environmental metabolomics

Metabolomics represents the functional terminus of the omics analysis chain. The goal of metabolomics is to observe and quantify the full complement of small endogenous molecules in a cell, tissue or whole organism (Viant, 2008). Whilst predominantly utilised to investigate human biology, in recent years environmental concerns have been increasingly studied with metabolomic analyses (Booth et al., 2011, Fiehn et al., 2008, Viant, 2008). Utilising state of the art mass spectrometry and nuclear magnetic resonance platforms, metabolomic studies can measure huge numbers of metabolites allowing both targeted monitoring of specific mechanisms of action and untargeted hypothesis generating analyses (Bundy et al., 2009). To date, the vast majority of

metabolomic studies have focussed on the smaller, polar metabolites, however, lipids contain great potential for the analysis of toxicant mechanisms of action.

1.4.2 - Lipidomics

Interest in lipid biochemistry began in earnest in the 1950s with the work of Eugene Kennedy (Kennedy, 1957). Facilitated by technological advances in Mass Spectrometry (MS) instrumentation, particularly the soft ionisation techniques Electrospray Ionisation (ESI) and Matrix Assisted Laser Desorption Ionisation (MALDI), lipidomics is now a rapidly expanding field with over 1,300 peer reviewed articles to date (WOK, 2014). Unsurprisingly, lipidomics derives its name from metabolomics and describes the analysis of the full complement of lipids within a cell, tissue or organism (Kishimoto et al., 2001). Important sub-components of the metabolome, lipids can be defined as generally hydrophobic biological substances often soluble in organic solvents (Sud et al., 2007). Intuitively this description covers a wide range of molecules with varied biological function, for example glycerolipids, well known as energy stores and glycerophospholipids, which are the focus of section 1.5, the major constituents of cellular membranes. A recent overhaul of lipid classification has defined eight sub-groups (Fahy et al., 2009): fatty acyls, glycerolipids, glycerophospholipids, sphingolipids, sterol lipids, prenol lipids, saccharolipids and polyketides. Species within these groups can vary by carbon chain length, double bond content and chain linkage chemistry to yield diverse ranges of compounds (Pulfer and Murphy, 2003).

1.4.2.1 - Lipid extraction from biological tissue

General lipid extraction is achieved with liquid-liquid phase extraction using the Bligh and Dyer or Folch methodologies (Bligh and Dyer, 1959, Folch et al., 1957). In these techniques, following cell lysis, metabolites are split into two phases based upon their affinity for the lower higher density chloroform (CHCl_3) layer or the upper lower density layer, a methanol/water ($\text{MeOH}/\text{H}_2\text{O}$) mix. Lipids are hydrophobic by definition and so are partitioned into the chloroform phase. These two methods have been used for the bulk of lipid extractions for lipidomic studies (Kosinska et al., 2013, Loizides-Mangold, 2013). However, recently lipid extraction by methyl-tert-butyl ether (MTBE) / MeOH has attracted interest (Donovan et al., 2013, Chen et al., 2013) as the lipid containing phase will be at the top due to the relatively higher density of MeOH over MTBE (Matyash et al., 2008). This avoids potential contamination of the lipid extract by remaining aqueous phase or protein layer which must be passed through for lipid phase retrieval in the CHCl_3 containing methods. Despite the contamination issue we have used the Bligh and Dyer methodology throughout this thesis as $\text{MeOH}/\text{H}_2\text{O}$ phases were used by other members of the group to assess changes in polar metabolites.

1.4.2.2 - Pre-analytical, chromatographic separation of lipids

For targeted analysis of specific lipids chromatographic techniques may be applied. Classically, Thin Layer Chromatography (TLC) was used to separate lipid classes, which has now been surpassed by Two-Dimensional High Performance TLC (2D- HPTLC) (Tyurin et al., 2008). Technological advances in separation techniques have also led to advances in lipidomic studies. For example, a variety Solid Phase Extraction (SPE)

columns exist which are capable of separating lipid classes e.g. glycerophospholipids (Perez-Palacios et al., 2007) or glycerolipids (Rizov and Doulis, 2001). Additionally, Liquid Chromatography (LC) is adept at separating both lipid classes by normal phase and specific lipid species by reversed phase based on their chain chemistry (Sommer et al., 2006). Finally, Gas Chromatography has been widely used for lipidomics particularly in the study of free and total Fatty Acid (FA) composition (Bychek and Gushchina, 1999)., however, this normally requires derivitisation of compounds to aid ionisation. For example, FAs require conversion to FAME. Whilst separation techniques can aid lipid identification, by reducing ion suppression (Annesley, 2003) from other lipids and adding meta-data such as retention time (RT), they come with an associated increase in analysis time, reducing the high throughput nature of lipidomics (Griffiths et al., 2010). For this purpose I have selected to use Direct Infusion MS (DIMS), for analytical work throughout this thesis, placing my work in the shotgun lipidomics category (Schwudke et al., 2007).

1.4.2.3 - Analytical platforms for lipidomic analysis

The major analytical platforms used for shotgun lipidomics are MS based, particularly when the MS is capable of high mass accuracy and resolution and samples are introduced via a soft ionisation technique (e.g. ESI). However, lipidomics has also been conducted using ^{31}P NMR spectroscopy (Kaffarnik et al., 2013). ^{31}P NMR has the advantage of being able to quantify phospholipid classes simply in a non-destructive manner; however, it is not capable of separating individual lipid species (Lutz and Cozzone, 2010) and as such is not utilised within this thesis.

1.4.2.3.1 - Mass spectrometry with a focus on DI nESI FT-ICR MS

MS is an analytical technique which ionises molecules, separates them based on their molecular mass and charge state, and detects them to yield a spectrum of mass/charge ratio (m/z) vs. intensity (related to abundance of the molecule). The four major components of a mass spectrometer are ion source, mass analyser, detector and data collection module (i.e. a computer) (Allwood and Goodacre, 2010). The ionisation source, creates ions from the sample for infusion into the mass spectrometer, while MALDI has also been used for lipidomic analysis, the work presented in this thesis uses ESI specifically nano-ESI (nESI, Advion). Electrical energy is used to create droplets of either positively or negatively charged ions which are subsequently evaporated and passed into the MS (Bruins, 1998). Molecular structure and sample matrix define how a compound will ionise, for example glycerophosphatidylcholines (PC) will readily form positive adducts such as protonated ($[M+H]^+$) (Murphy et al., 2001) or metal adducts ($[M+Na]^+$ and $[M+K]^+$) etc. due to their positively charged head group. PCs will not form deprotonated ions ($[M-H]^-$) and so are absent in negative mass spectra of lipid extracts, however, if the modifying agent ammonium acetate is added to the lipid extract PC molecules will be observed in negative spectra as acetate adducts ($[M+Ac]^-$).

Infused ions are then mass analysed. For top down shotgun lipidomics, high mass accuracy and resolution are required, leading primarily to the use of Fourier Transform Ion Cyclotron Resonance (FT-ICR) and Orbitrap mass analysers (Loizides-Mangold, 2013). The instrument used to acquire data within this thesis was a LTQ FT Ultra, a hybrid machine combining a linear ion trap (LTQ) and a High Resolution Fourier Transform MS (HR FT MS). Following ESI, the LTQ is used to regulate the number of

ions passing into the FT-ICR MS via an Automatic Gain Control (AGC) and can also be used to select specific ions of interest. After transition from the LTQ, ions are trapped in the ICR cell by a strong magnetic field, before excitation electrodes induce ions into radial motion dependant on their m/z . Finally detector plates record the charge of proximal groups of ions as a function of time and Fourier Transform is used to deconvolute signals into frequencies which are proportional to the m/z value of the ions. This detection methodology allows low mass error and extremely high peak resolution (<1 ppm and > 1,000,000 respectively). Mass error is the difference between the theoretical m/z and the observed m/z in a spectrum, normalised to the m/z (Equation 1-1). Where M is the m/z value of the peak and ΔM is the difference between the experimental m/z and the theoretical m/z .

Equation 1-1 Mass error equation

$$\text{Mass Error}_{(ppm)} = \frac{\Delta M}{M} \times 1,000,000$$

Mass resolution defines the ability to distinguish two peaks with similar m/z values and is defined by equation 1-2. Where M is the m/z value of the peak and ΔM is the Full Width of the peak at Half the Maximum peak intensity (FWHM).

Equation 1-2 Resolution equation

$$R = \frac{M}{\Delta M}$$

1.4.2.4 - Statistical analyses in metabolomic studies

The datasets produced by mass-spectrometric lipidomic studies are large with many hundreds of spectral features observed in many tens of sample numbers. In order to visualise this amount of data into a comprehensible format multivariate analysis is required. Throughout this thesis Principal Component Analysis (PCA) is used as an unsupervised method to highlight the mass spectral features most discriminating between treatment groups (Dettmer et al., 2007). PCA visualises the variation within a dataset and generates axes to visualise this where principal component 1 (PC1) contains the maximal variance and each subsequent axis the maximal variance remaining. A score is generated for each sample based upon its position along respective PC axes. Significant separation between treatment groups can be determined by performing a Student's t-test or (ANalysis Of VAriance) ANOVA on the PC scores for each group.

Univariate statistics can also be useful to identify the molecules of importance between groups. T-test and ANOVA were used to assess the significance of peak intensity changes across treatment groups. With large datasets however, the False Discovery Rate (FDR) will lead to a large number of erroneous significantly changing peaks. To account for this a Benjamini-Hochberg correction is applied creating adjusted p -values based on the number of calculations which can be used to determine significance more robustly (Benjamini and Hochberg, 1995).

1.4.2.5 - Identification of metabolites

Identification of the complex m/z profiles which derive from mass spectrometry metabolomic studies is one of the major challenges facing the community but crucial in order to draw biologically relevant conclusions (Breitling et al., 2008). (Sumner et al., 2007) have outlined criteria for the identification of spectral features with four levels of rigour. Level four contains the least information with features being identified only by analytical data. Level three contains putatively characterised compound classes based on characteristic physicochemical properties of a class of compounds. Level two contains putatively annotated compounds where physicochemical properties have been used to match features to spectral libraries and a compound name has been assigned. Level one contains identified compounds, the most comprehensive identification, which requires two independent and orthogonal analyses compared to identical measurements made on an authentic reference compound. In the case of MS lipidomic study, an unidentified m/z value would be a level four unknown, solubility in chloroform could add level three assignment as a putatively characterized lipid, matching the m/z value against a compound in the Lipid Metabolites and Pathways Strategy (LipidMAPS) database, discussed below, would increase the confidence to a level two putative annotation and the addition of tandem MS and retention time from LC information matched to reference libraries would increase the assignment to a level one identified compound.

Despite the relatively recent interest in lipidomics, there are an abundance of tools designed to aid the identification of lipids. The LipidMAPS consortium has a suite of online tools which can match mass spectra to their database of glycerolipids and

glycerophospholipids within a given ppm error range (LipidMAPS, 2014). In addition to this, there exist numerous freely available software packages which utilise MS and MS/MS data to identify lipids. These include LipidQA (Washington University, 2013), LipidView (AB Sciex, 2006), LIMSA (University of Helsinki, 2006), FAAT (UC Davis, 2006), LipidAT (Indiana University, 2009), SimLipid (Premier Biosoft, 2010), LipidomeDB (University of Kansas, 2011), etc.. All of these tools use accurate m/z measurements and / or data-dependant fragmentation data to annotate or identify the lipids present in a mass spectrum by matching them to databases. The major limiting factor for these tools is the content of their associated lipid database. LipidMAPS have the most comprehensive experimental lipid database, however, there are many lipid species which are not included in the database, or do not cover a broad range of chain chemistries. To improve on this situation Kind et al., 2013 have generated LipidBlast which takes the LipidMAPS database and expands it with *in silico* methods to yield a fragmentation database of some 119,200 lipid compounds. LipidBlast is used throughout this thesis for automated annotation of fragmentation patterns. For putative annotation of spectral features, the LipidMAPS database is used, however, as the online LipidMAPS tools are time-consuming and limited in flexibility, the MI-Pack software package was used to match experimental spectral features to ionic forms of database entries.

1.5 - Aim and objectives

The aim of this thesis is to explore peroxidation of biologically relevant lipids, from *in vitro* studies, through to aquatic *in vivo* studies in response to classic and novel toxicants.

1. Generate phospholipid oxidation products *in vitro* and identify them with tandem mass spectrometry (Chapter 3).
2. Optimise direct-infusion mass spectrometric methods to observe and annotate the lipidome of *D. magna* and *C. reinhardtii* (Chapter 4).
3. Oxidise lipidomes of *D. magna* and *C. reinhardtii* both *in vitro* and *in vivo* using hydrogen peroxide, silver nitrate and copper sulfate (Chapter 5).
4. Optimise conditions for *D. magna* silver nanoparticle exposures and assess nanoparticle perturbation of the lipidome (Chapter 6).

2 - Materials and methods

Methods presented in this chapter are those used in multiple chapters within this thesis. All *D. magna* used within this thesis were cultured with the conditions outlined in section 2.2 - and exposed with the methodologies outlined in sections 2.3 and 2.4 for acute toxicity assessment and lipidomic analysis respectively. The workflow outlined in section 2.4 was used for all lipidomic analyses in chapters 4 and 5. Materials and methods used only within a single chapter are detailed therein.

2.1 - Chemicals

All chemicals were obtained from Sigma-Aldrich Co. (UK) unless otherwise stated.

2.2 - Culturing of *Daphnia magna*

All *D. magna* used to complete *in vivo* experimental work presented in this thesis originated from a strain which was obtained from the University of Reading six years ago (2007) and cultured continuously since then under constant conditions recommended by the OECD (OECD, 2004). Modified OECD media was used to maintain each strain at a density of 20 organisms per 1.2 l media (section 2.2.1 -). Both strains received a diet of a suspension of *Chlorella vulgaris* cells (green algae); a solution of *Saccharomyces cerevisiae* (baker's yeast) and extract of *Ascophyllum nodosum* (seaweed) (Marinure, Wilfrid-Smith Ltd, UK) (section 2.2.2 -). Culture beakers were maintained under a light : dark cycle (16:8 h) at constant temperature (20 °C ±1) for a period of 14 days, allowing several reproductive broods for exposure studies before colonies were restarted with neonates (<24 h).

2.2.1 - OECD modified media preparation for culturing of *Daphnia magna*

Concentrated stock solutions were prepared by addition of salts to DI water, then further diluted to yield OECD modified media as required. Aerated media (>24 h) was used for the initiation of cultures and subsequent semi-weekly media changes for the duration of the colony. OECD modified media was prepared by the addition of sodium selenite (Keating and Dagbusan, 1984) to OECD ISO test media for exposure of *D. magna* (see Table 2-1) (OECD, 2004). Media pH was measured and adjusted with hydrochloric acid (HCl) or sodium hydroxide (NaOH) to the designated range (pH = 6-9).

Table 2-1 Composition of OECD modified media

| Compound | Empirical formulae | Stock conc. (mg/l) | Final conc. (mg/l) |
|--------------------|--------------------------------------|--------------------|--------------------|
| Calcium chloride | CaCl ₂ .2H ₂ O | 11760 | 294 |
| Magnesium sulfate | MgSO ₄ .7H ₂ O | 4930 | 123.25 |
| Sodium bicarbonate | NaHCO ₃ | 2590 | 64.75 |
| Potassium chloride | KCl | 230 | 5.75 |
| Sodium selenite | Na ₂ SeO ₃ | 40 | 0.002 |

2.2.2 - Supplement preparation and regimen

2.2.2.1 - *Chlorella vulgaris*

C. vulgaris, for use as *D. magna* feed, was cultured under semi-static sterile conditions in Bold's basal medium (BBM) (Bold, 1949) (pH 6.7 ± 0.3) (Table 2-2) under constant photosynthetic light and aeration. Replacement BBM was prepared from dissolved stocks and autoclaved prior to use.

Table 2-2 Composition of Bold's basal medium (BBM)

| Compound | Empirical formulae | Stock conc. (mg/l) | Final conc. (mg/l) |
|---|--------------------------------------|--------------------|--------------------|
| di-Potassium hydrogen orthophosphate | K ₂ HPO ₄ | 7500 | 75 |
| Potassium di-hydrogen orthophosphate | KH ₂ PO ₄ | 17500 | 175 |
| Magnesium sulfate | MgSO ₄ .7H ₂ O | 7500 | 75 |
| Sodium nitrate | NaNO ₃ | 25000 | 250 |
| Calcium chloride | CaCl ₂ .2H ₂ O | 2500 | 25 |
| Sodium chloride | NaCl | 2500 | 25 |
| EDTA tetrasodium salt | EDTA - Na ₄ | 50000 | 50 |
| & Potassium hydroxide | KOH | 31000 | 31 |
| Iron(II) sulfate & Sulfuric acid (0.1%) | FeSO ₄ .7H ₂ O | 4980 | 4.98 |
| Boric acid | H ₃ BO ₃ | 11420 | 11.42 |
| Zinc sulfate | ZnSO ₄ .7H ₂ O | 14120 | 1.412 |
| Manganese chloride | MnCl ₂ .4H ₂ O | 2320 | 0.232 |
| Cupric sulfate | CuSO ₄ .5H ₂ O | 2520 | 0.252 |

Optical density (A_{440nm}) of a ten-fold dilution of the algal suspension was used to ensure consistent cell density in feed. Retrieved algae was centrifuged (3000 rpm, 30 min), before the supernatant was discarded and the pellet re-suspended in the appropriate volume of DI water to yield the desired optical density ($A_{440nm} = 0.8$, Equation 2-1).

Equation 2-1 Equation to calculate required algal re-suspension volume

$$\frac{A_{440nm}(original) \times Vol (original)}{0.800} = Vol (resuspension)$$

D. magna were fed daily with set volumes of algal feed per culture beaker, increasing with age (1-2 d = 1 ml, 3-7 d = 1.5 ml, 8+ d = 2 ml). Algal feed was discarded if unused 14 days after removal from culture vessels.

2.2.2.2 - Baker's yeast

S. cerevisiae was suspended in deionised DI water (10 mg/100 ml) and stirred magnetically until dissolution was achieved (ca. 1 h). *D. magna* were fed daily with 0.5 ml solution per culture vessel. This solution was replaced every 14 days.

2.2.2.3 - Marinure

Marinure, a concentrated extract of the seaweed *Ascophyllum nodosum* was diluted approximately 100-fold with DI water to yield a stock with desired optical density when diluted an additional ten-fold ($A_{400nm} = 0.8 \pm 5\%$). The working stock was added to all fresh media at an organism, age-dependant volume (1-7 d = 3 ml, 8+ d = 4 ml). The stock solution was replaced at least every six months.

2.3 - Acute toxicity assessment

2.3.1 - Exposures

Immobilisation of *D. magna* was used to assess acute toxicity in accordance with OECD guidelines (OECD, 2004). Typically, *D. magna* neonates (<24 h) were exposed in groups to at least five toxicant doses alongside relevant controls to rule out background stress. Neonates were pooled from culture beakers into clean media and then split equally into exposure vessels containing clean media (200 ml). Exposure density was maximised with organism availability, ideally at least 10 animals per vessel were exposed with replication of $n=3$. Appropriate toxicant volumes were added to exposure vessels followed by a further aliquot of clean media (50ml) to aid chemical dispersal. Neonate immobilisation, defined as an inability of the organism to self-propel after gentle agitation (OECD, 2004), was assessed

visually after 24 and 48 hours. No supplements were administered during the exposure period.

2.3.2 - EC₅₀ calculation

The concentration predicted to immobilise 50% of a population of *D. magna* (EC₅₀) over a set timescale was estimated using the trimmed Spearman-Kärber (TSK) method (Hamilton et al., 1977). Prior to the estimation of the EC₅₀ any adjacent pairs of non-monotonically increasing immobilisation proportions were set to the mean of the pair. Should data not include dose groups with zero and dose groups with total immobilisation a trim was applied at the minimum value greater than immobilisation in the lowest dose and remaining mobility in the highest dose. The Spearman-Kärber equation (Equation 2-2) is then used to calculate the EC₅₀ where k is the number of doses, $p(i)$ is the smoothed and trimmed immobilised fraction at dose i and $x(i)$ is the natural log of the dose i .

Equation 2-2 Spearman-Kärber equation for calculation of EC₅₀

$$EC_{50} = \exp \left(\sum_{i=1}^{k-1} \left((p(i+1) - p(i)) \cdot \left(\frac{x(i) + x(i+1)}{2} \right) \right) \right)$$

2.4 - General workflow to obtain, analyse and process shotgun lipidomic samples

All lipidomic datasets presented in this thesis were achieved via a standard workflow in which *D. magna* were exposed to toxicants and flash frozen before homogenisation and lipid extraction. Lipid extracts were analysed by Direct Infusion Fourier-Transform Ion Cyclotron Resonance mass spectrometry (DI FT-ICR MS)

without any prior separation. Data was processed along the previously described Selective Ion Monitoring (SIM)-stitch methodology (Southam et al., 2007, Payne et al., 2009, Weber et al., 2011) before uni- and multi-variate statistical analysis to discern lipid concentration changes across dosed groups.

2.4.1 - Exposures

Exposures for lipid extraction had similar protocols to acute toxicity testing (see section 2.3.1 -). Exposure density was increased to 30 neonates per vessel in order to maximise lipid concentrations whilst maintaining study feasibility. Replication of dose groups varied between studies due to neonate availability in conjunction with the number of dosing groups, but minimally n=6 was used. Results from acute toxicity studies were used to identify sub-lethal doses for 24 and 48 h exposures. Following the exposure period, organisms were removed from solution with a fine mesh filter (0.2 µm), transferred to ceramic bead containing homogenisation tubes (Precellys, Stretton Scientific Ltd., UK) and flash frozen in liquid nitrogen. Frozen tissue samples were stored at -80 °C prior to biphasic extraction.

2.4.2 - Metabolite extraction

Bligh and Dyer, biphasic extraction was used to obtain hydrophilic (polar) and hydrophobic (lipid) fractions from frozen tissue and at least one homogenisation tube empty of biological material, an extract blank, as described previously (Bligh and Dyer, 1959, Wu et al., 2008). All solvents were HPLC grade and kept on ice, where possible, to reduce evaporation. Methanol (MeOH, 320 µl, Fisher Scientific, UK) and water (H₂O, 128µl, J.T. Baker) were added to each sample tube before

homogenisation (Precellys 24 homogeniser, 6400rpm, 2 x 10s). The homogenate was transferred to a glass vial (glass Pasteur pipette) with a second aliquot of water (160 μ l) and chloroform (320 μ l), all transfer of chloroform was via a glass syringe (Hamilton, UK) with metal plunger unless stated otherwise. Samples were vortex mixed (30 s) and allowed to separate (10 min) before centrifugation (10 min, 4000 rpm, 4 $^{\circ}$ C) yielded two well defined phases separated by a thin disc of protein. The majority of the upper MeOH:H₂O layer (300 μ l), containing the more polar molecules, was transferred to a micro test tube (Eppendorf, Germany) via glass syringe, washed thrice between samples to avoid cross contamination, and dried using vacuum centrifugation (3 h, 40 $^{\circ}$ C). Similarly, the lower CHCl₃ layer (200 μ l), containing hydrophobic compounds, was removed to a glass tube, avoiding disturbance of the protein layer as the syringe slid past. In contrast to the polar layer, CHCl₃ was removed under anoxic conditions in a nitrogen blow down sample concentrator (Techne, Bibby Scientific, UK) to reduce oxidative artefacts. All dried samples were stored at -80 $^{\circ}$ C until re-suspension for mass spectrometric analysis. The main focus of this thesis is the molecular contents of the chloroform fraction resulting from this biphasic extraction, however, the polar phase was utilised for chapter 5 where Alex Gavin took it forward for polar metabolomics analysis.

2.4.3 - Fourier transform ion cyclotron resonance mass spectrometry

2.4.3.1 - Sample preparation for mass spectrometry

Dried lipid residues were dissolved on ice in re-suspension solution for negative ion analysis (MeOH:CHCl₃, 2:1 w. ammonium acetate (5 mM), 50 μ l). Samples were vortex mixed and centrifuged (10 min, 4000 rpm, 4 $^{\circ}$ C) to remove solid contaminants.

A 384-well polymerase chain reaction (PCR) plate (ABgene, Thermo Fisher Scientific, USA) was placed on ice (10 min) before sample aliquots (6 μ l) were transferred by manual pipette in quadruplicate to individual wells with carbon pipette tips (Advion, USA) and immediately covered with strips of self-adhesive foil. Following completion of sample transfer, the self-adhesive strips were replaced by a single heat sealed foil sheet (ALPS 50V, Thermo Fisher Scientific, US).

2.4.3.2 - Acquisition of mass spectra

Samples were delivered to a hybrid 7-Tesla linear ion trap FT-ICR mass spectrometer with no prior separation via a nESI source (Advion, UK) in negative ion mode with settings maintained across all DIMS lipidomic studies as shown in Table 2-4.

Table 2-3 Electrospray ionisation settings for shotgun lipidomics.

| Parameter | Setting |
|--------------------------|----------|
| Sample volume (μ l) | 4 |
| Delivery time (s) | 210 |
| Gas pressure (psi) | 0.6 |
| Spray voltage (kV) | 1.7 |
| Polarity | Negative |

FT-ICR MS analysis was conducted in such a way to allow data processing by the previously reported SIM-stitch methodology, optimised for analysis of polar fractions (Weber et al., 2011, Payne et al., 2009, Southam et al., 2007). Mass spectra were collected as transients across the available range (70-2000 m/z) in ten, “wide-SIM” windows overlapping by 30 m/z . Shotgun lipidomic mass spectra of *D. magna* in negative ion mode show peaks predominantly between 600 and 900 m/z and, as such, windows in this region were 100 m/z wide, which was reported as optimal for this instrumental set up (Weber et al., 2011). Windows outside this range were

widened to avoid underfill, a scenario where too few ions are collected during the acquisition time leading to unreliable peak intensities (Figure 2-1). Order of sample analysis was randomised to avoid confusion between analysis drift and treatment effects, however, the four technical replicates were measured consecutively. Mass spectrometry parameters are summarised in Table 2-4.

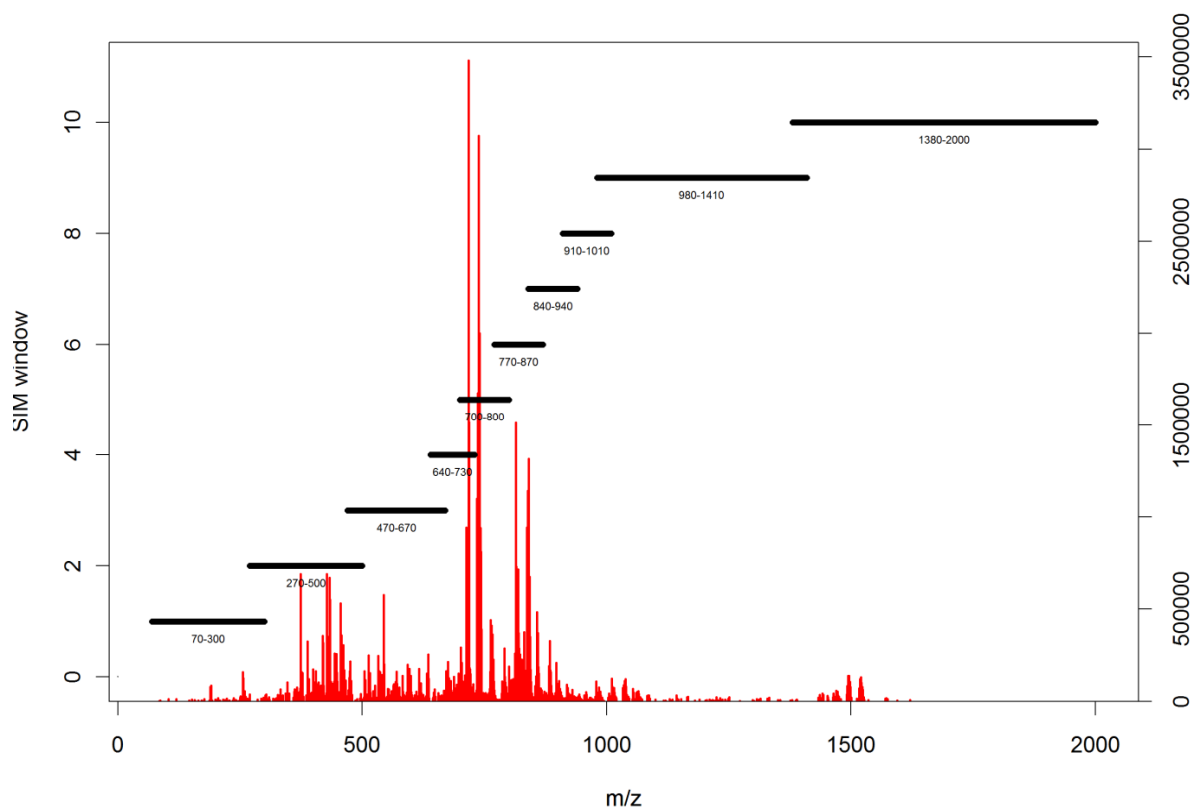


Figure 2-1 SIM-windows used during FT-ICR MS analysis. A typical post-processing spectrum from *D. magna* lipid extract is shown in red with SIM-windows shown in black.

Table 2-4 Mass spectrometry settings

| Parameter | Setting |
|-----------------------------|--------------------|
| Scan mode | Wide SIM |
| AGC target | 1×10^6 |
| Resolution | 100,000 |
| Window width (Da) | Variable (100-620) |
| Range (<i>m/z</i>) | 70-2000 |
| No. of windows | 10 |
| Acquisition delay (s) | 60 |
| Window acquisition time (s) | 15 |
| Acquisition time (s) | 210 |

2.4.4 - Processing mass spectral data to increase reliability and allow statistical analysis

An intensity matrix with rows and columns, corresponding to samples and m/z values of spectral features respectively, was produced along the SIM-stitch workflow (Payne et al., 2009). Briefly, transients were averaged, transformed into spectra with Fast Fourier Transform (FFT) (Comisarow and Melka, 1979) and calibrated using a list of defined spectral features (developed in chapter 4) for each SIM window. Calibrated SIM windows were 'stitched' together via alignment of peaks in overlapping (30 Da) windows to yield a single spectrum for each replicate of peaks above a selected signal-to-noise ratio (SNR = 10) with regularly observed 'high noise regions' removed ($m/z = (74.05-74.2); (90.50-90.58), (101.32-101.42); (101.6-102.1); (105.1-105.5);$ and $(116.37-116.5)$). Three spectra per sample were selected for further processing, allowing removal of low quality spectra, based on spray stability, total ion current (TIC) profile shape and file size. Spectral reliability was enhanced using a three-step filtering process. A replicate filter combined triplicate spectra, retaining only peaks present in a set fraction of the spectra (RF = 2/3) within a parts per million (ppm) error range (< 2 ppm), yielding a single robust spectrum for each exposure vessel. A blank filter then removed peaks with intensities less than 10-fold above that in the extract blank as these were considered to be artefacts of the extraction procedure. Finally a sample filter removed those peaks not present in 85 % of a single dosing group; previously, this was performed on the whole dataset irrespective of sample treatment, however, this could result in the loss of peaks which are only being observed in a single group which is the expected scenario for lipid peroxides (Weber et al., 2011). The intensity matrix produced requires further processing to allow

statistical analyses. Probable quotient normalisation (PQN) used intensities of ubiquitous peaks to remove variation arising from unavoidable sample concentration differences (Dieterle et al., 2006). Quotients of intensity over mean intensity across all spectra were calculated for each peak present in 100 % of samples, the median of all quotients within a SIM-window was defined as the most probable quotient and used to normalise all peaks within that window. Missing intensity values occurred in the matrix where the no mass feature of sufficient intensity and reproducibility was detected at the specified m/z for a particular sample. To avoid hugely exaggerated fold changes, these missing values were replaced with the minimum intensity from the matrix, representing a minimum detection level. Finally, multivariate statistics can be dominated by more intense peaks with intrinsically higher variation, to counter this and reduce technical variation the dataset underwent generalised logarithm (glog) transformation (Purohit et al., 2004). Glog involves a transformation parameter (λ), calibrated on a subset of data containing only technical variation, being applied to the whole dataset, emphasising biological variation in the subsequent multivariate statistical analyses.

2.4.5 - Putative metabolite identification

Column headers of processed data matrices represented accurate m/z values of measured ionic species arising from the lipid extract of *D. magna* homogenate. A peak list with associated mean intensities was input into MI-Pack software (Weber and Viant, 2010) which has previously been used in conjunction with the Kyoto Encyclopedia of Genes and Genomes (KEGG) LIGAND database to putatively identify polar metabolites in *D. magna* (Taylor et al., 2009). MI-Pack (v2 beta)

incorporates the database from the lipid metabolites and pathways strategy (LIPID MAPS) allowing increased annotation of apolar metabolite extracts (Fahy et al., 2009). In brief, MI-Pack calculated accurate m/z values for probable negative ions ($[M-H]^-$, $[M+35Cl]^-$, $[M+37Cl]^-$, $[M+Acetate(Ac)]^-$, $[M+K-2H]^-$, $[M+Na-2H]^-$) of all compounds in KEGG LIGAND and LIPID MAPS databases and assigned these to any peaks within a set ppm error range (<2 ppm).

2.4.6 - Statistical analysis of lipidomic spectra

2.4.6.1 - Univariate comparison of individual spectral feature intensities

Univariate statistics were applied to all pre-glog lipidomic datasets presented in this thesis as discussed in chapter 1. Student's t-test or ANOVA were used to identify statistically significant fold-changes from control to treated in single- and multi-dose experiments respectively. Due to the high number of fold changes being assessed large FDR of significance require control, as such, P-values were modified using a sequential Bonferroni-type procedure reported previously (Benjamini and Hochberg, 1995).

2.4.6.2 - Multivariate comparison of spectral feature intensities

PCA was used as an unbiased method to highlight the peaks most discriminating between treatment groups. All PCA models within this thesis contain six principal components and were created by the PLS toolbox (Eigenvector research, USA) in the MATLAB environment (Mathworks, USA). ANOVA or t-test of mean intragroup PC score was used to assess significance of group separation.

3 - In vitro oxidation of lipid standards for creation of OxyLipidBlast database tool

3.1 - Introduction

Lipid peroxidation is a well documented consequence of oxidative stress as described in Chapter 1. Short chain terminal products such as MDA and 4-HNE have been widely utilised as markers of lipid peroxidation in environmental toxicological testing, however, they offer no insight into the initial peroxidation target, so provide little mechanistic information (Gutteridge, 1986, Draper et al., 1993). Lipid peroxides, stable intermediary products in the reaction cascade (Moore and Roberts, 1998, Pryor and Castle, 1984), represent attractive markers for the oxidation of specific lipids and lipid classes, primarily as they maintain the lipid skeleton allowing greater insight into toxic mechanisms. Knowledge of the lipid classes which have been oxidised can potentially yield information on the organism or cellular location of the oxidation. For example PE species are known to exist primarily in the cytosolic layer of membranes (Bishop and Bell, 1988) and as such, oxidation of these may indicate intracellular oxidation while PC species are known to exist in the external membrane layer and so oxidation of these may indicate extracellular oxidative insult.

Identification of phospholipid species by m/z value alone can only putatively annotate lipid species (e.g. PE(36:1)) (Sumner et al., 2007), however, false positives will also be identified due to both isomeric overlap (e.g. PC(33:1)) and compounds of similar mass. The confidence in accurate (level 4) metabolite identification can be significantly enhanced by fragmentation information, MS² can yield head group information (e.g. PE), chain lengths (18:1, 18:0) and potentially chain position (sn1 /

sn2) (Murphy et al., 2001). For unambiguous lipid identification including double bond position and structural conformation, further analyses are required such as MS³ or selective reduction of the double bond such as the ozonolysis published previously (Thomas et al., 2006). The major classes of phospholipids have well defined MS² fragmentation patterns (Pulfer and Murphy, 2003) with chain chemistry information prevalent in negative ion mode (Khalil et al., 2010). While lipid oxidation products such as lipid peroxides have been identified and fragmented (Domingues et al., 2008), to my knowledge there has been no systematic study to date and there is no tool for the automated identification of these compounds. A hurdle for a study of this type is the lack of availability of lipid peroxide standards.

Here I address this limitation. Specifically this chapter describes my research to generate and identify lipid peroxidation products in order to observe systematic fragmentation patterns of oxidised lipids. Then, as part of a collaboration with Dr Tobias Kind at the University of California, Davis, these analytical measurements are used to generate an in silico oxidised lipid fragmentation database for integration into the LipidBlast tool for automated identification of lipid species (Kind et al., 2013). For the “wet lab” component of this collaboration at the University of Birmingham, seven species of PE were oxidised in vitro before applying FT-ICR mass spectrometry and LTQ ion trap mass spectrometry to yield accurate mass and fragmentation information, respectively, for all parent lipid species and oxidised products. The PE lipid class was selected because, in contrast to the other phospholipid classes, they ionise successfully in both positive and negative mode, allowing full characterisation of any oxidised products.

3.2 - Materials and methods

3.2.1 - Molecular structure of PE lipid standards

Isolated PE standards were purchased from Avanti lipids to cover a range of chain chemistries (Table 3-1): saturated - PE(14:0,14:0); monounsaturated - PE(16:0,18:1); polyunsaturated - PE(18:1,18:1) and PE(18:0,20:4); lyso - PE(14:0,0:0) and PE(18:1,0:0); and finally plasmalogen - PE(P-18, 18:1) (Purity>99%). All the fatty acyl chains contained within these PE species and the general lipid class have been identified previously in *D. magna* indicating these lipids are relevant to biological studies undertaken later in this thesis (Bychek et al., 2005, Persson and Vrede, 2006).

Table 3-1 Table detailing the PE standards used for oxidation, with chain chemistry, formula and neutral mass (Da).

| Lipid | sn1 chain | sn2 chain | Formula | Neutral mass (Da) |
|----------------|-----------|----------------------|---|-------------------|
| PE(14:0,0:0) | 14:0 | 0:0 | C ₁₉ H ₄₀ NO ₇ P | 425.25424 |
| PE(18:1,0:0) | 18:1(9Z) | 0:0 | C ₂₃ H ₄₆ NO ₇ P | 479.30119 |
| PE(14:0,14:0) | 14:0 | 14:0 | C ₃₃ H ₆₆ NO ₈ P | 635.45261 |
| PE(16:0,18:1) | 16:0 | 18:1(9Z) | C ₃₉ H ₇₆ NO ₈ P | 717.53086 |
| PE(P-18, 18:0) | P-18 | 18:1 | C ₄₁ H ₈₀ NO ₇ P | 729.56724 |
| PE(16:0,20:4) | 16:0 | 20:4(5Z,8Z,11Z,14Z)) | C ₄₁ H ₇₄ NO ₈ P | 739.51521 |
| PE(18:1,18:1) | 18:1(9Z) | 18:1(9Z) | C ₄₁ H ₇₈ NO ₈ P | 743.54651 |

3.2.2 - Oxidation of PE species

Chloroform was removed from PE standards under N₂, before residues were resuspended in sodium phosphate buffer solution (pH 7.4, 50 mM) with vortex spinning and sonication to yield 0.5 mM PE solutions (0.54 ml) containing crude liposomes. Samples were heated in an oven (38 °C) for 48 h, to aid oxidation, before the lipids and oxidised products were extracted using the modified biphasic Bligh and Dyer method (Bligh and Dyer, 1959). Ice cold MeOH (0.6 ml) and CHCl₃ (0.6 ml)

were added to the vials with vortex mixing, separated on ice (10 min) and centrifuged (4000 rpm, 15 min). The chloroform fraction was removed to a clean vial via glass syringe, dried under N₂ and stored at -80 °C until MS analysis. PE(16:0,18:1) was additionally oxidised for 24, 72 and 96 hours.

3.2.3 - Analysis of lipid species and oxidised products by FT-ICR and LTQ IT mass spectrometry.

Oxidised lipid residues were re-suspended in MeOH:CHCl₃ (3:1, 3 ml) and directly infused into the FT-ICR MS via nESI in both positive and negative ion modes. Data-dependant spectra of each oxidised sample were collected for two minutes. Scan 1 was collected in the FT-ICR MS with a resolution of 100,000, an AGC target of 200,000 and *m/z* range of 140 to 1600, and the top 4 most abundant mass features were fragmented by collision induced dissociation and recorded in the LTQ MS, yielding scans 2-5 (settings detailed in Table 3-2). Following multiple scans, mass features were added to an exclusion list to ensure maximum fragmentation coverage of the spectra.

Table 3-2 Mass spectrometry settings for data-dependant acquisition.

| Scan no. | Mass spectrometer | Fragmentation | Settings |
|----------|-------------------|-----------------------------|---|
| 1 | FT-ICR | None | Resolution = 100000 AGC = 200000 |
| 2 | LTQ-IT | 1 st intense ion | Isolation width = 1Da Activation Q = 0.25 Activation time = 30ms Collision energy = 33eV |
| 3 | | 2 nd intense ion | |
| 4 | | 3 rd intense ion | |
| 5 | | 4 th intense ion | |

3.2.4 - Peak assignment

Accurate mass data from the FT-ICR was used to putatively identify peaks with mass error cut-off <1ppm. MI-Pack (Weber and Viant, 2010) matched m/z values against the LIPID MAPS phospholipid database (Sud et al., 2007) to ascertain which adducts of the unmodified lipids were present. Putative modifications to the original lipid were identified using the Xcalibur formula generator.

Fragmentation spectra of unmodified lipids were matched to known fragmentation methods published previously (Pulfer and Murphy, 2003). In the absence of reference spectra, over 100 fragmentation spectra of modified lipids were manually assessed for fragmentation annotated with reference to the unmodified lipid, the modifications observed and fragmentation spectra of oxidised PC reported previously (Domingues et al., 2008).

3.2.5 - Creation of OxyLipidBlast conducted by Dr. Tobias Kind (UC Davis)

The fragmentation data discussed in section 3.3.2 - are being integrated into the LipidBlast database package to create OxyLipidBlast, an *in silico* generated database of oxidised PE lipids. The first phase is complete and a database of oxidised [PE-H]⁻ fragmentation patterns has been created. The primary fragments of deprotonated PE ions in negative ion mode are carboxylate anions of radyl chains, assuming they are ester bound to the lipid. The primary fragments from deprotonated oxidised PE ions in negative ion mode are carboxylate anions of the radyl chains plus neutral addition of oxygen molecules. For example [PE+O-H]⁻ will have major fragments of [FA₁+O-H]⁻ & [FA₂-H]⁻ or [FA₁-H]⁻ & [FA₂+O-H]⁻. [PE+O₂-H]⁻ could have fragments of [FA₁+O₂-H]⁻ & [FA₂-H]⁻, [FA₁+O-H]⁻ & [FA₂+O-H]⁻ or [FA₁-H]⁻ & [FA₂+O₂-H]⁻. These

species will also be observed as both keto and carboxylate neutral losses and finally a loss of H₂O is observed. The first version of OxyLipidBlast contains the most likely oxygen additions (up to seven) for all theoretically possible diacyl PE species yielding a database of 48,205 spectra. These spectra contain theoretical carboxylate ions of radical chains, neutral losses of these and losses of H₂O.

In order to assess the success of this instalment of the database, negative ion fragmentation patterns obtained in this chapter which contained significant oxidation products (i.e. PE(16:0,18:1), PE(18:1,18:1) & PE(16:0,20:4)) were retro-searched against the OxyLipidBlast database. A precursor mass error of ± 0.005 *m/z* was used and a fragment mass error of ± 1 *m/z*, reflecting the inaccuracy of ion trap analyses. Dot product and reverse dot product scores were calculated, which represent the intensity and mass weighted similarity between a library spectrum and a collected spectrum. Annotation success was assessed using reverse dot product scores as they only assign weight to peaks in the library spectra and therefore avoid inherent noise present in fragmentation spectra from biological sources (Stein, 2012).

3.2.6 - Validation of the OxyLipidBlast database

To assess whether the OxyLipidBlast database could annotate oxidation in a more complex sample matrix, oxidation of a mixture of PE species was undertaken. Initial studies indicated that the soft peroxidation used earlier in the chapter may have little observable effect in a mixture and so was supplemented with a hydrogen peroxide / copper chloride system which has been used previously to oxidise lipids (Khaselev and Murphy, 2000). Egg yolk, total PE extract (Sigma-Aldrich Co., UK) was resuspended in sodium phosphate buffer (50 mM, pH = 7.4) with vortex mixing (30 s)

and sonication (15 min) to an approximate molarity of 0.5 mM based on an atomic mass of 750 Da. Six aliquots (0.24 ml) were separated into vials before additional buffer (0.3 ml) was added to three vials, alternatively H₂O₂ (0.15 ml, 70 mM) and CuCl₂ (0.15 ml, 100 μM) were added to the remaining vials. H₂O₂ containing vials were stored at 37 °C for two hours, the three remaining vials for 24 h. Vials were retrieved and placed on ice before cold methanol (0.6 ml) and chloroform (0.6 ml) were added with vortex mixing. Phases were separated further by centrifugation (10 min, 4000 rpm) and the chloroform layer was removed by glass syringe. Chloroform extracts were dried under N₂ and re-suspended in MeOH:CHCl₃ (3:1, 3 ml). Mass spectra were obtained identically to the method described in section 3.2.3.

OxyLipidBlast was used to determine whether any oxidised spectral features could be observed with settings as defined above, a precursor mass error of ± 0.005 *m/z* was used and a fragment mass error of ± 1 *m/z*.

3.3 - Results and discussion

Mass spectrometric measurements of oxidation products

Initial annotation of spectral features was successful in both ion modes. The uncalibrated data yielded consistent mass errors which were coincidentally negative in negative ion mode and positive in positive ion mode (appendix A1). Unmodified lipids were predominantly identified as de-protonated ions [M-H]⁻ in negative ion mode with a small amount of chlorinated adducts [M+35Cl]⁻ (

Table 3-3), in positive ion mode sodiated ions $[M+Na]^+$ were the most commonly observed adduct followed by disodiated $[M+2Na-H]^+$, protonated $[+H]^+$ and traces of potassiated species $[M+K]^+$ (

Table 3-4). Tables summarising this data for all PE species are contained in appendix A1, representative tables from oxidation of PE(16:0,18:1) are included within this chapter for reference (Table 3-3 to Table 3-10 inclusive). Additionally as expected, ^{13}C isotope containing structures were observed for all species at high enough concentrations. As the most abundant ion forms, all discussion of ions from here will be deprotonated in negative ion mode and sodiated in positive mode unless explicitly mentioned.

Oxidation was observed by the presence of spectral features at oxygen mass differences ($15.99491\ m/z$) above the unmodified lipid within a mass error $< 1\ \text{ppm}$ (Figure 3-2). For the two saturated PE species, PE(14:0,0:0) and PE(14:0,14:0), no oxygen additions were observed. This is expected as SFA do not possess either bisallylic or allylic hydrogen moieties which are vulnerable to abstraction. Additionally, no oxygen additions were seen to the plasmalogen species, PE(P-18,18:1), despite the presence of an allylic hydrogen on the sn2 chain and the vinylic bond binding the sn1 chain (Figure 3-2). This is surprising and goes against previous publications which suggest plasmalogens are readily oxidisable and in fact may function as ROS scavengers protecting cellular membranes (Lessig and Fuchs, 2009). However, it has also been reported that plasmalogen species have a strong affinity for hexagonal formation which contributes to membrane fusion (Maeba and Ueta, 2003). Stronger liposomes may prevent attack of either the vinylic bond or the allylic hydrogen on the sn2 18:1 chain. Multiple oxidised products of other unsaturated lipids were observed in both positive and negative spectra. The least oxidised product was PE(18:1, 0:0) with only single and double oxygen mass differences observed in both ion modes. A double oxygen addition represents lipid peroxidation, it is unsurprising that this

occurs only once on PE(18:0,0:0) as there is only one vulnerable molecular region and it is well documented that MUFAs are more resistant to oxidation than PUFAs (Sparvero et al., 2010). More surprising is that the PE(16:0,18:1) species showed oxidation of up to four oxygen additions in negative ion mode and up to three oxygen additions in positive ion mode despite also having only a single double bond. However, single and double oxygen additions had much higher relative intensities than three and four and the likely reason that four oxygen additions were not observed in positive ion mode is the low abundance of the molecule which only had a relative intensity of 1 % in negative ion mode (**Error! Reference source not found.**). The poly unsaturated species had the highest relative intensities of three and four oxygen additions, reflecting the fact that they contain multiple allylic and bisallylic hydrogen moieties allowing further oxidation following the initial attack. The relative intensity of double oxygen addition was much higher in PE(18:1, 18:1) where all other oxygen additions showed similar relative intensities across the two species. This appears surprising as PE(16:0,20:4) contains three bisallylic and two allylic hydrogen moieties in comparison to only four allylic hydrogen moieties on PE(18:1,18:1). Figure 3-2 shows the relative intensities of oxidatively modified PE species. In general, oxidation appears to increase as carbon chain saturation decreases from left to right. The nature of the modifications observed will be further explored via fragmentation patterns in the next section.

Table 3-3 Negative ion mode mass spectra from oxidised PE(16:0,18:1). M represents the unmodified lipid (PE(16:0,18:1)).

| Observed | | Identification | | | | |
|------------|-----------|-------------------|-----------|------------------|------------|-----------------|
| <i>m/z</i> | Intensity | Formula | Ion Form | Theoretical Mass | Mass Error | ID |
| 716.52429 | 1102247.0 | C39H76NO8P | [M-H]- | 716.52358 | -0.991 | PE(16:0,18:1) |
| 717.52766 | 465170.8 | C38(13C)H76NO8P | [M-H]- | 717.52693 | -1.017 | M(13C) |
| 748.51445 | 196788.5 | C39H76NO10P | [M-H]- | 748.51341 | -1.389 | M+O2 |
| 732.51928 | 136384.5 | C39H76NO9P | [M-H]- | 732.51849 | -1.078 | M+O |
| 718.53066 | 102584.0 | C37(13C2)H76NO8P | [M-H]- | 718.53029 | -0.515 | M(13C2) |
| 749.51797 | 80438.1 | C38(13C)H76NO10P | [M-H]- | 749.51676 | -1.614 | M+O2(13C) |
| 744.51939 | 76871.0 | C40H76NO9P | [M-H]- | 744.5185 | -1.202 | M+CO |
| 730.50365 | 73369.8 | C39H74NO9P | [M-H]- | 730.50284 | -1.109 | (M+O2)-H2O |
| 733.52288 | 55978.7 | C38(13C)H76NO9P | [M-H]- | 733.52185 | -1.404 | M+O(13C) |
| 746.49831 | 38922.4 | C39H74NO10P | [M-H]- | 746.49776 | -0.737 | (M+O3)-H2O |
| 764.50947 | 34205.5 | C39H76NO11P | [M-H]- | 764.50832 | -1.504 | M+O3 |
| 745.52271 | 30422.4 | C38(13C)H76NO9P | [M-H]- | 745.52185 | -1.154 | M+CO(13C) |
| 731.50709 | 30085.0 | C38(13C)H74NO9P | [M-H]- | 731.5062 | -1.224 | (M+O2)-H2O(13C) |
| 752.50082 | 29342.8 | C39H76NO8P | [M+35Cl]- | 752.50026 | -0.747 | PE(16:0,18:1) |
| 728.82474 | 26170.9 | - | - | - | - | Unknown |
| 762.49351 | 25377.6 | C39H74NO11P | [M-H]- | 762.49267 | -1.108 | (M+O4)-H2O |
| 760.51413 | 14983.2 | C40H76NO10P | [M-H]- | 760.51341 | -0.947 | M+CO2 |
| 780.50412 | 14716.4 | C39H76NO12P | [M-H]- | 780.50323 | -1.140 | M+O4 |
| 750.52037 | 14479.3 | C37(13C2)H76NO10P | [M-H]- | 750.52012 | -0.340 | M+O2(13C2) |
| 765.51265 | 12317.8 | C38(13C)H76NO11P | [M-H]- | 765.51168 | -1.274 | M+O3(13C) |
| 747.50153 | 11796.5 | C38(13C)H74NO10P | [M-H]- | 747.50112 | -0.555 | (M+O3)-H2O(13C) |
| 776.50905 | 11096.0 | C40H76NO11P | [M-H]- | 776.50833 | -0.934 | M+CO3 |

Table 3-4 Positive ion mode mass spectra from oxidised PE(16:0,18:1). M represents the unmodified lipid (PE(16:0,18:1)).

| Observed | | Identification | | | | |
|------------|-----------|-------------------|------------------------|------------------|------------|---------------------|
| <i>m/z</i> | Intensity | Formula | Ion Form | Theoretical Mass | Mass Error | ID |
| 740.51964 | 3273760.8 | C39H76NO8P | [M+Na] ⁺ | 740.52008 | 0.587 | PE(16:0,18:1) |
| 741.52301 | 1392710.5 | C38(13C)H76NO8P | [M+Na] ⁺ | 741.52343 | 0.566 | M(13C) |
| 756.51467 | 741855.9 | C39H76NO9P | [M+Na] ⁺ | 756.51499 | 0.423 | M+O |
| 772.50938 | 615908.6 | C39H76NO10P | [M+Na] ⁺ | 772.50991 | 0.680 | M+O2 |
| 754.49890 | 548833.6 | C39H74NO9P | [M+Na] ⁺ | 754.49934 | 0.583 | (M+O2)-H2O |
| 795.33430 | 484209.9 | - | - | - | - | Blank peak |
| 757.51795 | 317315.3 | C38(13C)H76NO9P | [M+Na] ⁺ | 757.51835 | 0.521 | M+O(13C) |
| 742.52623 | 302462.9 | C37(13C2)H76NO8P | [M+Na] ⁺ | 742.52679 | 0.747 | M(13C2) |
| 773.51272 | 253885.6 | C38(13C)H76NO10P | [M+Na] ⁺ | 773.51326 | 0.698 | M+O2(13C) |
| 796.33771 | 232362.3 | - | - | - | - | Blank peak |
| 770.49379 | 223782.1 | C39H74NO10P | [M+Na] ⁺ | 770.49426 | 0.604 | (M+O3)-H2O |
| 755.50212 | 218802.5 | C38(13C)H74NO9P | [M+Na] ⁺ | 755.50270 | 0.761 | (M+O2)- H2O(13C) |
| 786.48879 | 126764.8 | C39H74NO11P | [M+Na] ⁺ | 786.48917 | 0.483 | (M+O4)-H2O |
| 728.83231 | 111130.9 | - | - | - | - | Blank peak |
| 771.49715 | 91858.8 | (M+O3)-H2O(13C) | [M+Na] ⁺ | 771.49761 | 0.596 | (M+O3)- H2O(13C) |
| 788.50476 | 88428.5 | C39H76NO11P | [M+Na] ⁺ | 788.50482 | 0.076 | M+O3 |
| 758.66837 | 68236.6 | - | - | - | - | Blank peak |
| 811.30789 | 62239.4 | - | - | - | - | Blank peak |
| 718.53782 | 56000.4 | C39H76NO8P | [M+H] ⁺ | 718.53813 | 0.431 | PE(16:0,18:1) |
| 792.64999 | 51266.5 | - | - | - | - | Unknown |
| 762.50183 | 46200.1 | C39H76NO8P | [M+2Na-H] ⁺ | 762.50202 | 0.249 | PE(16:0,18:1) |
| 774.51541 | 43860.0 | C37(13C2)H76NO10P | [M+Na] ⁺ | 774.51662 | 1.556 | M+O2(13C2) |
| 797.34090 | 39720.6 | - | - | - | - | Blank peak |
| 787.49217 | 36875.3 | C38(13C)H74NO11P | [M+Na] ⁺ | 787.49253 | 0.451 | (M+O4)- H2O(13C) |

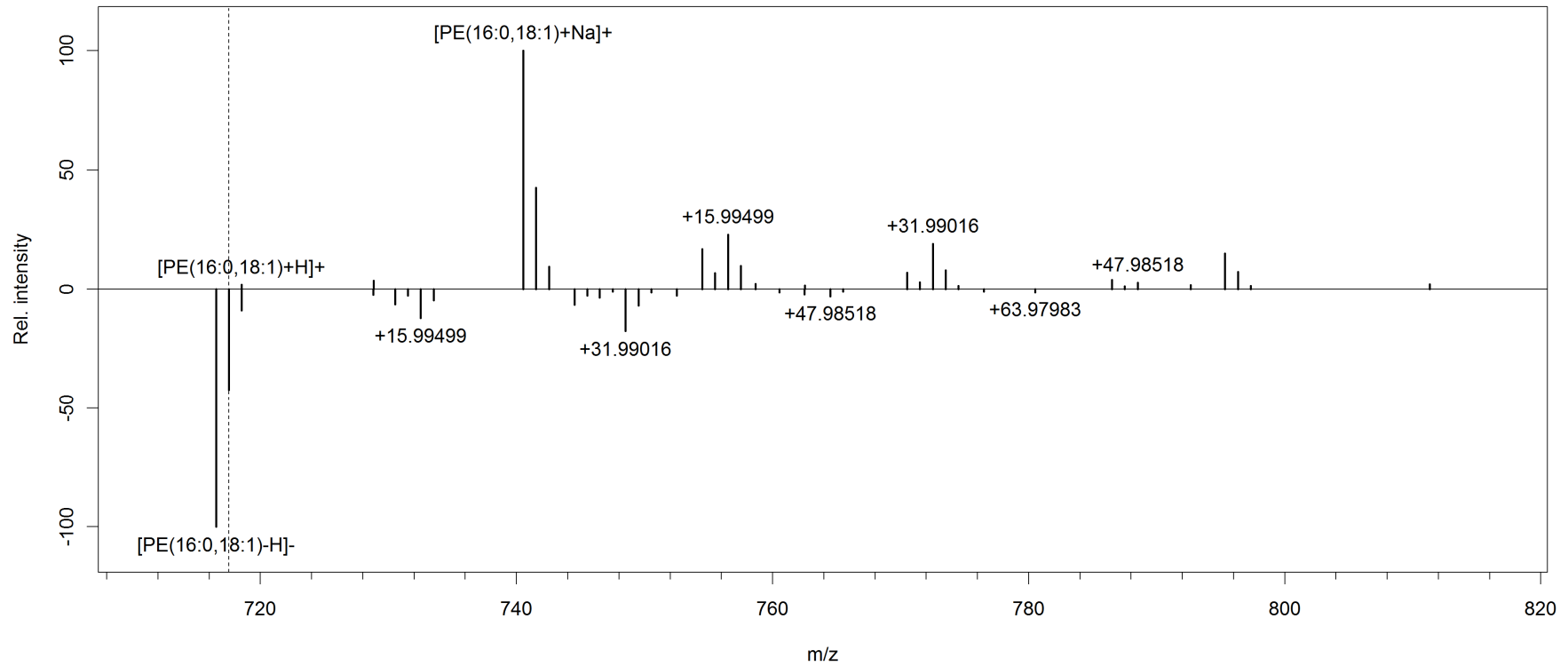


Figure 3-1 FT-ICR mass spectrum of PE(16:0,18:1) and oxidised products. Hashed line at $m/z = 717.53$ denotes neutral mass of unmodified lipid. Named peaks indicate adducts of unmodified lipids, peak mass additions indicate oxygen modifications. Positive ion mode is shown above the x-axis and negative ion mode below.

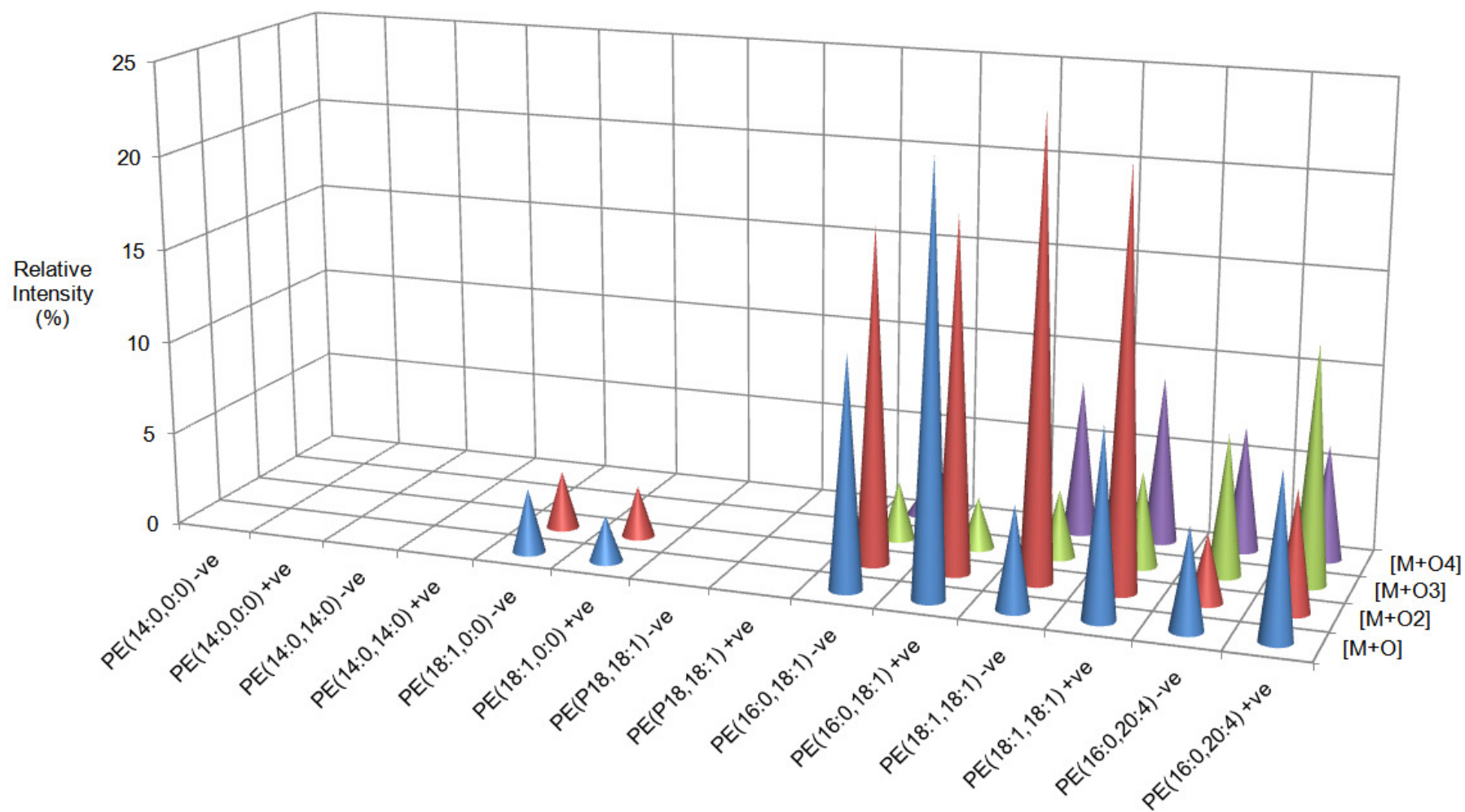


Figure 3-2 Summary of oxidative modifications observed in PE molecules with varying chain chemistry. Relative intensities are represented by cones, single oxygen addition = blue, double oxygen addition = red, triple oxygen addition = green, quadruple oxygen addition = purple. Where cones are absent species was not observed with relative intensity above 1%.

3.3.1 - Oxidation time-course

The intensities of oxidatively modified PE(16:0,18:1) relative to unmodified PE(16:0,18:1) were used to monitor oxidation rate over a 96 hour period. Features representing single, double, triple and quadruple oxygen addition were present at m/z 732, 748, 764 and 780 respectively. For all four oxidised lipids oxidation occurred linearly for the first 72 hours following which there was a sharp increase in the oxidised product with the ratio rising to at 96 hours (Figure 3-3). This shows that the proportion of oxidised products grew with time and so oxidation was occurring continuously over the time-course. Whilst this is what you would expect from an oxidation timeline, this validates our soft methodology, without an oxidant, is appropriate for the induction of oxidation. Sonication of the PE molecules in an aqueous matrix will form liposomes due to the amphipathic nature of the lipid species. The sharp upturn in oxidation at 96 hours could be due to breakdown of these spherical lipid conglomerates, increasing fatty acyl chain exposure to the aqueous environment. Internalisation of carbon chains into hydrophobic bilayers should afford some protection against oxidative attack as ROS are, by nature, polar and thus will be externalised. Bilayer disruption would occur where chain oxidation reduces the efficiency of Van der Waals binding between phospholipid molecules, membrane packing would be reduced allowing an influx of ROS (Reis et. al., 2007).

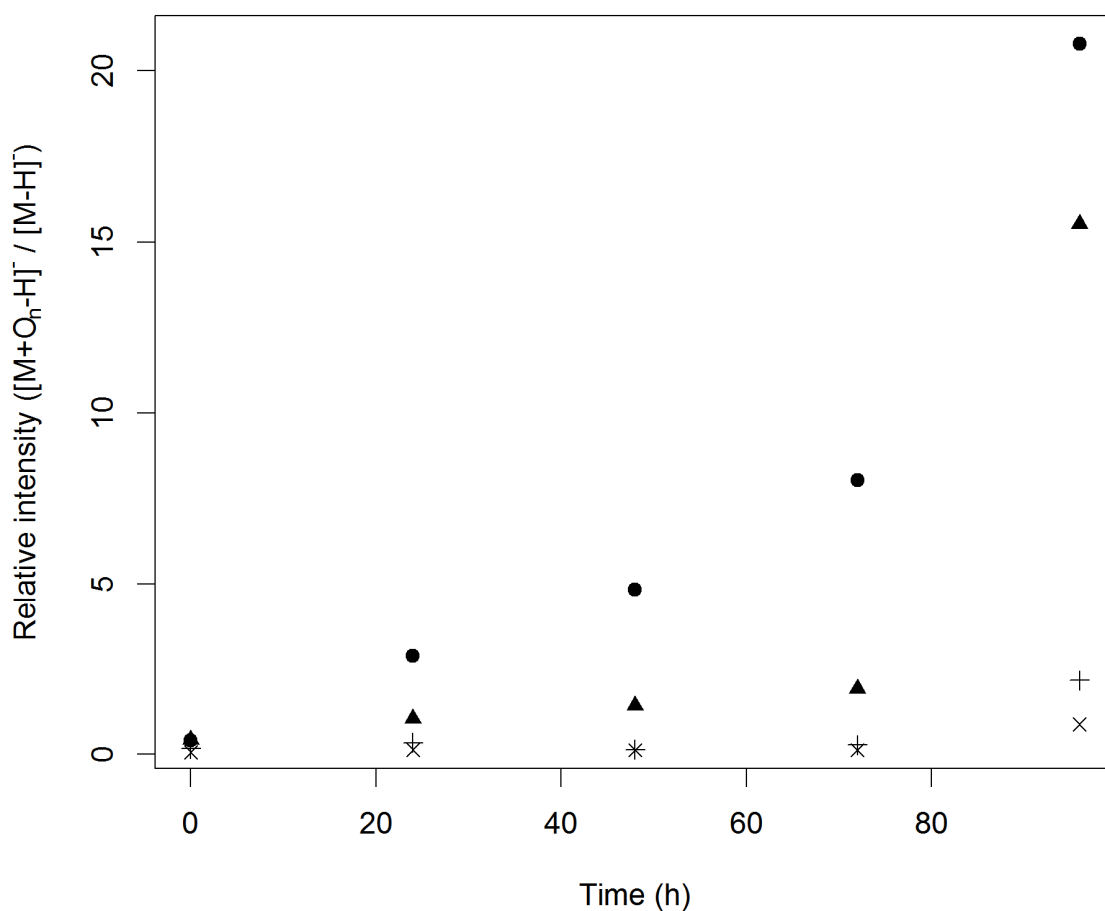


Figure 3-3 Intensities of oxidatively modified lipids relative to the unmodified lipid PE(16:0,18:1(9Z)) across a 96 hour period (n=1). Triangles (▲) represent single oxygen addition (M+O), circles (●) represent double oxygen addition (M+O2), plus signs (+) represent triple oxygen addition (M+O3) and crosses (×) represent quadruple oxygen addition (M+O4).

3.3.2 - Annotation and interpretation of fragmentation patterns

Annotation of fragmentation patterns from unmodified and oxidised species was undertaken manually. Over 100 fragmentation patterns were assessed and annotated utilising existing PE fragmentation patterns, fragmentation patterns of other oxidised phospholipids published previously and chemical knowledge. A complete collection of annotated spectra can be found in the appendix of this thesis (Appendix All), in this section I will use the fragmentation patterns of PE(16:0,18:1)

and the oxidative products thereof to illustrate the general fragmentation profiles which are maintained well across the PE species.

3.3.2.1 - Unmodified PE (positive ion mode)

In positive mode, all sodiated unmodified PE species produced a fragment due to the loss of aziridine (C_2H_5N , $-43 m/z$), additionally two peaks (-123 , $-141 m/z$) representing neutral head group loss and one peak ($-163 m/z$) from sodiated head group loss were observed from the diacyl PE species and the plasmalogen (Figure 3-4, Table 3-5). Alternatively lyso species showed losses of water ($-18 m/z$) and water + aziridine ($-61 m/z$) (Appendix All). Further fragments were observed from the loss of fatty acyl moieties from both sn1 and sn2 positions both with and without aziridine, however, when detected the intensity was near the limit of detection and they were not identified in all compounds. These fragmentations are consistent with those reported previously (Pulfer and Murphy, 2003). They have strong utility for identification of lipid class, however, due to the low abundance of chain loss fragments, they have little value in elucidating chain chemistry.

Table 3-5 Fragments of unmodified [PE(16:0,18:1)+Na]⁺ and associated annotation.

| Parent <i>m/z</i> | 740.52 | | | |
|---------------------|---|--------------------|--|-----------------------------|
| Ion form | [M+Na] ⁺ | | | |
| ID | PE(16:0,18:1) | | | |
| Formula | C ₃₉ H ₇₆ NO ₈ PNa | | | |
| | Observed | | Identification | |
| Fragment <i>m/z</i> | Neutral loss | Relative Intensity | Formula | Annotation |
| 697.37 | 43.15 | 100 | C ₃₇ H ₇₁ O ₈ PNa | - Aziridine |
| 599.49 | 141.03 | 20 | C ₃₇ H ₆₈ O ₄ Na | - Head group(PE) |
| 577.51 | 163.01 | 5 | C ₃₇ H ₆₉ O ₄ | - Sodiated head group |
| 617.52 | 123.00 | 3 | C ₃₇ H ₇₀ O ₅ Na | -Head group (PE) |
| 441.31 | 299.21 | 2 | C ₂₁ H ₃₉ O ₆ PNa | - Palmitic acid & aziridine |

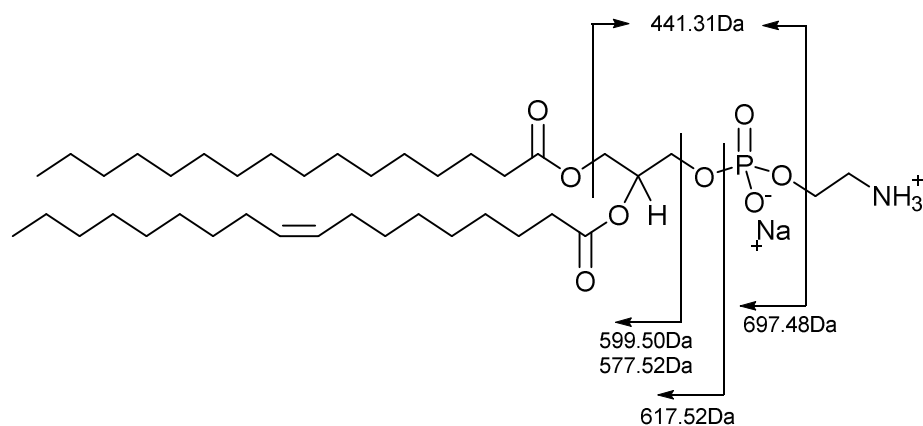


Figure 3-4 Structure showing the major fragments of [PE(16:0,18:1)+Na]⁺. Arrows indicate observed fragments and *m/z* values.

3.3.2.2 - Oxidised PE (positive ion mode)

Species formed by the addition of a single oxygen atom [PE+O+Na]⁺ were observed for all diacyl PEs with any unsaturated bond, these generated similar fragmentation patterns to the unmodified lipids. Neither the loss of sodiated head groups (-163 *m/z*) nor the loss of radyl chains were observed, however, the losses from H₂O and H₂O + aziridine (-18 & -61 *m/z*), previously only observed for lyso species, were observed for all molecules. A previously unobserved fragment due to the loss of head group +

water (-159 m/z) was observed for the three diacyl but not the lyso $[PE+O+Na]^+$ (Figure 3-5, Table 3-6). These fragments, can be used to distinguish $[PE+O+Na]^+$ from $[PE +Na]^+$, however, they do not give any indication as to the location of the oxygen modification and so have limited value in identification over putative annotation with accurate m/z values.

Table 3-6 Fragments of [PE(16:0,18:1)+O+Na]⁺ and associated annotation.

| Parent <i>m/z</i> | 756.51 | | | |
|---------------------|---|--------------------|---|-------------------------------------|
| Ion form | [M+Na] ⁺ | | | |
| ID | PE(16:0,18:1)+O | | | |
| Formula | C ₃₉ H ₇₆ NO ₉ PNa | | | |
| | Observed | | Identification | |
| Fragment <i>m/z</i> | Neutral loss | Relative Intensity | Formula | Annotation |
| 713.42 | 43.09 | 100 | C ₃₇ H ₇₁ O ₉ PNa | - Aziridine |
| 738.39 | 18.12 | 57 | C ₃₉ H ₇₄ NO ₈ PNa | -H ₂ O |
| 615.52 | 140.99 | 41 | C ₃₇ H ₆₈ O ₅ Na | - Head group(PE) |
| 712.44 | 44.07 | 15 | - | Unknown |
| 695.39 | 61.12 | 14 | C ₃₇ H ₆₉ O ₈ PNa | - Aziridine & H ₂ O |
| 633.52 | 122.99 | 10 | C ₃₇ H ₇₀ O ₆ Na | - Head group(PE) |
| 614.52 | 141.99 | 6 | - | Unknown |
| 597.46 | 159.05 | 2 | C ₃₇ H ₆₆ O ₄ Na | - Head group(PE) & H ₂ O |

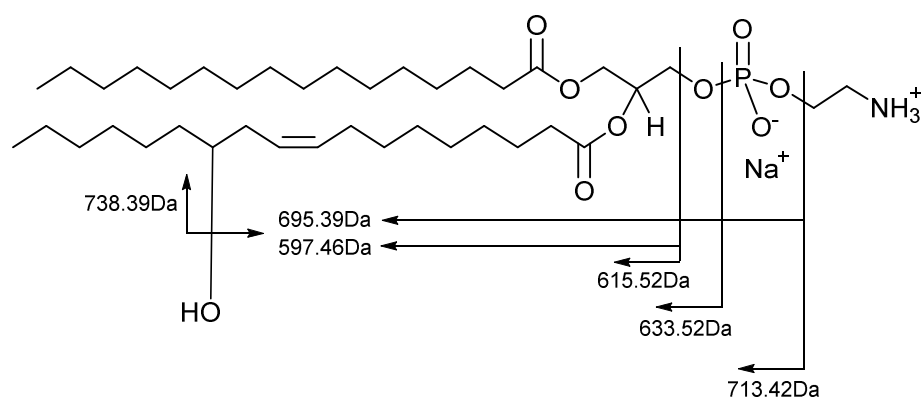


Figure 3-5 Structure showing the major fragments of [PE(16:0,18:1)+O+Na]⁺. Arrows indicate observed fragments and *m/z* values. Hydroxyl group position is for illustrative purposes only as not defined by MS² analysis.

Species formed by the addition of two oxygen atoms [PE+O₂+Na]⁺ were observed for all diacyl PEs with a degree of saturation. Again, sodiated head group loss (-163 *m/z*) was absent, and loss of H₂O and H₂O + aziridine (-18 & -61 *m/z*) were observed for all peaks. A new peak at -34 *m/z*, representing loss of hydrogen peroxide was observed for all peaks. This hydrogen peroxide peak can be used to distinguish the fragmentation pattern of [PE+O₂+Na]⁺ from [PE+O+Na]⁺ and [PE +Na]⁺. As with the

single oxygen addition there is no molecular information for the oxygen additions, including location and the nature of the oxidation. For example, a single oxygen could be added to the head group and one to a chain as hydroxyl moieties. However, the widely reported mechanism of lipid peroxidation would suggest that the predominant modification is a peroxy-moiety attached to an unsaturated chain, as lipid peroxides are the first intermediate product of lipid peroxidation (Horton and Fairhurst, 1987). This is a limitation of positive ion mode fragmentation in the identification of oxidised lipid products.

Table 3-7 Fragments of [PE(16:0,18:1)+O2+Na]⁺ and associated annotation.

| Parent <i>m/z</i> | 772.51 | | | |
|---------------------|------------------|--------------------|----------------|------------------------|
| Ion form | [M+Na] | | | |
| ID | PE(16:0,18:1)+O2 | | | |
| Formula | C39H76NO10PNa | | | |
| | Observed | | Identification | |
| Fragment <i>m/z</i> | Neutral loss | Relative Intensity | Formula | Annotation |
| 729.41 | 43.10 | 100 | C37H71O10PNa | - Aziridine |
| 631.51 | 141.00 | 55 | C37H68O6Na | - Head group(PE) |
| 754.42 | 18.09 | 39 | C39H74NO9PNa | -H2O |
| 711.42 | 61.09 | 33 | C37H69O9PNa | - Aziridine & H2O |
| 613.49 | 159.02 | 22 | C37H66O5Na | - Head group(PE) & H2O |
| 649.49 | 123.02 | 19 | C37H70O7Na | - Head group(PE) |
| 656.35 | 116.16 | 18 | - | Unknown |
| 738.42 | 34.09 | 17 | C39H74NO8PNa | - H2O2 |
| 642.36 | 130.15 | 15 | - | Unknown |
| 415.28 | 357.23 | 8 | - | Unknown |
| 638.40 | 134.11 | 7 | - | Unknown |
| 612.39 | 160.12 | 6 | - | Unknown |
| 736.48 | 36.03 | 6 | C39H72NO8PNa | -2(H2O) |
| 695.39 | 77.12 | 5 | - | Unknown |
| 624.40 | 148.11 | 5 | - | Unknown |
| 598.36 | 174.15 | 4 | - | Unknown |
| 361.30 | 411.21 | 3 | - | Unknown |
| 458.26 | 314.25 | 3 | - | Unknown |
| 530.27 | 242.24 | 2 | - | Unknown |
| 587.29 | 185.22 | 2 | - | Unknown |
| 772.51 | 0.00 | 2 | C39H76NO10PNa | Parent |
| 291.25 | 481.26 | 2 | - | Unknown |
| 332.13 | 440.38 | 2 | - | Unknown |
| 626.57 | 145.94 | 2 | - | Unknown |
| 693.37 | 79.14 | 2 | - | Unknown |
| 346.14 | 426.37 | 2 | - | Unknown |
| 489.39 | 283.12 | 2 | - | Unknown |
| 475.35 | 297.16 | 2 | - | Unknown |
| 503.42 | 269.09 | 2 | - | Unknown |
| 652.38 | 120.13 | 2 | - | Unknown |

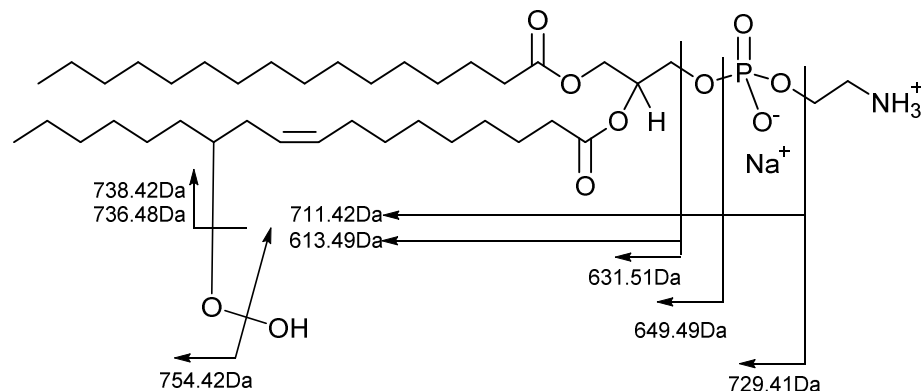


Figure 3-6 Structure showing the major fragments of $[\text{PE}(16:0,18:1)+\text{O}_2+\text{Na}]^+$. Arrows indicate observed fragments and m/z values. Peroxyl group position is for illustrative purposes only as not defined by MS^2 analysis.

3.3.2.3 - Unmodified PE (negative ion mode)

In negative ion mode the primary fragments from deprotonated unmodified lipids were radyl anions, the exception being the vinyl-bound species from the plasmalogen, which cannot form a carboxylate ion. Peaks were also observed from losses of the radyl chains as keto and carboxyl groups with the former being the more intense. As reported previously (Hvattum et al., 1998) the abundance of sn2 carboxylate anions was higher than sn1 in the two species with disparate chain chemistry (Figure 3-7, Table 3-8). While lacking a specific PE identifying fragment, head group ID can be calculated from the radyl and precursor m/z values. The predominant carboxylate anions allow great structural elucidation, identifying both the chain lengths and the number of double bonds in the sn1 and sn2 chains. This is a significant advantage of negative ion phospholipid fragmentation over positive ion.

Table 3-8 Fragments of unmodified [PE(16:0,18:1)-H]⁻ and associated annotation.

| Parent (<i>m/z</i>) | 716.52 | | | |
|-----------------------|---|--------------------|---|-------------------------|
| Ion form | [M-H] ⁻ | | | |
| ID | PE(16:0,18:1) | | | |
| Formula | C ₃₉ H ₇₅ NO ₈ P | | | |
| | Observed | | Identification | |
| Fragment <i>m/z</i> | Neutral loss | Relative Intensity | Formula | Annotation |
| 281.35 | 435.17 | 100 | C ₁₈ H ₃₃ O ₂ | Oleic acid anion |
| 255.34 | 461.18 | 48 | C ₁₆ H ₃₁ O ₂ | Palmitic acid anion |
| 452.37 | 264.15 | 13 | C ₂₁ H ₄₃ NO ₇ P | -Oleic acid (ketene) |
| 478.36 | 238.16 | 5 | C ₂₃ H ₄₅ NO ₇ P | -Palmitic acid (ketene) |
| 434.39 | 282.13 | 2 | C ₂₁ H ₄₁ NO ₆ P | -Oleic acid |
| 460.36 | 256.16 | 1 | C ₂₃ H ₄₃ NO ₆ P | -Palmitic acid |

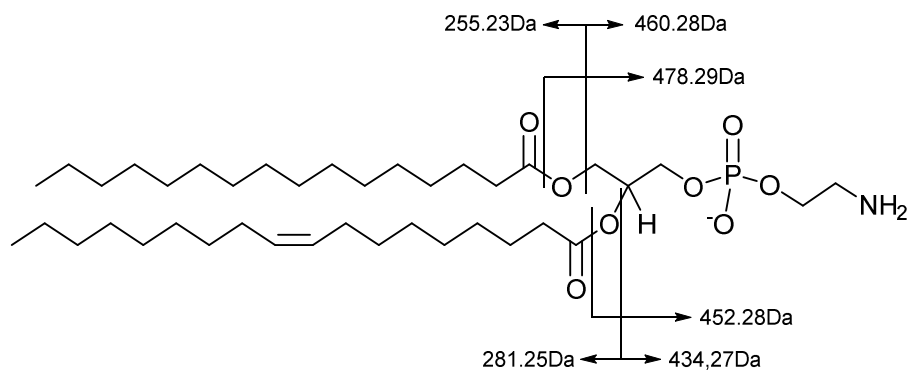


Figure 3-7 Structure showing the major fragments of [PE(16:0,18:1)-H]⁻. Arrows indicate observed fragments and *m/z* values.

3.3.2.4 - Oxidised PE (negative ion mode)

For all phospholipid fatty acyl chains with a degree of unsaturation, single oxygen addition was observed [PE+O-H]⁻. Oxygen modified carboxylate ions were observed (FA+O or FA+16 *m/z*) as well as dehydration products of the modified chains ((FA+O)-H₂O or FA-2 *m/z*). Additionally loss of these unsaturated modified chains was repeatedly observed as keto moieties but only once as a carboxylate group in the case of the PUFA in [PE(16:0,20:4)+O]. Unmodified carboxylate ions of unsaturated chains were also observed but not as neutral losses (carboxylate nor

keto). Unexpectedly, oxygen addition was also observed on saturated fatty acid chains [FA + O], however these were weak signals and neither dehydration products nor loss of oxidatively modified saturated chains were recorded. Additionally, unmodified saturated chains were observed as carboxylate ions and neutral losses (keto and carboxylate) (Figure 3-8, Table 3-9). This fragmentation data indicates that single oxygen modifications were occurring on the MUFA and PUFA chains, a situation we would expect given the labile sites for hydrogen abstraction on these groups. The weak presence of SFA chains with oxygen addition and neutral losses of unmodified unsaturated chains suggest there may also be a slight amount of oxidation occurring on SFA chains, which is unexpected due to the more strongly bound hydrogen atoms and fact that no oxidative products were observed for the saturated phospholipid compounds. It is most likely that the compounds produced will be hydroxyl phospholipids which are a reduction product of lipid hydroperoxides. The position of the hydroxyl group along the chain cannot be verified by MS/MS analysis although it is likely that it will lie adjacent to the double bond due to allylic hydrogen abstraction.

Table 3-9 Fragments of [PE(16:0,18:1)+O-H]⁻ and associated annotation.

| Parent <i>m/z</i> | 732.51 | | | |
|---------------------|---|--------------------|---|---------------------------------------|
| Ion form | [M-H] ⁻ | | | |
| ID | PE(16:0,18:1)+O | | | |
| Formula | C ₃₉ H ₇₅ NO ₉ P | | | |
| | Observed | | Identification | |
| Fragment <i>m/z</i> | Neutral loss | Relative Intensity | Formula | Annotation |
| 297.34 | 435.17 | 100 | C ₁₈ H ₃₃ O ₃ | Oleic acid anion +O |
| 255.33 | 477.18 | 45 | C ₁₆ H ₃₁ O ₂ | Palmitic acid anion |
| 452.38 | 280.13 | 12 | C ₂₁ H ₄₃ NO ₇ P | -(Oleic acid anion +O) (ketene) |
| 494.37 | 238.14 | 6 | C ₂₃ H ₄₅ NO ₈ P | - Palmitic acid (ketene) |
| 279.34 | 453.17 | 5 | C ₁₈ H ₃₁ O ₂ | Oleic acid anion +O -H ₂ O |
| 281.35 | 451.16 | 3 | C ₁₈ H ₃₃ O ₂ | Oleic acid anion |
| 295.33 | 437.18 | 2 | - | Unknown |
| 476.28 | 256.23 | 2 | C ₂₃ H ₄₃ NO ₇ P | -Palmitic acid |
| 296.39 | 436.12 | 2 | - | Unknown |
| 256.38 | 476.13 | 1 | - | Unknown |
| 271.30 | 461.21 | 1 | C ₁₆ H ₃₁ O ₃ | Palmitic acid anion +O |

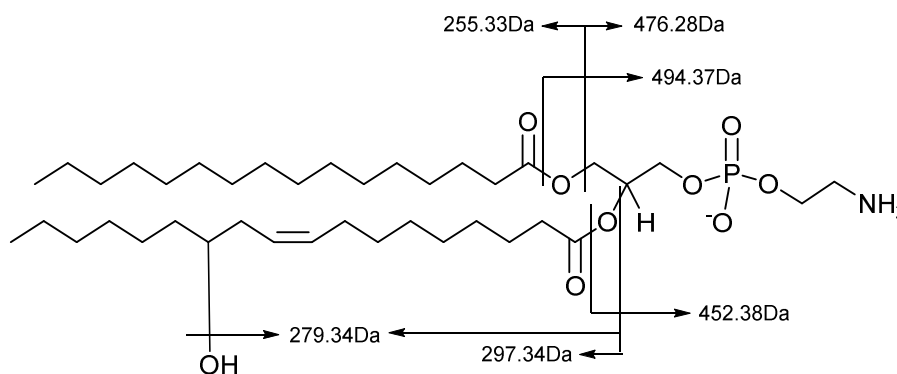


Figure 3-8 Structure showing the major fragments of [PE(16:0,18:1)+O-H]⁻. Arrows indicate observed fragments and *m/z* values. Hydroxyl group position is for illustrative purposes only as not defined by MS² analysis.

Fragmentation patterns of double oxygen addition [PE+O₂-H]⁻ followed a similar pattern to the single additions [PE+O-H]⁻. Key differences were the loss of water ([M-H₂O] at M-18 *m/z*) and molecular oxygen ([M-O₂] at M-32 *m/z*) although the latter was not observed in the modified lyso ([PE(18:1,0:0)+O₂]). Modified carboxylate ions

were observed for unsaturated fatty acids $[FA+O_2]^-$, and dehydration products of these $[FA+O_2-H_2O]^-$, as well as neutral losses as carboxylate and keto groups ($[M-(FA_{(keto)}+O_2)]$ & $[M-(FA_{(carboxylate)}+O_2)]$) were also observed. Modified carboxylate ions of dehydration products $[FA+O_2-H_2O-H]^-$ were also observed for unsaturated chains but they were not observed as neutral losses (Figure 3-9, Table 3-10). Single oxygen addition was also observed as carboxylate ions of both unsaturated and saturated chains, this indicates the presence of multiple oxidation products. Using the fragmentation pattern of $[PE(16:0,18:1)+O_2]$ these products could include: $[PE(16:0-OH,18:1-OH)]$, $[PE(16:0,18:1-OOH)]$, $[PE(16:0,18:1(-OH)_2)]$. These are all feasible, however, the relative abundance of unmodified $[16:0]$ and $[18:1+O_2]$ suggests the modification takes place predominantly on the unsaturated chain and knowledge of the lipid peroxidation mechanism indicates a lipid peroxide molecule as the most likely product.

Table 3-10 Fragments of [PE(16:0,18:1)+O2-H]⁻ and associated annotation.

| Parent <i>m/z</i> | 748.51 | | | |
|---------------------|--------------------|--------------------|----------------|-----------------------------|
| Ion form | [M-H] ⁻ | | | |
| ID | PE(16:0,18:1)+O2 | | | |
| Formula | C39H75NO10P | | | |
| | Observed | | Identification | |
| Fragment <i>m/z</i> | Neutral loss | Relative Intensity | Formula | Annotation |
| 313.34 | 435.17 | 100 | C18H33O4 | Oleic acid + O2 anion |
| 255.33 | 493.18 | 76 | C16H31O2 | Palmitic acid anion |
| 295.32 | 453.19 | 53 | C18H31O3 | Oleic acid + O2 -H2O anion |
| 730.52 | 17.99 | 33 | C39H73NO9P | -H2O |
| 452.36 | 296.15 | 20 | C21H43NO7P | -(Oleic acid + O2) (ketene) |
| 297.32 | 451.19 | 12 | C18H33O3 | Oleic acid + O anion* |
| 510.36 | 238.15 | 8 | C23H45NO9P | - Palmitic acid (ketene) |
| 492.35 | 256.16 | 8 | C23H43NO8P | -Palmitic acid |
| 271.33 | 477.18 | 6 | C16H31O3 | Palmitic acid anion +O* |
| 281.36 | 467.15 | 5 | C18H33O2 | Oleic acid anion* |
| 312.36 | 436.15 | 3 | - | Unknown |
| 311.32 | 437.19 | 2 | - | Unknown |
| 256.36 | 492.15 | 2 | - | Unknown |
| 269.37 | 479.14 | 2 | - | Unknown |
| 293.28 | 455.23 | 2 | - | Unknown |
| 434.39 | 314.12 | 2 | C21H41NO6P | -(Oleic acid + O2) |
| 287.39 | 461.12 | 1 | - | Unknown |
| 468.35 | 280.16 | 1 | - | Unknown |
| 257.39 | 491.12 | 1 | - | Unknown |
| 716.61 | 31.90 | 1 | C39H75NO8P | -O2 |

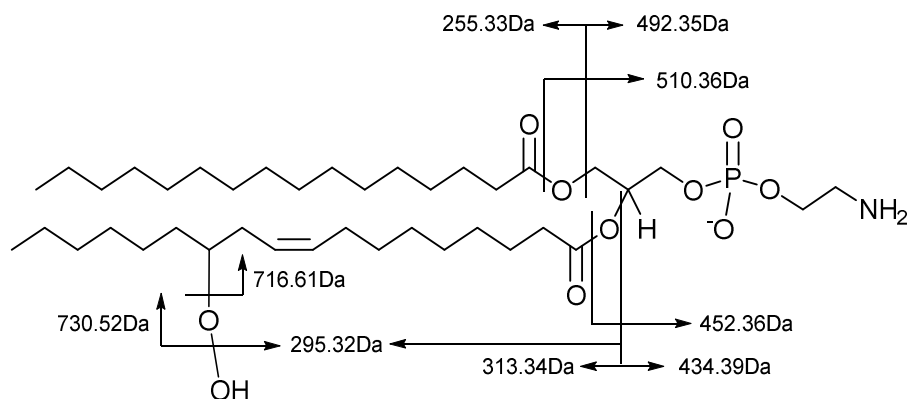


Figure 3-9 Structure showing the major fragments of [PE(16:0,18:1)+O2-H]⁻. Arrows indicate observed fragments and *m/z* values. Peroxyl group position is for illustrative purposes only as not defined by MS² analysis.

3.3.3 - Utilisation of OxyLipidBlast to identify oxidised products

All oxygen additions observed on the diacyl PE species above were successfully annotated by OxyLipidBlast (Table 3-11). Reverse dot product scores were notably higher than the 600 set out by Kind et al., 2013 as a benchmark for competent matching. However, additional multiple false positives were identified. The correctly identified [PE(18:1,18:1)+O2], was also spuriously annotated as [PE(17:2/19:0)+O2] and [PE(19:1/17:1)+O2]. This is due to the fact that using a 1 Da mass error on the fragment features a lot of pseudo-isomeric overlap is created. For LTQ collected fragmentation data it was found that a mass error this large is required (see Appendix All), however, the errors were largely offset in a single direction which indicated that improved calibration both pre data collection and during data processing would allow more stringent mass errors on fragments and reduce false positives. Alternatively, fragment ions could be analysed in the FT-ICR cell, this would allow greater mass accuracy which would allow much more stringent mass error settings, however, there would be an associated loss in sensitivity which could preclude the analysis of low intensity oxidised phospholipids.

Table 3-11 Table showing ability of OxyLipidBlast to annotate oxidised peaks. Numerical values represent reverse dot product scores which assess how well the theoretical spectrum matches the experimental one, scores run from 0 (no match) to 999 (perfect match).

| | Spectral match (rev dot score) | | |
|--------|--------------------------------|---------------|---------------|
| | PE(16:0,18:1) | PE(18:1,18:1) | PE(16:0,20:4) |
| [M+O] | 852 | 855 | 823 |
| [M+O2] | 840 | 872 | 958 |
| [M+O3] | 847 | 805 | 831 |
| [M+O4] | 833 | 846 | 831 |

3.3.4 - Validation of the OxyLipidBlast database

Oxidation of a PE mixture was used to assess the success of the first iteration of OxyLipidBlast. Two methodologies were used, the soft oxidation analogous to that which oxidised the individual standards earlier in the chapter and a H_2O_2 / CuCl_2 matrix which has been used previously (Khaselev and Murphy, 2000). In addition to the fragmentation patterns of oxidised PE lipids, OxyLipidBlast retains the fragmentation patterns of unmodified PE species. Across the six analyses, twelve unmodified PE molecules were observed, with chain lengths with even parity primarily between 34 and 40, and bond lengths between 1 and 6 which reflect common fatty acids in biological organisms. There was a PE species which did not fall within these common parameters PE(42:9), however, this peak has isomeric overlap with PE(38:5) + O3 which may indicate it as a false positive. In both datasets multiple spectral features were identified as oxidised products by OxyLipidBlast (Table 3-12). Additions of one, two, three and four oxygen atoms were observed in the soft oxidation spectra for five, six, two and three species respectively. Oxidation seemed to be more widespread in the H_2O_2 exposed lipids which is expected from the addition of a chemical oxidant, additions of one, two, three, four, five and six oxygen atoms were observed in the H_2O_2 spectra for five, six, six, three, one and two species respectively. In addition to the greater number of oxygen additions, 11 of 12 species were oxidised by H_2O_2 compared to 7 of 12 in the soft oxidation (Table 3-12). As all the identified lipids were unsaturated, it is no surprise to see oxidised products from the majority of them, however, it is reassuring that a maximum of double oxygen addition is observed on the monounsaturated PE species as these should be more resilient to oxidation. All reverse dot scores were > 600 , the standard set for

fragmentation confidence set by Kind et al., 2013. The rational annotation of oxidised species by OxyLipidBlast adds confidence in its use as a tool for identification of oxidative modifications, the first tool available for this use.

Table 3-12 Table showing the oxidised products identified by OxyLipidBlast. Numerical values represent the reverse dot product score which assesses how well the theoretical spectrum matches the experimental spectrum, 0 = no match, 1000 = perfect match.

| | Unmodified lipids | O1 | O2 | O3 | O4 | O5 | O6 |
|-------------------------------|-------------------|-----|-----|-----|-----|-----|-----|
| Auto-oxidation | PE 34:1 | | 790 | | | | |
| | PE 34:2 | | | | | | |
| | PE 36:1 | 834 | | | | | |
| | PE 36:2 | 794 | 829 | | 592 | | |
| | PE 36:3 | 854 | 834 | | | | |
| | PE 36:4 | | | | | | |
| | PE 38:4 | 792 | 805 | 830 | 845 | | |
| | PE 38:5 | | 884 | 849 | 914 | | |
| | PE 38:6 | | | | | | |
| | PE 40:5 | 814 | 756 | | | | |
| | PE 40:6 | | | | | | |
| | PE 42:9 | | | | | | |
| H ₂ O ₂ | PE 34:1 | | 803 | | | | |
| | PE 34:2 | 799 | 723 | | | | |
| | PE 36:1 | 651 | 975 | | | | |
| | PE 36:2 | 827 | 897 | 908 | | | |
| | PE 36:3 | 859 | | 850 | | | |
| | PE 36:4 | | | 925 | | | |
| | PE 38:4 | | 857 | | 834 | | 656 |
| | PE 38:5 | | | 780 | 852 | 803 | 653 |
| | PE 38:6 | | | 838 | 858 | | |
| | PE 40:5 | | | 794 | | | |
| | PE 40:6 | | | | | | |
| | PE 42:9 | 644 | 642 | | | | |

3.4 - Conclusions

Peak intensity ratios of unmodified versus oxidised PE(16:0, 18:1) indicate that oxidation increases with time in an aqueous environment. Oxidised products of PE species are observed in both positive and negative ion mode predominantly as deprotonated and sodiated adducts respectively. In addition to this temporal nature, chain saturation also has an impact with increasing oxidation occurring with multiple double bonds.

Fragmentation patterns of oxidised species in both positive and negative mode contain peaks that are unique to the fragments of their unmodified analogues, and they were well preserved across disparate chain chemistry. In positive mode loss of water (-18 m/z) and loss of azaridine plus water (-61 m/z) were both indicators of general oxidative modification. Uniquely for double oxygen addition [PE+O₂], loss of H₂O₂ (-34 m/z) was a major fragment. Negative ion fragmentation was more structurally revealing as fatty acyl chains which had undergone oxygen addition could be observed as carboxylate ions [FA+O_x]⁻, dehydration products [FA+O_x-H₂O]⁻ and as carboxylate and keto neutral losses [(PE+O_x)-(FA+O_x)]. The repeatability of these fragmentation patterns allows the creation of a database of oxidised PE compounds for automated identification of compounds. MS² data is not able to elucidate the position or nature of the oxygen addition to the fatty acyl chains, although it is likely that it will occur as peroxidation at the allylic and bisallylic positions in SUFA and PUFA respectively for double oxygen addition as has been well documented (Reis and Spickett, 2012). To address the inability to distinguish the carbon position along the radical chain upon which the oxidative modification occurs, it may be possible to perform a further fragmentation step or derivatise the products.

MS³ has been used to identify long-chain oxidation products arising from a single PE species (Maskrey et al., 2007). Furthermore, addition of silver salts to oxidised PC species has been shown to yield positionally specific cleavage between the peroxidised carbon and its distal neighbour (Milne and Porter, 2001). Whilst this information would be interesting and make this work more comprehensive it wouldn't be suitable for inclusion into OxyLipidBlast due to the extra experimental steps required.

Complexity of fragmentation spectra increased significantly as the number of oxygen additions increased. This is likely due to increased potential for isomers (e.g. oxygen addition on different chains) and reduced molecular stability.

To our knowledge, this study represents the first attempt to systematically annotate fragmentation patterns of oxidised PE species with the intention of creating a comprehensive *in silico* database, covering all possible PE products. Most previous work has focussed on PC species as these represent the most abundant phospholipid species in most eukaryotic organisms (Domingues et al., 2008).

However, PE was an ideal starting point for this work as species of this class readily ionise in both positive and negative mode for MS analysis. The data generated within this chapter has been used successfully to create an initial version of OxyLipidBlast, however, this is not yet the envisaged resource. To enable expansion of OxyLipidBlast to a comprehensive database, covering all polar lipids, the work presented within this chapter would have to be repeated on species from the remaining classes of phospholipids (PC, PA, PS, PG, PI etc.). Furthermore increased coverage of lyso- and plasmalogen species would be required for their inclusion into the OxyLipidBlast database as the few representatives in this study are insufficient

for *in silico* expansion. In the case of plasmalogens this is currently infeasible as the few available standards have limited chain chemistry (Avanti polar lipids, 2014). Whilst the current OxyLipidBlast version represents a step forward in the identification of oxidised products in biological samples as there are currently no other software resources for identification of oxidised lipid products, the utility of the software is currently limited. Completion of oxidation in the other classes of phospholipids would create a cross-platform tool which could be used in all lipidomic studies employing tandem mass-spectrometry techniques to identify oxidative damage, regardless of test organism.

4 - Optimisation of mass spectrometric lipidomics and baseline lipidome characterisation of *D. magna* and *C. reinhardtii*

4.1 - Introduction

The lipidome of the keystone ecotoxicological organism *D. magna* is relatively unexplored. To date, there have been no lipidomic studies in *D. magna* and only a small number related to environmental concerns (Degenkolbe et al., 2012, Shen et al., 2012, Yan et al., 2012). Algae been more widely studied due to the interest in algal lipids as a potential biofuel source (Simionato et al., 2013), however, only one lipidomic study has been undertaken in *C. reinhardtii* which was published in Chinese (Yang et al., 2013). FT-ICR MS is an excellent tool for analysis of complex mixtures due to high mass accuracy and resolution (Weber et al., 2011), which has been reflected in its successful use for environmental metabolomics of polar metabolites (Taylor et al., 2009, Taylor et al., 2010, Southam et al., 2011). Shotgun lipidomics, however, has additional inherent challenges as detailed in chapter 1, with isomeric overlap, sample degradation and plasticiser leachate (Lewis et al., 2010) adding complexities compared to the more established polar analysis.

Here we present the first shotgun lipidomic study of *D. magna* to our knowledge. Our first aim was to optimise the polar lipid concentration, handling and subsequent MS analysis to facilitate the shotgun lipidomic workflow outlined in section 2.4. To maintain high throughput extraction whilst avoiding plasticiser leachate, several sample handling methodologies, including two types of leach resistant tips (Polytetrafluoroethylene

(PTFE) and carbon) attached to manual and auto pipettes and a glass syringe, were compared as well as two analysis plate sealing methods, heat-sealing and self-adhesive. The PCR plate used to store samples prior to analysis is a potential source of significant concentrations of plasticiser leachate, however, a viable non-plastic alternative could not be found. Lipid extract resuspension volume is a crucial variable in MS studies as lipid concentration must be maximised from feasible organism numbers whilst yielding workable volumes. In order to find an optimal balance between these factors we assessed the spectra yielded from multiple resuspension concentrations of *D. magna* and *C. reinhardtii* lipid extracts. With an optimised sample analysis methodology achieved, our second aim was to enhance spectral processing by creating robust lists of metabolites which could be used to internally calibrate spectra (Payne et al., 2009). DIMS/MS and accurate mass matching against databases were used to annotate abundant metabolites which should always be present to be calibrated against with accurate m/z values. With robust analytical methods our final aim was to produce annotated baseline polar lipidomes for two ecotoxicological sentinel species, *D. magna* and *C. reinhardtii*. This will improve upon the paucity of research available in this area, as discussed in chapter 1, where only several studies have been conducted with main focus being on total FA composition rather than complete polar lipid species.

4.2 - Materials and methods

4.2.1 - Optimising the preparation of samples for lipidomics analysis

Chloroform extracts from cardiac tissue of cow (*Bos primigenius taurus*) and sheep (*Ovis aries*) extracted previously (Kirwan et al., 2013) were retrieved from storage at -80

°C and pooled to yield a homogenous stock (2 ml, 60 mg/ml tissue wet mass). Mammalian tissue was utilised in this study for ease of access and to minimise time and cost, the aim of this study does not require specific *D. magna* or *C. reinhardtii* tissue. This stock was dried under N₂ and resuspended in non-polar negative ion MS solvent (2.4 ml), vortex-mixed and split into glass vials (n=35). Vials were divided equally into five groups (A-E) prepared along different methods. Aliquots were transferred in quadruplicate to a 384-well PCR plate (Abgene) on ice via a pipette with carbon tip (Advion) (groups A&D), a F1 pipette (Finnpipette, Thermo, US) with PTFE tip (group B), or a Novus auto-pipette (Finnpipette, Thermo, US) with PTFE tip (group E) or a glass syringe (group C), and immediately covered with self-adhesive foil. Following sample transfer completion the self adhesive foil was removed from groups A, B, C and E and resealed with a heat sealer (Thermo-Fisher) (Table 4-1).

Table 4-1 Sample preparation differences.

| Group | Sealant | Dispense | |
|-------|---------------|---------------|-------------|
| | | Tips | Manual/Auto |
| A | Heat | Carbon | Manual |
| B | Heat | PTFE | Manual |
| C | Heat | Glass syringe | Manual |
| D | Self-adhesive | Carbon | Manual |
| E | Heat | PTFE | Auto |

The resultant PCR plate was analysed along the shotgun lipidomic workflow described in section 2.4. For data processing, a stringent sample filter (100 %) was applied with only mass features present in every sample retained in the output matrix. Relative

standard deviations (RSD, Equation 4-1) of peak intensity were calculated for every mass species observed.

Equation 4-1 RSD equation where σ and \bar{x} are standard deviation and mean of peak intensity respectively.

$$RSD = \frac{\sigma}{\bar{x}} \times 100$$

4.2.2 - Optimising the concentration of *D. magna* and *C. reinhardtii* extracts for mass spectrometric analysis in collaboration with Dr. Nadine Taylor (U of Birmingham)

D. magna neonates (800, <24 h) were grown (48 h), harvested and extracted to replicate control groups of omics exposures detailed in Section 2.4. Chloroform extracts were pooled, vortex mixed, separated into glass vials (n = 8) and dried under a gentle stream of nitrogen. Residues were re-suspended in non-polar negative ion solution (100 μ l, MeOH:CHCl₃, 2:1 w. ammonium acetate (5 mM)) to yield a concentration of 1 neonate μ l⁻¹. Sequential dilutions were made to yield four further concentration groups (0.50, 0.33, 0.17 and 0.08 neonate μ l⁻¹).

C. reinhardtii was cultured in sterile 2 l Erlenmeyer flasks in a shaking incubator (120 rpm) (Multitron, Infors HT) under a 12:12 light : dark regime at 22 °C in BBM media (without EDTA, section 2.2.2.1). Optical density at 660 nm was used to determine cell density with comparison to a growth curve. *C. reinhardtii* cells in exponential growth at a density of 1x10⁶ cells ml⁻¹ were retrieved in 1 ml aliquots (n=8) and added to ice cold methanol (1 ml), mixing by inversion. Cell suspensions were centrifuged (2 min, -9 °C,

16,000 rpm) and the supernatant discarded before storage at -80 °C prior to extraction. Lipids from *C. reinhardtii* were extracted analogously to *D. magna* (section 2.4) with different solvent volumes (CHCl₃:MeOH:H₂O = 500:500:450 μl). Chloroform extracts were dried under N₂ before re-suspension in non-polar negative ion MS solvent and sequential dilution to yield four concentrations (1.33x10⁵, 6.65 x10⁴, 2.66 x10⁴, 1.33 x10⁴ cells μl⁻¹).

All re-suspended lipid extracts were then analysed and processed along the shotgun lipidomic workflow detailed in section 2.4. Dilution group spectra were processed independently in order to compare the respective output matrices.

4.2.3 - Definitive identification of selected lipids to form a robust calibration list in collaboration with Dr. Nadine Taylor (U of Birmingham)

Groups of 30 *D. magna* neonates (<24 h) and aliquots of *C. reinhardtii* (inoculation density = 1x10⁶ cells ml⁻¹) were grown for 48 and 72 h respectively, harvested, extracted and re-suspended as detailed in section 2.4 and 4.2.2 to yield lipid extracts ready for MS analysis. Data dependant *D. magna* spectra were obtained analogously to the method utilised in section 3.2.3. Accurate *m/z* data and MS/MS scans were recorded in negative ion mode for each SIM-window used in shotgun lipidomic MS analysis (Section 2.4). Accurate *m/z* values were matched against the entire LipidMAPS and KEGG databases via MI-Pack to give potential peak identities. Fragmentation patterns were used to confirm or refute these identities. Deprotonated fatty acids were confirmed by the loss of CO₂ and H₂O and the loss of propanoate (M-(CH₂)₂CO₂) which has been reported previously (Kerwin et al., 1996). Phospholipids were identified by appropriate

carboxylate ions and corresponding neutral losses which matched the sn1 and sn2 chains in the putative ID. Additionally, loss of serine (M-87 Da) was indicative of [PS-H]⁻, loss of methyl acetate (M-74 Da) of [PC+Ac]⁻, and loss of inositol (M-163 Da) of [PI-H]⁻. LipidBlast was also used to match in silico fragmentation patterns to experimental fragmentation patterns using a precursor ion accuracy cut off of <2 ppm. *C. reinhardtii* extracts were analysed and processed along the shotgun lipidomic workflow with a stringent signal to noise ratio to ensure robust calibrant peaks (SNR = 100, section 2.4). Algal lipids were putatively annotated via accurate *m/z* comparison (<2 ppm) to the unicellular algal lipidome reported previously (He et al., 2011).

4.2.4 - Annotation of baseline lipidomes of *D. magna* and *C. reinhardtii*

Groups of 30 *D. magna* neonates (<24 h, n = 11) and aliquots of *C. reinhardtii* (starting density = 1×10^6 cells μl^{-1}) were collected and grown for 48 and 72 h respectively to replicate lipidomic exposures (Section 2.4). Organisms and cells were harvested, lipids extracted and analysed with FT-ICR MS in negative ion mode as detailed in section 2.4 and 4.2.2. A 2/3 replicate filter was applied followed by an 85 % sample filter. The *m/z* values and mean intensities from the output matrices were used to create peak lists which were matched against the LipidMAPS database modified by the most abundant negative adducts ([M-H]⁻, [M+35Cl]⁻, [M+37Cl]⁻, [M+Ac]⁻) with MI-Pack software using a defined mass error cut-off (determined from results presented below to be <2 ppm). A further MS² analysis was implemented by Dr. A Southam to separate the isomeric species [PS-H]⁻ and [PC+Ac]⁻. A *D. magna* lipid extract was prepared and directly infused into the FT-ICR MS as described in section 2.4. Spectral features were isolated

in m/z 100 wide SIM windows and fragmented with CID (collision energy = 80 kV). Fragments were collected in the FT-ICR MS in windows m/z 100 wide and m/z 80 Da lower than the isolation window. The resulting fragmentation spectra were processed analogously to DIMS spectra along the SIM-stitch workflow. The resulting mass list containing the major fragments from all spectral features was transformed with the exact mass of methyl acetate (m/z 74.03677) and serine – H₂O (m/z 87.03203) to yield two new peak lists containing potential [PC+Ac]⁻ and [PS-H]⁻ ionic masses respectively. These peak lists were matched against LipidMAPS phospholipid database using MI-Pack with a mass error cut-off <2 ppm. The “PC” and “PS” peak lists were used to confirm or refute putative PC and PS annotations from the baseline lipidome annotation.

4.3 - Results and discussion

4.3.1 - Optimisation of the sample preparation methodology for mass spectrometric lipidomic analysis

Only four out of seven MS analyses successfully ran for samples in group D (self adhesive sealant), compared to seven out of seven in the other groups (heat sealed). These MS failures occurred increasingly with run time, indicating solvent evaporation as the crucial factor. This evaporation occurs despite counteractive precautions such as ice for sample preparation and a cooled plate holder during MS analysis. The failure to avoid solvent escape discounts self adhesive as a plate cover for future experiments and so group D is only included in further discussion for interest.

Peak intensity variability represented by median RSD across the whole dataset ($RSD_{(639)}$) and RSD across the 100 most intense, reproducible peaks ($RSD_{(100)}$) is

detailed in Table 4-2 Table showing median RSD values from sample preparation optimisation analysis. Grey shading denotes lack of reliable sample spray from group D resulting in 3/7 analyses failing.. From the normalised output matrix (639 *m/z* values) median RSD values identified group A as being the most reproducible ($RSD_{A(639)} = 13.49\%$, $RSD_{A(100)} = 9.18\%$). The most variable analysis was group E using the automatic pipette fitted with solvent resistant PTFE tip ($RSD_{E(639)} = 18.21\%$, $RSD_{E(100)} = 14.21\%$), followed by group C with the glass syringe ($RSD_{C(639)} = 16.57\%$, $RSD_{C(100)} = 13.10\%$), and group B with the PTFE tip ($RSD_{B(639)} = 15.03\%$, $RSD_{B(100)} = 9.59\%$). This data suggests manual pipetting is more reproducible over both automated pipetting and manual syringing, probably due to instrumental and human error respectively. Carbon tips appear slightly more reproducible than PTFE tips which may be due to a smaller aperture allowing greater control over the aliquot. The methodology used for group A will be utilised for all sample handling from here. In addition to reproducibility, methodology A avoids sample cross-over from re-use of the glass syringe, and while some leachate from the carbon tip is likely, this would occur during sample delivery unavoidably, a significant advantage over any leachate from PTFE tips which would otherwise be absent.

Table 4-2 Table showing median RSD values from sample preparation optimisation analysis. Grey shading denotes lack of reliable sample spray from group D resulting in 3/7 analyses failing.

| Group | Sealant | Dispense | | Median RSD (all peaks) | Median RSD (top 100) |
|-------|---------------|---------------|-------------|---------------------------|-------------------------|
| | | Tips | Manual/Auto | | |
| A | Heat | Carbon | Manual | 13.49% | 9.18% |
| B | Heat | PTFE | Manual | 15.03% | 9.59% |
| C | Heat | Glass syringe | Manual | 16.57% | 13.10% |
| D | Self-adhesive | Carbon | Manual | 12.14% | 8.54% |
| E | Heat | PTFE | Auto | 18.21% | 14.21% |

4.3.2 - Optimisation of the concentration of *D. magna* and *C. reinhardtii* extracts for mass spectrometric analysis

In *D. magna* intensity matrices, peak number decreased with sample concentration across all five sample concentration groups (Figure 4-1). This is expected, as low abundance compounds will fall below the limit of detection as they are diluted (Long and Winefordner, 1983). A linear increase in peak numbers was only observed within the four most dilute groups ($r^2 = 0.998$), above this, increasing concentration had a much lesser impact on peak number. This is likely attributed to ion suppression effects from the more abundant ionic species (Annesley, 2003).

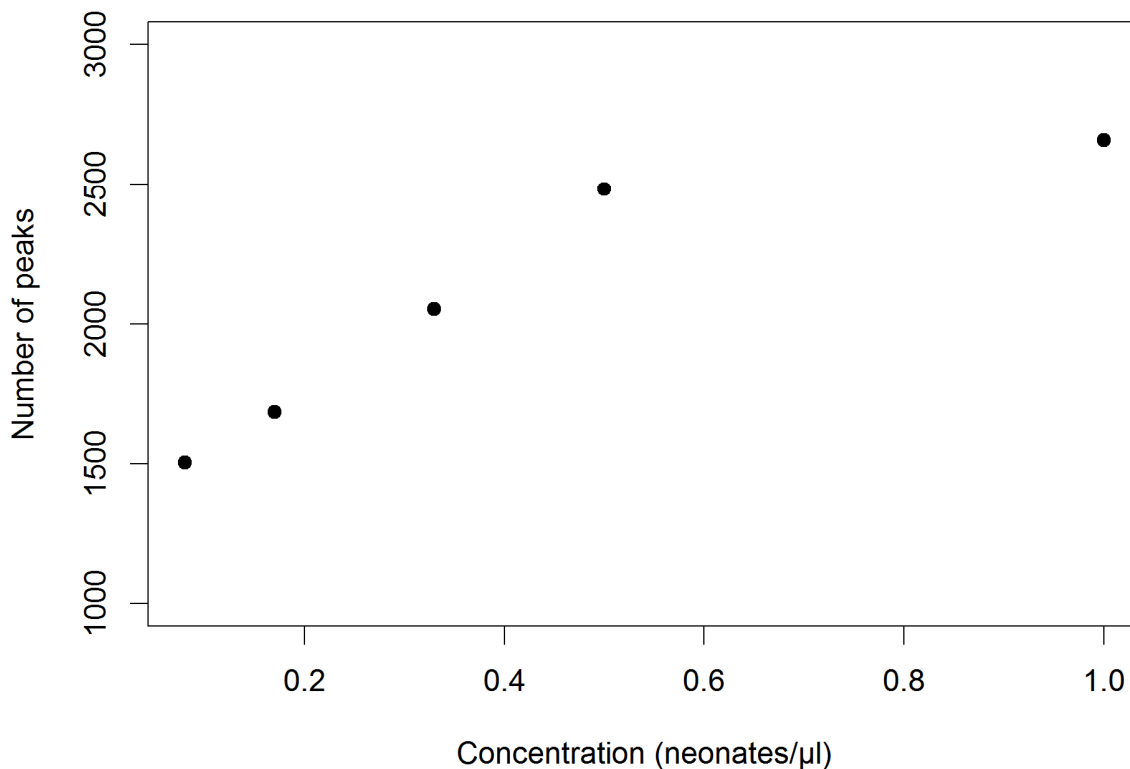


Figure 4-1 Scatter plot showing correlation between mass spectral features and sample concentration of *D. magna* lipid extract. Points represent mean spectral features across concentration groups (n=8).

A lipid extract concentration of 0.5 neonates / μl was chosen for all following *D. magna* lipidomic analyses. Whilst some peaks will be lost using this concentration it will allow more flexibility in handling samples as re-suspension volume will be 60 μl from which 20 μl is required compared to 20 μl from 30 μl at 1 neonate / μl.

In *C. reinhardtii* intensity matrices, peak number did not increase monotonically with sample concentration (Figure 4-2), however, there was a general linear increase ($r^2 = 0.766$). Across the ten-fold dilution there was only a 10 % reduction in peak number

across the ten-fold dilution compared to a 43 % reduction in peak number across the ten-fold dilution of *D. magna* samples.

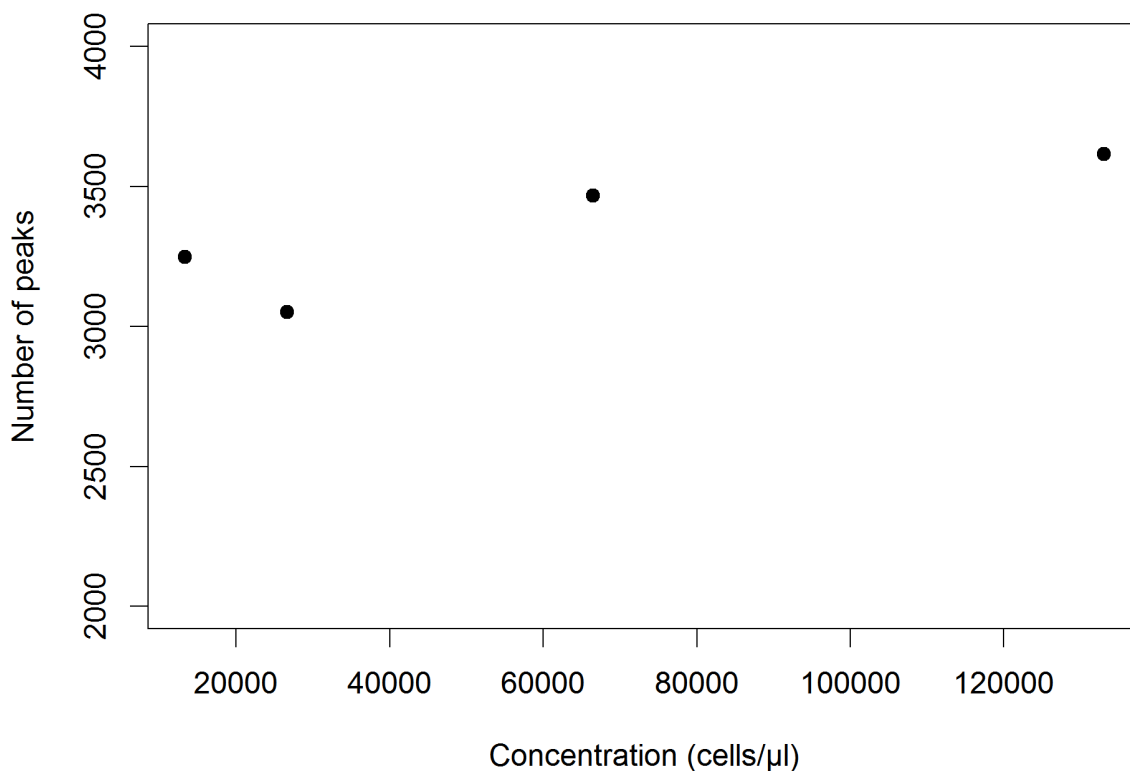


Figure 4-2 Scatter plot showing correlation between mass spectral features and sample concentration of *C. reinhardtii* lipid extract. Points represent mean spectral features across concentration groups (n=8).

Due to the lack of clear saturation point in peak increase with concentration in *C. reinhardtii* a concentration of 6×10^4 cells / μl was selected to allow ease of sample handling. This concentration also requires 60 μl resuspension volume, matching that selected for *D. magna*.

4.3.3 - Creation of calibration list from identified lipids

A m/z list used to internally calibrate negative ion *D. magna* DIMS spectra during processing was created from the fragmentation data obtained above (Table 4-3). As these samples arose from biological tissue unlike the standards in chapter 3, settings could not be tuned to each species and multiple species were fragmented within an isolation window ($m/z=1$), as a result coherent fragments were often not achieved reducing the potential compounds for identification. At low m/z , ions arising from the added ammonium acetate dominate with the deprotonated acetate dimer (m/z 119.03498) and the sodiated equivalent (m/z 141.01692). Free fatty acids are then seen at regular intervals from m/z 143.10775 to 283.26425. One lyso PE species (PE(18:3,0:0)) was observed at m/z 474.26261. Unsaturated PE species were the most commonly observed phospholipid with seven species and five ^{13}C isotopes yielding identifiable fragmentation patterns. Three PS and three PI species were also observed at higher m/z .

Fragmentation patterns of many identified phospholipids showed isomeric chain chemistry. For example in the fragments of m/z 742.53923 carboxylate ions of fatty acids 18:0 (m/z 283), 18:1 (m/z 281) and 18:2 (m/z 279) were all identified. Accurate mass matches for this peak included de-protonated PE(18:1(9Z),18:1(9Z)), PE(18:0,18:2(9Z,12Z)) and PE(18:2(9Z,12Z),18:0). These peaks all have equal mass with the only difference being double bond positions and are inseparable in DIMS. This isomeric situation can include many tens of species particularly with increasing double bond content. To avoid lengthy listing of species, bulk nomenclature will be used from here i.e. PE(18:1(9Z),18:1(9Z)), PE(18:0,18:2(9Z,12Z)) and PE(18:2(9Z,12Z),18:1) are

combined to PE(36:2). All phospholipids manually identified had chain lengths of 34, 36 or 38 reflecting the prevalence of 16, 18 and 20 long fatty acids discussed in chapter 1 as combinations of these chain lengths can only yield 32, 34, 36, 38 and 40 carbon atoms (Bychek et al., 2005, Persson and Vrede, 2006). LipidBlast correctly annotated eight of the 14 manually annotated phospholipids which were contained in the LipidBlast database with reverse dot product scores well in excess of the 600 required suggested by (Kind et al., 2013).

Table 4-3 Identified species used as internal calibrants for *D. magna* lipidomic datasets. LipidBlast column shows the reverse dot product score indicating match success, NA indicates compound is not in the LipidBlast library and No ID indicates the compound is in the database but was not identified.

| ID | Ion form | Theoretical <i>m/z</i> | LipidBlast rev dot score |
|---------------------|------------------------|---------------------------|-----------------------------|
| Acetate dimer | [M-H] ⁻ | 119.03498 | NA |
| Acetate dimer (C13) | [M-H] ⁻ | 120.03833 | NA |
| Acetate dimer | [M+Na-2H] ⁻ | 141.01692 | NA |
| 8:0 | [M-H] ⁻ | 143.10775 | NA |
| 10:0 | [M-H] ⁻ | 171.13905 | NA |
| 12:0 | [M-H] ⁻ | 199.17035 | NA |
| 16:0 | [M-H] ⁻ | 255.23295 | NA |
| 16:0 (13C) | [M-H] ⁻ | 256.23630 | NA |
| 18:3 | [M-H] ⁻ | 277.21730 | NA |
| 18:2 | [M-H] ⁻ | 279.23295 | NA |
| 18:1 | [M-H] ⁻ | 281.24860 | NA |
| 18:1 (13C) | [M-H] ⁻ | 282.25195 | NA |
| 18:0 | [M-H] ⁻ | 283.26425 | NA |
| 18:0 (13C) | [M-H] ⁻ | 284.26760 | NA |
| PE(18:3,0:0) | [M-H] ⁻ | 474.26261 | 998 |
| PE(34:3) | [M-H] ⁻ | 712.49232 | 961 |
| PE(34:3) (13C) | [M-H] ⁻ | 713.49567 | NA |
| PE(34:2) | [M-H] ⁻ | 714.50797 | 984 |
| PE(36:6) | [M-H] ⁻ | 734.47663 | No ID |
| PE(36:6) (13C) | [M-H] ⁻ | 735.47998 | NA |
| PE(36:5) | [M-H] ⁻ | 736.49228 | No ID |
| PE(36:5) (13C) | [M-H] ⁻ | 737.49563 | NA |
| PE(36:4) | [M-H] ⁻ | 738.50793 | 983 |
| PE(36:4) (13C) | [M-H] ⁻ | 739.51128 | NA |
| PE(36:3) | [M-H] ⁻ | 740.52358 | No ID |
| PE(36:3) (13C) | [M-H] ⁻ | 741.52693 | NA |
| PE(36:2) | [M-H] ⁻ | 742.53923 | 994 |
| PS(36:3) | [M-H] ⁻ | 784.51341 | No ID |
| PS(36:2) | [M-H] ⁻ | 786.52906 | No ID |
| PS(36:0) | [M-H] ⁻ | 790.56036 | 985 |
| PI(36:4) | [M-H] ⁻ | 857.51855 | No ID |
| PI(36:3) | [M-H] ⁻ | 859.53420 | 839 |
| PI(38:5) | [M-H] ⁻ | 883.53420 | 807 |

As with the *D. magna* spectra, low *m/z* regions of the *C. reinhardtii* spectra were dominated by acetate dimers and fatty acids (Table 4-4). Only a single phospholipid was identified, PI(34:1). However, other polar lipids associated with algae were observed,

four SQDG, three DGDG and two IPC analogues alongside four novel sulphur containing polar lipids first reported by (He et al., 2011).

Table 4-4 Putatively annotated species used as internal calibrants for *C. reinhardtii* lipidomic datasets.

| Putative annotation | Ion form | Theoretical m/z |
|---------------------|------------------------|-------------------|
| Acetate dimer | [M-H] ⁻ | 119.03498 |
| Acetate dimer | [M+Na-2H] ⁻ | 141.01692 |
| 14:0 | [M-H] ⁻ | 227.20165 |
| 16:1 | [M-H] ⁻ | 253.21730 |
| 16:0 | [M-H] ⁻ | 255.23295 |
| 18:2 | [M-H] ⁻ | 279.23295 |
| 18:1 | [M-H] ⁻ | 281.24860 |
| 18:0 | [M-H] ⁻ | 283.26425 |
| C31H60O4S1, DBE=2 | [M-H] ⁻ | 527.41396 |
| C31H62O4S1, DBE=1 | [M-H] ⁻ | 529.42961 |
| C30H62O5S1, DBE=0 | [M-H] ⁻ | 533.42452 |
| C31H64O5S1, DBE=0 | [M-H] ⁻ | 547.44017 |
| IPC (d33:2) | [M-H] ⁻ | 762.49268 |
| IPC (d33:1) | [M-H] ⁻ | 764.50833 |
| SQDG (31:2) | [M-H] ⁻ | 775.46718 |
| SQDG (31:1) | [M-H] ⁻ | 777.48283 |
| SQDG (32:2) | [M-H] ⁻ | 789.48283 |
| SQDG (33:1) | [M-H] ⁻ | 805.51413 |
| SQDG (34:3) | [M-H] ⁻ | 815.49848 |
| PI (34:1) | [M-H] ⁻ | 835.53421 |
| DGDG (34:5) | [M+Ac] ⁻ | 969.57923 |
| DGDG (34:3) | [M+Ac] ⁻ | 973.61053 |
| DGDG (36:6) | [M+Ac] ⁻ | 995.59488 |

4.3.4 - Annotation of baseline lipidomes of *D. magna* and *C. reinhardtii*

Processed spectra for *D. magna* and *C. reinhardtii* basal lipidomes were quite different, with peak clusters appearing in different m/z regions (Figure 4-3, Figure 4-4). More

spectral features were retained following replicate, sample and blank filters in *C. reinhardtii* compared to *D. magna* (2340 vs. 1638) (Table 4-5). However, putative annotation of spectral features by matching to the LipidMAPS database was more successful for the *D. magna* spectra with 32 % of m/z values being assigned at least one lipid ID. Numerically, more peaks were putatively annotated in *C. reinhardtii* (587 vs. 532), however, this represented only 25 % of the retained spectra.

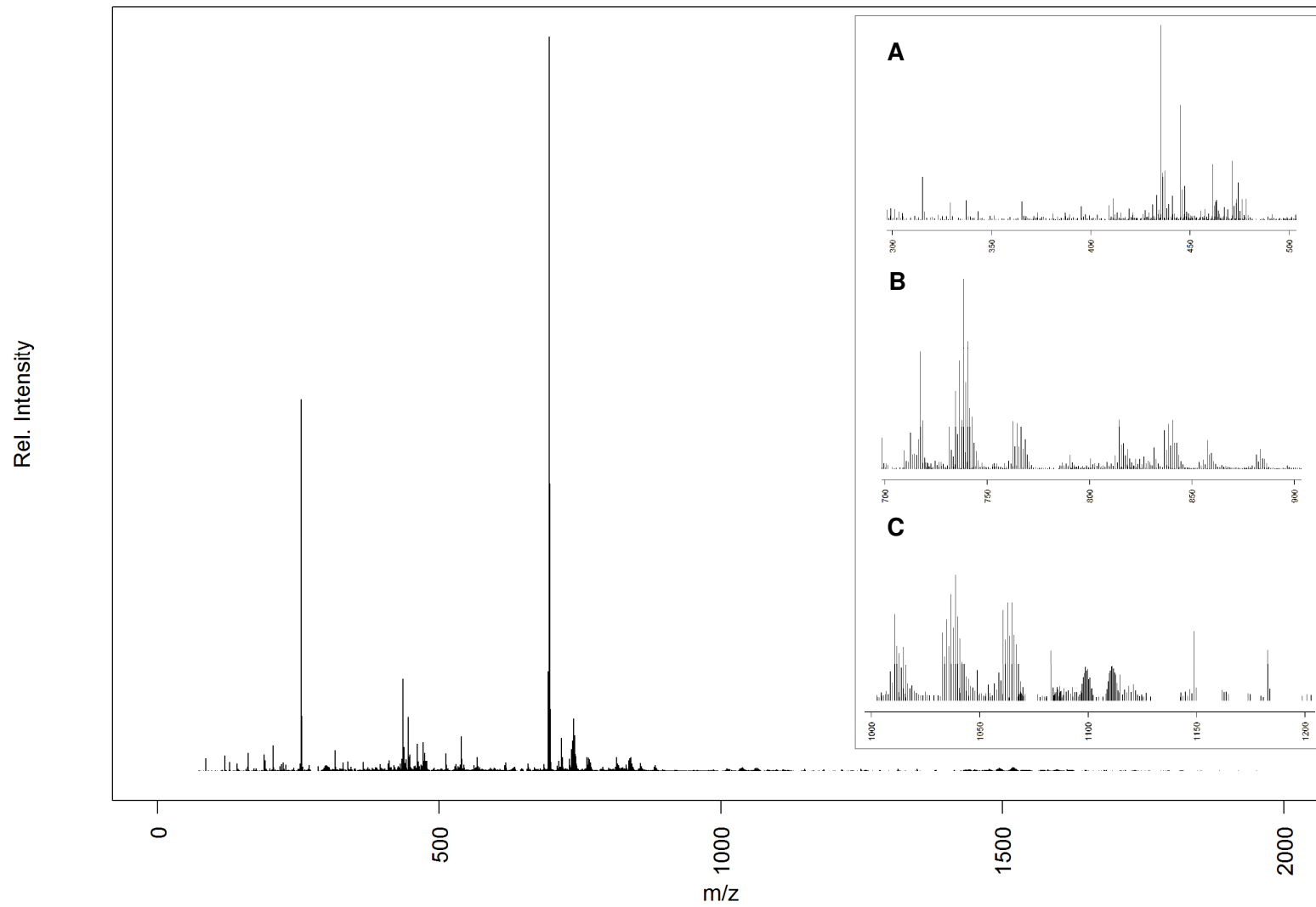


Figure 4-3 Representative mass spectrum of *D. magna* lipid extract. Spectra were collected in m/z range 70-2000. Inserts show zoomed regions containing peaks clusters (A) m/z 300-500, (B) m/z 700-900 (C) m/z 1000-1200. Relative intensity is normalised to peaks contained in zoomed regions.

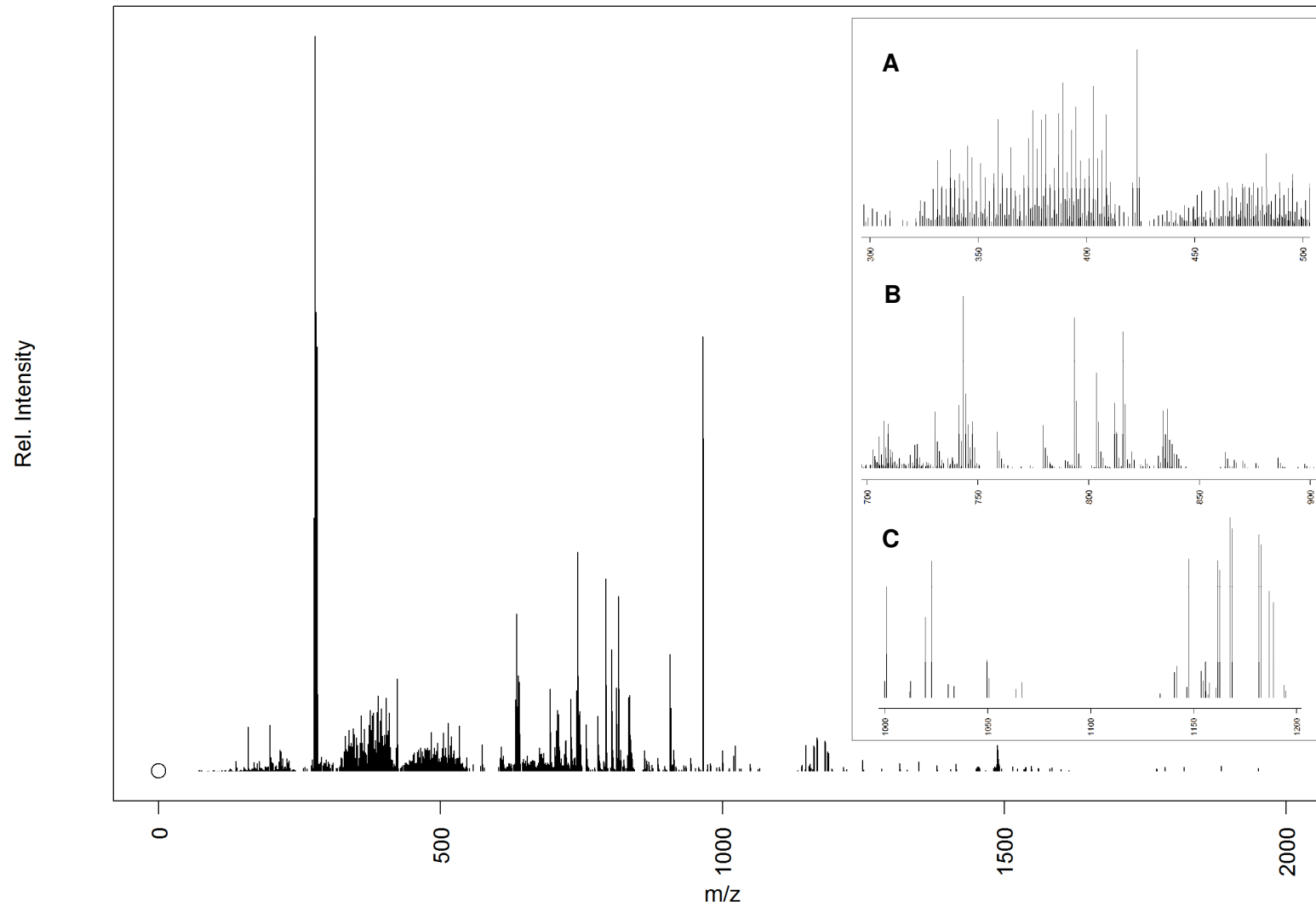


Figure 4-4 Representative mass spectrum of *C. reinhardtii* lipid extract. Spectra were collected in m/z range 70-2000. Inserts show zoomed regions containing peaks clusters (A) m/z 300-500, (B) m/z 700-900 (C) m/z 1000-1200. Relative intensity is normalised to peaks contained in zoomed regions.

Table 4-5 Baseline lipidome peak lists retained following peak lists. Processed peak no. denotes spectral features remaining following processing filters.

| | <i>D. magna</i> | <i>C. reinhardtii</i> |
|--------------------------------------|-----------------|-----------------------|
| Processed peak no. | 1638 | 2340 |
| Annotated with ≥ 1 LipidMAPS ID | 532 (32 %) | 587 (25 %) |

Focussing on the major classes of polar lipids, annotation of the *D. magna* lipidome was significantly greater than the algae (Table 4-6). At least a single adduct of 374 bulk polar lipids were putatively annotated to a mass spectral feature in *D. magna* compared to 133 in *C. reinhardtii* despite the inclusion of the major algal lipids in the filtering. This may reflect the fact that while the LipidMAPS consortium acknowledges and incorporates algal lipids into their database (Sud et al., 2007), there are very few currently included. For example SQDG has been reported as the most abundant polar lipid in *Nannochloropsis oculata* (He et al., 2011) with at least 32 analogues identified, however, the LipidMAPS database currently only includes six, restricting its utility for algal lipid identification. This pattern is repeated with DGTS, DGDG, MGDG, and worse for DGMG, MGMG and MGTS which are completely absent from the database.

Table 4-6 Summary of polar lipids annotated in baseline analysis of *D. magna* and *C. reinhardtii*. Features include lyso and plasmalogens. Lipid annotations are counted only once regardless of multiple ion forms.

| | PA | PC | PE | PG | PI | PS | MGDG | SQDG | DGDG | Total polar lipids |
|-----------------------|----|----|-----|----|----|----|------|------|------|--------------------|
| <i>D. magna</i> | 30 | 87 | 107 | 32 | 35 | 80 | 3 | - | - | 374 |
| <i>C. reinhardtii</i> | 49 | 4 | 14 | 35 | 12 | 11 | 5 | 2 | 1 | 133 |

Histograms were used to visualise ppm across the four adducts ($[M-H]^-$, $[M+Ac]^-$, $[M+^{35}Cl]^-$, $[M+^{37}Cl]^-$) as a guide to most prevalent ion forms and remove false positive annotations (Figure 4-5). Both the $[M-H]^-$ and $[M+Ac]^-$ histograms show putative identifications clustered between -2 and 2ppm error, whereas there is no pattern observed in either of the chlorine isotopes in *D. magna*. Additionally where the ^{37}Cl adduct is observed, it is expected that the ^{35}Cl isotope would also be present due to a greater natural abundance. However, this only happened twice out of 89 Cl ion form annotations with more ^{37}Cl ion forms being annotated in total (38 vs 51). Therefore Cl adducts were removed from the baseline annotation of *D. magna* as unreliable, although it is noted that this probably removes some true positive annotations. In contrast, mass errors of Cl ion forms in *C. reinhardtii* behaved similarly to deprotonated and acetate forms and as such were retained for further analysis (Figure 4-6). Despite robust calibration, a positive mass error offset appeared in five of the six bell shaped histogram plots, with 0.5-1 ppm being the most abundant error bin.

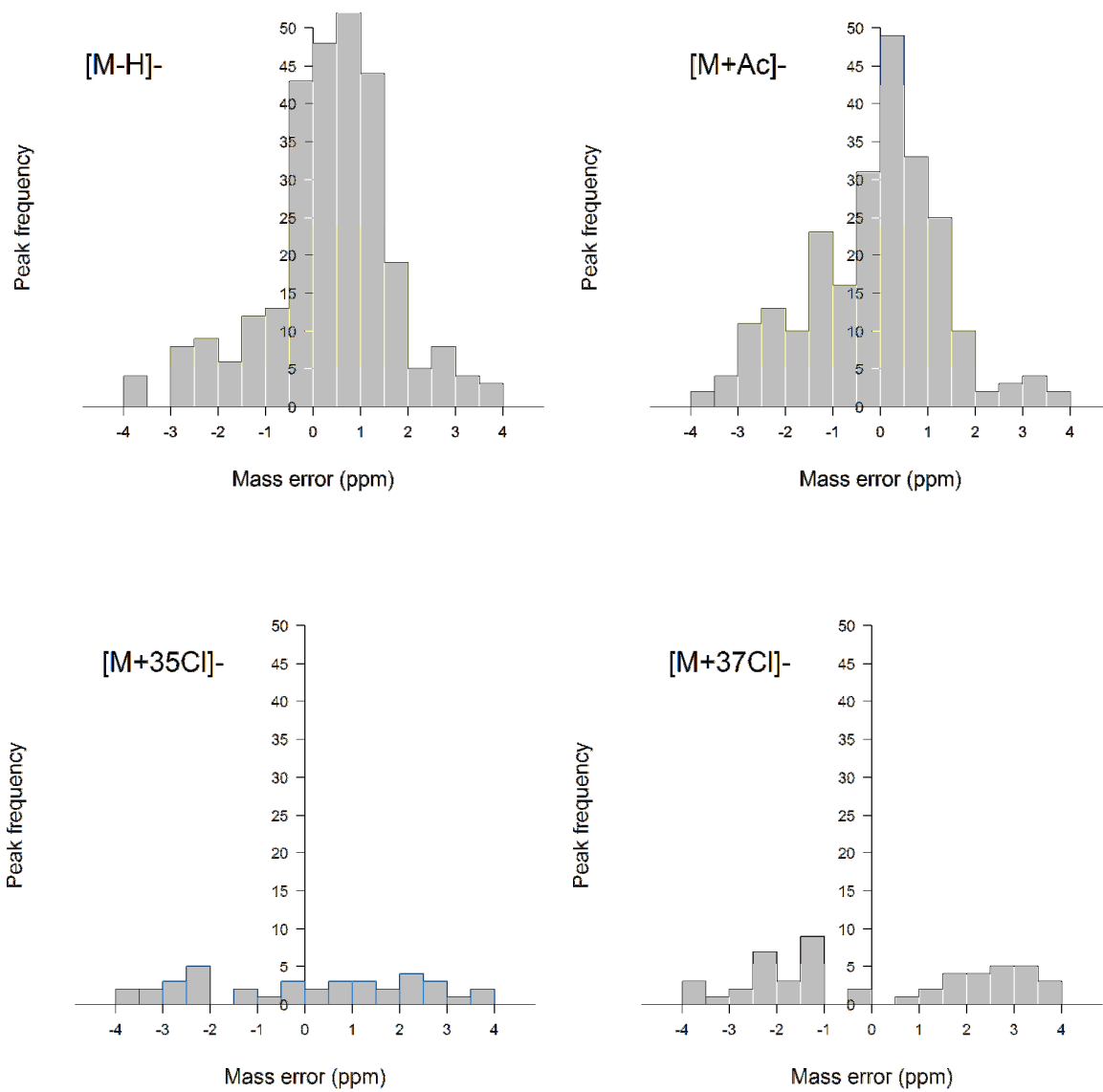


Figure 4-5 Histograms depicting mass error distributions of putatively annotated ion forms within the baseline lipidome of *D. magna*.

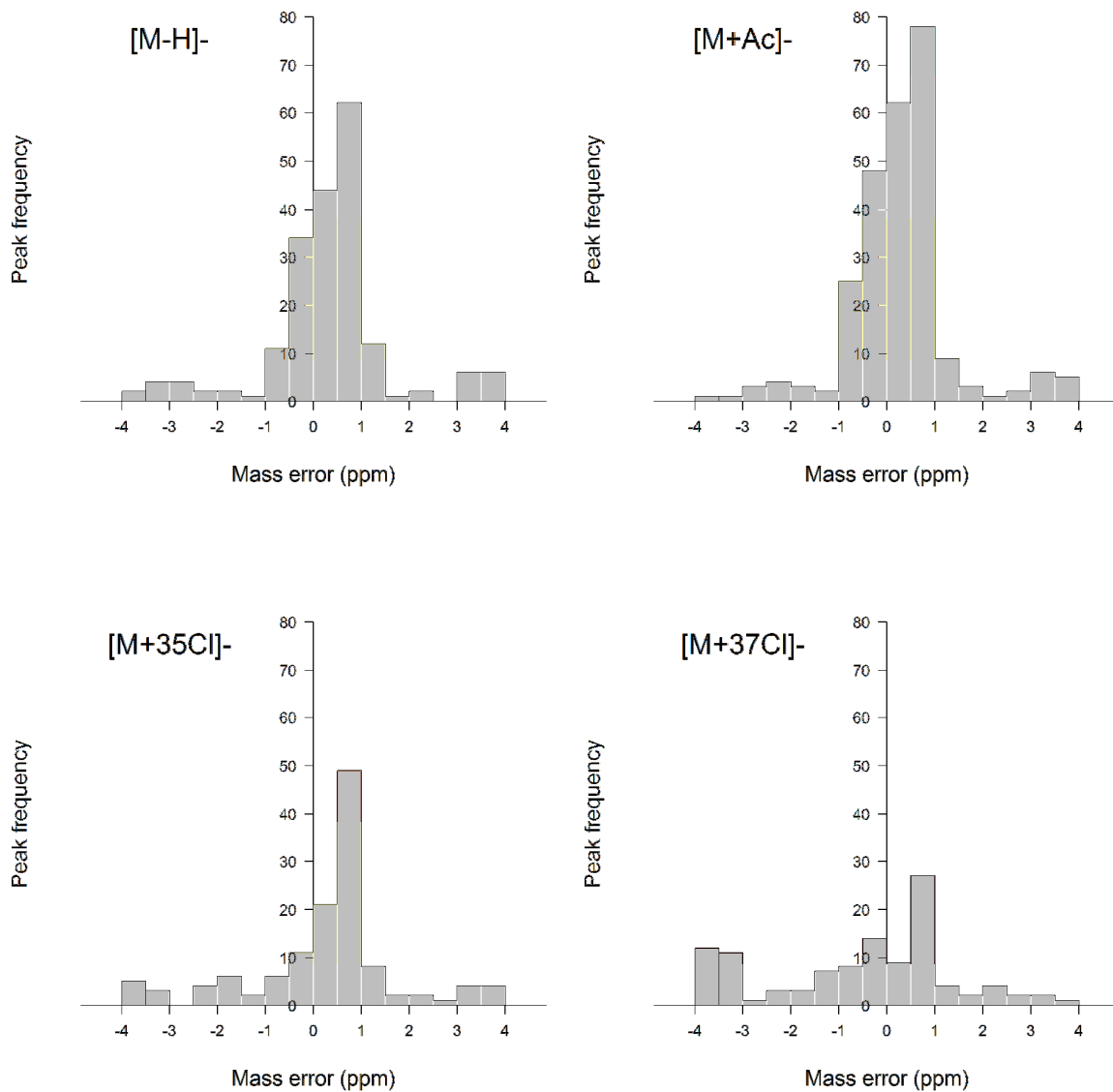


Figure 4-6 Histograms depicting mass error distributions of putatively annotated ion forms within the baseline lipidome of *C. reinhardtii*.

As mentioned previously, isomeric overlap is rife within lipid species: PC/PE, PS/PC, PA/PG all have isomeric overlap. It has been well reported that PC species do not form de-protonated ions with ESI (Pulfer and Murphy, 2003) and so any $[PC-H]^-$ annotations

were also removed from the baseline annotation, there were an abundance of these as [PC-H]⁻ isomerically overlaps with [PE-H]⁻ which should be highly expressed (Bychek et al., 2005). Fragmentation data added a degree of confidence to the putative annotation of 63 of 148 PC/PS species (Appendix III). There was almost total overlap between [PG-H]⁻ and [PA+Ac]⁻, however, PA adducts were almost exclusively odd chained 2 of 17 and de-protonated PGs almost exclusively even chained 15 of 16 (Figure 4-7, Figure 4-10) suggesting that the latter are correct and the PA adducts false positives as odd fatty acyl chains are rare in *D. magna*. Finally, there is isomeric overlap between plasmalogens with a vinyl ether bond at the sn1 position and the lipid subspecies with an ether bond at sn1 should it contain an extra double bond on one of the chains (e.g. PE(P-34:3) & PE(O-34:4)). These species differ only by a single double bond position and as such are extremely challenging to separate and so are treated as single entities for the purpose of this thesis.

Chain length and double bond number both show identifiable but different trends across phospholipid classes. Chain length parity for [PA+Ac]⁻ annotations is predominantly odd (87 % odd), however, this was the only lipid class where that was the case with parity predominantly even in all other classes [PC+Ac]⁻ (53 % even), [PE-H]⁻ (71 % even), [PG-H]⁻ (93 % even), [PI-H]⁻ (71% even) and [PS-H]⁻ (55 % even) (Figure 4-7 - Figure 4-12). A low ratio of odd to even chain lengths is expected given the vast prevalence of even chained fatty acids in *D. magna* with only 15:0 and 17:0 being reported previously in relatively small concentrations (Bychek and Gushchina, 1999, Persson and Vrede, 2006). [PA+Ac]⁻ ion forms were retained in baseline annotation, however, the isomeric overlap with [PG-H]⁻ and extremely high odd chain abundance indicates these

annotations may be false positives as mentioned above. The relatively equal ratios in PC and PS are probably related to the presence of even chained [PE+Ac]⁻ which would appear at the same *m/z* values as odd [PC+Ac]⁻ and [PS-H]⁻. However, in the cases where odd chains were annotated, the adjacent even chains consistently dominated in terms of intensity, as expected, in all classes but PA (Figure 4-13).

The most abundant chain lengths were 34 in PG, 36 in PC and PE, 38 in PI, 40 in PS and 35 in PA species. These chain lengths are expected as they are all potential products of even integers between 16 and 20, the major radical chain lengths in *D. magna* (Persson and Vrede, 2006, Bychek et al., 2005), with 35 for PA likely a false positive (see above). Saturation was split similarly across lipid classes with the following dominant double bond annotations: 2 in PA, PG and PS; 3 in PC; and 4 in PE and PI. A total intensity comparison of double bond annotation creates a bell shaped curve with the abundance order 4 > 3 > 5 > 2 > 6 > 1 > 0 > 7 > 8 > 10 with no annotations of nine double bonds (Figure 4-14). Again this matches previously reported saturations of total FA (Persson and Vrede, 2006, Bychek et al., 2005) as ten out of the possible eleven double bond combinations (0-10) are covered. PI had an unusual double bond pattern with very few species observed with double bond count almost exclusively four-six (Figure 4-14). Comparisons of the relative abundance of SFA to MUFA and PUFA is not possible without fragmentation data, as whilst we know a saturated PL has two SFA chains and a monounsaturated PL has a single SFA and a single MUFA, double bond annotations from 2-6 could all include combinations of SFA, MUFA and PUFA until 7+ double bond annotations most likely arise from two PUFA chains.

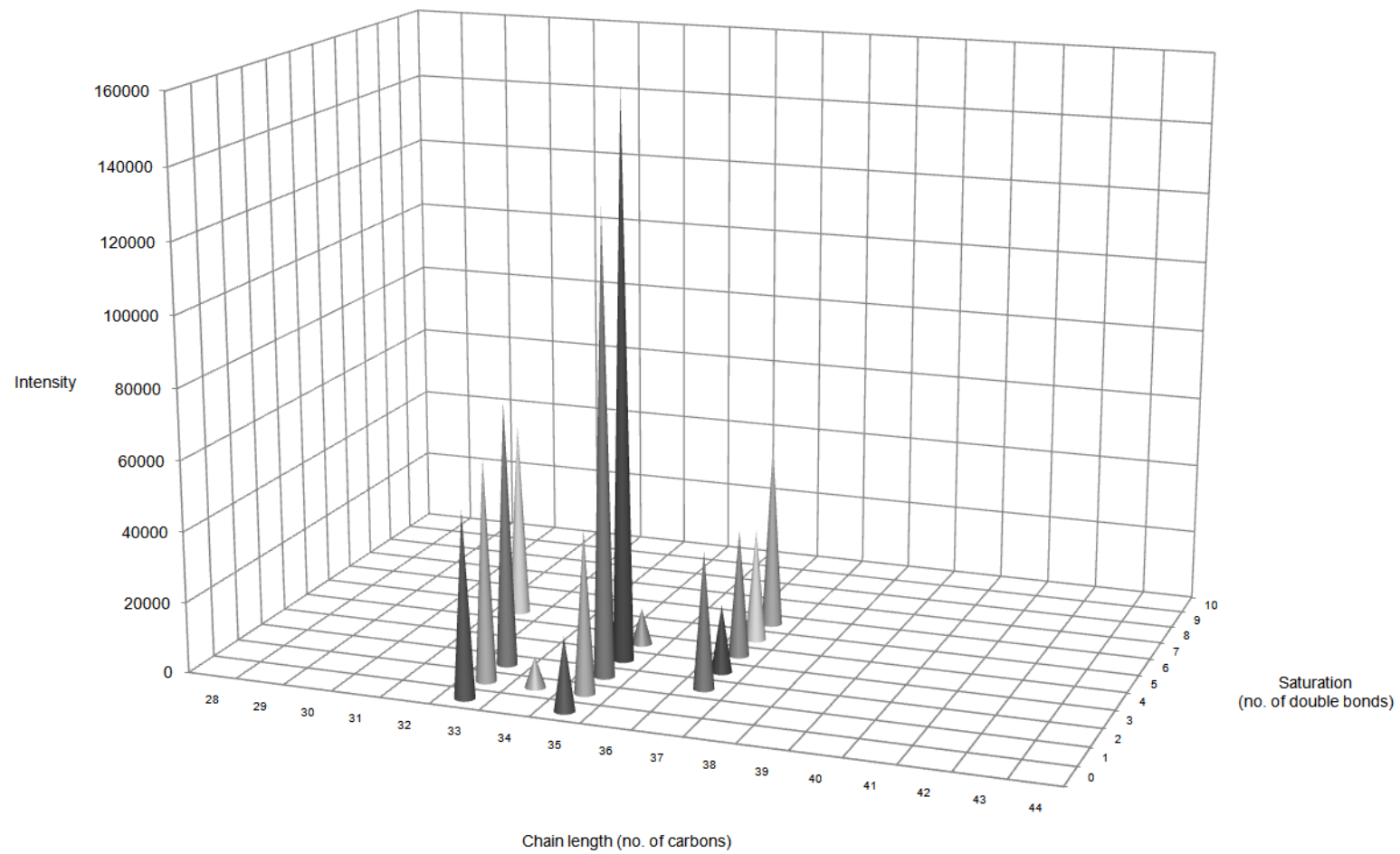


Figure 4-7 Chart showing specific [PA+Ac]- putative annotations of features observed in the basal *D. magna* lipidome. Species are separated along the x-axis by cumulative carbon chain length (sn1+sn2) and along the z-axis by saturation (number of double bonds).

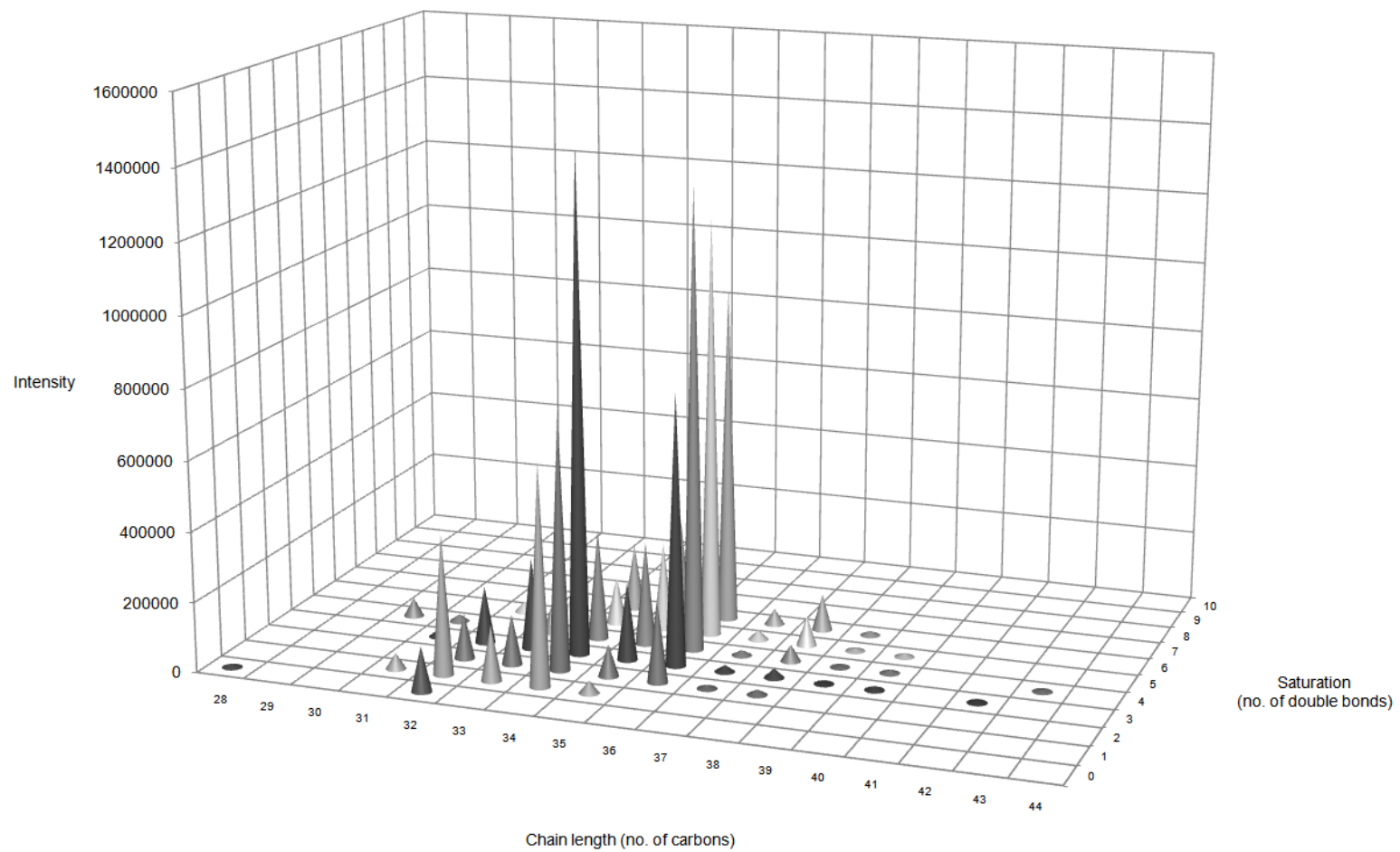


Figure 4-8 Chart showing specific [PC+Ac]- putative annotations of features observed in the basal *D. magna* lipidome. Species are separated along the x-axis by cumulative carbon chain length (sn1+sn2) and along the z-axis by saturation (number of double bonds).

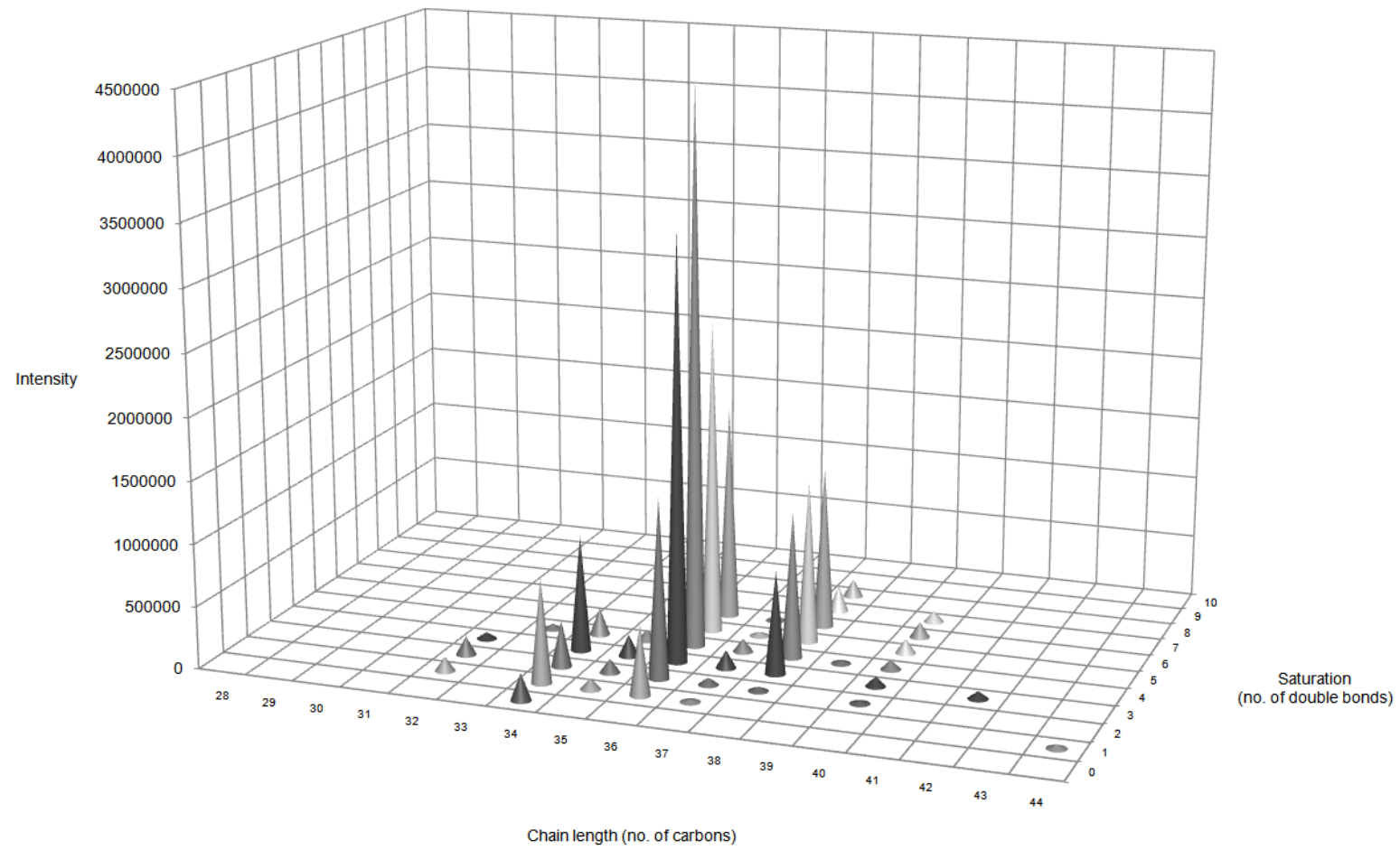
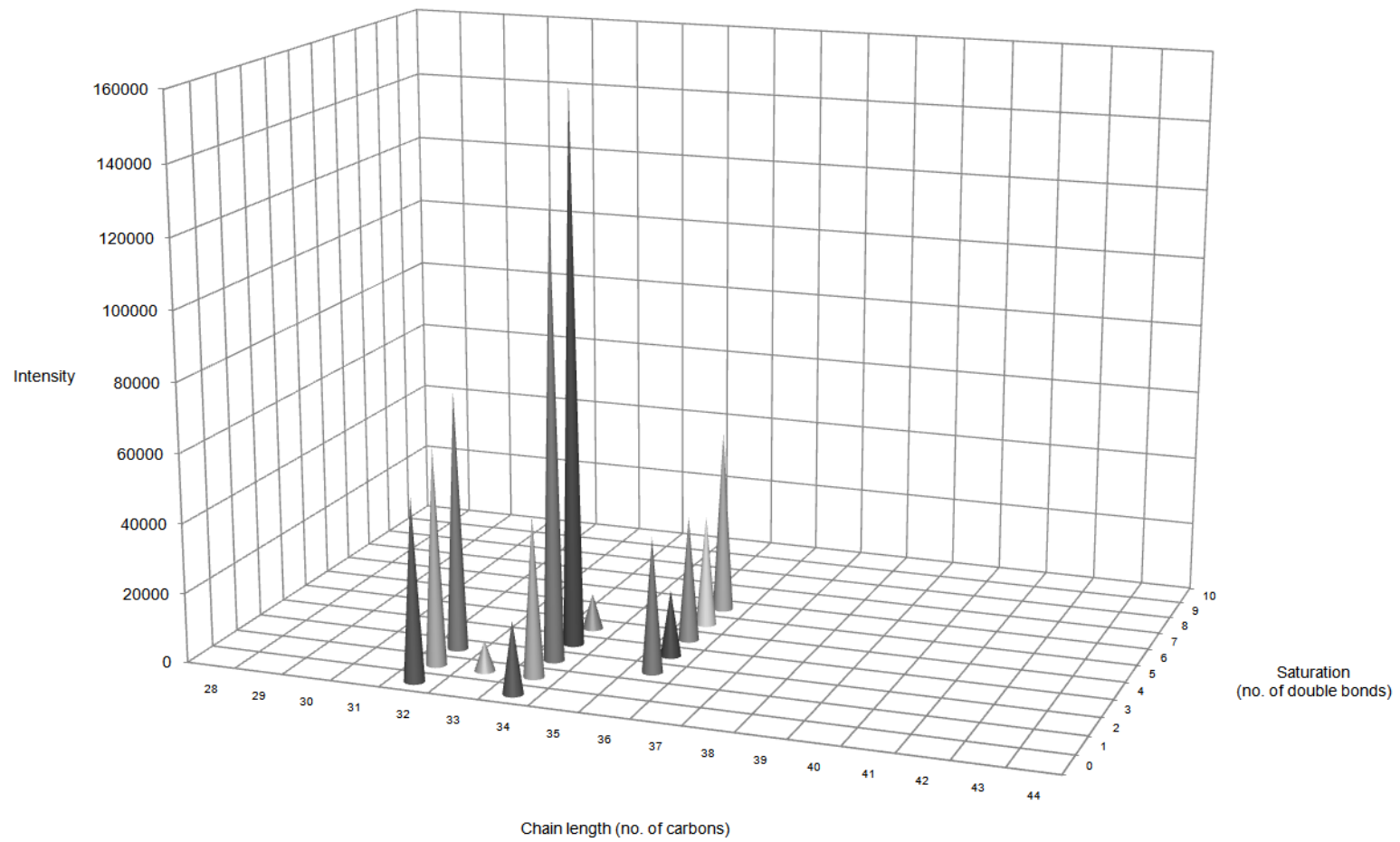


Figure 4-9 Chart showing specific [PE-H]- putative annotations of features observed in the basal *D. magna* lipidome. Species are separated along the x-axis by cumulative carbon chain length (sn1+sn2) and along the z-axis by saturation (number of double bonds).



2 10

Figure 4-10 Chart showing specific [PG-H]- putative annotations of features observed in the basal *D. magna* lipidome. Species are separated along the x-axis by cumulative carbon chain length (sn1+sn2) and along the z-axis by saturation (number of double bonds).

3 10

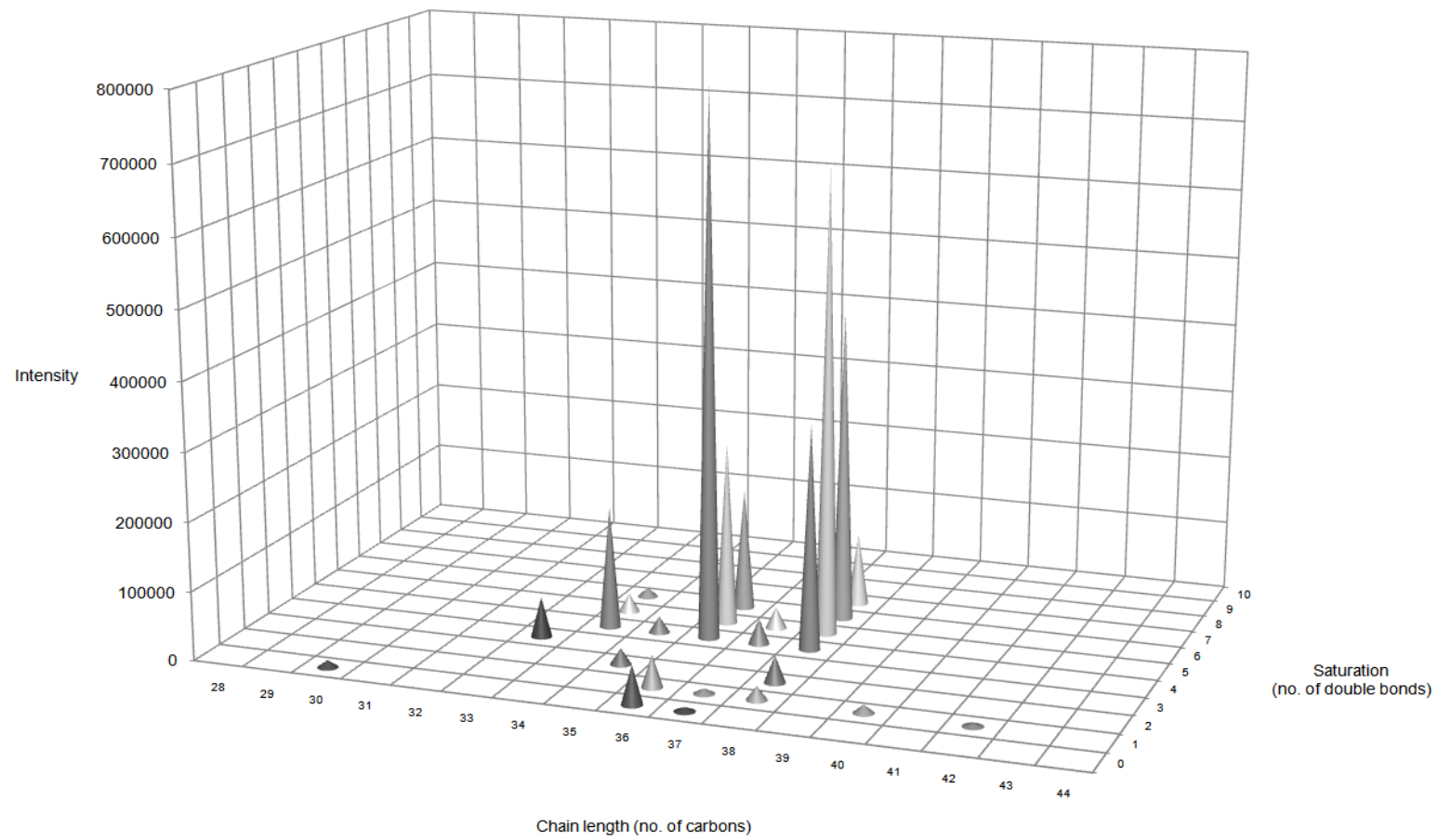


Figure 4-11 Chart showing specific [PI-H]- putative annotations of features observed in the basal *D. magna* lipidome. Species are separated along the x-axis by cumulative carbon chain length (sn1+sn2) and along the z-axis by saturation (number of double bonds).

4 10

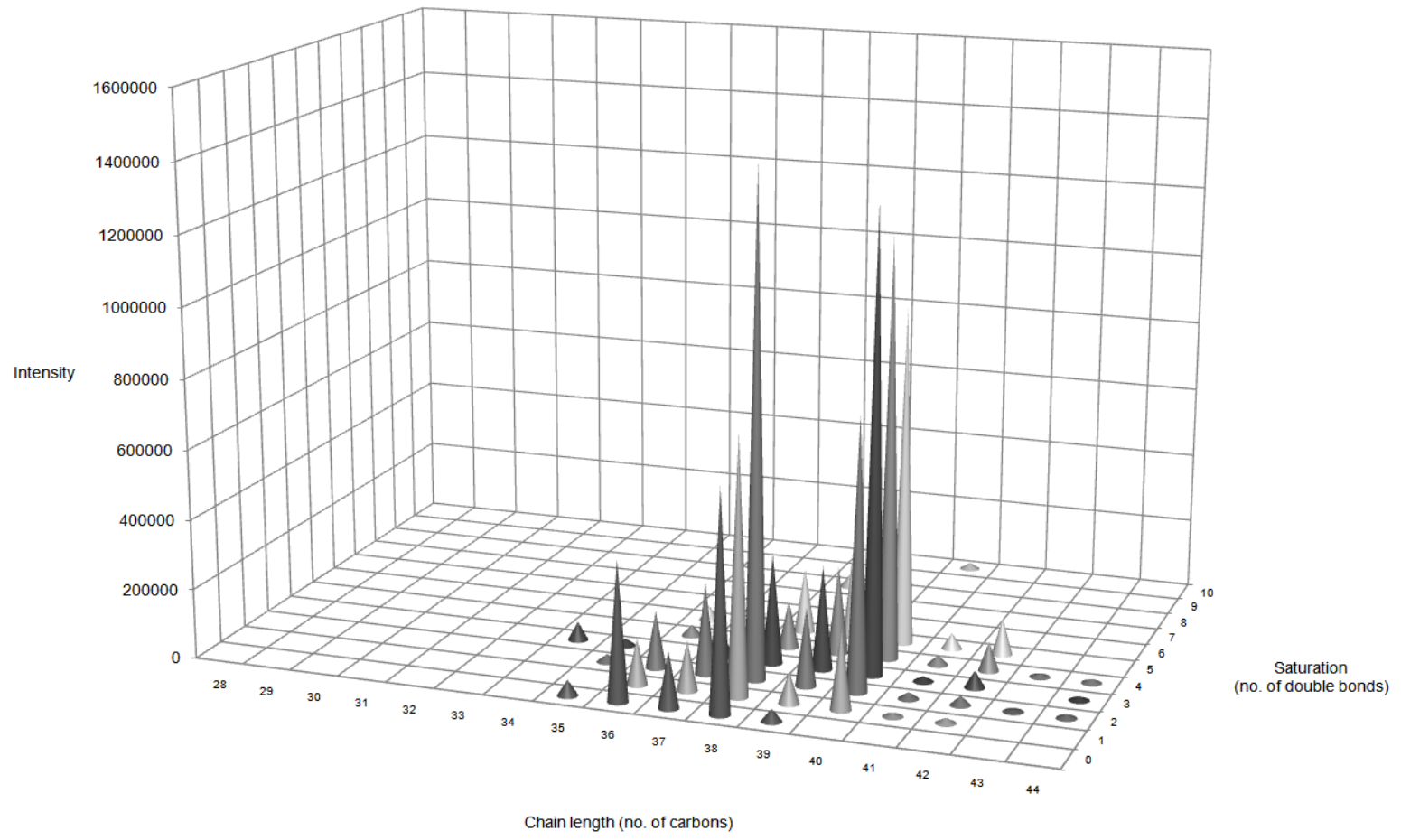


Figure 4-12 Chart showing specific [PS-H]- putative annotations of features observed in the basal *D. magna* lipidome. Species are separated along the x-axis by cumulative carbon chain length (sn1+sn2) and along the z-axis by saturation (number of double bonds).

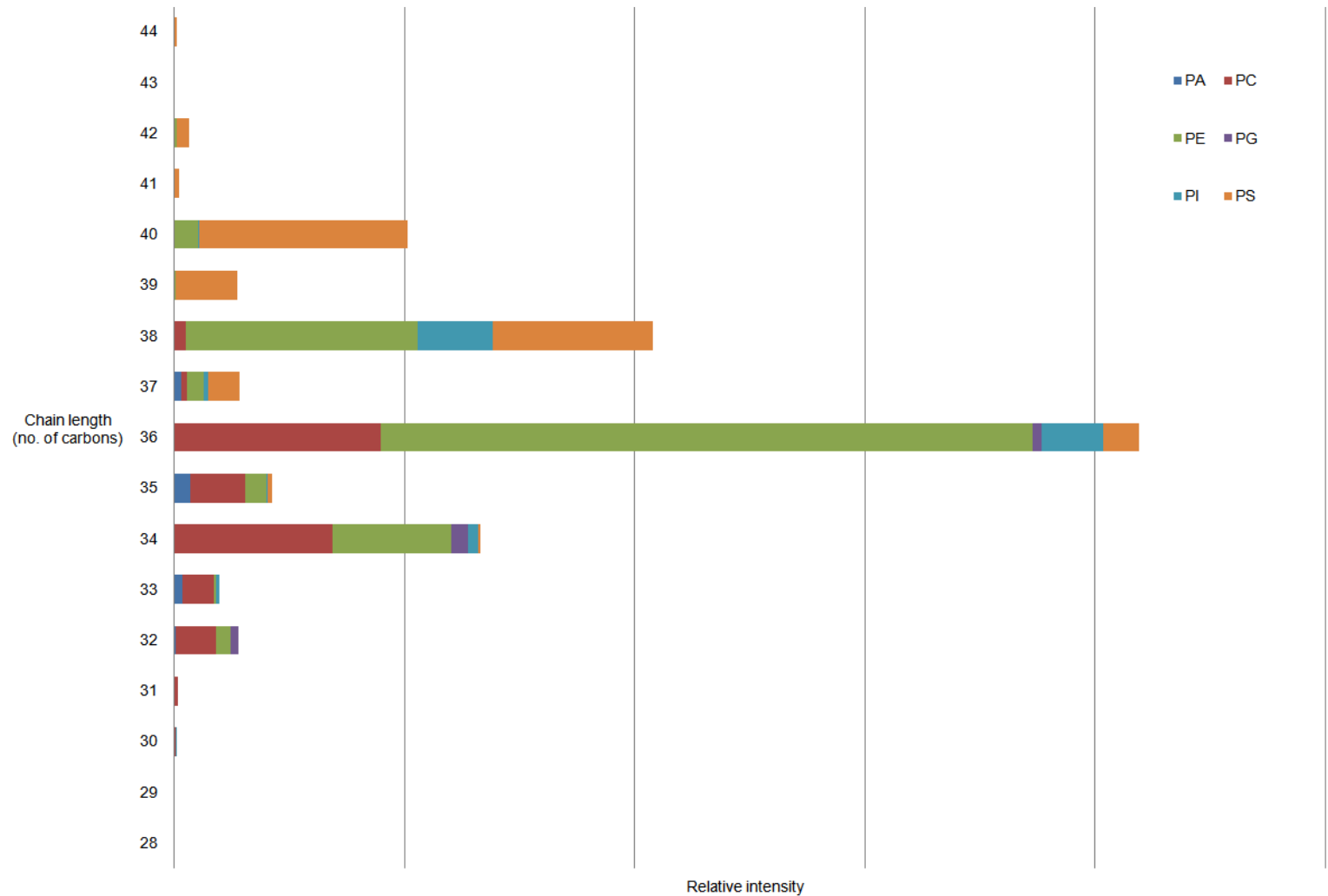


Figure 4-13 Chart showing putatively annotated chain lengths in *D. magna* baseline lipidome. Phospholipid class is shown by colour and order, left to right: navy blue = PA, red =PC, green = PE, purple = PG, teal = PI and orange = PS.

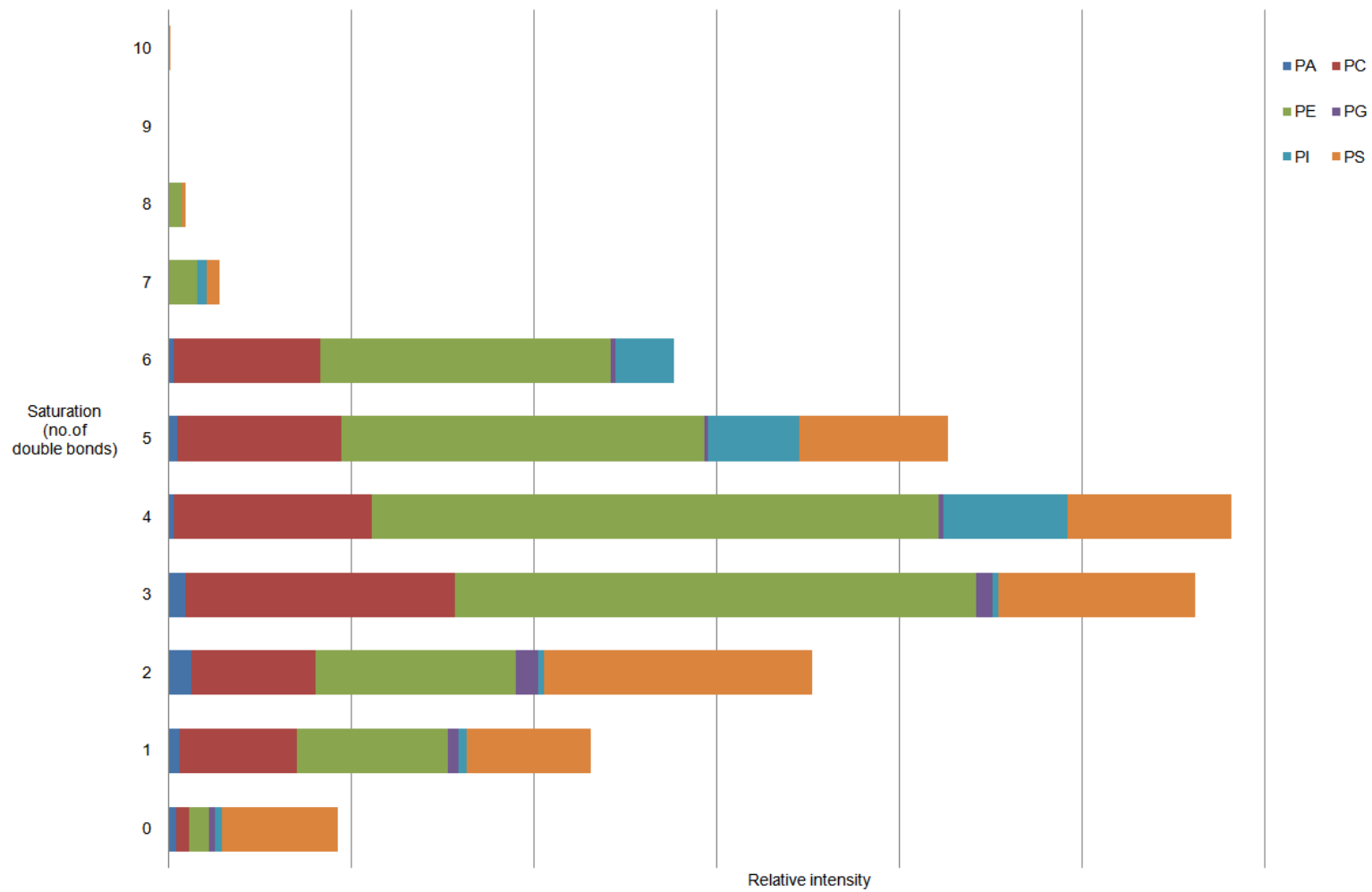


Figure 4-14 Chart showing putatively annotated double bond number in *D. magna* baseline lipidome. Phospholipid class is shown by colour and order, left to right: navy blue = PA, red =PC, green = PE, purple = PG, teal = PI and orange = PS

With far less annotation of polar lipids in *C. reinhardtii*, particularly for phospholipids, similar conclusive data summaries as above are difficult (Appendix IV). The predominant phospholipid classes which were identified were PG and PA, again the isomeric nature of these may account for the dual abundance and while both of these classes have been reported in eukaryotic green algae, PA is noted as a minor compound while PG makes up 10-20 % of the polar lipid component (Lu et al., 2013a, Lu et al., 2013b, Arts et al., 2009). Again the PA annotations had predominantly odd chain parity (54 %) where as the PG species were predominantly even annotations (81 %), suggesting PA annotations may be false positives. Chain parity was predominantly even (79 %) over the other polar lipid classes in line with PG as would be expected. Only eight putative annotations were made for other algal polar lipids, two deprotonated SQDG molecules as reported previously (Yang et al., 2013), a single DGDG acetate adduct and five MGDG ion forms were annotated, three acetate and two ³⁷Cl adducts. While the acetate adducts may indeed be true positives, it is unlikely the ³⁷Cl annotations will be, as we would expect to see equivalent ³⁵Cl adducts with approximately four-fold relative intensity (Kaufmann, 2010).

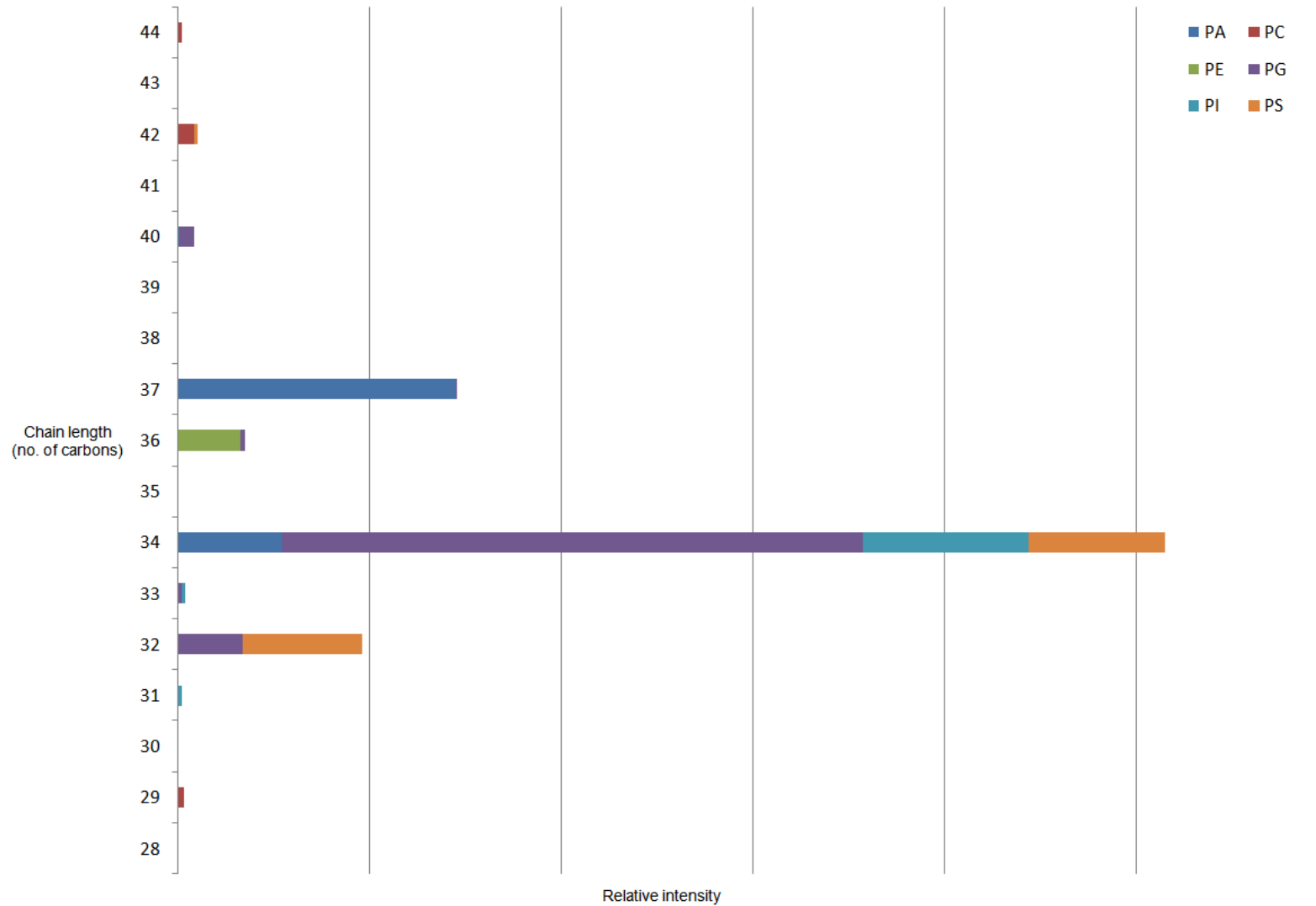


Figure 4-15 Chart showing putatively annotated chain lengths in *C. reinhardtii* baseline lipidome. Phospholipid class is shown by colour and order, left to right: navy blue = PA, red =PC, green = PE, purple = PG, teal = PI and orange = PS

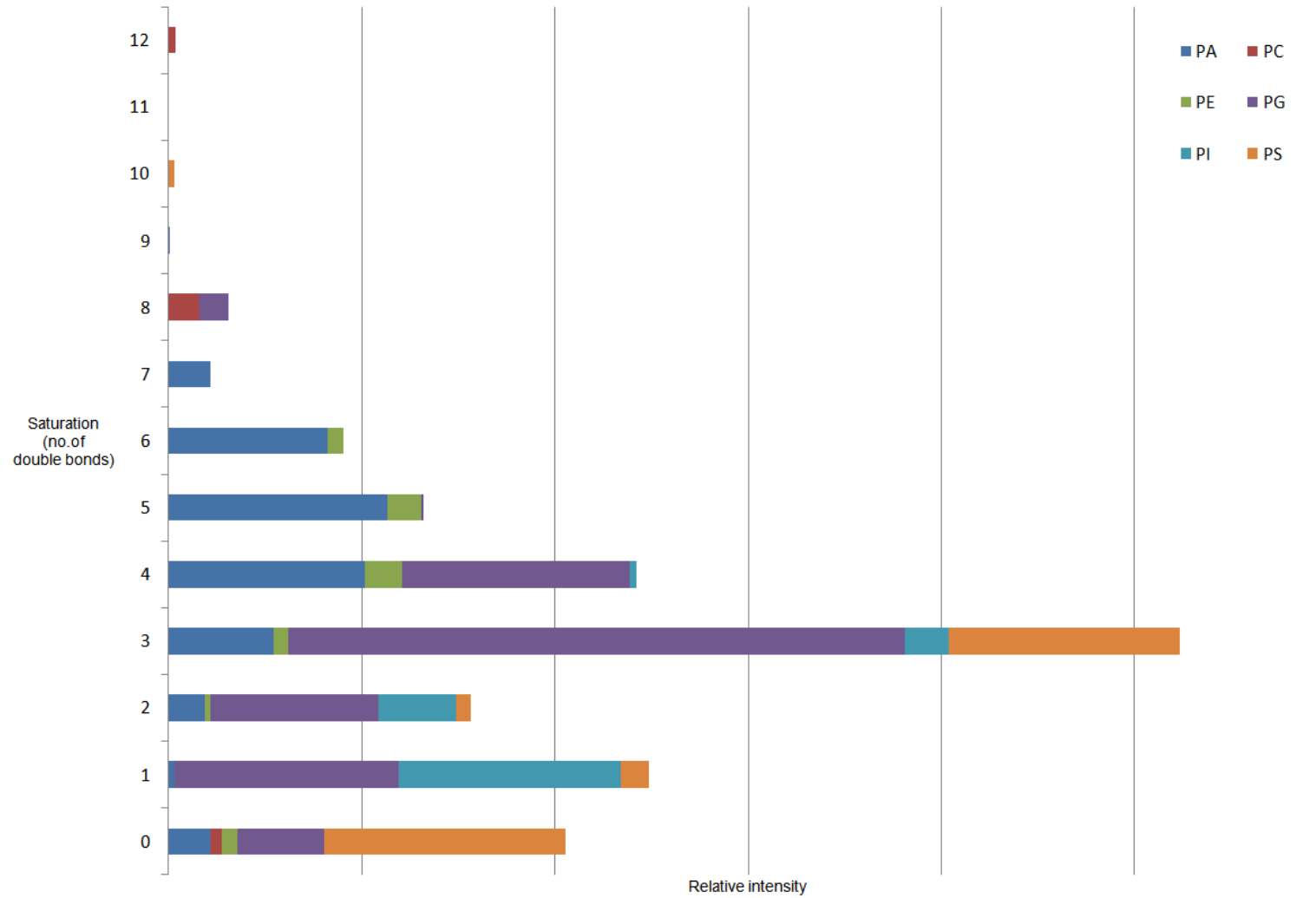


Figure 4-16 Chart showing putatively annotated double bond number in *D. magna* baseline lipidome. Phospholipid class is shown by colour and order, left to right: navy blue = PA, red =PC, green = PE, purple = PG, teal = PI and orange = PS

4.4 - Conclusions

To my knowledge this study represents the first attempt to use shotgun MS lipidomics to annotate the polar lipidomes of *D. magna*, a keystone toxicological species and *C. reinhardtii*, also a widely used toxicological model species.

High quality spectra were obtained following optimisation of lipid handling, and tissue concentration, with mass accuracy further enhanced by internal calibration with abundant peaks identified by MS/MS in *D. magna* and matched to previously identified species in *C. reinhardtii*.

We have identified ion forms of all the major phospholipid classes in both organisms, however, with much greater spectral coverage in *D. magna*. In the freshwater crustacean, chain parity, length and saturation agreed with previously reported total fatty acid and phospholipid class with even chains dominating and a majority of lipids unsaturated to some extent (Bychek and Gushchina, 1999, Persson and Vrede, 2006). PG and PA were the dominant lipid annotations in the *C. reinhardtii* lipidome, with PA more likely false positives, however, there were very few annotations in the other polar lipid classes including algal lipid classes such as DGDG, SQDG and MGDG. The lack of annotation of the features observed from *C. reinhardtii* highlights that while algal lipids have been included within the LipidMAPS database (Fahy et al., 2009), there is still scope for further expansion. Furthermore, it again highlights the major hurdle for lipidomic and metabolomic studies of achieving feature annotation whilst retaining high-throughput analysis (Weber et al., 2011).

The novel, bulk fragmentation methodology implemented by Dr. A. Southam added confidence to PS and PC annotations in the *D. magna* baseline lipidome, however, for

comprehensive annotation separation techniques would be needed to fully negate isomeric overlap. Traditionally this has been done with HPTLC (Tyurin et al., 2009), however, 2D LC is the current gold standard, separating polar lipids by head group along a normal phase column and then by chain chemistry along a reversed phase column (Lee et al., 2013, Brouwers, 2011). While metabolite identification could be achieved with separation techniques the scope for high-throughput analysis is vastly decreased as analysis time is significantly increased. Therefore we did not explore this approach here, since my focus was on the optimisation and application of methods that could be used in high throughput toxicity screening of chemicals and nanomaterials.

5 - Oxidation of the *D. magna* and *C. reinhardtii* lipidomes by *in vitro* and *in vivo* stressors

5.1 - Introduction

Lipidomic analysis has the potential to offer mechanistic insight into the toxicity of both established and novel toxicants, particularly in the detection and localisation of lipid peroxidation during oxidative stress (Reis and Spickett, 2012). Previously, lipid peroxidation has been identified predominantly by increased levels of terminal products such as MDA and 4-HNE, however, these lack specific information such as the class(es) of lipid affected as well as (by implication) the potential to determine the biological location of the toxicity, and few studies have identified individual lipid peroxides *in vivo* (Tyurin et al., 2008). As shown in Chapter 3, ESI DI FT-ICR MS can detect oxidised products of phospholipids which occur from lipid peroxidation with double oxygen addition the most abundant product followed by reduction to single oxygen addition (Horton and Fairhurst, 1987).

Having annotated baseline lipidomes for *D. magna* and *C. reinhardtii* in the previous chapter and oxidised individual lipid standards in chapter 3, here we attempt to use *in vitro* methods to oxidise biological lipid extracts from the two model organisms. We would expect the direct interaction of lipid species and oxidising agents *in vitro* to result in exaggerated oxidative modification compared to *in vivo* oxidative stress, facilitating visualisation of oxidised products.

Oxidative stress was applied to lipid extracts *in vitro* via exposure to air for simplicity, and a more widely reported hydrogen peroxide copper catalysed system ($\text{H}_2\text{O}_2 / \text{CuCl}_2$) shown to cause greater oxidative modification in chapter 3 (Khaselev and Murphy, 2000).

Secondly we aim to induce lipid peroxidation *in vivo* using three xenobiotics shown previously to cause oxidative insult in biological systems: copper, silver and hydrogen peroxide (Cortese-Krott et al., 2009, Gonzalez-Sanchez et al., 2013, Pervaiz and Clement, 2002, Schwarz et al., 2013, Rhee et al., 2013). Despite being an essential trace element for *D. magna*, copper also has significant toxicity at higher doses. The prevalent hypothesis for copper toxicity is the enhancement of ROS formation, which has been supported by numerous *in vivo* studies including a recent metabolomic study in *D. magna* which showed depletion of antioxidant, glutathione (GSH) (Stohs and Bagchi, 1995, Taylor et al., 2009, Bopp et al., 2008). Silver is less studied than copper as an environmental toxicant, however, has been shown to induce lipid peroxidation in mice (Rungby and Ernst, 1992). Finally, hydrogen peroxide is often used in bioremediation and as a disinfectant in aquaculture where it breaks down into harmless oxygen and water, however, it is also classed as a ROS and at high enough doses will cause toxicity in aquatic organisms as shown in *Dicentrarchus labrax* and *Pterophyllum scalare* (Sanabria et al., 2009, Roque et al., 2010). All three compounds represent good models for environmental oxidative stress.

The shotgun lipidomic pathway presented in section 2.4 will be used to assess changes between control and exposed lipidomes in order to detect phospholipid peroxides. If successful, this would yield a high-throughput analytical technique capable of detecting

oxidative stress, in particular lipid peroxidation, but also yielding some mechanistic insight.

5.2 - Materials and methods

5.2.1 - In vitro oxidation of lipid extracts of *D. magna* and *C. reinhardtii*

Groups of 30 *D. magna* neonates (<24 h, n=40) and aliquots of *C. reinhardtii* (inoculation density = 1×10^6 cells mL^{-1} , n=20) were grown for 48 h to mimic control organisms in a lipidomic study and harvested, extracted and dried as outlined previously (section 2.4) to yield lipid extracts stored at -80 °C. Dried samples were subsequently oxidised by one of two methods.

5.2.1.1 - Oxidation of *D. magna* and *C. reinhardtii* lipid extracts by exposure to air

Vials containing *D. magna* (n = 10) and *C. reinhardtii* (n = 10) lipid extracts were retrieved from storage. Lids were removed to expose lipid residues to air (Yamada et al., 1993) and left lightly covered for 168hrs. Air exposed lipid extracts were then re-suspended, analysed, processed and annotated as described in section 2.4, alongside control lipid extracts from *D. magna* and *C. reinhardtii* (n = 10) retrieved from -80 °C storage. PCA was used to identify spectral differences between control and air exposed lipid extracts.

5.2.1.2 - Oxidation of *D. magna* lipid extracts by hydrogen peroxide and copper chloride

Similar to the OxyLipidBlast validation in chapter 3 the remaining *D. magna* lipid extracts (n=20) were retrieved from storage and resuspended in sodium phosphate buffer (0.24 ml, 50 mM, pH = 7.4) with vortex mixing (30 s) and sonication (15 min). Additional buffer (0.3 ml) was added to control vials and H₂O₂ (0.15 ml, 70 mM) and CuCl₂ (0.15 ml, 100 μM) were added to exposed vials. All vials were stored at 37 °C for two hours. Vials were retrieved and placed on ice before cold methanol (0.6 ml) and chloroform (0.6 ml) were added with vortex mixing. Phases were separated further by centrifugation (10 min, 4000 rpm) and the chloroform layer was removed by glass syringe. Chloroform extracts were dried under N₂, re-suspended in non-polar mass spec solvent, analysed and processed along the shotgun lipidomic workflow (section 2.4). Differences between peak intensities in control and exposed lipid extracts were assessed by multivariate PCA and univariate T-tests with a FDR correction to avoid false significance from this large dataset.

5.2.1.3 - Putative annotation of potential oxidation

Spectral features which appeared at a mass difference of one or two oxygen atoms (+O = 15.99492 *m/z*, +O₂ = 31.98983 *m/z*) higher than a second feature within a mass error range of 2ppm were identified by a bespoke script in MATLAB and highlighted as potentially oxidised products. Spectral features which appeared at +O or +O₂ above a second feature and -O or -O₂ below a third feature were also highlighted. These

spectral features could be oxidatively modified lipids which were subsequently oxidised a second time as was observed in chapter 3 or lipids with inherent oxygen differences which were oxidised. Targeted annotation of oxidised lipids was achieved by a similar method by assigning +O and +O₂ to spectral features which were appropriate mass differences higher than lipids annotated in the baseline lipidome created in chapter 4. Annotated lipids which appeared at +O and +O₂ mass differences above a second annotated lipid were also highlighted, these would likely mask oxidation of the second lipid as oxidised products are unlikely to be more abundant than an endogenous species.

5.2.2 - Assessing the acute toxicity of AgNO₃, and H₂O₂ to *D. magna* and *C. reinhardtii*

D. magna acute toxicity assays were performed for silver nitrate (AgNO₃), and hydrogen peroxide (H₂O₂) as described in section 2.3.

C. reinhardtii acute toxicity assays were performed for AgNO₃ following standard toxicity test guidelines (OECD, 2011). Briefly, exponentially growing algal cells were inoculated into sterile Erlenmeyer flasks (50 ml) stoppered with a foam bung at a starting density of 5*10⁴ cells ml⁻¹. AgNO₃ was added to exposure vessels at a range of concentrations and cells were exposed for 72 h under constant light before cell density was determined (section 4.2.2). Cell growth was reported as exposed cell density relative to control cell density.

EC₅₀ estimations for *D. magna* immobilisation and algal cell growth were calculated using the trimmed Spearman-Kärber equation. The highest exposure level without organism immobilisation or cell growth inhibition, the no observed adverse effect level (NOAEL) was recorded.

5.2.3 - In vivo exposure of *D. magna* and *C. reinhardtii* to oxidative stressors

Groups of 30 *D. magna* neonates (<24 h, n = 8) were exposed to one of three compounds at high (NOAEL) and low (NOAEL / 10) concentrations for 48 h (Table 5-1). Groups of 30 *D. magna* (n = 8) were grown in exposure vessels for 48 h with no xenobiotic stress to yield control organisms for comparison.

Table 5-1 Table showing the concentrations of oxidative stressors to which *D. magna* neonates were exposed. *NOAEL for CuSO₄ communicated from Dr N. Taylor (University of Birmingham).

| Compound | High concentration (µg/l) | Low concentration (µg/l) |
|--|---------------------------|--------------------------|
| Silver nitrate (AgNO ₃) | 0.8 | 0.08 |
| Copper sulphate (CuSO ₄)* | 20 | 2 |
| Hydrogen peroxide (H ₂ O ₂) | 2 | 0.2 |

After 48 h neonates were harvested and quenched in liquid N₂ before lipid extraction, MS analysis and processing as described in section 2.4.

C. reinhardtii aliquots (n = 8, initial density = 1x10⁶) were exposed to AgNO₃ at high (8 µg/l, EC₅₀ / 10) and low (0.8 µg/l, EC₅₀ / 100) concentrations for 72 h, alongside vessels with no xenobiotic stress acting as control samples. Following exposure, samples were quenched, extracted and analysed with MS as described in sections 2.4 and 4.2.2.

Data analysis included PCA and univariate techniques to discern differences between exposures. Mass differences of 15.99491 between spectral features were determined in MATLAB using a custom built script and combined with fold change and significance to identify potential lipid peroxidation as described in section 5.2.1.3 -.

5.3 - Results and discussion

5.3.1 - In vitro oxidation of *D. magna* and *C. reinhardtii* lipid extracts

Intensity matrices were obtained for each *in vitro* lipidomic experiment following replicate, sample and blank filtering (*D. magna* Air & H₂O₂, *C. reinhardtii* Air) (Table 5-3). Prior to matrix processing, the percentage of missing values was assessed for each sample to confirm spectral quality, samples with missing values higher than the 95 % confidence interval were discarded. This led to the removal of only one (of 10) *D. magna* air exposed sample and one (of 10) control sample from the H₂O₂ matrix. Matrices were then PQN normalised, missing values replaced with minimum intensities and glog transformed. Principal component analysis (PCA) was completed on glog modified matrices to visualise differences between control and oxidatively modified lipids (Figure 5-1). Significant separation was observed between control and exposed samples in all three studies along PC1 showing that control lipidomes were significantly perturbed *in vitro* both by air exposure and the H₂O₂ / CuCl₂ system (Table 5-2).

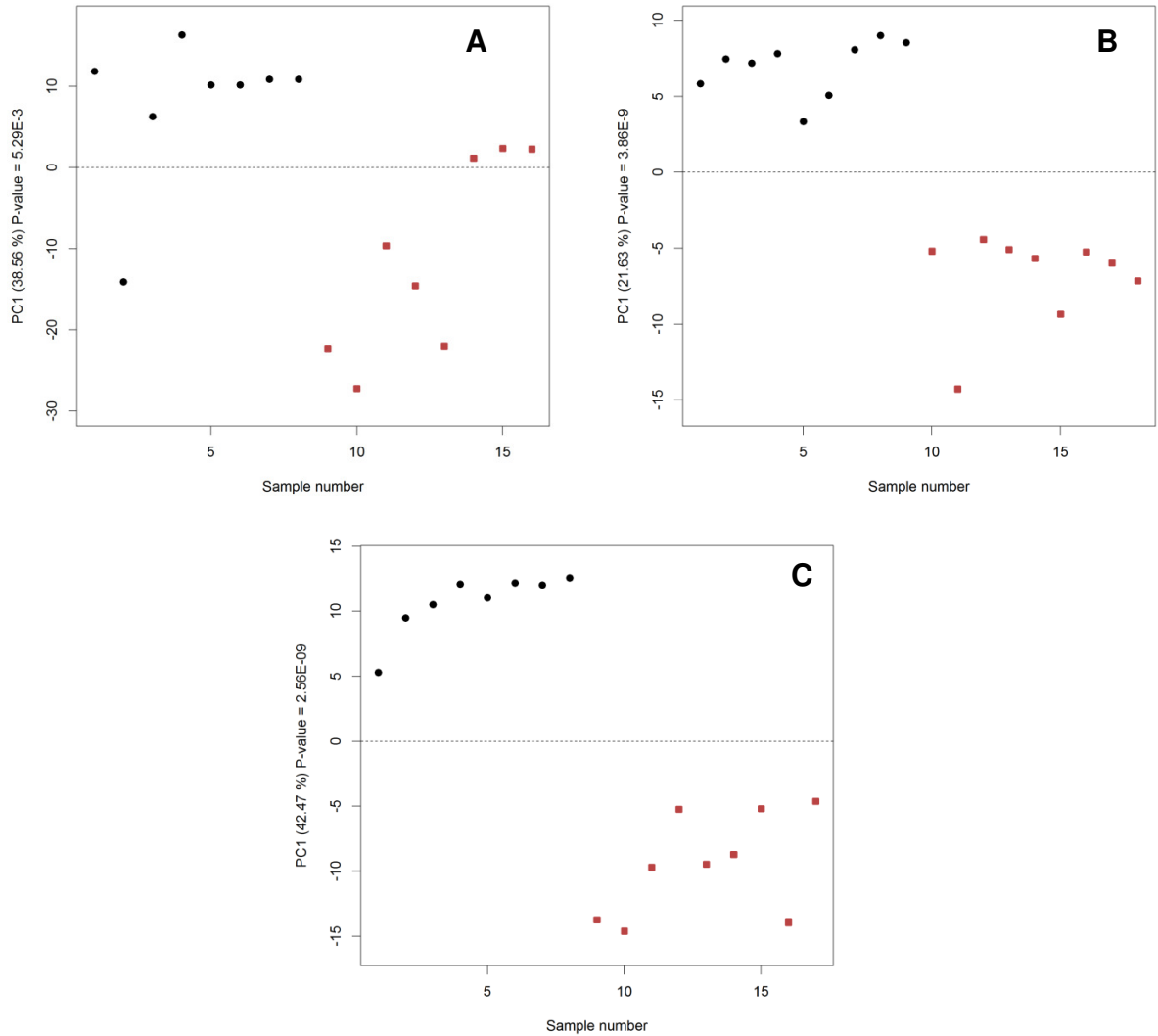


Figure 5-1 Scores plot showing sample number vs. principal component 1 (PC1) for *in vitro* lipid extract exposures. Control samples are denoted by black circles, exposed samples are denoted by red squares. (A) H₂O₂ / CuCl₂ exposure to *D. magna* lipid extract. Significant separation between control and exposed is observed ($P=5.29 \times 10^{-3}$). (B) Air exposure to *D. magna* lipid extract. Significant separation between control and exposed is observed ($P=3.86 \times 10^{-9}$). (C) Air exposure to *C. reinhardtii* lipid extract. Significant separation between control and exposed is observed ($P=2.56 \times 10^{-9}$).

Table 5-2 Table showing significant group separation by principal scores of processed *in vitro* perturbed lipid extracts. * = P<0.05, * = P<0.001.**

| Study | Organism | Principal component significance | | | | | |
|----------------------|-----------------------|----------------------------------|-------|--------|-------|-------|-------|
| | | PC1 | PC2 | PC3 | PC4 | PC5 | PC6 |
| H2O2 <i>in vitro</i> | <i>D. magna</i> | 5.29E-03* | 0.194 | 0.0641 | 0.947 | 0.291 | 0.714 |
| Air <i>in vitro</i> | <i>D. magna</i> | 3.86E-09*** | 0.973 | 0.657 | 0.948 | 0.922 | 0.342 |
| | <i>C. reinhardtii</i> | 2.56E-09*** | 0.322 | 0.689 | 0.800 | 0.916 | 0.904 |

Univariate statistics were used to identify which peaks were changing significantly between control and exposed groups and by how much. Fold changes and FDR corrected *p*-values were calculated for each peak in each of the three data sets. All three matrices had a large number of significantly changing peaks (i.e. 44-67 % of the total datasets) with predictably large associated fold changes (Table 5-3, Figure 5-2). This massive change in lipid extract composition reflects the “heavy handed” nature of the *in vitro* oxidative stress studies. The significance of the separation between control and exposed sample groups was far greater in the air exposures than the H₂O₂/CuCl₂. This may appear surprising due to the passive nature of the air oxidation, however, the exposure lengths (air = 168 h, H₂O₂/CuCl₂ = 2 h) probably accounts for this. There were numerous spectral features which were present in only the control or exposed group (Table 5-3). These unique peaks are not unexpected given that there should be few oxidised lipids present in control samples and potential for species to be oxidatively degraded to the extent where they would drop below the level of detection in exposed samples. Many of the fold changes reported are created artificially by the missing value

imputation particularly those for unique peaks. However, it allows ready visualisation of data which would be impossible with the infinite fold changes associated with a spectral feature only appearing in one sample group. Indeed despite their artificial nature, fold changes of unique peaks give an idea of the abundance of that peak above the low detection limit.

Table 5-3 Table showing peak matrix size and univariate statistical results for *in vitro* oxidation studies. Peak number is the amount of spectral features which passed the filtering steps of processing. Spectral features with associated significant intensity changes between sample groups (FDR corrected $P < 0.05$) are counted in the significantly changing column. Unique peaks are those which are only observed in one sample group. Min and max fold changes are the highest and lowest intensity fold changes between sample groups $\log_2(\text{exposed} / \text{control})$.

| Study | Organism | Univariate statistics | | | Fold change (\log_2) | |
|--|-----------------------|-----------------------|------------------------|--------------|--------------------------|-------|
| | | Peak number | Significantly changing | Unique peaks | Min | Max |
| H ₂ O ₂ in vitro | <i>D. magna</i> | 1047 | 690 | 154 | -6.9 | 5.9 |
| Air in vitro | <i>D. magna</i> | 1097 | 479 | 118 | -13.37 | 15.31 |
| | <i>C. reinhardtii</i> | 1537 | 1038 | 611 | -9.11 | 9.61 |

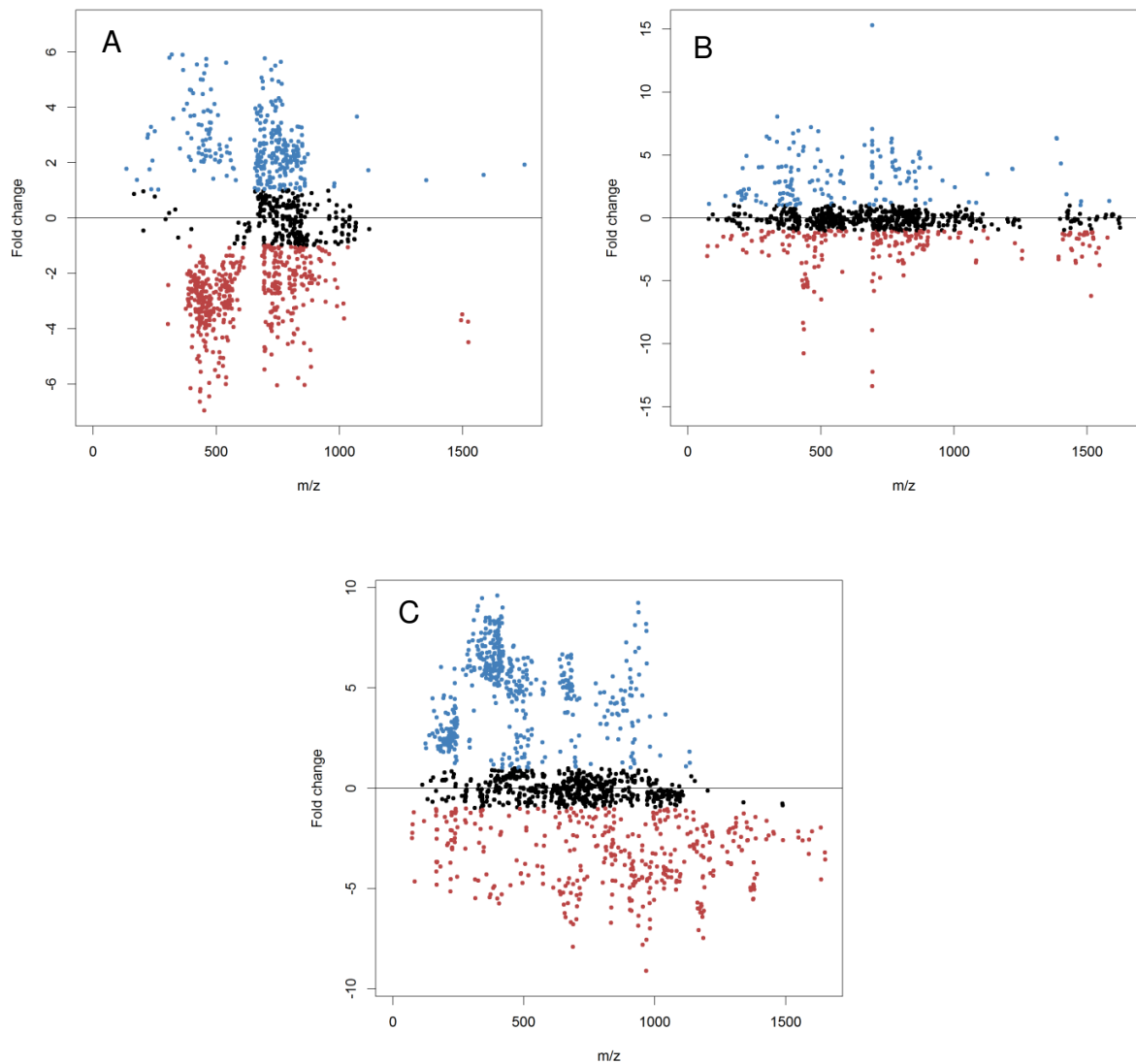


Figure 5-2 Exposed / control log₂ fold changes for *in vitro* exposed lipid extracts. Species with changes of more than 1 or less than -1 (i.e. an arbitrary two-fold change) are highlighted in blue and red respectively. (A) H₂O₂ / CuCl₂ exposure to *D. magna* lipid extract. (B) Air exposure to *D. magna* lipid extract. (C) Air exposure to *C. reinhardtii* lipid extract.

Potentially oxidised peaks were identified by matching m/z differences of one and two oxygen molecules (15.99491 and 31.98983, <2 ppm error) within the peak matrix representing the two major oxidative modifications observed in chapter 3. Numerous single and double oxygen mass differences were observed in all three datasets. If the control sample groups contain only unmodified lipids and the exposed samples many oxidatively modified lipids then the former should have high negative \log_2 fold changes and the latter high positive fold changes. However, this was not the case in any of the three *in vitro* studies (Figure 5-3, Figure 5-4), as the unmodified (shown in black) and oxidised (shown in blue) annotated lipids appeared with both positive and negative fold changes with little sign of correlation. Adding to the complexity there were some peaks which were both oxygen mass differences above and below another peak which could be oxidised products which were oxidised further, shown as red circles in Figure 5-3 and Figure 5-4. Inherent single and double oxygen structural differences could also be adding noise to this data, for example diacyl phospholipid species will always be observed at a single oxygen m/z difference above corresponding plasmalogen and ester linked phospholipid species. In order to apply a more focused lipid oxidation search, the baseline lipidome for *D. magna*, compiled in chapter 4 was used as an unmodified lipid list and single and double oxygen additions identified to indicate potential oxidised products.

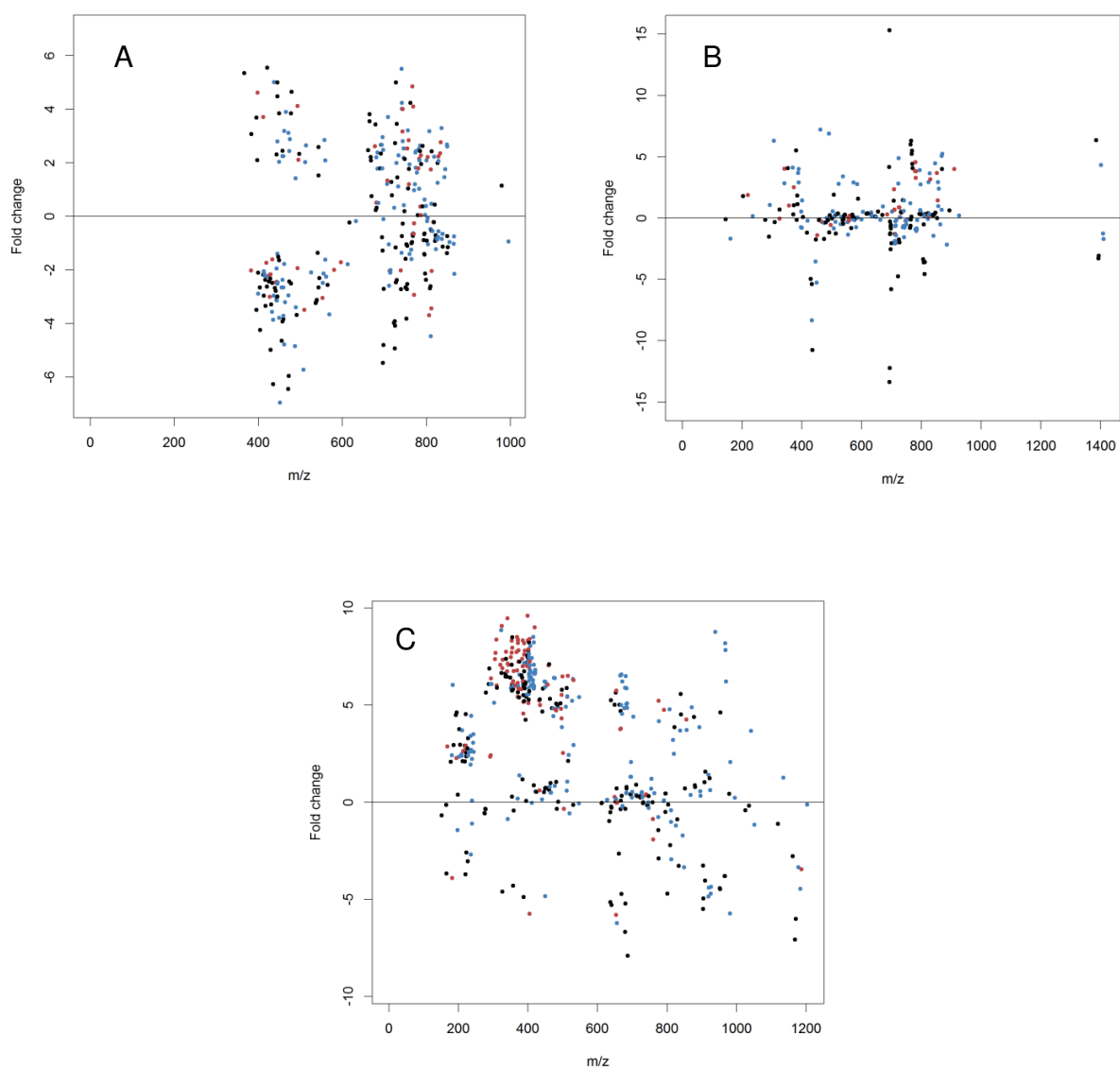


Figure 5-3 Log₂ fold changes (exposed / control) of unmodified (black), and potentially oxidatively modified (+O, blue) spectral features. (A) = *in vitro* H₂O₂ (*D. magna*). (B) = *in vitro* Air (*D. magna*). (C) = *in vitro* Air (*C. reinhardtii*). Spectral features which could be unmodified or modified are shown in red.

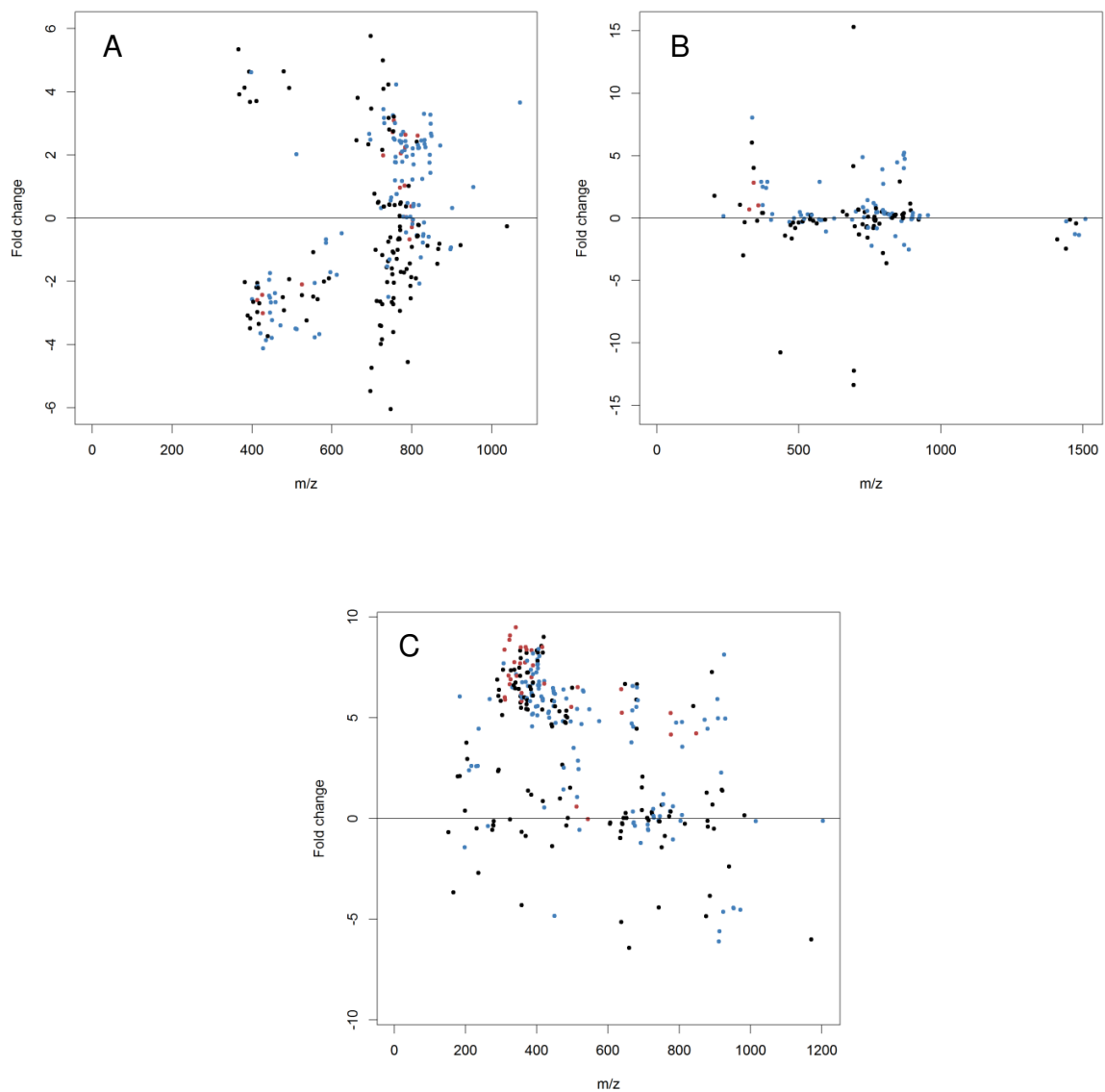


Figure 5-4 Log₂ fold changes (exposed / control) of unmodified (black), and potentially oxidatively modified (+O₂, blue) spectral features. (A) = *in vitro* H₂O₂ (*D. magna*). (B) = *in vitro* Air (*D. magna*). (C) = *in vitro* Air (*C. reinhardtii*). Spectral features which could be unmodified or modified are shown in red.

Targeted lipid oxidation annotation yielded more interpretable results in H₂O₂ exposed *D. magna* lipid extracts. A total of 112 spectral features were matched against 227 unique masses in the baseline lipidome. From these, 33 single oxygen and 38 double oxygen mass additions (highlighted blue) were observed in the dataset as a whole (Figure 5-5). Of the 33 single oxygen additions, 19 had log₂ fold changes <1, however, 12 of these were annotated as other lipids (highlighted red). In contrast, of the 14 spectral features with log₂ fold change >1 none had putative lipid annotations. A similar situation was observed with double oxygen addition, of the 38 spectral features 15 had log₂ fold changes <1, eight of which were putatively annotated as lipids. 23 had log₂ fold changes >1 with only two having a putative lipid annotation. This indicates that lipid peroxidation is taking place with >10% of the baseline lipidome being oxidatively modified, the fold changes of the lipid oxides and peroxides are relatively low which reflects their intensities being close to the level of detection. In the air exposed *D. magna* lipid extracts (Figure 5-6), a similar situation is observed for single oxygen addition, 26 oxidised compounds were observed of which 13 had log₂ fold changes > 1 only two of which with lipid annotations in contrast to 13 with log₂ fold changes < 1 of which 8 had lipid annotations. However, the 25 double oxygen additions, i.e. lipid peroxidation, did not follow the same trend with only four log₂ fold changes >1 although none were annotated and 21 log₂ fold changes <1 with nine putatively annotated. This is unexpected and suggests that oxidation in from air exposure does not take place via a peroxidative mechanism. Both data sets highlight that observed lipid oxidation may be masked by inherent structural oxygen differences, the major source of this in these datasets is the isomeric nature of plasmalogens + O and diacyl lipids of the same class.

The application of targeted oxidative annotation in the air exposed *C. reinhardtii* lipid extracts had very little impact (Figure 5-7). Only five spectral features were annotated as potentially oxidised species across both single and double oxygen addition of which three were identified as other lipids. The only single oxygen addition annotation without a lipid annotation had a negative \log_2 fold change of -3.0, the opposite of what would be expected for an oxidised product. The double oxygen addition annotation without a lipid annotation had a positive \log_2 fold change of 4.2 which is expected but little significance can be drawn from a single peak. A lack of success for targeted oxidative annotation of *C. reinhardtii* is probably attributed to the lack of polar lipid annotation in the baseline lipidome. Only 46 spectral features in the air oxidised dataset were matched to the baseline lipidome, however, this still represented 37% of the 122 unique m/z values comprising the *C. reinhardtii* baseline lipidome. From targeted oxidative annotation of the three datasets it appears that H_2O_2 / CuCl_2 is a more successful technique for modelling oxidation *in vitro* than air exposure, yet with no separation prior to MS analysis complexity will always exist due to isomeric overlap with existing lipids.

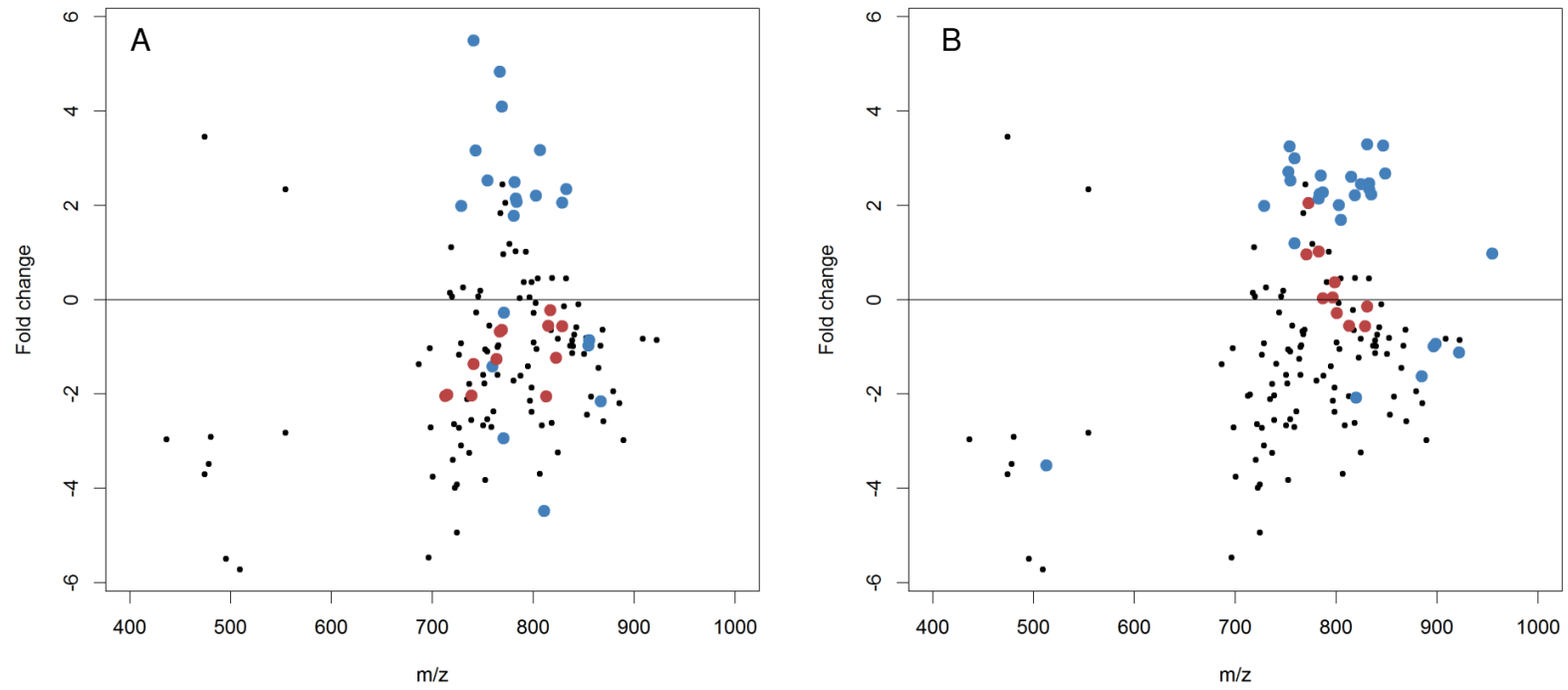


Figure 5-5 Scatter plots showing putatively annotated oxidation in H₂O₂ exposed *D. magna* lipid extracts. Exposed / control intensity log₂ fold changes of baseline lipidome matched spectral features (black), oxygen addition features (blue) and oxygen added features with an unmodified lipid annotation (red). (A) single oxygen addition. (B) double oxygen addition.

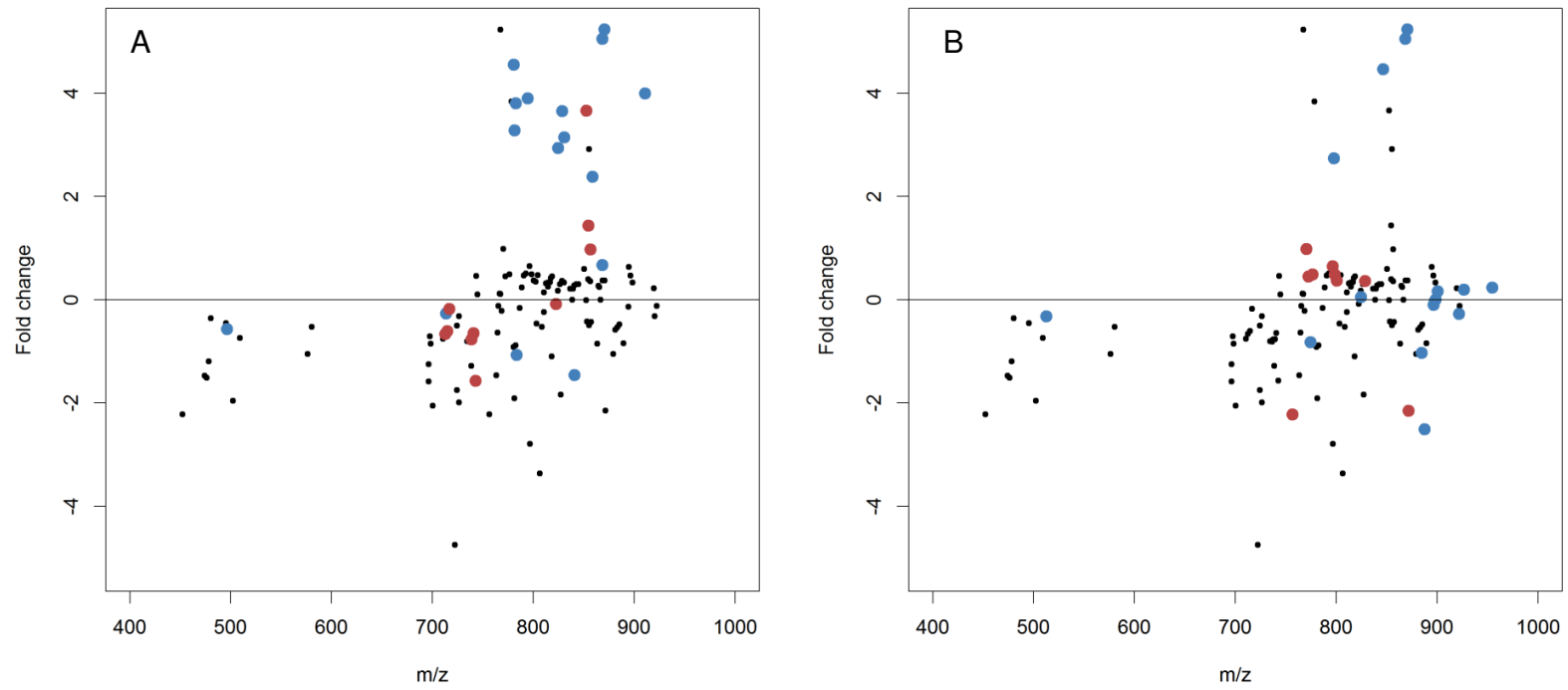


Figure 5-6 Scatter plots showing putatively annotated oxidation in air exposed *D. magna* lipid extracts. Exposed / control intensity log₂ fold changes of baseline lipidome matched spectral features (black), oxygen addition features (blue) and oxygen added features with an unmodified lipid annotation (red). (A) single oxygen addition. (B) double oxygen addition.

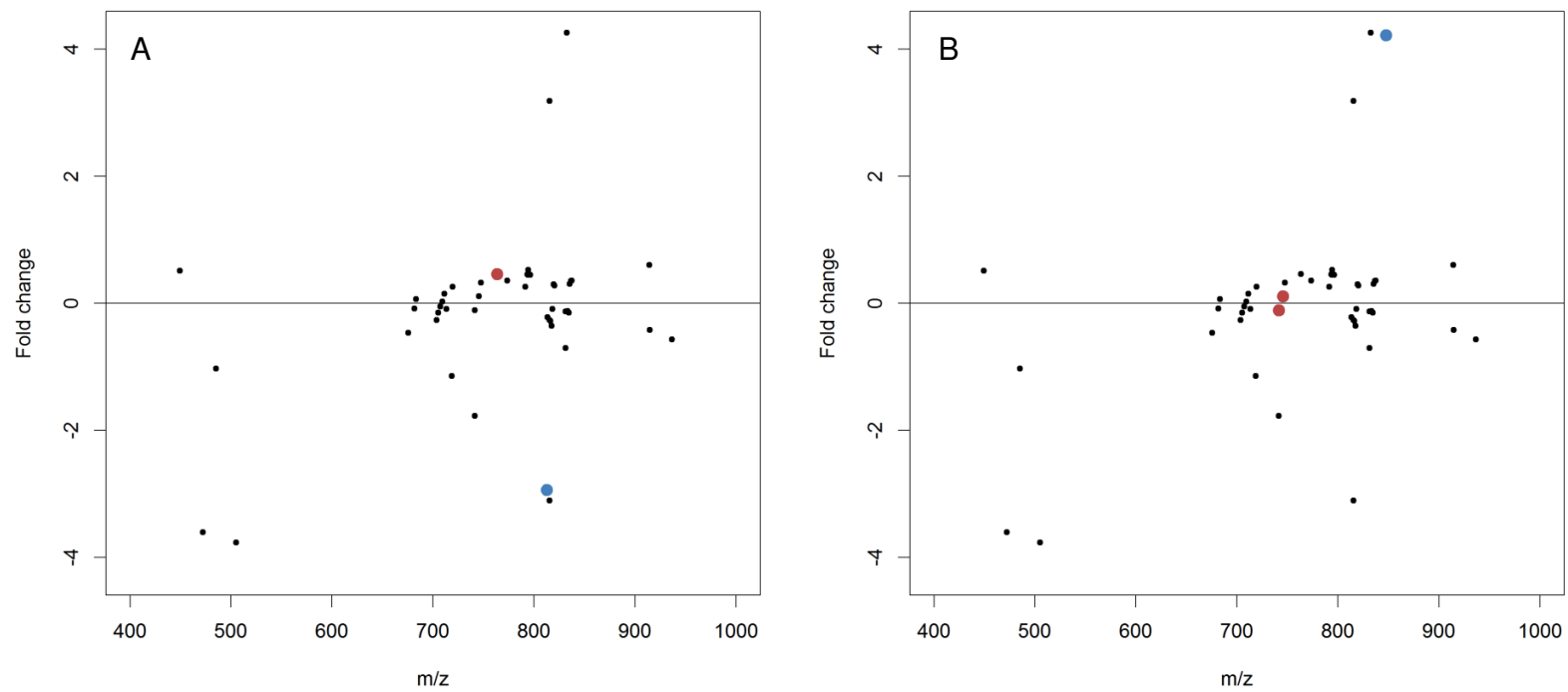


Figure 5-7 Scatter plots showing putatively annotated oxidation in air exposed *C. reinhardtii* lipid extracts. Exposed / control intensity log₂ fold changes of baseline lipidome matched spectral features (black), oxygen addition features (blue) and oxygen added features with an unmodified lipid annotation (red). (A) single oxygen addition. (B) double oxygen addition.

5.3.2 - Acute toxicity of AgNO₃ and H₂O₂ to *D. magna* and *C. reinhardtii*

D. magna neonates responded to both AgNO₃ and H₂O₂ to yield sigmoidal concentration-response curves (Figure 5-8). TSK predicted 1.49 µg/l and 1.34 µg/l as the EC₅₀ values for AgNO₃ at 24 and 48 hour exposures respectively. The NOAEL fell from 1 µg/l to 0.8 µg/l between 24 and 48 h. Over 70, 48hr EC₅₀ values for *D. magna* exposed to AgNO₃ have been reported to date, according to the ECOTOX database (USEPA, 2014). The mean EC₅₀ of these studies is 7.86 µg/l, which is less toxic than the value reported here, however, this is skewed by a few studies with large values, the median EC₅₀ of these studies is 2.41 µg/l, which when accepting inter-lab variation in methodology and *D. magna* strain is remarkably similar.

TSK predicted 9.44 mg/l and 7.35 mg/l as the EC₅₀ values for H₂O₂ for 24 and 48 h exposures respectively. The NOAEL fell from 3.2 to 2.1 mg/l between 24 and 48 h. There is little EC₅₀ data available for immobilisation of *D. magna* exposed to H₂O₂, with only three hits from the ECOTOX database (USEPA, 2014). These studies suggest EC₅₀s of 2.3 mg/l (Watanabe et al., 2007), 2.32 mg/l and 20 mg/l (USEPA, 2014), whilst only the first of these values was accessible for confirmation, they lie within the same effect levels observed in our experiment. The similarity between our *D. magna* acute toxicity studies and those reported in the literature add strength to the validity of our exposure procedures.

C. reinhardtii cell growth was also inhibited by AgNO₃ in the expected sigmoidal, concentration-response manner (Figure 5-9). TSK predicted 73.17 µg/l as the EC₅₀ value for AgNO₃ at 72 hours (Figure 5-8). As mentioned in the introduction, there is less

toxicological literature available for *C. reinhardtii*, and indeed only a single publication in the ECOTOX database quotes growth inhibition figures for exposure to AgNO₃ (Howe and Merchant, 1992). This study reports a concentration of 850 µg/l of AgNO₃ required for inhibition of cell growth without affecting cell viability. This is far higher than the EC₅₀ reported here, however, the timescale along which this work was undertaken was much shorter at approximately 10 minutes which would intuitively require much higher concentrations of toxicant to induce similar, if less defined, results.

Acute toxicity results allowed the selection of sub-lethal doses for lipidomic exposures. For lipidomic analysis, NOAELs at 48 hours were used as high doses for AgNO₃ and H₂O₂ with a ten-fold dilution of each used as the corresponding low dose in *D. magna*. An identical strategy was used for CuSO₄ using a NOAEL of 20 µg/l as reported previously (Taylor, 2010). For AgNO₃ exposures to *C. reinhardtii*, 10 and 1 % of the EC₅₀ were used as high and low dose respectively.

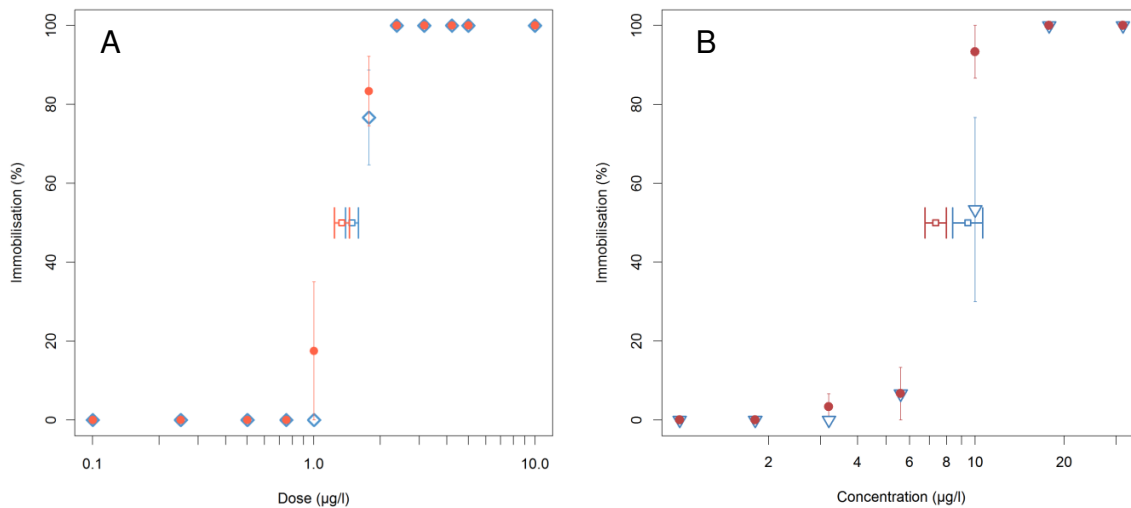


Figure 5-8 Concentration-response curves for immobilisation of *D. magna*. Blue diamonds (◊) indicate immobilisation at 24 hours, red circles (●) indicate immobilisation at 48 hours. EC₅₀s are indicated by squares. Vertical error bars represent standard error of the mean (SEM), horizontal error bars show 95% EC₅₀ confidence intervals. (A) AgNO₃ EC₅₀ = 1.49 µg/l (24hrs), 1.34 µg/l (48hrs). (B) H₂O₂ EC₅₀ = 9.44 mg/l (24hrs), 7.35 mg/l (48hrs).

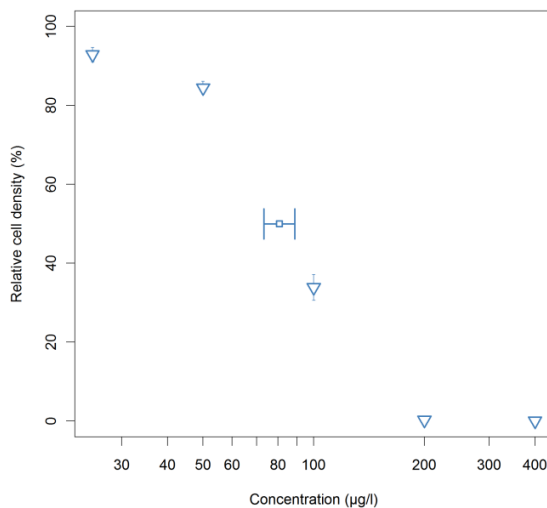


Figure 5-9 Concentration-response curve for cell growth inhibition of *C. reinhardtii* exposed to AgNO₃. 72hour EC₅₀ is indicated by square with horizontal error bars representing 95% confidence interval and has a value of 73.17 µg l⁻¹. Vertical error bars represent standard error of the mean (SEM), horizontal error bars show 95% EC₅₀ confidence intervals.

5.3.3 - Lipidomic responses of *D. magna* and *C. reinhardtii* to *in vivo*

oxidative stressors

Processed intensity matrices were assessed for each *in vivo* study with samples removed should their missing value percentage lie above the 95 % confidence interval. This resulted in one low dose sample from the *D. magna* AgNO₃ dataset, one control and one high dose sample from the *C. reinhardtii* dataset, one control sample from the H₂O₂ *D. magna* dataset and two low dose samples from the CuSO₄ dataset being removed. Following PQN and minimum value imputation PCA was conducted to observe differences between control and exposed (low and high) groups. Significant separations were seen in the CuSO₄ and H₂O₂ *D. magna* studies along PC4 and PC2 respectively, with Tukey's post-hoc analysis confirming the separation was between control and high dosed groups. No significant separations were observed in the AgNO₃ *D. magna* dataset, however, in the AgNO₃ *C. reinhardtii* dataset, significant separations were observed along PC1, 5 and 6 between low and high doses, control and high doses and low and control doses respectively (Figure 5-10).

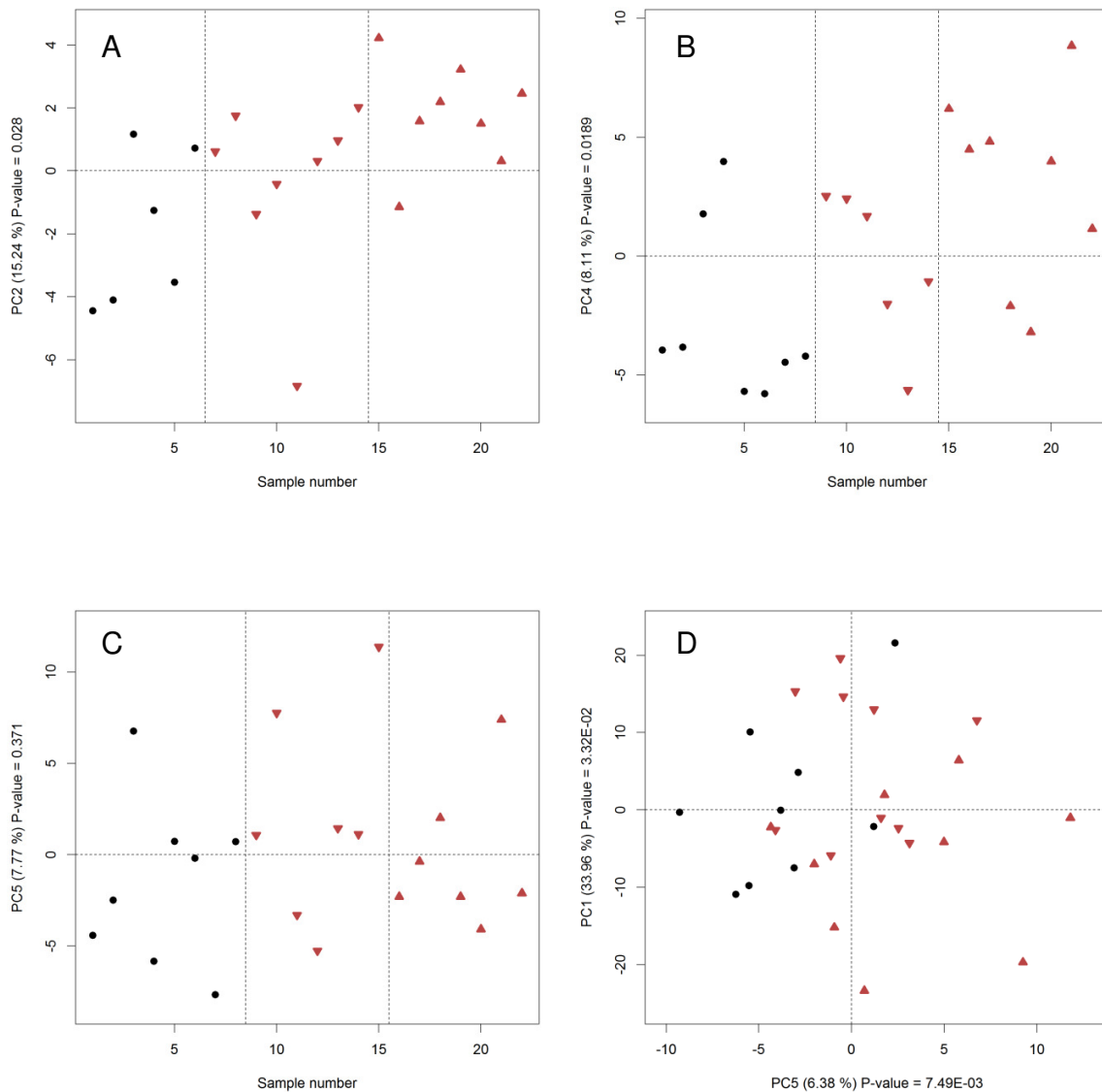


Figure 5-10 Scores plot showing sample number vs. most significant principal component for *in vivo* oxidative stress exposures. Control samples are denoted by black circles, low dose exposed samples are denoted by red down triangles and high dose exposed samples denoted by red up triangles. Vertical lines in A-C separate sample groups. (A) H₂O₂ exposure to *D. magna*. Significant separation between control and high dose is observed along PC2 (P=0.028). (B) CuSO₄ exposure to *D. magna*. Significant separation between control and high dose is observed along PC4 (P=0.019). (C) AgNO₃ exposure to *D. magna*. No significant separation observed, PC5 is shown as the most significant PC axis (P = 0.371) (D) AgNO₃ exposure to *C. reinhardtii* Significant separations seen along PC1 between low and high doses and PC5 between control and high dose (P= 0.033 and 0.0075 respectively).

Table 5-4 Table showing significant group separation by principal scores of processed *in vivo* *D. magna* and *C. reinhardtii* exposed to oxidative stress. * = P(<0.05).

| Study | Organism | Principal component significance | | | | | |
|--|-----------------------|----------------------------------|---------|-------|---------|--------|--------|
| | | PC1 | PC2 | PC3 | PC4 | PC5 | PC6 |
| H ₂ O ₂ <i>in vivo</i> | <i>D. magna</i> | 0.300 | 0.0280* | 0.223 | 0.824 | 0.734 | 0.498 |
| CuSO ₄ <i>in vivo</i> | <i>D. magna</i> | 0.480 | 0.461 | 0.301 | 0.0189* | 0.958 | 0.488 |
| AgNO ₃ <i>in vivo</i> | <i>D. magna</i> | 0.401 | 0.974 | 0.741 | 0.771 | 0.371 | 0.547 |
| | <i>C. reinhardtii</i> | 0.0332* | 0.132 | 0.983 | 0.809 | 0.007* | 0.022* |

There is far less perturbation of the lipidomic profiles of both *D. magna* and *C. reinhardtii* in response to *in vivo* oxidative stress. Only 15 unique peaks, i.e. spectral features only observed in control or exposed groups, were observed across all four datasets. This is reflected by the much smaller number of log₂ fold changes observed above 1 or below -1 between control and high dose samples (Figure 5-11). Only 41 spectral features were significantly changing across the datasets most of which occurring in CuSO₄ exposed *D. magna*. Whilst a lack of significantly changing species is disappointing it is unsurprising that the perturbation of the lipidomes of *D. magna* and *C. reinhardtii* was far less in these *in vivo* studies than *in vitro* studies presented above.

Table 5-5 Table showing peak matrix size and univariate statistical results for *in vitro* oxidation studies.

| Study | Organism | Univariate statistics | | | Fold change (log ₂) | |
|---------------------------------------|-----------------------|-----------------------|------------------------|--------------|---------------------------------|------|
| | | Peak number | Significantly changing | Unique peaks | Min | Max |
| H ₂ O ₂ in vivo | <i>D. magna</i> | 1638 | 22 | 10 | -5.82 | 4.41 |
| CuSO ₄ in vivo | <i>D. magna</i> | 1289 | 11 | 3 | -5.11 | 3.02 |
| AgNO ₃ in vivo | <i>D. magna</i> | 1375 | 1 | 1 | -3.30 | 1.86 |
| | <i>C. reinhardtii</i> | 2514 | 7 | 1 | -2.50 | 2.67 |

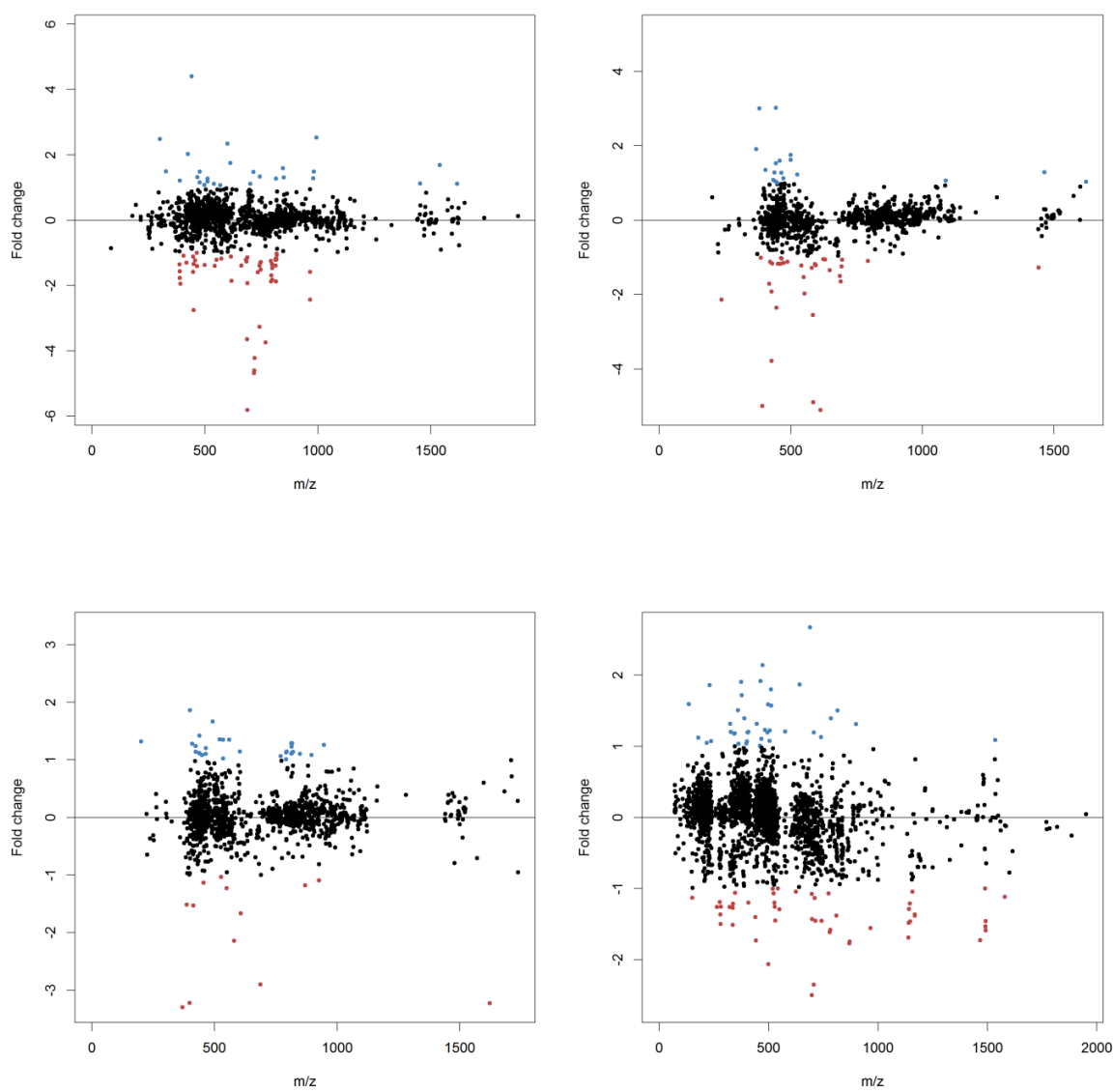


Figure 5-11 High dose exposed / control log₂ fold changes for *in vivo* exposures. Species with changes of more than 1 or less than -1 (i.e. a two-fold change) are highlighted in blue and red respectively. (A) H₂O₂ exposure to *D. magna*. (B) CuSO₄ exposure to *D. magna*. (C) AgNO₃ exposure to *D. magna*. (D) AgNO₃ exposure to *C. reinhardtii*.

Targeted annotation of oxidatively modified peaks also yielded little of note. Over one hundred spectral features were matched to the baseline lipidome of *D. magna* or *C. reinhardtii* in each of the four datasets. Many single and double oxygen additions were annotated from these matched features, however, there was no identifiable trend in the \log_2 fold changes with no spectral features changing positively or negatively by two-fold (Figure 5-12, Figure 5-13, Figure 5-14, Figure 5-15).

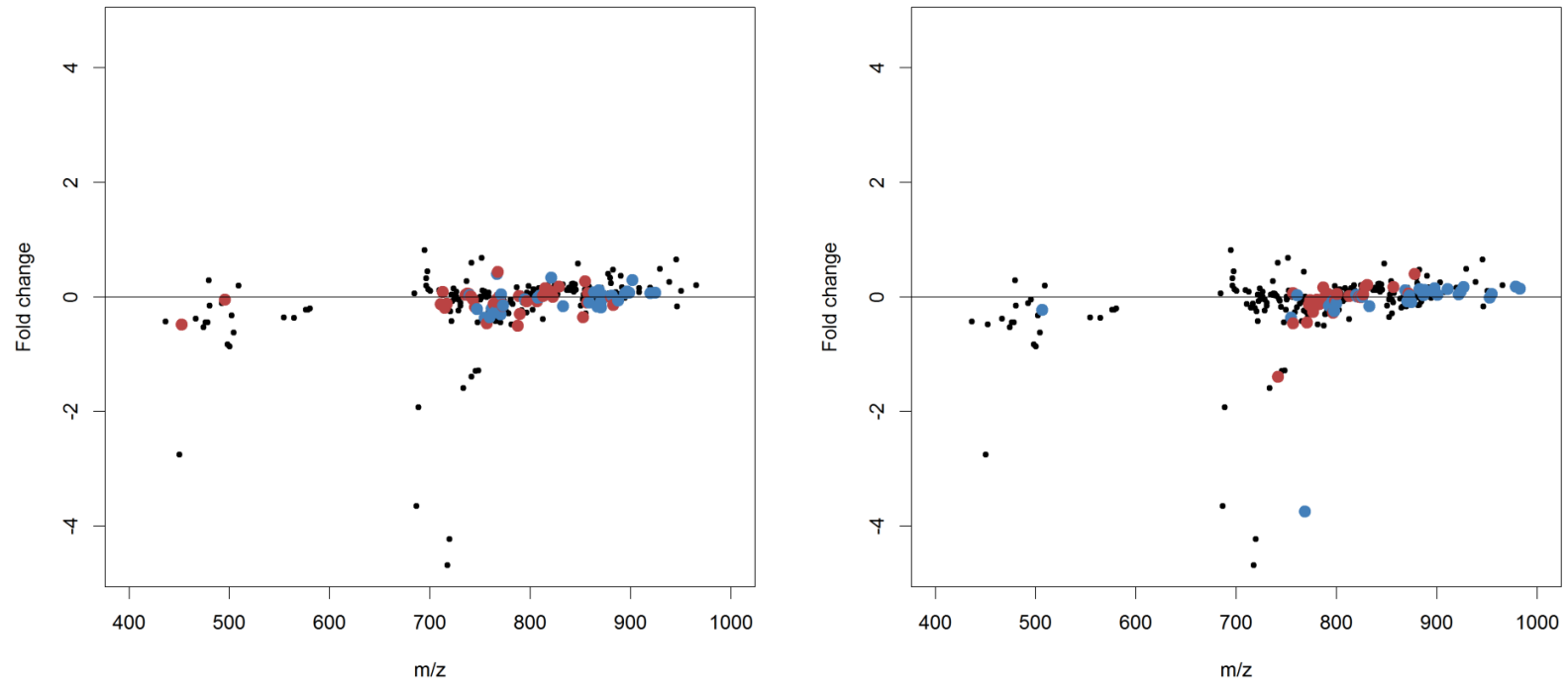


Figure 5-12 Scatter plots showing putatively annotated oxidation in H_2O_2 exposed *D. magna* lipid extracts. Exposed / control intensity \log_2 fold changes of baseline lipidome matched spectral features (black), oxygen addition features (blue) and oxygen added features with an unmodified lipid annotation (red). (A) single oxygen addition. (B) double oxygen addition.

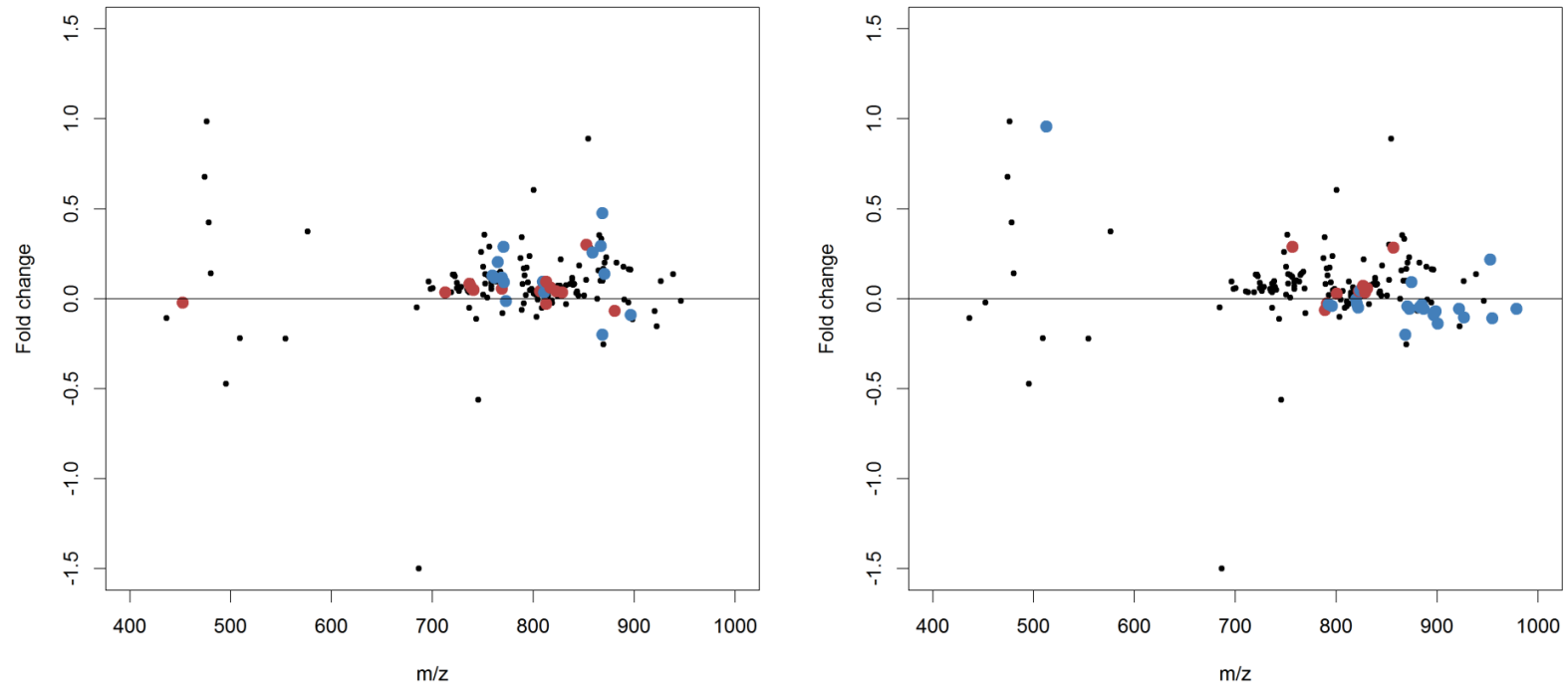


Figure 5-13 Scatter plots showing putatively annotated oxidation in CuSO_4 exposed *D. magna* lipid extracts. Exposed / control intensity \log_2 fold changes of baseline lipidome matched spectral features (black), oxygen addition features (blue) and oxygen added features with an unmodified lipid annotation (red). (A) single oxygen addition. (B) double oxygen addition.

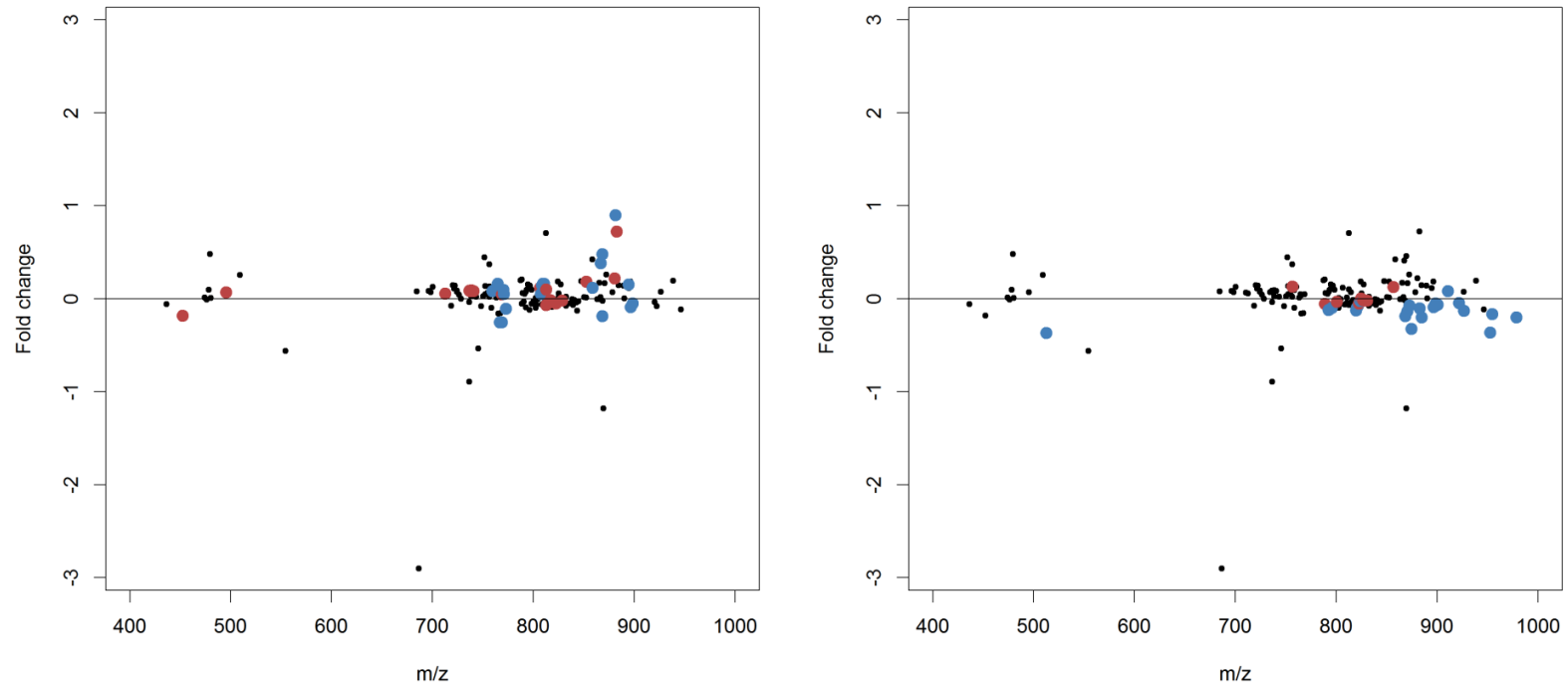


Figure 5-14 Scatter plots showing putatively annotated oxidation in AgNO_3 exposed *D. magna* lipid extracts. Exposed / control intensity \log_2 fold changes of baseline lipidome matched spectral features (black), oxygen addition features (blue) and oxygen added features with an unmodified lipid annotation (red). (A) single oxygen addition. (B) double oxygen addition.

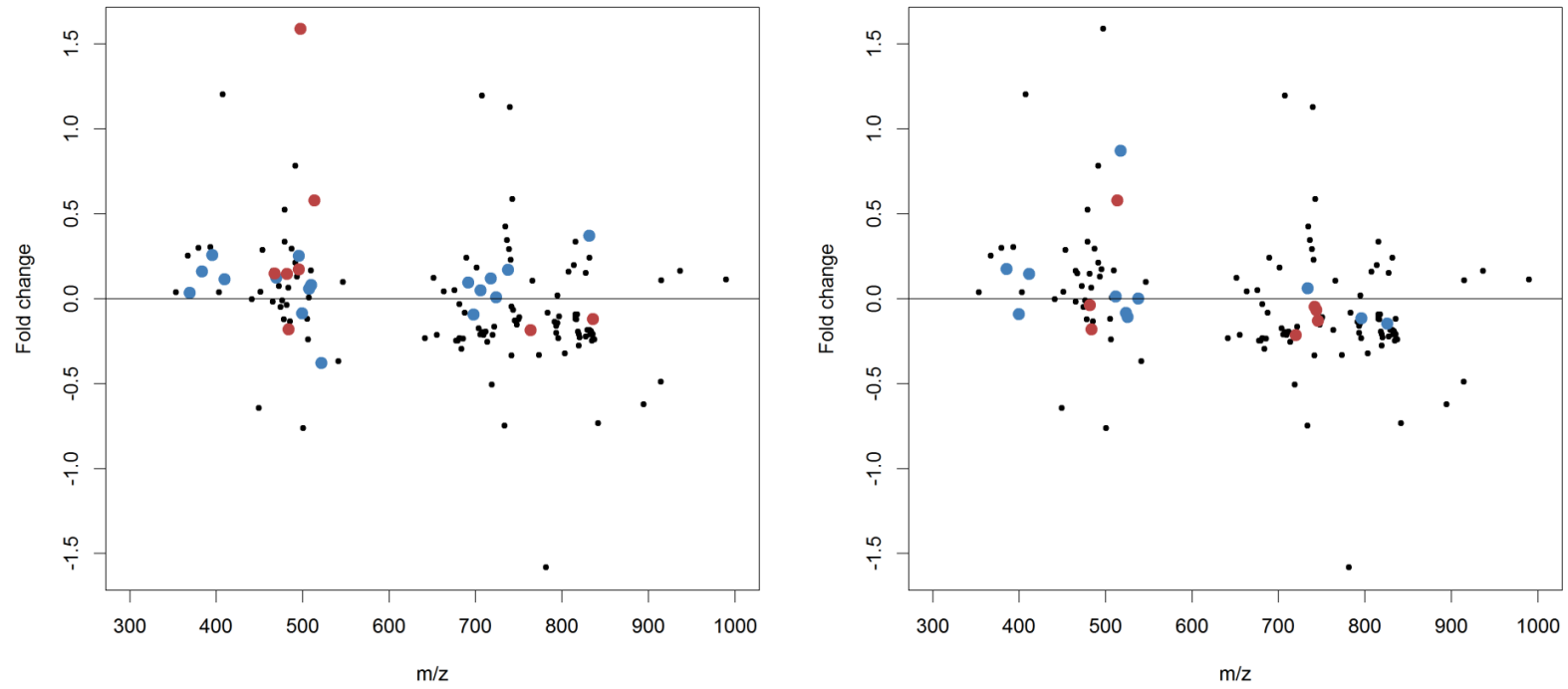


Figure 5-15 Scatter plots showing putatively annotated oxidation in AgNO₃ exposed *C. reinhardtii* lipid extracts. Exposed / control intensity log₂ fold changes of baseline lipidome matched spectral features (black), oxygen addition features (blue) and oxygen added features with an unmodified lipid annotation (red). (A) single oxygen addition. (B) double oxygen addition.

5.4 - Conclusions

Oxidative perturbation of the *D. magna* baseline lipidome was attempted with air and H₂O₂ and the *C. reinhardtii* lipidome with air only. Untargeted analysis of the data did not reveal oxidative modifications despite many hundreds of spectral features and large significant fold changes between control and exposed groups. Targeted inspection of the baseline lipidomes, however, showed large positive fold changes of putatively annotated oxygen additions between control *D. magna* lipid extracts and both H₂O₂ and air exposed extracts. Numerous oxygen additions with log₂ fold changes less than 1 were observed but these were predominantly annotated as other lipid species due to the isomeric nature of plasmalogen and diacyl phospholipids. The positively changing oxygen additions from control to exposed lipids were predominantly single from air perturbation, this indicates lipid peroxidation may not be the mechanism of action where lipid peroxides (+O₂) are the primary product and lipid hydroxides are subsequently formed via reduction reactions (Tyurin et al., 2008). Targeted annotation of *in vitro* oxidation in *C. reinhardtii* was less successful, potentially exacerbated by the lack of spectral coverage in the baseline lipidome. To progress this study further, confirmation of oxidative annotations would be the logical next step, with tandem mass spectrometry coupled to OxyLipidBlast, as presented in the previous chapter, the logical tools. However, the isolation width of 1 Da used in this work would not be sufficient to fragment a single ion, this would complicate the fragmentation pattern, particularly if the feature of interest was low abundant (Hartler et al., 2013). Two methodologies have been widely utilised to improve spectral annotation of lipidomes, precursor ion scanning with DIMS

(Han et al., 2012) and prior chromatographic separation, specifically LC (Nakanishi et al., 2009). To enable implementation of OxyLipidBlast, LC separation would be the preferred tool as it reduces the ion suppression of low-abundance compounds and can separate the various phospholipid classes (Hartler et al., 2013). Increased annotation of the *C. reinhardtii* lipidome could also be achieved with similar methodologies as the LipidBlast software contains extensive *in silico* fragmentation patterns of algal lipids (Kind et al., 2013).

D. magna were exposed to multiple oxidative stressors *in vitro* and *C. reinhardtii* to a single one at well-defined toxicologically relevant concentrations, supported by both acute toxicity data presented here and previous studies reported in the literature (USEPA 2014, Watanabe et al., 2007). While significant separation of high dose groups from control were observed in all but the AgNO₃ exposed *D. magna*, lipid peroxidation was not observed in any significant way and fold changes were largely less than two fold positively or negatively. As numerous other studies have reported oxidative stress and resulting lipid peroxidation as toxicological effects of these xenobiotics using non-lipidomic methodologies (Cortese-Krott et al., 2009, Gonzalez-Sanchez et al., 2013, Pervaiz and Clement, 2002, Schwarz et al., 2013, Rhee et al., 2013), it is likely that lipid peroxides are present but not observed in DIMS spectra. Therefore, use of these DIMS techniques for analysis of phospholipid peroxides and related compounds *in vivo* may be undermined by the low abundance of these molecular species (Sparvero et al., 2010).

6 - Lipidomic analysis of silver nanoparticle toxicity in *D. magna* following extensive exposure optimisation[–]

6.1 - Introduction

As discussed in chapter 1 commercial use of AgNP is becoming increasingly widespread despite insufficient toxicological knowledge (Borm et al., 2006).

Environmental exposure would most likely occur via waste water indicating freshwater bodies as potential terminal sinks and *D. magna* as an ideal ecotoxicity test organism.

The majority of nanoparticle aquatic toxicity studies to date are mostly lacking in two fundamental aspects: proper characterisation of nanoparticles, due mostly to the use of commercial preparations, and insight into mechanistic toxicity due to the use of classic endpoints such as immobilisation in *D. magna* and / or appropriate controls to rule out ionic toxicity (Zhao and Wang, 2012, Allen et al., 2010, Gaiser et al., 2011).

To best elucidate the toxic effect of nanoparticles it is ideal for them to remain mono-dispersed. It has been shown that citrate capped silver nanoparticles (AgNP-cit) agglomerate in high ionic strength media (Römer et al., 2013). Ideally the ionic concentration of exposure media would be minimised to avoid particle agglomeration, however, this may cause organism stress which could render toxicity studies irrelevant.

The aim of this study is to use comprehensively characterised particles and optimal experimental conditions to elucidate lipid perturbations in *D. magna* exposed to silver nanoparticles. Initially we will optimise the ionic concentration of exposure media to ensure nanoparticle dispersal without detrimental biological effects to facilitate robust

[–] Contents of this chapter, including the figures have been published in Journal of Chromatography A: Roemer, I., T. A. White, et al. (2011). Aggregation and dispersion of silver nanoparticles in exposure media for aquatic toxicity tests. *Journal of Chromatography A* **1218** (27): 4226-4233.

toxicity testing. Modelling the dissolution of nanoparticles in experimental conditions will allow ionic silver controls to be matched to nanoparticle exposures to determine whether there is a nano-specific effect to the *D. magna* lipidome. Finally a comprehensive lipidomic study will be undertaken, with exposure concentrations led by acute toxicity studies, to elucidate any effect of AgNPs on the lipidome of *D. magna*. As mentioned in chapter 1, extensive toxicological studies have been undertaken with AgNPs, with many in *D. magna* (Asghari et al., 2012, Hoheisel et al., 2012, Zhao and Wang, 2011). This study represents the first use of lipidomic techniques to assess ecotoxicological AgNP toxicity. Indeed there have been only two, published metabolomic studies (Hadrup et al., 2012, Kim et al., 2011) and a single lipidomic study (Tentschert et al., 2013) assessing AgNP mediated toxicity. The lipidomic study focuses on the membrane composition of human macrophages exposed to 20nm, peptide-capped, silver nanoparticles and observes significant differences between control and exposed cells, predominantly in PC species (Tentschert et al., 2013). Whilst there is no mention of lipid peroxidation, they show addition of N-acetyl cysteine, a well-known anti-oxidant, to exposure vessels reduces membrane disruption supporting the hypothesis that oxidative stress plays an important role in AgNP mediated toxicity. Similarly, Kim et al., 2011 showed depletion of glutathione in hepatocytes exposed to AgNPs. Glutathione formed from N-acetyl cysteine is also an important anti-oxidant, which would be reduced under oxidative stress by ROS (Timbrell, 2000). The second metabolomic paper reveals purine metabolism to be affected by AgNPs (Hadrup et al., 2012), which would not be directly observed in a lipidomic dataset.

6.2 - Materials and methods

6.2.1 - Acid washing of equipment

Prior to experimentation, all plastic and glass-ware was submerged in nitric acid (10 %) for at least 24 h, rinsed thrice with ultrapure (UP) H₂O (18.2 Ω, Purelab) and submerged in UP H₂O for 24 h. Finally, items were rinsed a further 3 times and dried naturally. This process removed any trace silver which may contaminate experiments conducted at low concentrations of AgNP.

6.2.2 - Silver nanoparticle preparation conducted by Dr. Isabella Römer and Mila Tejamaya (U of Birmingham)

AgNPs capped with citrate (AgNP-cit) were prepared by Dr. Isabella Römer as reported previously, from reduction of AgNO₃ in sodium citrate (Roemer et al., 2011). Briefly, sodium citrate (100 ml, 0.31 mM) and AgNO₃ (100 ml, 0.25 mM) were prepared in UP H₂O, vigorously mixed, slowly heated and boiled (90 min). After cooling, the mixture was reduced with sodium borohydride (NaBH₄, 6 ml, 0.25 mM) and boiled for a further 10 min.

AgNPs capped with polyvinylpyrrolidone (AgNP-PVP) were prepared similarly by the reduction of AgNO₃ (60 ml, 1 mM) with NaBH₄ (180 ml, 2 mM) (Tejamaya et al., 2012) however, this time in the presence of PVP₁₀.

Particulate matter greater than 100 nm was removed from all nanoparticle solutions by filtration through a cellulose nitrate membrane (Millipore USA) and excess reagents removed via diafiltration using a regenerated cellulose membrane (1 kDa) in a stirred ultrafiltration cell under N₂, volume was maintained with capping agent solution (sodium

citrate or PVP). Particles underwent diafiltration 3 times following preparation and a further 3 times prior to all exposure work.

6.2.2.1 - Silver nanoparticle characterisation

The AgNP-cit and AgNP-PVP used within this chapter were characterised by Dr. I Römer and M. Tejamaya respectively with Flow Field Flow Fractionation (FIFFF), Dynamic Light Scattering (DLS) and Transition Electron Microscopy (TEM) to confirm particle size and aggregation. Initial characterisation was conducted in UP H₂O to determine production size and stability, followed by characterisation in OECD modified media and dilutions thereof, to ascertain particle behaviour in *D. magna* exposures. DLS measurements were made at 21 °C, using a refractive index of 0.54 and an absorption of 3 in a Zetasizer 5000 (Malvern, UK) with replication of at least five. Particle separation based on size was achieved in an asymmetrical flow-field flow fractionator (AF2000, Postnova Analytics, Germany). Eluting AgNPs were detected by an ultraviolet (UV) spectrometer at 400nm and size was determined by comparison to elution times of polyacrylamide beads with known size.

TEM imaging was conducted on a Tecnai F20 (Philips, Netherlands) with data recorded and analysed using Digital Micrograph software (Gatan, US).

6.2.3 - Media dilution acute stress assessment

The acute effects of reducing the ionic concentration of exposure media were assessed analogously to the acute toxicity tests described in section 2.3. Groups of ten *D. magna* neonates (<24 h) were rinsed in DI water, to avoid unwanted strengthening of diluted

media, then transferred to exposure vessels containing one of four dilutions of media in quadruplicate (Full-strength = Media1, two-fold dilution = Media2, five-fold dilution = Media5, ten-fold dilution Media10 and DI water). Immobilisation was visually assessed at 24 and 48 h alongside any other signs of stress such as surface trapping.

6.2.4 - Media dilution chronic stress assessment

Chronic *D. magna* reproductive toxicity tests following OECD guidelines (OECD, 1998) were performed using media dilutions suggested by the apparent no observed effect level (NOEL) in the acute toxicity tests. Single *D. magna* neonates (<24 h) were rinsed and immediately transferred to 250 ml beakers containing media1, media10, media20 (media1 diluted by a factor of 20) and DI water (100 ml, n = 5 per media concentration). Animals were maintained in these beakers for 21 days, with twice weekly media replacement and daily algal feeding (*Chlorella vulgaris*, 100µl on days 1–2, 150µl on days 3–7, 200µl on days 8–21) but with no additional supplements. To assess reproductive capability, the number of offspring were counted and removed from the test vessel daily. Again, any other irregularities were recorded.

6.2.5 - Acute toxicity conducted in collaboration with Alex Gavin (U of Birmingham)

All AgNP toxicity studies were performed in conjunction with Alex Gavin, University of Birmingham. EC₅₀s were determined for AgNP-cit, AgNP-PVP and AgNO₃ as outlined in chapter 2. Briefly, groups of *D. magna* neonates (<24 h) were exposed to increasing toxicant concentrations between 0.1 & 10 µg/l in media10 for 48 h with visual

immobilisation assessment after 24 and 48 h. EC₅₀ with 95 % confidence interval estimates were calculated using the Trimmed Spearman-Kärber equation.

6.2.6 - Nanoparticle dissolution conducted in collaboration with Alex Gavin (U of Birmingham)

All AgNP dissolution studies were performed in conjunction with Alex Gavin, University of Birmingham. The release of silver ions from AgNP-PVP under exposure conditions in the absence of *D. magna* was assessed over the acute toxicity time period (48 h) by ultra-centrifugation and ultra-filtration. AgNP-PVP were added to exposure beakers containing media10 (200 ml) in triplicate before mixing with a second aliquot of the media10 (50 ml) to yield a nominal final concentration of 5 ppm. Two techniques were used, ultracentrifugation and ultrafiltration, to separate the nano and ionic silver components prior to Inductively Coupled Plasma Mass Spectrometry (ICP-MS) to assess particle dissolution.

6.2.6.1 - Ultracentrifugation separation of ionic and nano silver

Aliquots (5 ml) were transferred directly from exposure vessels to centrifuge tubes (14 ml, Ultra-Clear™, Beckman Coulter USA) and diluted with UP H₂O (5 ml). Samples were covered with minimal paraffin film (Parafilm USA) and vortex mixed (5 s) before ultracentrifugation (30000 rpm, 10 °C, 1 hour, L7, Beckman Coulter USA). The resulting solution was split into top and bottom fractions (4.9 ml & 5.1 ml respectively) and acidified with nitric acid (2 %, trace metal grade). Top (ionic) and bottom (nano + ionic) samples were stored at 4 °C until submission for ICP-MS.

6.2.6.2 - Ultrafiltration separation of ionic and nano silver

Aliquots (10 ml) were transferred directly to ultrafiltration cells (10 ml, Millipore (UK)) fitted with filters (1 kDa NMWL, 25 mm, Ultracel regenerated cellulose) after 0, 24 and 48 h. Cells were pressurised with nitrogen (N₂, ca. 1 hour, PRESSURE) until ca. 5 ml filtrate containing only silver ions had passed into a clean scintillation vial. Pressure was relieved before a 4 ml aliquot was transferred to clean vials from both the filtrate (ionic) and filtrand (nano + ionic). Aliquots were acidified using HNO₃ (trace metal grade, 2 %), vortex mixed and stored at 4 °C until submission for ICP-MS.

6.2.6.3 - Inductively coupled plasma mass spectrometry analysis of silver conducted by Dr Steve Baker (U of Birmingham)

Acidified ionic and nanoparticle containing samples were submitted for ICP-MS analysis to Dr. S. Baker at the University of Birmingham. ICP-MS analysis specifically measured the elemental Ag concentration with a lower detection limit of 0.5 parts per billion (ppb). Acidified Ag solutions were atomised and ionised by the plasma torch (ca. 10,000 K) before measurement on a mass spectrometer. Ag concentration is determined by comparison to a calibration curve (Mitrano et al., 2012).

6.2.6.4 - Calculation of nano and ionic silver concentrations from ICP-MS results

Ionic silver concentration in the exposure vessel was calculated with Equation 6-1, where $[Ag^+]_E$ is the ionic silver concentration in the exposure vessel, $[Ag^+]_I$ is the

measured silver concentration of the acidified 'ionic' fraction (top/filtrate) and D is the sample preparation dilution factor.

Equation 6-1 Ionic silver concentration calculation from ICP-MS measurement

$$[Ag^+]_E = \frac{[Ag^+]_I}{D}$$

Nanoparticle concentration was calculated from Equation 6-2, where $[AgNP]_E$ is the concentration of silver nanoparticles in the exposure vessel, $[Ag^+]_{NP+I}$ is the measured silver concentration of the acidified 'nano + ionic' fraction (bottom and filtrand), $[Ag^+]_E$ is the ionic silver concentration in the exposure vessel, D is the sample preparation dilution factor, and C is the nanoparticle concentration factor from filtration.

Equation 6-2 Nano silver concentration calculation from ICP-MS measurement

$$[AgNP]_E = C \left(\frac{[Ag^+]_{NP+I}}{D} - [Ag^+]_E \right)$$

Percentage dissolution was calculated from Equation 6-3, where %_{Diss} is the percentage dissolution, $[AgNP]_E$ is the concentration of nanoparticles in the exposure vessel and $[Ag^+]_E$ is the ionic concentration in the exposure vessel.

Equation 6-3 Percentage dissolution calculation

$$\%_{Diss} = \frac{[Ag^+]_E}{[Ag^+]_E + [AgNP]_E} \times 100$$

6.2.7 - Lipidomic analysis of *D. magna* exposed to PVP capped silver nanoparticles conducted in collaboration with Alex Gavin

All exposures for AgNP lipidomic studies were performed in conjunction with Alex Gavin, University of Birmingham, all extractions, mass spectrometry and data analysis were performed by the author. Groups of *D. magna* neonates (< 24 h) were exposed to AgNP-PVP, AgNO₃, PVP or bulk silver alongside control organisms free of xenobiotic stress. AgNP-PVP concentrations were selected with reference to acute toxicity studies described in section 6.2.5. A nominal high concentration of 4.7 µg/l was selected as the lowest observed affect level (LOAEL), followed by three lower concentrations at two-fold intervals (medium = 2.4, low = 1.2 and very low = 0.6 µg/l). AgNO₃ exposure concentrations were matched to the AgNP-PVP concentrations with reference to dissolution data described in section 6.2.6. Nominal concentrations of AgNO₃ (282, 141, 71 and 35 ng (Ag)/l) were used for high, medium, low and very low exposures respectively. A final ionic silver exposure group was created by exposing neonates to the filtrate from the final wash of the particles, which was diluted and dosed identically to high dose AgNP-PVP representing the minimum possible ionic silver in the high dose should no dissolution occur. Potential capping agent effects were modelled by exposing neonates to the maximum possible concentration of PVP in the AgNP-PVP high dose, 6x10⁻⁷ % (w/v). Similarly, potential aggregation effects were modelled by exposing neonates to bulk silver, mass matched to high dose AgNP-PVP at 4.7 µg/l. All dose groups contained n = 6 replication, except high AgNP-PVP where some immobilisation was expected and replication was n = 8 to allow substitution of any immobilised neonates whilst maintaining exposure replication. Neonates were exposed for 24 h in

conditions described in section 2.4. Following exposure neonates were harvested and flash frozen as described in section 2.4. Lipids were extracted as described in section 2.4, however, prior to chloroform addition an aliquot of the homogenate (113 μ l) was removed for RNA extraction and an equal volume of MeOH:H₂O added. Lipid extracts were resuspended, analysed with FT-ICR MS and processed along the shotgun lipidomic workflow described in section 2.4.

6.3 - Results and discussion

6.3.1 - Silver nanoparticle characterisation

Qualitative TEM analysis identifies both the citrate and PVP-stabilised AgNPs as spherical in shape. The citrate stabilised nanoparticles were synthesised with an average diameter of 7 nm when measured by FIFFF and TEM in UP H₂O. DLS measured the same particles at 16 nm, however, is known to overestimate particle diameter (Roemer et al., 2011). All three techniques gave larger measurements for the AgNP PVP particles in UP H₂O. TEM analysis gave an average particle diameter of 10.8 nm compared to a DLS measurement of 28.3 nm. The disparity between FIFFF particle estimation (25.6 nm) and TEM in this case is due to the shell created by the PVP capping agent, TEM does not visualise this and so represents the Ag core of the nanoparticle, the additional 14.8 nm added in the FIFFF measurement represents the PVP coating (Tejamaya et al., 2012). Crucially, all these measurements lie comfortably within the nano boundary (1-100 nm).

Table 6-1 Characterisation of AgNP-cit and AgNP-PVP in UP H₂O

| | Size (nm) | |
|-----------------|-----------|----------|
| | AgNP-cit | AgNP-PVP |
| DLS (z average) | 16 | 28.3 |
| FIFFF | 7.2 | 25.6 |
| TEM | 7.0 | 10.8 |

In OECD modified media, AgNP-cit aggregated to such an extent that sedimentation occurred and a loss of colour was observed in the solution precluding further analytical measurements. However, in media10, a ten-fold dilution of OECD modified media, AgNP-cit particles did not aggregate significantly with mean particle diameters of 10 nm when measured by both TEM and FIFFF, showing only a slight increase in size. Comparatively, AgNP-PVP were more stable in OECD modified media with little to no sedimentation. However, significant aggregation was observed with DLS as particle size increased from 28 to 80 nm. This change in size was much less pronounced in media10 with particle size rising slightly to 41 nm. Only qualitative TEM data was obtained for AgNP-PVP with dispersed particles observed in both media concentrations. Aggregation of both particles in OECD modified media to the extent of sedimentation in the case of AgNP-cit limits the utility of this media in AgNP toxicity studies. Maximisation of nano-specific toxic effects requires well dispersed particles and as such media10 is a significant improvement in comparison to OECD modified media for both capping agents (Roemer et al, 2011).

6.3.2 - Acute effects of diluting culture media on *D. magna*

Neonate immobilisation was not induced by dilution of exposure media; however, there was a single immobilised neonate in media1 after 24 h (Table 6-2). Immobilisation was observed in DI H₂O increasing from 25 % at 24 h to 35 % after 48 h. Some surface trapping was observed, however, it was not observed in a concentration dependant manner. This lack of immobilisation reflects the resilience of *D. magna* to environmental stresses (Rider et al., 2005), however, does not preclude subtler sub-lethal effect which could impair lipidomic results.

Table 6-2 Acute toxicity of various media concentrations to *Daphnia magna*

| Media concentration | Starting pH | Ending pH | 24 h Immobilisation (%) | 48 h Immobilisation (%) |
|---------------------|-------------|-----------|-------------------------|-------------------------|
| Media1 | 7.33 | 7.28 | 3 | 3 |
| Media2 | 7.01 | 6.98 | 0 | 0 |
| Media5 | 6.72 | 6.65 | 0 | 0 |
| Media10 | 6.37 | 6.37 | 0 | 0 |
| DI water | 6.05 | 6.09 | 25 | 35 |

6.3.3 - Chronic effects of diluting culture media on *D. magna*

Although complete immobilisation was not observed in DI H₂O during an acute exposure (48 h) it was observed by 96 h, before reproductive maturity and so zero neonates were produced. Immobilisation was absent in all media dilutions. Mean neonate production was 61.8 ± 4 per organism across the 21-day period in media1 (Table 6-3). Fecundity was not reduced significantly by maintenance in media10, however, media20 caused major reproductive effects. The mean reproductive output in media20 was significantly reduced ($p < 0.01$) to 10.6 ± 5 , with additional immobilised neonates being produced. A lack of particle aggregation, *D. magna* immobilisation and reproductive inhibition

indicates that media10 is an optimal matrix to expose *D. magna* to AgNPs regardless of capping agent (Roemer et al., 2011).

Table 6-3 Chronic toxicity of various media concentrations to *Daphnia magna*

| Media | Immobilisation (%) | No. of offspring produced | Comments |
|----------|--------------------|---------------------------|---|
| Media1 | 0 | 61.8 ± 4.0 | - |
| Media10 | 0 | 56.8 ± 12.3 | - |
| Media20 | 0 | 10.6 ± 5.1* | Immobilised neonates and surface trapping |
| DI water | 100** | 0** | - |

6.3.4 - Acute toxicity of silver nanoparticles capped by citrate and PVP to *D. magna*

The EC₅₀ of AgNO₃ was converted to that of Ag⁺ to yield 0.94 and 0.84 µg/l at 24 and 48 h respectively (Table 6-4). This conversion allows comparisons with AgNP exposures; ICP-MS measures total silver content only. The nitrate moiety is unlikely to cause toxicity at these concentrations as it is a major component of *D. magna* culture media (OECD, 1998). In comparison to Ag⁺, both AgNP-cit and AgNP-PVP were less toxic in terms of Ag concentration. AgNP-cit had EC₅₀ values of 7.46 and 5.36 µg/l at 24 and 48 h respectively (Figure 6-1). AgNP-PVP had EC₅₀ values of 6.30 and 4.06 at 24 and 48 h respectively. Overlap of the 95 % confidence intervals for the EC₅₀ values at both 24 and 48 h indicates that AgNP-PVP is not notably more toxic than AgNP-cit. These EC₅₀ values are the same order of magnitude as those reported for *D. magna* exposed to other similarly prepared AgNPs (Hoheisel et al., 2012, Asghari et al., 2012). The particles used for toxicity exposures in Asghari et al., 2012 are citrate capped, in the size

range, 5-25nm and yield a 48 hour EC₅₀ of 4 µg/l. Similarly Hoheisel et al., 2012 show the EC₅₀ of 10 nm uncapped AgNPs to be 4.31 µg/l rising steadily with particle size to 24.48 µg/l at 50nm. This similarity in acute toxicity of the AgNPs used in this study to those reported in the literature is reassures our experimental procedure. It is worth noting that EC₅₀ values also vary widely for disparately prepared AgNPs, such as the commercially obtained nanopowder (EC₅₀ = 187 µg/l) also tested in Asghari et al., 2013 or the 26-fold change in EC₅₀ observed by Zhao et al., 2012 in particles differing only by their surface chemistry.

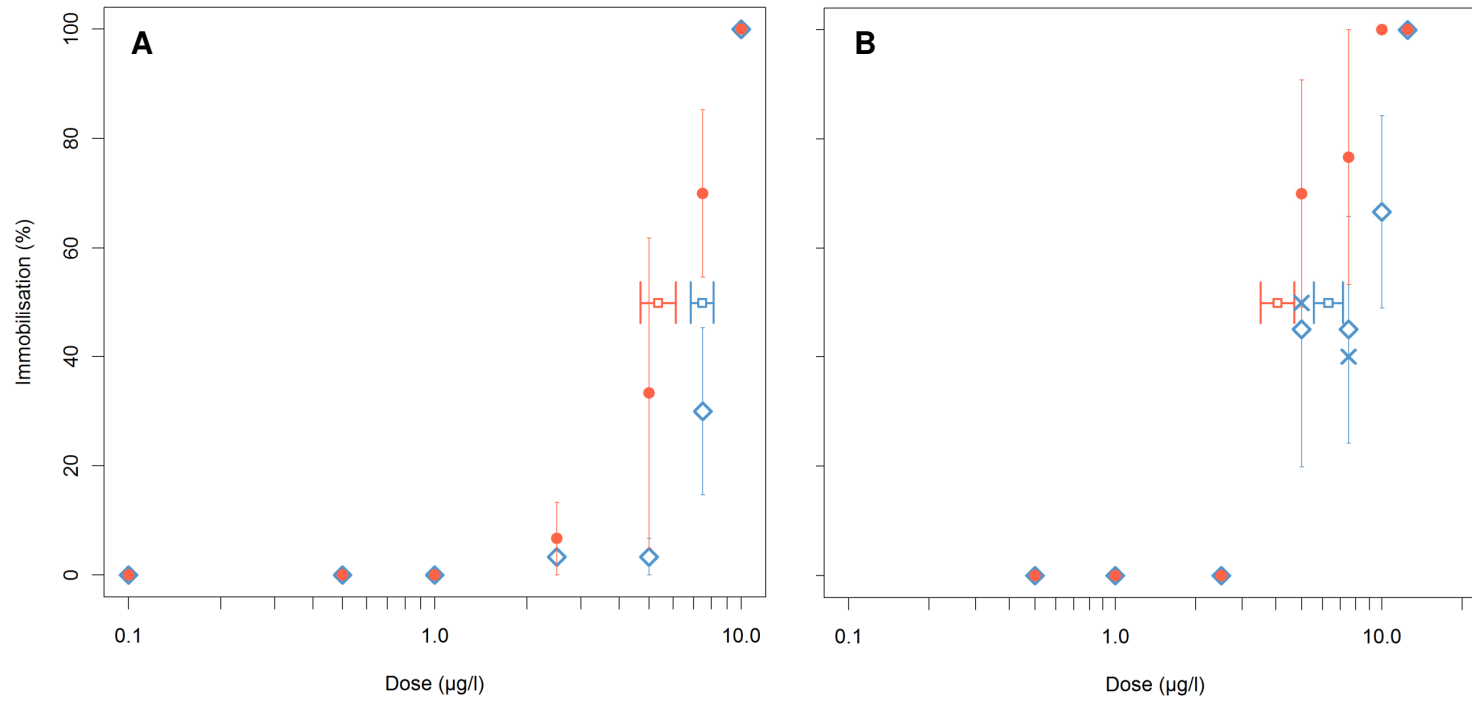


Figure 6-1 Dose-response curves for immobilisation of *D. magna* exposed to (A) AgNP-cit and (B) AgNP-PVP. Blue diamonds (\diamond) indicate immobilisation at 24 h, blue crosses (X) represent pre-adjustment values for non-monotonically increasing immobilisation at 24 h, red circles (\bullet) indicate immobilisation at 48 h. 24 h and 48 h EC_{50} s are indicated by squares. Vertical error bars represent standard error of the mean (SEM), horizontal error bars show 95 % EC_{50} confidence intervals

Table 6-4 EC₅₀ values for Ag⁺ (converted from AgNO₃), AgNPs-cit and AgNPs-PVP with 95 % confidence intervals at 24 and 48 h.

| Toxicant | EC ₅₀ 24 h (µg/l) | EC ₅₀ 48 h (µg/l) |
|-----------------|------------------------------|------------------------------|
| Ag ⁺ | 0.94 ± 0.07 | 0.84 ± 0.07 |
| AgNPs-cit | 7.46 ± 0.6 | 5.36 ± 0.8 |
| AgNPs-PVP | 6.30 ± 0.8 | 4.06 ± 0.6 |

6.3.5 - Dissolution of silver nanoparticles over the time-course of an acute exposure

The two techniques used to separate AgNP from Ag⁺ resulted in disparate results. Ultracentrifugation resulted in non-monotonically increasing values across the 48 h period with an average percentage dissolution of 86.5 % (Figure 6-2). This suggests that AgNP-PVP are almost completely converted into Ag⁺ instantly upon exposure vessel dosing. Ag concentration was greater in the bottom portion of all centrifuged samples indicating a degree of successful separation; however, both the acute toxicity results and nanoparticle characterisation preclude this from being accurate dissolution data. Should 80+ % of total silver be ionic, the EC₅₀ for AgNP-PVP would be much lower. As reported in section 6.3.4 the ionic silver EC₅₀ is 0.94 µg/l at 24 h which is only 15 % of the AgNP-PVP EC₅₀ at 24 h, these values should be much closer together if the Ag is predominantly ionic in the AgNP exposures. As mentioned in section 6.3.1, nanoparticles were characterised after suspension in media₁₀, although theoretically this would be possible with < 15 % of particles remaining, they would have been extremely difficult to find with TEM, additionally loss of yellow colour would also have been observed, neither of these were the case. It is probable that ultracentrifugation is

inefficient for particles of such small size or the AgNP pellet is not sufficiently strong to avoid re-suspension of particles prior to splitting.

Ultrafiltration separation identified increasing AgNP-PVP dissolution with time as we would expect (Figure 6-2). At 0 h, the start of an exposure, 4.0 % of Ag was in ionic form rising to 5.7 % after 24 h and 8.2 % at 48 h, the end of exposures. Variation also increased across the time course. Dissolution data was used to select concentrations for lipidomic exposures, ionic silver concentration at 6 % of each AgNP-PVP concentration were used to distinguish nano effects from silver dissolution effects.

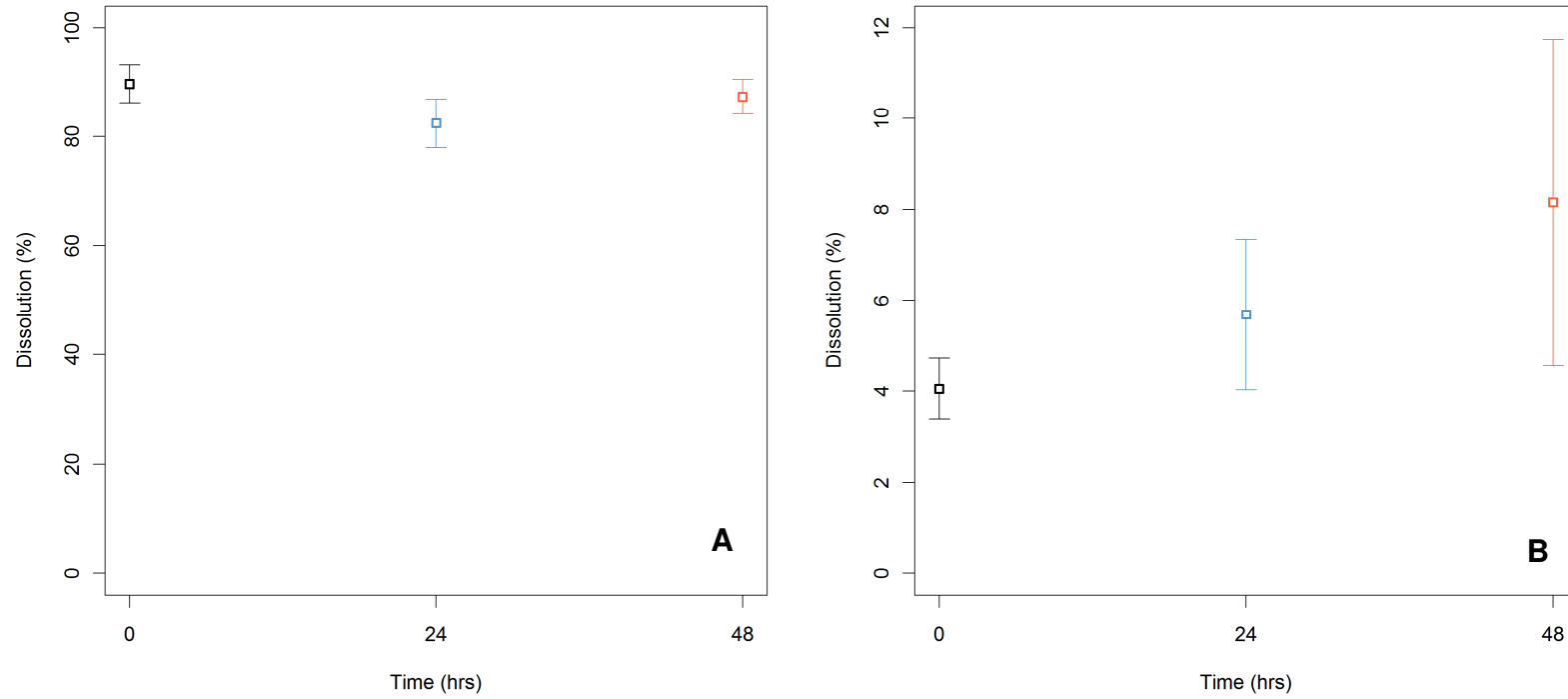


Figure 6-2 Dissolution of silver nanoparticles across acute toxicity time course. Error bars show standard error of the mean (n=3). (A) Ultracentrifugation separation (B) Ultrafiltration separation.

6.3.6 - Lipidomic perturbations caused by silver nanoparticles to *D. magna*

Immobilisation was seen in a greater proportion of *D. magna* neonates than expected from acute toxicity assessment (section 6.3.4). This led to the loss of two exposure groups from the high dose AgNP-PVP and one from the medium dose of AgNP-PVP. This shows that AgNP-PVP exposures were having significant macro effect and so metabolic, and by extension lipidomic, responses should be large. Additionally, one exposure group was lost from ionic silver high due to a loose cap during homogenisation.

PCA of glog modified output matrices was undertaken to visualise differences between exposure groups. Table 6-5, summarises the significance of separation between groups along the six principal components containing the most variance. Significant separation was observed between groups along PC3 ($p = 0.004$) and PC5 ($p = 7.814 \times 10^{-6}$). Tukey's post-hoc analysis identified that the separation along PC3 lay between the negative control group and high doses of both AgNP-PVP and Ag^+ , which is an expected result, however, low dose of AgNP-PVP was also significantly different to the negative control (Figure 6-3). Whilst this suggests there may be a perturbation occurring in the high doses, there is no separation from the PVP and bulk controls which makes it difficult to draw strong conclusions. Far more significant is the separation along PC5. Medium and very low silver concentrations separate significantly from their nano counterparts as well as PVP and negative controls. Additionally these ionic groups are visibly pulling away from the remaining nano and control groups. However, this is a strange result given that the ionic high concentration clusters very well into the other groups. The limited

separation observed along all PCs limits the utility of further analysis and was disappointing given the toxicity of particles in the exposures.

To simplify univariate analysis, comparison between negative control and high dose AgNP-PVP and Ag⁺ exposure groups were selected as these should experience the greatest effect and thus represent the most likely opportunity to view lipid peroxidation should it be occurring. Large positive and negative fold changes were observed from control to high doses in both ionic and nano exposures, however, only 62 of 1634 observed spectral features were significantly changing of which only 16 were annotated by LipidMAPS comparison (Figure 6-4). There was little similarity between the identifications made, and no correlation between fold changes in either nano or ionic exposures. It may be that the large fold changes observed are artifacts of a high number of missing values due to the large number of groups and small number of replication (n=4-6).

Table 6-5 Table showing significant group separation by principal scores of groups of *D. magna* exposed to varying concentrations of AgNP-PVP, AgNO₃, PVP or bulk silver. ** = P<0.005, * = P<0.001.**

| PC1 | PC2 | PC3 | PC4 | PC5 | PC6 |
|-------|-------|---------|-------|-------------------------|-------|
| 0.165 | 0.059 | 0.004** | 0.209 | 7.814x10 ^{-6*} | 0.589 |

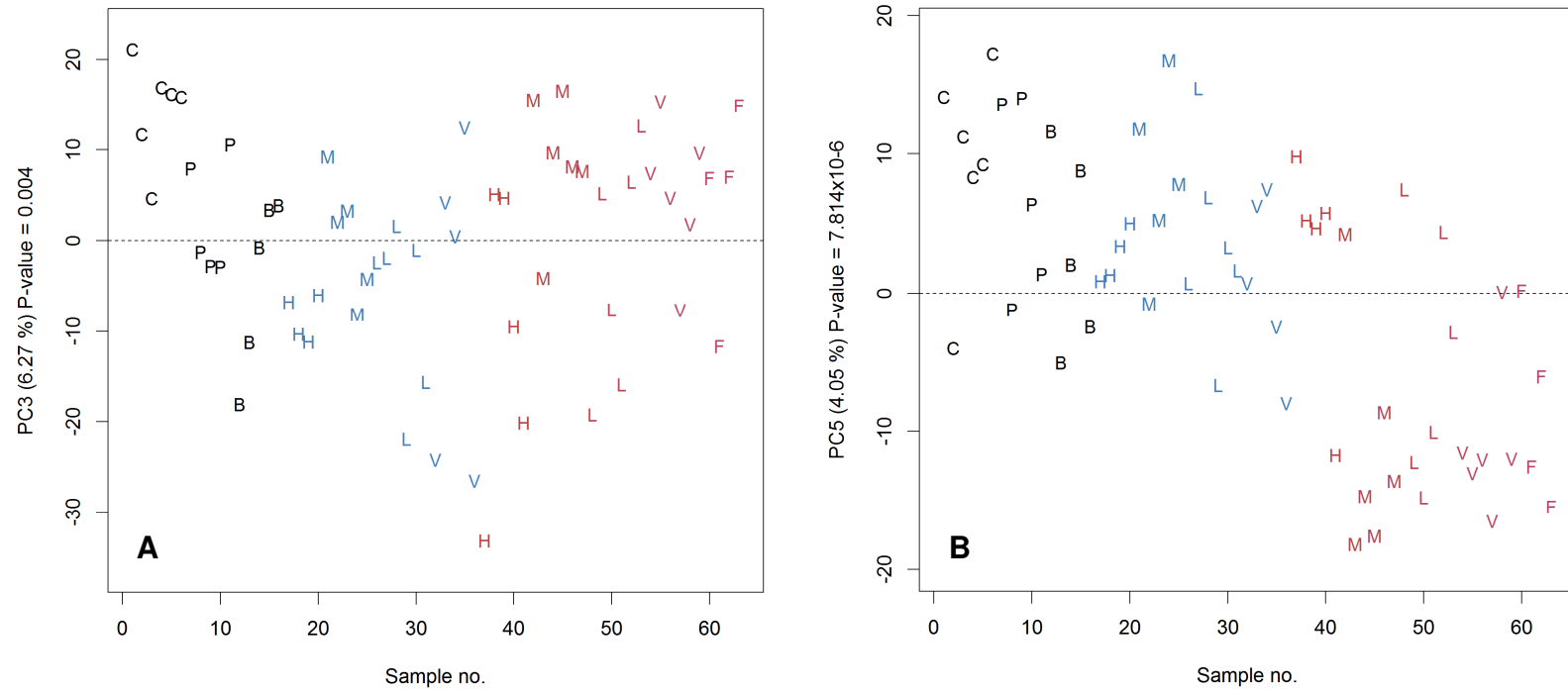


Figure 6-3 PCA scores plots showing the most significant separation between exposure groups. Colour signifies toxicant, Black = control, Blue = AgNP-PVP, Red = silver ions. Letters signify concentration in toxicant groups H= High, M = Medium, L= Low, V = Very Low. Letters signify type in control groups, C = negative control, P = PVP, B = bulk silver. (A) PC3, (B) PC5.

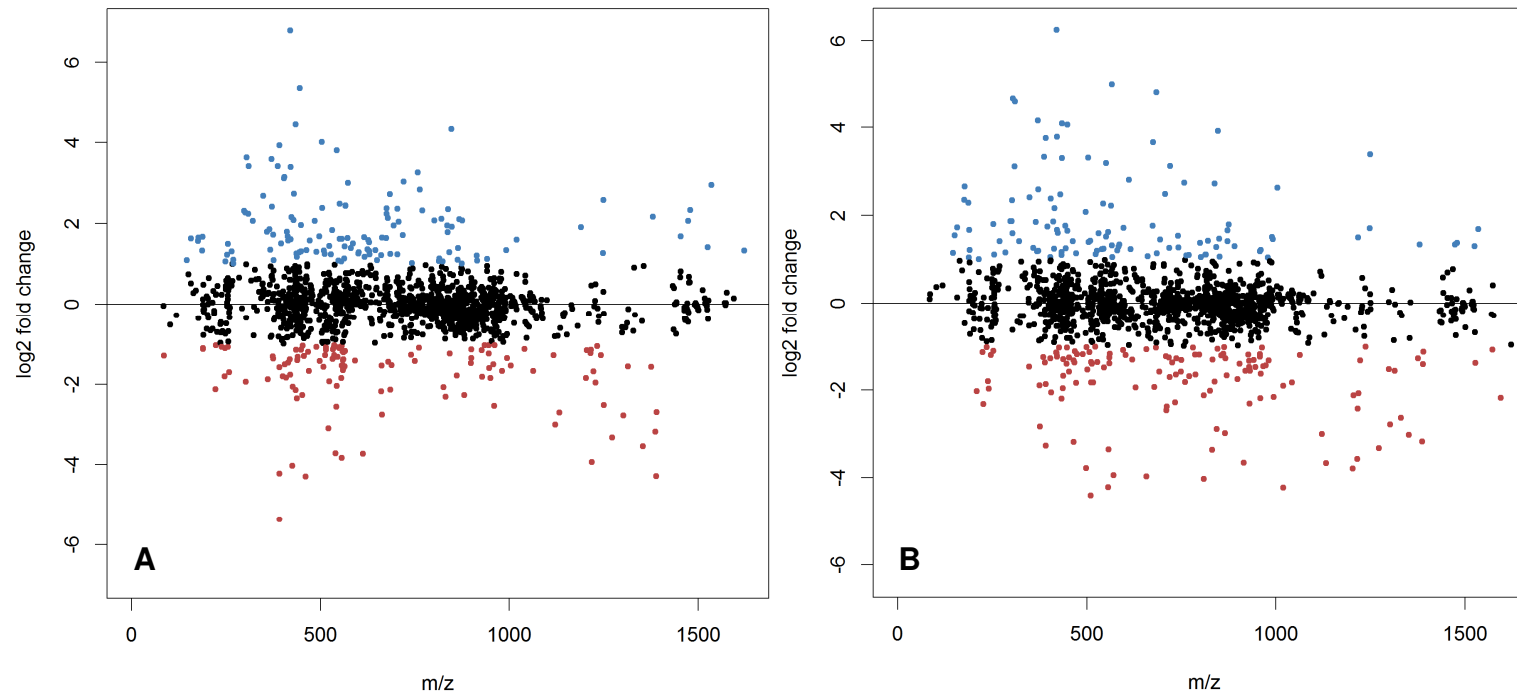


Figure 6-4 Scatter plot showing log₂ fold changes of lipid species (high dose / control) versus *m/z*. Positive fold changes are shown in blue, negative fold changes are shown in red. (A) Ionic silver high dose, (B) AgNP-PVP high dose.

In light of the limited perturbations observed by multi- and uni-variate statistics, focus reverted to oxidation detection. Untargeted annotation of oxygen addition to all peaks in the output matrix yielded 211 +O and 133 +O₂ spectral features. These peaks did not show fold changes which differed from the data as a whole in either ionic or nano high doses, spread evenly around a log₂ fold change of zero, i.e. no change and very few above an absolute value of 1, an arbitrary two-fold change (Figure 6-5, Figure 6-6). Targeted annotation of oxygen addition yielded similar results. 145 peaks were matched to baseline annotated lipid peaks within a mass error of 2ppm. From these baseline spectral features, 27 +O and 32 +O₂ additions were observed of which 12 and 10 were annotated as unmodified lipids (Figure 6-7, Figure 6-8). The fold changes associated with these annotations were almost exclusively between -1 and 1, indicating very little change within these compounds. Should lipid peroxidation be occurring significantly the fold change situation should minimally mirror that from the *in vitro* studies in chapter 4, however, it is more similar to the *in vitro* studies where little was observed. This suggests that there is little oxidative perturbation occurring from exposure to these AgNP-PVP. Given that immobilisation, almost synonymous with mortality, was occurring in the high dose of AgNP-PVP this would further suggest that lipid peroxidation is not the major mechanism of toxic action of these particles. However, it may be the case that individual lipid peroxides are not present in large enough concentrations to be observed *in vivo* using shotgun lipidomics, to rule this out further studies would be required with sample pre-separation using LC or TLC for example (Sparvero et al., 2010).

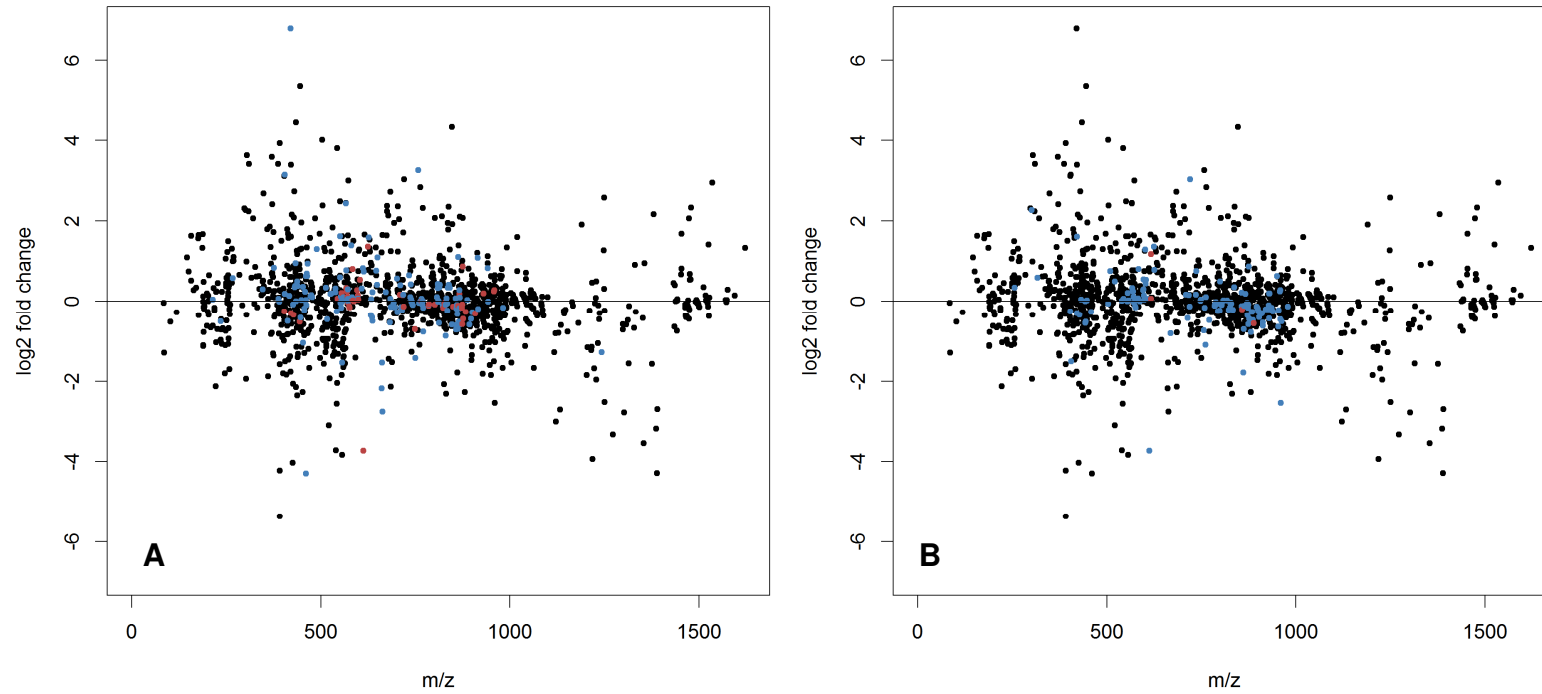


Figure 6-5 Log₂ fold changes (High dose ionic / negative control) of unmodified (black), and potentially oxidatively modified (blue) spectral features. Spectral features which could correspond to unmodified or oxidatively modified are shown in red. (A) shows +O modifications, (B) shows +O₂ modifications.

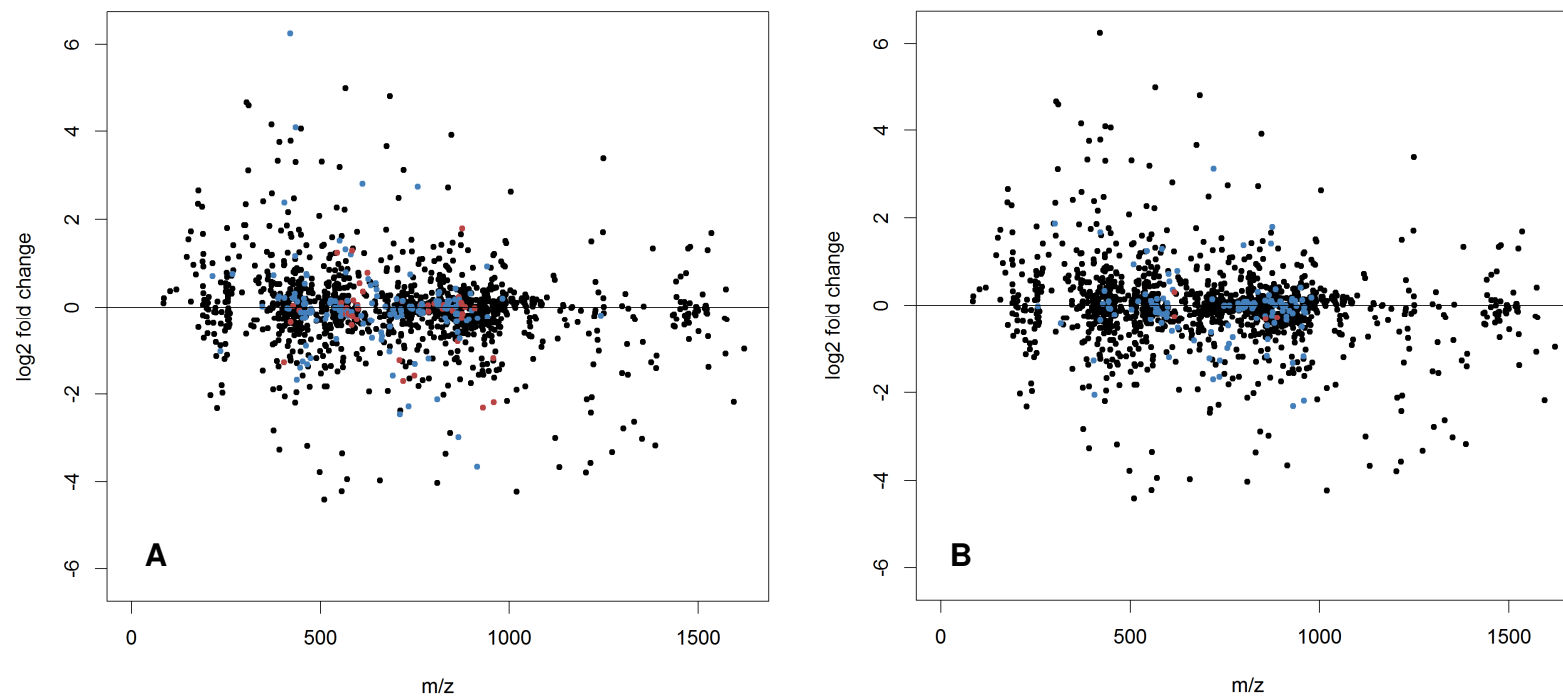


Figure 6-6 Log₂ fold changes (High dose AgNP-PVP / negative control) of unmodified (black), and potentially oxidatively modified (blue) spectral features. Spectral features which could correspond to unmodified or oxidatively modified are shown in red. (A) shows +O modifications, (B) shows +O₂ modifications.

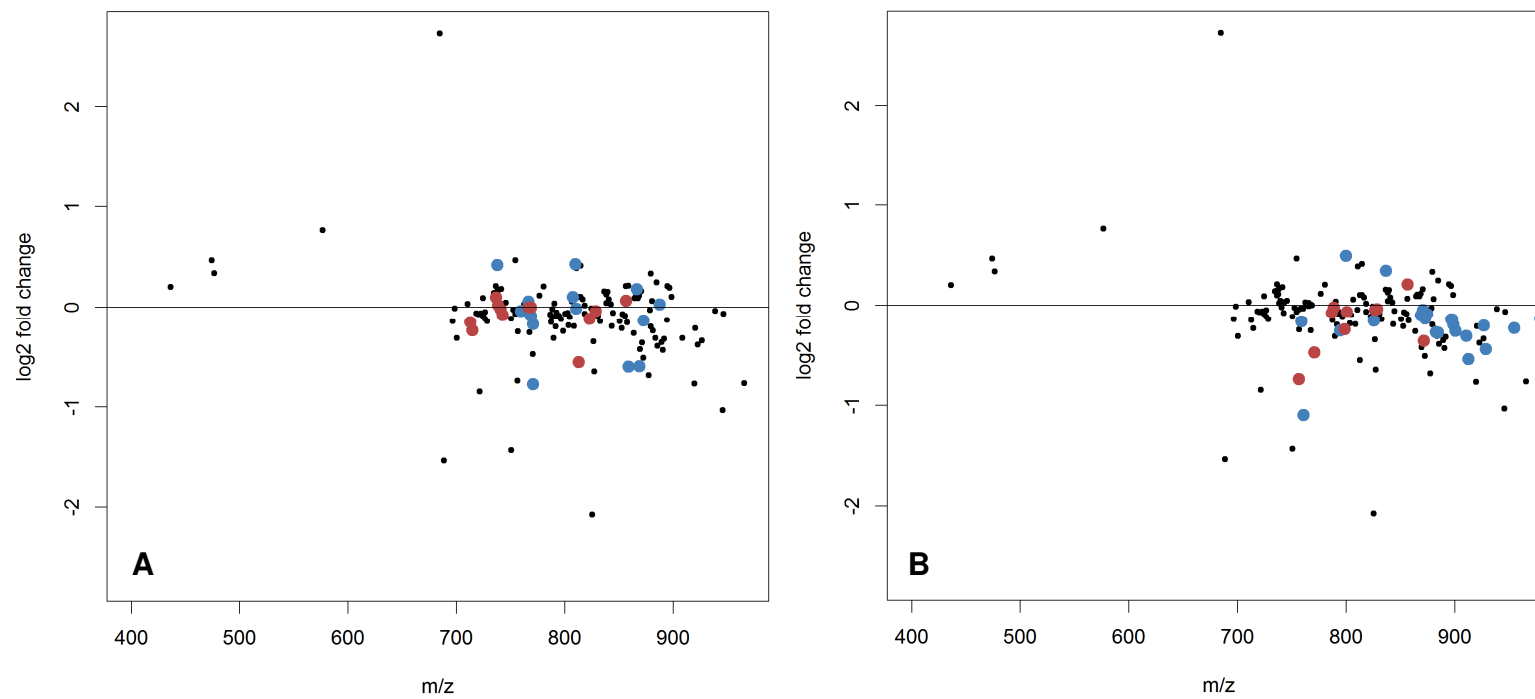


Figure 6-7 Scatter plots showing putatively annotated oxidation in high dose ionic silver exposed *D. magna* lipid extracts. Exposed / control intensity log₂ fold changes of baseline lipidome matched spectral features (black), oxygen addition features (blue) and oxygen added features with an unmodified lipid annotation (red). (A) single oxygen addition. (B) double oxygen addition.

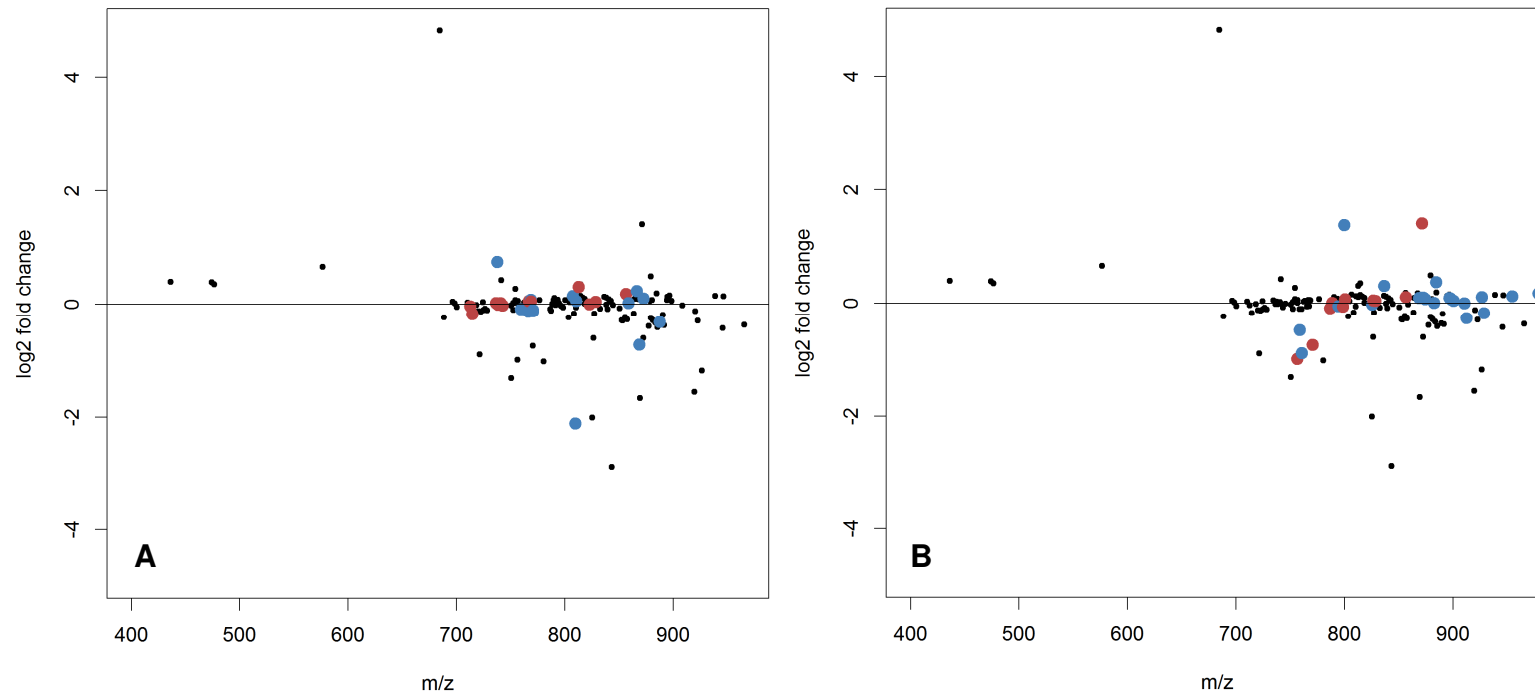


Figure 6-8 Scatter plots showing putatively annotated oxidation in high dose AgNP-PVP exposed *D. magna* lipid extracts. Exposed / control intensity log₂ fold changes of baseline lipidome matched spectral features (black), oxygen addition features (blue) and oxygen added features with an unmodified lipid annotation (red). (A) single oxygen addition. (B) double oxygen addition.

6.4 - Conclusions

The work presented in this chapter represents the first attempt to elucidate mechanisms of silver nanoparticle toxicity with lipidomic techniques in *D. magna* and proceeds only one published lipidomic AgNP toxicity study (Tentschert et al., 2013).

Optimisation of media conditions, particle dissolution and multi-platform nanoparticle characterisation allowed for robust toxicity studies which has been absent in many other toxicological studies to date (Römer et al., 2013). We have shown that ionic strength of exposure media is a key variable in the design of toxicity assays which, if not modified may lead to significant aggregation of particles which must be considered in any results. The nanoparticle dissolution observed here has confirmed that significant concentrations of ionic silver will always be present for these PVP capped particles unless chelating agents such as EDTA are added to exposures. Characterisation and dissolution data collected alongside these studies is necessary in order to draw robust conclusions about the mechanism of AgNP toxicology. This is so crucial as the surface area : size ratio of nanomaterials is the source of their special properties, changes in these will affect their mechanism of action (Jiang et al., 2009).

Acute toxicity assessment of two synthetic AgNPs capped with PVP and citrate showed that they are less toxic than ionic silver in terms of mass per volume calculations which matches findings in previously published studies with disparately capped AgNPs (Hoheisel et al., 2012, Asghari et al., 2012, Griffitt et al., 2008). Unfortunately, estimation of environmental release of AgNPs is complicated by a dearth of methodologies which can detect, quantify and characterise NMs in complex environmental or

biological media (Gottschalk et al., 2010). However, repeatable, inter-laboratory toxicity data will be essential in setting environmental exposure limits.

With such comprehensive development of exposures and monitoring of nanoparticle chemistry it is disappointing that little lipidomic perturbation was observed. There was no indication of the increases in PC species shown in human macrophages (Tentschert et al., 2013) or lipid peroxidation caused by increased ROS indicated by previous metabolomic study (Kim et al., 2011). There was some significant separation shown by PCA, however, this did not follow dose-response relationships raising significant questions in its validity. Whilst *D. magna* exposed to high doses of AgNP-PVP and Ag⁺ separate significantly from negative control in PCA, very low dosed AgNP-PVP organisms do also. Toxic effects observed at high doses and very low doses should also be observed at low and medium doses, in this case they were not suggesting PCA separation may be an artefact of many groups with small replication (Kirwan et al., 2013).

The lack of evidence of lipid peroxidation, mirrored the *in vivo* studies from chapter 5, coupled with the immobilisation observed at high doses suggests top-down shotgun lipidomics may not have great utility for observation of oxidative stress in *D. magna*. As mentioned above, previous metabolomic and lipidomic studies in have indicated oxidative stress in model organisms other than *D. magna*. It may be possible to confirm or more comprehensively refute the presence of oxidative stress in this case using more targeted assays such as fluorometric measurement of ROS or HPLC measurement of GSH as described previously in *D. magna* (Becker et al., 2011).

7 - General conclusions and future work

In chapter one, four research objectives were set out to explore the potential toxic effects of established and novel toxicants on aquatic systems using mass spectrometric lipidomic analyses. Firstly, the ability to induce and observe lipid peroxidation from individual lipids was assessed in chapter 3. Subsequently lipidomic annotation of two sentinel ecotoxicology species, *D. magna* and *C. reinhardtii*, was undertaken in chapter 4. Oxidation of these lipidomes was then attempted utilising *in vitro* and *in vivo* methodologies in chapter 5. Finally, analysis of lipid perturbation in *D. magna* by novel ecotoxicants silver nanoparticles was attempted using robust exposure techniques and particle characterisation, absent in many of the other publications on this subject, in chapter 6.

In chapter 3 a soft oxidation technique was successfully used to induce oxidation of biologically relevant unsaturated lyso and diacyl PE species including up to five oxygen additions to fatty acyl chains. Extensive manual annotation was successfully undertaken to yield well-maintained fragmentation patterns across oxidised products, with particularly informative fragments produced in negative ion mode. To my knowledge this is the first study to systematically observe and fragment long chain oxidised products of PE and annotate the resulting patterns. The success of this wet lab aspect has allowed the generation of a new tool for the analysis of lipid oxidation. In its initial form, OxyLipidBlast contains 40,000+ *in silico* fragmentation patterns comprising the major anions observed in section 3.3 of this thesis: $[FA_1-H]^-$, $[FA_2+O_x-H]^-$, $[M+O_x-FA_1(keto)-H]^-$, $[M+O_x-FA_1(carboxyl)-H]^-$, $[M+O_x-FA_2(keto)+O_x-H]^-$, $[M+O_x-FA_2(carboxyl)+O_x-H]^-$ and $[M-H_2O-H]^-$. Utilising this novel tool the original oxidised

products were successfully retro-annotated and a number of oxidised products were successfully annotated from a more complex PE mixture. The obvious future for this study is to expand the oxidised structures to include all the major phospholipid classes; PC, PA, PI, PG and PS. This would make the dual ion mode analysis challenging due to the propensity of the other phospholipid classes to ionise exclusively as positive or negative species. However, PC can be modified by the addition of modifying agents, for example ammonium acetate used extensively in this thesis, to yield negative adducts. Negative ions would be the optimal choice for the expansion of OxyLipidBlast as their fragmentation patterns yield greater structural information. This chapter successfully achieved its stated objective and has aided the creation of a tool which will allow the annotation of oxidised lipids for subsequent lipidomic studies. Automated annotation of oxidised lipids, made possible by OxyLipidBlast, will drastically decrease data analysis time in oxidative lipidomic studies such as those conducted in the Kagan group in Pittsburgh (Sparvero et al, 2010, Tyurin et al., 2009). Additionally, it could provide fresh lipid modification insights in studies which may have not specifically attempted to detect oxidised lipids as they do not appear in the LipidMAPS database or tools (Fahy et al., 2009). Negative results are rarely reported in scientific literature (Dirnagl and Lauritzen, 2010), so assumptions about what was assessed in previous lipidomics studies should be made extremely tentatively, however, it may be that studies which reported oxidative stress in lipid systems such as Tentschert et al, 2013, may have observed lipid peroxides if they had utilised OxyLipidBlast as a quick, cross-platform, data analysis tool.

Chapter 4 presents the first annotated lipidome of the sentinel ecotoxicological species *D. magna*. The optimisation of analytical techniques for the analysis of lipid extracts from *D. magna* allowed annotation of all the major classes of phospholipids to be identified with chain length and parity in agreement with previously published studies of total fatty acids (Bychek et al., 2005, Persson and Vrede, 2006). PE was by far the most abundant PL, which would be expected in negative ion mode, given that PE was the second most abundant PL reported by Bychek et al, 2005 coupled with the lower ionisation efficiency of PC in negative mode (Pulfer and Murphy, 2003). Less success was achieved in the annotation of the *C. reinhardtii* lipidome although significant concentrations of PG were observed as would be expected from previously reported studies of algal polar lipids (Arts et al., 2009). The lesser coverage of *C. reinhardtii* lipids may be due to the lack of algal lipids currently contained in the LipidMAPS database. Increased coverage of both species could be enhanced with MS/MS analyses, however, sample separation would be required as direct infusion yields complex matrices where numerous compounds are fragmented together clouding fragmentation patterns. Fragmentation patterns could then be matched against the LipidBlast databases which contain algal lipids, both experimental and *in silico* (Kind et al., 2013). Annotated lipidomes represent strong foundations for further analyses of lipids in *D. magna* including but not limited to toxicity testing and other studies, such as those assessing fatty acid composition of *Daphnia* under differing environmental stresses (Bychek et al., 2005), would be greatly enhanced by information regarding the origin of those fatty acids. Oxidation of biological lipids was attempted in chapter 5, initially *in vitro* and then *in vivo*. Repeated single and double oxygen additions were induced by lipid extract

exposure to air, however, as expected results were more pronounced with hydrogen peroxide exposure. This also highlighted a major limitation in the detection of lipid peroxidation with shotgun lipidomics as numerous spectral features were observed which appeared at oxygen additions above unmodified lipids but were also annotated as lipids themselves, identifying common intrinsic oxygen differences in lipid extracts, primarily between ester and ether bound species. Attempts to translate lipid peroxidation into *in vivo* systems were less successful. *D. magna* exposed to H₂O₂, CuSO₄ and AgNO₃ and AgNP showed little sign of lipid peroxidation although significant perturbation to the lipid extract as a whole was identified by principal component scores. All of these xenobiotics have been shown to cause oxidative stress and lipid peroxidation in various model systems with targeted assays (Cortese-Krott et al., 2009, Gagne et al., 2012, Vieira et al., 2009, Watanabe et al., 2009), and so the lack of success in observing lipid peroxidation in response to any of these suggests that the techniques used here are unlikely to have wide utility in the field of oxidative lipidomics.

Overall, it appears that observation of lipid peroxides and other oxidised products is achievable using shotgun mass spectrometric lipidomic techniques. However, it is yet to be proven whether they have utility in ecotoxicological testing, which may be supported by the lack of literature in this area, with most oxidative lipidomics toxicity studies utilising separation of lipid classes via chromatography (Tyurin et al., 2009) or online fragmentation techniques such as those described in Han et al., 2012. Separation of lipid extracts using chromatography represents the most attractive enhancement to these techniques, allowing purification of the sample matrix, removing isomeric overlap and temporally separating compounds to allow

fragmentation enhancing compound knowledge from annotation to identification (Hartler et al., 2013). However, separation techniques come at the cost of analysis time and require greater sample concentration so are less useful for high-throughput analysis. To enhance the scope of this work, greater identification of the baseline lipidome would be the ideal next step. As mentioned in chapter 4, only 32% of the 1638 spectral features observed in *D. magna* lipid extracts were annotated. Utilising chromatographic separation, tandem fragmentation and new *in silico* databases such as LipidBlast and OxyLipidBlast expanding this coverage and enhancing annotations to identifications would be possible (Sumner et al., 2007). Complete identification of metabolomes and lipidomes is still the greatest challenge facing the field (Weber et al., 2011), however, analytical technology and novel data analysis methodologies are continually progressing. A comprehensive lipidome would remove false positive annotations and allow far greater biological insight into perturbations such as those caused in chapter 5 by xenobiotics.

To conclude the work conducted in this thesis has indicated the limitations of shotgun lipidomics in ecotoxicology testing. However, has also yielded the first lipidomic annotation of *D. magna* and facilitated the production of a new analytical tool, the first to aid identification of oxidised lipid products.

8 - References

- AB Sciex (2006) *LipidView* [Online] Available from:
<http://www.absciex.com/products/software/lipidview-software?country=Australia>
[Accessed: 13th January 2014]
- Allen, H. J., Impellitteri, C. A., Macke, D. A., Heckman, J. L., Poynton, H. C., Lazorchak, J. M., Govindaswamy, S., Roose, D. L. & Nadagouda, M. N. (2010) Effects from filtration, capping agents, and presence / absence of food on the toxicity of silver nanoparticles to *Daphnia magna*. *Environmental Toxicology and Chemistry*, 29, 2742-2750.
- Allwood, J. W. & Goodacre, R. (2010). An Introduction to Liquid Chromatography-Mass Spectrometry Instrumentation Applied in Plant Metabolomic Analyses. *Phytochemical Analysis*, 21, 33-47.
- Annesley, T. M. (2003). Ion suppression in mass spectrometry. *Clinical Chemistry*, 49, 1041-1044.
- Arisz, S. A., Van Himbergen, J. A. J., Musgrave, A., Van Den Ende, H. & Munnik, T. (2000). Polar glycerolipids of *Chlamydomonas moewusii*. *Phytochemistry*, 53, 265-270.
- Arts, M. T., Brett, M. T. & Kainz, M. J. (2009). *Lipids in Aquatic Ecosystems*, Springer.
- Asghari, S., Johari, S. A., Lee, J. H., Kim, Y. S., Jeon, Y. B., Choi, H. J., Moon, M. C. & Yu, I. J. (2012). Toxicity of various silver nanoparticles compared to silver ions in *Daphnia magna*. *Journal of Nanobiotechnology*, 10.
- Avanti polar lipids Inc. (2014) *Avanti Polar Lipids – Plasmalogens* [Online] Available from:
http://avantilipids.com/index.php?option=com_content&view=article&id=131&Itemid=139
[Accessed: 13th January 2014]
- Barnett, R. (2014). *Female adult and neonate Daphnia magna*. [Photograph] University of Birmingham.
- Becker, D., Brinkmann, B. F., Zeis, B. & Paul, R. J. (2011). Acute changes in temperature or oxygen availability induce ROS fluctuations in *Daphnia magna* linked with fluctuations of reduced and oxidized glutathione, catalase activity and gene (haemoglobin) expression. *Biology of the Cell*, 103, 351-363.
- Benjami, N. I., Y. & Hochberg, Y. (1995). Controlling the false discovery rate - a practical and powerful approach to multiple testing. *Journal of the Royal Statistical Society Series B-Methodological*, 57, 289-300.
- Benn, T. M. & Westerhoff, P. (2008). Nanoparticle silver released into water from commercially available sock fabrics. *Environmental Science & Technology*, 42, 4133-4139.

- Bishop, W. R. & Bell, R. M. (1988). Assembly of phospholipids into cellular membranes - biosynthesis, transmembrane movement and intracellular translocation. *Annual Review of Cell Biology*, 4, 579-610.
- Bligh, E. G. & Dyer, W. J. (1959). A rapid method of total lipid extraction and purification. *Canadian Journal of Biochemistry and Physiology*, 37, 911-917.
- Bold, H. C. (1949). The Morphology of *Chlamydomonas chlamydogama*, Sp. Nov. *Bulletin of the Torrey Botanical Club*, 26, 101-108.
- Booth, S. C., Workentine, M. L., Weljie, A. M. & Turner, R. J. (2011). Metabolomics and its application to studying metal toxicity. *Metallomics*, 3, 1142-1152.
- Bopp, S. K., Abicht, H. K. & Knauer, K. (2008). Copper-induced oxidative stress in rainbow trout gill cells. *Aquatic Toxicology*, 86, 197-204.
- Borm, P. J., Robbins, D., Haubold, S., Kuhlbusch, T., Fissan, H., Donaldson, K., Schins, R., Stone, V., Kreyling, W., Lademann, J., Krutmann, J., Warheit, D. & Oberdorster, E. (2006). The potential risks of nanomaterials: a review carried out for ECETOC. *Particle and Fibre Toxicology*, 3, 11.
- Breitholtz, M., Ruden, C., Hansson, S. O. & Bengtsson, B. E. (2006). Ten challenges for improved ecotoxicological testing in environmental risk assessment. *Ecotoxicology and Environmental Safety*, 63, 324-335.
- Breitling, R., Vitkup, D. & Barrett, M. P. (2008). New surveyor tools for charting microbial metabolic maps. *Nature Reviews Microbiology*, 6, 156-161.
- Brouwers, J. F. (2011). Liquid chromatographic-mass spectrometric analysis of phospholipids. Chromatography, ionization and quantification. *Biochimica Et Biophysica Acta-Molecular and Cell Biology of Lipids*, 1811, 763-775.
- Bruins, A. P. (1998). Mechanistic aspects of electrospray ionization. *Journal of Chromatography A*, 794, 345-357.
- Bundy, J. G., Davey, M. P. & Viant, M. R. (2009). Environmental metabolomics: a critical review and future perspectives. *Metabolomics*, 5, 3-21.
- Bychek, E. A. & Gushchina, I. A. (1999). Age-dependent changes of lipid composition in daphnia magna. *Biochemistry Biokhimiia*, 64, 543-545.
- Bychek, E. A., Dobson, G. A., Harwood, J. L. & Guschina, I. A. (2005). Daphnia magna can tolerate short-term starvation without major changes in lipid metabolism. *Lipids*, 40, 599-608.
- Carvalho, G. R. & Hughes, R. N. (1983). The effect of food availability, female culture-density and photoperiod on ehippia production in *Daphnia-magna straus* (crustacea, cladocera). *Freshwater Biology*, 13, 37-46.
- Catala, A. (2012). Lipid peroxidation modifies the picture of membranes from the "Fluid

Mosaic Model" to the "Lipid Whisker Model". *Biochimie*, 94, 101-109.

Chen, S., Hoene, M., Li, J., Li, Y., Zhao, X., Haering, H. U., Schleicher, E. D., Weigert, C., Xu, G. & Lehmann, R. (2013). Simultaneous extraction of metabolome and lipidome with methyl tert-butyl ether from a single small tissue sample for ultra-high performance liquid chromatography/mass spectrometry. *Journal of Chromatography A*, 1298, 9-16.

Colbourne, J. K., Pfrender, M. E., Gilbert, D., Thomas, W. K., Tucker, A., Oakley, T. H., Tokishita, S., Aerts, A., Arnold, G. J., Basu, M. K., Bauer, D. J., Caceres, C. E., Carmel, L., Casola, C., Choi, J. H., Detter, J. C., Dong, Q. F., Dusheyko, S., Eads, B. D., Frohlich, T., Geiler-Samerotte, K. A., Gerlach, D., Hatcher, P., Jogdeo, S., Krijgsveld, J., Kriventseva, E. V., Kultz, D., Laforsch, C., Lindquist, E., Lopez, J., Manak, J. R., Muller, J., Pangilinan, J., Patwardhan, R. P., Pitluck, S., Pritham, E. J., Rechtsteiner, A., Rho, M., Rogozin, I. B., Sakarya, O., Salamov, A., Schaack, S., Shapiro, H., Shiga, Y., Skalitzky, C., Smith, Z., Souvorov, A., Sung, W., Tang, Z. J., Tsuchiya, D., Tu, H., Vos, H., Wang, M., Wolf, Y. I., Yamagata, H., Yamada, T., YE, Y. Z., Shaw, J. R., Andrews, J., Crease, T. J., Tang, H. X., Lucas, S. M., Robertson, H. M., Bork, P., Koonin, E. V., Zdobnov, E. M., Grigoriev, I. V., Lynch, M. & Boore, J. L. (2011). The Ecoresponsive Genome of *Daphnia pulex*. *Science*, 331, 555-561.

Colvin, V. L. (2003). The potential environmental impact of engineered nanomaterials. *Nature Biotechnology*, 21, 1166-1170.

Comisarow, M. B. & Melka, J. D. (1979). Error estimates for finite zero-filling in fourier-transform spectrometry. *Analytical Chemistry*, 51, 2198-2203.

Cortese-Krott, M. M., Munchow, M., Pirev, E., Hessner, F., Bozkurt, A., Uciechowski, P., Pallua, N., Kroncke, K. D. & Suschek, C. V. (2009). Silver ions induce oxidative stress and intracellular zinc release in human skin fibroblasts. *Free Radical Biology and Medicine*, 47, 1570-1577.

Degenkolbe, T., Giavalisco, P., Zuther, E., Seiwert, B., Hinch, D. K. & Willmitzer, L. (2012). Differential remodeling of the lipidome during cold acclimation in natural accessions of *Arabidopsis thaliana*. *Plant Journal*, 72, 972-982.

Dettmer, K., Aronov, P. A. & Hammock, B. D. (2007). Mass spectrometry-based metabolomics. *Mass Spectrometry Reviews*, 26, 51-78.

Dhawan, A. & Sharma, V. (2010). Toxicity assessment of nanomaterials: methods and challenges. *Analytical and Bioanalytical Chemistry*, 398, 589-605.

Dieterle, F., Ross, A., Schlotterbeck, G. & Senn, H. (2006). Probabilistic quotient normalization as robust method to account for dilution of complex biological mixtures. Application in H-1 NMR metabolomics. *Analytical Chemistry*, 78, 4281-4290.

Dirnagl, U. & Lauritzen, M. (2010). Fighting publication bias: introducing the Negative Results section. *Journal of Cerebral Blood Flow and Metabolism*, 30, 1263-1264.

Dodson, S. I. & Hanazato, T. (1995). Commentary on effects of anthropogenic and natural organic-chemicals on development, swimming behavior, and reproduction of

Daphnia, a key member of aquatic ecosystems. *Environmental Health Perspectives*, 103, 7-11.

Doma, S. (1979). Ehippia of Daphnia-magna straus - technique for their mass-production and quick revival. *Hydrobiologia*, 67, 183-188.

Domingues, M. R. M., Reis, A. & Domingues, P. (2008). Mass spectrometry analysis of oxidized phospholipids. *Chemistry and Physics of Lipids*, 156, 1-12.

Donovan, E. L., Pettine, S. M., Hickey, M. S., Hamilton, K. L. & Miller, B. F. (2013). Lipidomic analysis of human plasma reveals ether-linked lipids that are elevated in morbidly obese humans compared to lean. *Diabetology & Metabolic Syndrome*, 5.

Draper, H. H., Squires, E. J., Mahmoodi, H., Wu, J., Agarwal, S. & Hadley, M. (1993). A comparative-evaluation of thiobarbituric acid methods for the determination of malondialdehyde in biological-materials. *Free Radical Biology and Medicine*, 15, 353-363.

Ebert, D. (2005). *Ecology, Epidemiology, and Evolution of Parasitism in Daphnia*, Bethesda.

Elsaesser, A. & Howard, C. V. (2012). Toxicology of nanoparticles. *Advanced Drug Delivery Reviews*, 64, 129-137.

Fadok, V. A., de Cathelineau, A., Daleke, D. L., Henson, P. M. & Bratton, D. L. (2001). Loss of phospholipid asymmetry and surface exposure of phosphatidylserine is required for phagocytosis of apoptotic cells by macrophages and fibroblasts. *Journal of Biological Chemistry*, 276, 1071-1077.

Fahy, E., Subramaniam, S., Murphy, R. C., Nishijima, M., Raetz, C. R., Shimizu, T., Spener, F., Van Meer, G., Wakelam, M. J. & Dennis, E. A. (2009). Update of the LIPID MAPS comprehensive classification system for lipids. *Journal of Lipid Research*, 50 Suppl, S9-14.

Fan, W. H., Wang, X. L., Cui, M. M., Zhang, D. F., Zhang, Y., Yu, T. & Guo, L. (2012). Differential Oxidative Stress of Octahedral and Cubic Cu₂O Micro/Nanocrystals to Daphnia magna. *Environmental Science & Technology*, 46, 10255-10262.

Fiehn, O., Wohlgemuth, G., Scholz, M., Kind, T., Lee Do, Y., Lu, Y., Moon, S. & NIKOLAU, B. (2008). Quality control for plant metabolomics: reporting MSI-compliant studies. *The Plant Journal: for Cell and Molecular Biology*, 53, 691-704.

Fisher, L., Kennedy, D., Ryan, J. & Williams, S. The Project on emerging nanotechnologies [Online]. Available: <http://www.nanotechproject.org/>.

Folch, J., Lees, M. & Stanley, G. H. S. (1957). A simple method for the isolation and purification of total lipides from animal tissues. *Journal of Biological Chemistry*, 226, 497-509.

Frisch, D., Morton, P. K., Chowdhury, P. R., Culver, B. W., Colbourne, J. K., Weider, L.

- J. & Jeyasingh, P. D. (2013). A millennial-scale chronicle of evolutionary responses to cultural eutrophication in *Daphnia*. *Ecology Letters*, n/a-n/a.
- Gagne, F., Andre, C., Skirrow, R., Gelinas, M., Auclair, J., Van Aggelen, G., Turcotte, P. & Gagnon, C. (2012). Toxicity of silver nanoparticles to rainbow trout: A toxicogenomic approach. *Chemosphere*, 89, 615-622.
- Gaiser, B. K., Biswas, A., Rosenkranz, P., Jepson, M. A., Lead, J. R., Stone, V., Tyler, C. R. & Fernandes, T. F. (2011). Effects of silver and cerium dioxide micro- and nano-sized particles on *Daphnia magna*. *Journal of Environmental Monitoring*, 13, 1227-1235.
- Garcia-Reyero, N. & Perkins, E. J. (2011). Systems biology: leading the revolution in ecotoxicology. *Environmental Toxicology and Chemistry*, 30, 265-273.
- Garcia-Reyero, N., Escalon, B. L., Loh, P. R., Laird, J. G., Kennedy, A. J., Berger, B. & Perkins, E. J. (2012). Assessment of Chemical Mixtures and Groundwater Effects on *Daphnia magna* Transcriptomics. *Environmental Science & Technology*, 46, 42-50.
- Giroud, C., Gerber, A. & Eichenberger, W. (1988). Lipids of *Chlamydomonas-reinhardtii* - analysis of molecular-species and intracellular site(s) of biosynthesis. *Plant and Cell Physiology*, 29, 587-595.
- Gonzalez-Sanchez, M. I., Gonzalez-Macia, L., Perez-Prior, M. T., Valero, E., Hancock, J. & Killard, A. J. (2013). Electrochemical detection of extracellular hydrogen peroxide in *Arabidopsis thaliana*: a real-time marker of oxidative stress. *Plant Cell and Environment*, 36, 869-878.
- Gottschalk, F., Sonderer, T., Scholz, R. W. & Nowack, B. (2010). Possibilities and limitations of modeling environmental exposure to engineered nanomaterials by probabilistic material flow analysis. *Environmental Toxicology and Chemistry*, 29, 1036-1048.
- Greenberg, M. E., Li, X. M., Gugiu, B. G., Gu, X. D., Qin, J., Salomon, R. G. & Hazen, S. L. (2008). The lipid whisker model of the structure of oxidized cell membranes. *Journal of Biological Chemistry*, 283, 2385-2396.
- Griffiths, W. J., Koal, T., Wang, Y. Q., Kohl, M., Enot, D. P. & Deigner, H. P. (2010). Targeted Metabolomics for Biomarker Discovery. *Angewandte Chemie-International Edition*, 49, 5426-5445.
- Griffitt, R. J., Brown-Peterson, N. J., Savin, D. A., Manning, C. S., Boube, I., Ryan, R. A. & Brouwer, M. (2012). Effects of chronic nanoparticulate silver exposure to adult and juvenile sheepshead minnows (*Cyprinodon variegatus*). *Environmental Toxicology and Chemistry*, 31, 160-167.
- Griffitt, R. J., Luo, J., Gao, J., Bonzongo, J. C. & Barber, D. S. (2008). Effects of particle composition and species on toxicity of metallic nanomaterials in aquatic organisms. *Environmental Toxicology and Chemistry*, 27, 1972-1978.
- Gullingsrud, J. & Schulten, K. (2004). Lipid bilayer pressure profiles and

mechanosensitive channel gating. *Biophysical Journal*, 86, 3496-3509.

Guschina, I. A. & Harwood, J. L. (2006). Lipids and lipid metabolism in eukaryotic algae. *Progress in Lipid Research*, 45, 160-186.

Gutteridge, J. M. (1986). Aspects to consider when detecting and measuring lipid peroxidation. *Free Radical Research Communications*, 1, 173-84.

Hadrup, N., Lam, H. R., Loeschner, K., Mortensen, A., Larsen, E. H. & Frandsen, H. (2012). Nanoparticulate silver increases uric acid and allantoin excretion in rats, as identified by metabolomics. *Journal of Applied Toxicology*, 32, 929-933.

Hamilton, M. A., Russo, R. C. & Thurston, R. V. (1977). Trimmed Spearman-Kärber method for estimating median lethal concentrations in toxicity bioassays. *Environmental Science & Technology*, 11, 714-719.

Han, X. L., Yang, K. & Gross, R. W. (2012). Multi-dimensional mass spectrometry-based shotgun lipidomics and novel strategies for lipidomic analyses. *Mass Spectrometry Reviews*, 31, 134-178.

Han, X. L., Yang, K. & Gross, R. W. (2012). Multi-dimensional mass spectrometry-based shotgun lipidomics and novel strategies for lipidomic analyses. *Mass Spectrometry Reviews*, 31, 134-178.

Harris, E. H. (2001). Chlamydomonas as a model organism. *Annual Review of Plant Physiology and Plant Molecular Biology*, 52, 363-406.

Hartler, J., Tharakan, R., Kofeler, H. C., Graham, D. R. & Thallinger, G. G. (2013). Bioinformatics tools and challenges in structural analysis of lipidomics MS/MS data. *Briefings in Bioinformatics*, 14, 375-390.

He, H., Rodgers, R. P., Marshall, A. G. & Hsu, C. S. (2011). Algae Polar Lipids Characterized by Online Liquid Chromatography Coupled with Hybrid Linear Quadrupole Ion Trap/Fourier Transform Ion Cyclotron Resonance Mass Spectrometry. *Energy & Fuels*, 25, 4770-4775.

Hendren, C. O., Mesnard, X., Droege, J. & Wiesner, M. R. (2011). Estimating Production Data for Five Engineered Nanomaterials As a Basis for Exposure Assessment. *Environmental Science & Technology*, 45, 2562-2569.

Hobaek, A. & Larsson, P. (1990). Sex determination in Daphnia-magna. *Ecology*, 71, 2255-2268.

Hoheisel, S. M., Diamond, S. & Mount, D. (2012). Comparison of nanosilver and ionic silver toxicity in Daphnia magna and Pimephales promelas. *Environmental Toxicology and Chemistry / SETAC*, 31, 2557-63.

Honda, Z., Ishii, S. & Shimizu, T. (2002). Platelet-activating factor receptor. *Journal of Biochemistry*, 131, 773-779.

- Horton, A. A. & Fairhurst, S. (1987). Lipid-Peroxidation and Mechanisms of Toxicity. *CRC Critical Reviews in Toxicology*, 18, 27-79.
- Hosokawa, M. (2007). *Nanoparticle Technology Handbook*, Elsevier.
- Howe, G. & Merchant, S. (1992). Heavy metal-activated synthesis of peptides in *Chlamydomonas reinhardtii*. *Plant Physiology*, 98, 127-136.
- Hu, Q., Sommerfeld, M., Jarvis, E., Ghirardi, M., Posewitz, M., Seibert, M. & Darzins, A. (2008). Microalgal triacylglycerols as feedstocks for biofuel production: perspectives and advances. *Plant Journal*, 54, 621-639.
- Hvattum, E., Hagelin, G. & Larsen, A. (1998). Study of mechanisms involved in the collision-induced dissociation of carboxylate anions from glycerophospholipids using negative ion electrospray tandem quadrupole mass spectrometry. *Rapid Communications in Mass Spectrometry*, 12, 1405-1409.
- Indiana University (2009) *LipidAT* [Online] Available from: <http://mendel.informatics.indiana.edu/~chuyu/LipidAT/software.html> [Accessed: 13th January 2014]
- Jiang, J., Oberdorster, G. & Biswas, P. (2009). Characterization of size, surface charge, and agglomeration state of nanoparticle dispersions for toxicological studies. *Journal of Nanoparticle Research*, 11, 77-89.
- Kaffarnik, S., Ehlers, I., Grobner, G., Schleucher, J. & Vetter, W. (2013). Two-Dimensional P-31,H-1 NMR Spectroscopic Profiling of Phospholipids in Cheese and Fish. *Journal of Agricultural and Food Chemistry*, 61, 7061-7069.
- Kaufmann, A. (2010). Strategy for the elucidation of elemental compositions of trace analytes based on a mass resolution of 100 000 full width at half maximum. *Rapid Communications in Mass Spectrometry*, 24, 2035-2045.
- Keating, K. I. & Dagbusan, B. C. (1984). Effect of selenium deficiency on cuticle integrity in the cladocera (crustacea). *Proceedings of the National Academy of Sciences of the United States of America-Biological Sciences*, 81, 3433-3437.
- Kennedy, E. P. (1957). Metabolism of lipides. *Annual Review of Biochemistry*, 26, 119-148.
- Kerwin, J. L., Wiens, A. M. & Ericsson, L. H. (1996). Identification of fatty acids by electrospray mass spectrometry and tandem mass spectrometry. *Journal of Mass Spectrometry*, 31, 184-192.
- Khalil, M. B., Hou, W., Zhou, H., Elisma, F., Swayne, L. A., Blanchard, A. P., Yao, Z., Bennett, S. A. L. & Figeys, D. (2010). Lipidomics Era: Accomplishments and Challenges. *Mass Spectrometry Reviews*, 29, 877-929.
- Khaselev, N. & Murphy, R. C. (2000). Peroxidation of arachidonate containing plasmenyl glycerophosphocholine: Facile oxidation of esterified arachidonate at carbon-

5. *Free Radical Biology and Medicine*, 29, 620-632.

Kilham, S. S., Kreeger, D. A., Lynn, S. G., Goulden, C. E. & Herrera, L. (1998). COMBO: a defined freshwater culture medium for algae and zooplankton. *Hydrobiologia*, 377, 147-159.

Kim, S., Kim, S., Lee, S., Kwon, B., Choi, J., Hyun, J. W. & Kim, S. (2011). Characterization of the Effects of Silver Nanoparticles on Liver Cell Using HR-MAS NMR Spectroscopy. *Bulletin of the Korean Chemical Society*, 32, 2021-2026.

Kind, T., Liu, K.-H., Lee, D. Y., Defelice, B., Meissen, J. K. & Fiehn, O. (2013). LipidBlast in silico tandem mass spectrometry database for lipid identification. *Nature Methods*, advance online publication.

Kirwan, J. A., Broadhurst, D. I., Davidson, R. L. & Viant, M. R. (2013). Characterising and correcting batch variation in an automated direct infusion mass spectrometry (DIMS) metabolomics workflow. *Analytical and Bioanalytical Chemistry*, 405, 5147-5157.

Kishimoto, K., Urade, R., Ogawa, T. & Moriyama, T. (2001). Nondestructive quantification of neutral lipids by thin-layer chromatography and laser-fluorescent scanning: Suitable methods for "lipidome" analysis. *Biochemical and Biophysical Research Communications*, 281, 657-662.

Klabunde, K. J. & Richards, R. M. (2009). *Nanoscale materials in chemistry*, Hoboken, New Jersey, John Wiley & Sons, Inc.

Kosinska, M. K., Liebisch, G., Lochnit, G., Wilhelm, J., Klein, H., Kaesser, U., Lasczkowski, G., Rickert, M., Schmitz, G. & Steinmeyer, J. (2013). A Lipidomic Study of Phospholipid Classes and Species in Human Synovial Fluid. *Arthritis and Rheumatism*, 65, 2323-2333.

Lee, J. Y., Lim, S., Park, S. & Moon, M. H. (2013). Characterization of oxidized phospholipids in oxidatively modified low density lipoproteins by nanoflow liquid chromatography-tandem mass spectrometry. *Journal of Chromatography A*, 1288, 54-62.

Lessig, J. & Fuchs, B. (2009). Plasmalogens in Biological Systems: Their Role in Oxidative Processes in Biological Membranes, their Contribution to Pathological Processes and Aging and Plasmalogen Analysis. *Current Medicinal Chemistry*, 16, 2021-2041.

Lewis, L. K., Robson, M. H., Vecherkina, Y., Ji, C. & Beall, G. W. (2010). Interference with spectrophotometric analysis of nucleic acids and proteins by leaching of chemicals from plastic tubes. *Biotechniques*, 48, 297-301.

LipidMAPS (2014) *LIPID MAPS Tools: LIPID MAPS Lipidomics Gateway* [Online] Available from: <http://www.lipidmaps.org/tools/> [Accessed: 13th January 2014]

Loizides-Mangold, U. (2013). On the future of mass-spectrometry-based lipidomics.

Febs Journal, 280, 2817-2829.

Long, G. L. & Winefordner, J. D. (1983). Limit of detection. *Analytical Chemistry*, 55, A712-&.

Lu, N., Wei, D., Chen, F. & Yang, S. T. (2013a). Lipidomic profiling reveals lipid regulation in the snow alga *Chlamydomonas nivalis* in response to nitrate or phosphate deprivation. *Process Biochemistry*, 48, 605-613.

Lu, S., Wang, J., Ma, Q., Yang, J., Li, X. & Yuan, Y. J. (2013b). Phospholipid Metabolism in an Industry Microalga *Chlorella sorokiniana*: The Impact of Inoculum Sizes. *PLoS One*, 8, e70827.

Lutz, N. W. & Cozzone, P. J. (2010). Multiparametric Optimization of (31)P NMR Spectroscopic Analysis of Phospholipids in Crude Tissue Extracts. 1. Chemical Shift and Signal Separation. *Analytical Chemistry*, 82, 5433-5440.

Maeba, R. & Ueta, N. (2003). Ethanolamine plasmalogens prevent the oxidation of cholesterol by reducing the oxidizability of cholesterol in phospholipid bilayers. *Journal of Lipid Research*, 44, 164-171.

Masclaux, H., Bec, A., Kainz, M. J., Perriere, F., Desvillettes, C. & Bourdier, G. (2012). Accumulation of polyunsaturated fatty acids by cladocerans: effects of taxonomy, temperature and food. *Freshwater Biology*, 57, 696-703.

Maskrey, B. H., Bermudez-Fajardo, A., Morgan, A. H., Stewart-Jones, E., Dioszeghy, V., Taylor, G. W., Baker, P. R. S., Coles, B., Coffey, M. J., Kuehn, H. & O'Donnell, V. B. (2007). Activated platelets and monocytes generate four hydroxyphosphatidylethanolamines via lipoxygenase. *Journal of Biological Chemistry*, 282, 20151-20163.

Masters, S. (2013). Shell close to deal over 'ruinous' oil spill in Niger Delta. *The Independent*.

Matyash, V., Liebisch, G., Kurzchalia, T. V., Shevchenko, A. & Schwudke, D. (2008). Lipid extraction by methyl-tert-butyl ether for high-throughput lipidomics. *Journal of Lipid Research*, 49, 1137-1146.

McCarthy, M. P., Carroll, D. L. & Ringwood, A. H. (2013). Tissue specific responses of oysters, *Crassostrea virginica*, to silver nanoparticles. *Aquatic Toxicology*, 138, 123-128.

Merchant, S. S., Prochnik, S. E., Vallon, O., Harris, E. H., Karpowicz, S. J., Witman, G. B., Terry, A., Salamov, A., Fritz-Laylin, L. K., Marechal-Drouard, L., Marshall, W. F., Qu, L. H., Nelson, D. R., Sanderfoot, A. A., Spalding, M. H., Kapitonov, V. V., Ren, Q. H., Ferris, P., Lindquist, E., Shapiro, H., Lucas, S. M., Grimwood, J., Schmutz, J., Cardol, P., Cerutti, H., Chanfreau, G., Chen, C. L., Cognat, V., Croft, M. T., Dent, R., Dutcher, S., Fernandez, E., Fukuzawa, H., Gonzalez-Ballester, D., Gonzalez-Halphen, D., Hallmann, A., Hanikenne, M., Hippler, M., Inwood, W., Jabbari, K., Kalanon, M., Kuras, R., Lefebvre, P. A., Lemaire, S. D., Lobanov, A. V., Lohr, M., Manuell, A., Meir, I., Mets, L., Mittag, M., Mittelmeier, T., Moroney, J. V., Moseley, J., Napoli, C., Nedelcu, A. M.,

Niyogi, K., Novoselov, S. V., Paulsen, I. T., Pazour, G., Purton, S., Ral, J. P., Riano-Pachon, D. M., Riekhof, W., Rymarquis, L., Schroda, M., Stern, D., Umen, J., Willows, R., Wilson, N., Zimmer, S. L., Allmer, J., Balk, J., Bisova, K., Chen, C. J., Elias, M., Gendler, K., Hauser, C., Lamb, M. R., Ledford, H., Long, J. C., Minagawa, J., Page, M. D., Pan, J. M., Pootakham, W., Roje, S., Rose, A., Stahlberg, E., Terauchi, A. M., Yang, P. F., Ball, S., Bowler, C., Dieckmann, C. L., Gladyshev, V. N., Green, P., Jorgensen, R., Mayfield, S., Mueller-Roeber, B., Rajamani, S., Sayre, R. T., Brokstein, P., et al. (2007). The *Chlamydomonas* genome reveals the evolution of key animal and plant functions. *Science*, 318, 245-251.

Milne, G. L. & Porter, N. A. (2001). Separation and identification of phospholipid peroxidation products. *Lipids*, 36, 1265-1275.

Ming, H. (2013). Life inside a Chinese mining company. *The Guardian*.

Mitrano, D. M., Leshner, E. K., Bednar, A., Monserud, J., Higgins, C. P. & Ranville, J. F. (2012). Detecting nanoparticulate silver using single-particle inductively coupled plasma-mass spectrometry. *Environmental Toxicology and Chemistry*, 31, 115-121.

Moore, K. & Roberts, L. J. (1998). Measurement of lipid peroxidation. *Free Radical Research*, 28, 659-671.

Mueller, N. C. & Nowack, B. (2008). Exposure modeling of engineered nanoparticles in the environment. *Environmental Science & Technology*, 42, 4447-4453.

Murphy, R. C., Fiedler, J. & Hevko, J. (2001). Analysis of nonvolatile lipids by mass spectrometry. *Chemical Reviews*, 101, 479-526.

Nakanishi, H., Ogiso, H. & Taguchi, R. (2009). Qualitative and quantitative analyses of phospholipids by LC-MS for lipidomics. *Methods in molecular biology (Clifton, N.J.)*, 579, 287-313.

Newton, K. M., Puppala, H. L., Kitchens, C. L., Colvin, V. L. & Klaine, S. J. (2013). Silver nanoparticle toxicity to *Daphnia magna* is a function of dissolved silver concentration. *Environmental Toxicology and Chemistry / SETAC*, 32, 2356-64.

Niki, E. (2008). Lipid peroxidation products as oxidative stress biomarkers. *Biofactors*, 34, 171-180.

Nowack, B., Krug, H. F. & Height, M. (2011). 120 Years of Nanosilver History: Implications for Policy Makers. *Environmental Science & Technology*, 45, 1177-1183.

OECD (1998). Guidelines for testing of chemicals, no. 211 — *Daphnia magna* reproduction test. Paris: Organisation for Economic Cooperation and Development.

OECD (2004). Guidelines for testing of chemicals, No. 202 — *Daphnia sp.* acute immobilisation test. Paris: Organisation for Economic Cooperation and Development.

OECD (2011). Guidelines for testing of chemicals, no. 201: Freshwater alga and cyanobacteria, growth inhibition test. Paris: Organisation for Economic Cooperation and

Development.

Oukarroum, A., Bras, S., Perreault, F. & Popovic, R. (2012). Inhibitory effects of silver nanoparticles in two green algae, *Chlorella vulgaris* and *Dunaliella tertiolecta*. *Ecotoxicology and Environmental Safety*, 78, 80-85.

Payne, T. G., Southam, A. D., Arvanitis, T. N. & Viant, M. R. (2009). A signal filtering method for improved quantification and noise discrimination in fourier transform ion cyclotron resonance mass spectrometry-based metabolomics data. *Journal of the American Society for Mass Spectrometry*, 20, 1087-1095.

Perez-Palacios, T., Ruiz, J. & Antequera, T. (2007). Improvement of a solid phase extraction method for separation of animal muscle phospholipid classes. *Food Chemistry*, 102, 875-879.

Persson, J. & Vrede, T. (2006). Polyunsaturated fatty acids in zooplankton: variation due to taxonomy and trophic position. *Freshwater Biology*, 51, 887-900.

Pervaiz, S. & Clement, M. V. (2002). Hydrogen peroxide-induced apoptosis: Oxidative or reductive stress? *Redox Cell Biology and Genetics, Part A*, 352, 150-159.

Poynton, H. C., Varshavsky, J. R., Chang, B., Cavigiolo, G., Chan, S., Holman, P. S., Loguinov, A. V., Bauer, D. J., Komachi, K., Theil, E. C., Perkins, E. J., Hughes, O. & Vulpe, C. D. (2007). *Daphnia magna* ecotoxicogenomics provides mechanistic insights into metal toxicity. *Environmental Science & Technology*, 41, 1044-1050.

Premier Biosoft (2010) *SimLipid* [Online] Available from: <http://www.premierbiosoft.com/lipid/index.html> [Accessed: 13th January 2014]

Pritchard, J. B. (1993). Aquatic toxicology - past, present, and prospects. *Environmental Health Perspectives*, 100, 249-257.

Pryor, W. A. & Castle, L. (1984). Chemical methods for the detection of lipid hydroperoxides. *Methods in Enzymology*, 105, 293-299.

Pulfer, M. & Murphy, R. C. (2003). Electrospray mass spectrometry of phospholipids. *Mass Spectrometry Reviews*, 22, 332-364.

Purohit, P. V., Rocke, D. M., Viant, M. R. & Woodruff, D. L. (2004). Discrimination models using variance-stabilizing transformation of metabolomic NMR data. *Omics-a Journal of Integrative Biology*, 8, 118-130.

Reidy, B., Haase, A., Luch, A., Dawson, K. A. & Lynch, I. (2013). Mechanisms of Silver Nanoparticle Release, Transformation and Toxicity: A Critical Review of Current Knowledge and Recommendations for Future Studies and Applications. *Materials*, 6, 2295-2350.

Reis, A. & Spickett, C. M. (2012). Chemistry of phospholipid oxidation. *Biochimica Et Biophysica Acta-Biomembranes*, 1818, 2374-2387.

- Reis, A., Domingues, M. R. M., Amado, F. M. L., Ferrer-Correia, A. J. & Domingues, P. (2007). Radical peroxidation of palmitoyl-linoleoyl-glycerophosphocholine liposomes: Identification of long-chain oxidised products by liquid chromatography-tandem mass spectrometry. *Journal of Chromatography B-Analytical Technologies in the Biomedical and Life Sciences*, 855, 186-199.
- Rhee, J.-S., Yu, I. T., Kim, B. M., Jeong, C. B., Lee, K. W., Kim, M. J., Lee, S. J., Park, G. S. & Lee, J. S. (2013). Copper induces apoptotic cell death through reactive oxygen species-triggered oxidative stress in the intertidal copepod *Tigriopus japonicus*. *Aquatic Toxicology*, 132, 182-189.
- Rider, C. V., Gorr, T. A., Olmstead, A. W., Wasilak, B. A. & Leblanc, G. A. (2005). Stress signaling: coregulation of hemoglobin and male sex determination through a terpenoid signaling pathway in a crustacean. *Journal of Experimental Biology*, 208, 15-23.
- Rizov, I. & Doulis, A. (2001). Separation of plant membrane lipids by multiple solid-phase extraction. *Journal of Chromatography A*, 922, 347-354.
- Roemer, I., White, T. A., Baalousha, M., Chipman, K., Viant, M. R. & Lead, J. R. (2011). Aggregation and dispersion of silver nanoparticles in exposure media for aquatic toxicity tests. *Journal of Chromatography A*, 1218, 4226-4233.
- Römer, I., Gavin, A. J., White, T. A., Merrifield, R. C., Chipman, J. K., Viant, M. R. & Lead, J. R. (2013). The critical importance of defined media conditions in *Daphnia magna* nanotoxicity studies. *Toxicology letters*, in press.
- Roque, A., Yildiz, H. Y., Carazo, I. & Duncan, N. (2010). Physiological stress responses of sea bass (*Dicentrarchus labrax*) to hydrogen peroxide (H₂O₂) exposure. *Aquaculture*, 304, 104-107.
- Rungby, J. & Ernst, E. (1992). Experimentally induced lipid-peroxidation after exposure to chromium, mercury or silver - interactions with carbon-tetrachloride. *Pharmacology & Toxicology*, 70, 205-207.
- Sanabria, C., Diamant, A. & Zilberg, D. (2009). Effects of commonly used disinfectants and temperature on swim bladder non-inflation in freshwater angelfish, *Pterophyllum scalare* (Lichtenstein). *Aquaculture*, 292, 158-165.
- Scheidegger, C., Sigg, L. & Behra, R. (2011). Characterization of lead induced metal-phytochelatin complexes in *Chlamydomonas reinhardtii*. *Environmental Toxicology and Chemistry*, 30, 2546-2552.
- Schluesener, J. K. & Schluesener, H. J. 2013. Nanosilver: application and novel aspects of toxicology. *Archives of Toxicology*, 87, 569-576.
- Schmelzer, K., Fahy, E., Subramaniam, S. & Dennis, E. A. (2007). The lipid maps initiative in lipidomics. *Methods in Enzymology*, 432, 171-183.
- Schwarz, J. A., Mitchelmore, C. L., Jones, R., O'Dea, A. & Seymour, S. (2013).

Exposure to copper induces oxidative and stress responses and DNA damage in the coral *Montastraea franksi*. *Comparative Biochemistry and Physiology C-Toxicology & Pharmacology*, 157, 272-279.

Schwarzenbach, R. P., Egli, T., Hofstetter, T. B., Von Gunten, U. & Wehrli, B. (2010). Global Water Pollution and Human Health. *In: Gadgil, A. & Liverman, D. M. (eds.) Annual Review of Environment and Resources, Vol 35.*

Schwudke, D., Hannich, J. T., Surendranath, V., Grimard, V., Moehring, T., Burton, L., Kurzchalia, T. & Shevchenko, A. (2007). Top-down lipidomic screens by multivariate analysis of high-resolution survey mass spectra. *Analytical Chemistry*, 79, 4083-4093.

Scoma, A., Krawietz, D., Faraloni, C., Giannelli, L., Happe, T. & Torzillo, G. (2012). Sustained H-2 production in a *Chlamydomonas reinhardtii* D1 protein mutant. *Journal of Biotechnology*, 157, 613-619.

Shen, Q., Wang, Y., Gong, L., Guo, R., Dong, W. & Cheung, H.-Y. (2012). Shotgun Lipidomics Strategy for Fast Analysis of Phospholipids in Fisheries Waste and Its Potential in Species Differentiation. *Journal of Agricultural and Food Chemistry*, 60, 9384-9393.

Simionato, D., Basso, S., Giacometti, G. M. & Morosinotto, T. (2013). Optimization of light use efficiency for biofuel production in algae. *Biophysical Chemistry*, 182, 71-8.

Smith, E. F. & Lefebvre, P. A. (1996). PF16 encodes a protein with armadillo repeats and localizes to a single microtubule of the central apparatus in *Chlamydomonas flagella*. *Journal of Cell Biology*, 132, 359-370.

Snape, J. R., Maund, S. J., Pickford, D. B. & Hutchinson, T. H. (2004). Ecotoxicogenomics: the challenge of integrating genomics into aquatic and terrestrial ecotoxicology. *Aquatic Toxicology*, 67, 143-154.

Soetaert, A., Vandenbrouck, T., Van Der Ven, K., Maras, M., Van Remortel, P., Blust, R. & de Coen, W. M. (2007). Molecular responses during cadmium-induced stress in *Daphnia magna*: Integration of differential gene expression with higher-level effects. *Aquatic Toxicology*, 83, 212-222.

Sommer, U., Herscovitz, H., Welty, F. K. & Costello, C. E. (2006). LC-MS-based method for the qualitative and quantitative analysis of complex lipid mixtures. *Journal of Lipid Research*, 47, 804-814.

Southam, A. D., Lange, A., Hines, A., Hill, E. M., Katsu, Y., Iguchi, T., Tyler, C. R. & Viant, M. R. (2011). Metabolomics Reveals Target and Off-Target Toxicities of a Model Organophosphate Pesticide to Roach (*Rutilus rutilus*): Implications for Biomonitoring. *Environmental Science & Technology*, 45, 3759-3767.

Southam, A. D., Payne, T. G., Cooper, H. J., Arvanitis, T. N. & Viant, M. R. (2007). Dynamic range and mass accuracy of wide-scan direct infusion nano-electrospray fourier transform ion cyclotron resonance mass spectrometry-based metabolomics increased

by the spectral stitching method. *Analytical Chemistry*, 79, 4595-4602.

Sparvero, L. J., Amoscato, A. A., Kochanek, P. M., Pitt, B. R., Kagan, V. E. & Bayir, H. (2010). Mass-spectrometry based oxidative lipidomics and lipid imaging: applications in traumatic brain injury. *Journal of Neurochemistry*, 115, 1322-1336.

Stein, S. (2012). Mass Spectral Reference Libraries: An Ever-Expanding Resource for Chemical Identification. *Analytical Chemistry*, 84, 7274-7282.

Stohs, S. J. & Bagchi, D. (1995). Oxidative mechanisms in the toxicity of metal-ions. *Free Radical Biology and Medicine*, 18, 321-336.

Sud, M., Fahy, E., Cotter, D., Brown, A., Dennis, E. A., Glass, C. K., Merrill, A. H., JR., Murphy, R. C., Raetz, C. R., Russell, D. W. & Subramaniam, S. (2007). LMSD: LIPID MAPS structure database. *Nucleic Acids Research*, 35, D527-32.

Sumner, L. W., Amberg, A., Barrett, D., Beale, M. H., Beger, R., Daykin, C. A., Fan, T. W. M., Fiehn, O., Goodacre, R., Griffin, J. L., Hankemeier, T., Hardy, N., Harnly, J., Higashi, R., Kopka, J., Lane, A. N., Lindon, J. C., Marriott, P., Nicholls, A. W., Reily, M. D., Thaden, J. J. & Viant, M. R. (2007). Proposed minimum reporting standards for chemical analysis. *Metabolomics*, 3, 211-221.

Taipale, S., Kankaala, P., Hamalainen, H. & Jones, R. I. (2009). Seasonal shifts in the diet of lake zooplankton revealed by phospholipid fatty acid analysis. *Freshwater Biology*, 54, 90-104.

Tang, B. H., Zhu, L. Y. & Zhou, Q. X. (2011). Joint effects of Penta-BDE and heavy metals on *Daphnia magna* survival, its antioxidant enzyme activities and lipid peroxidation. *Frontiers of Environmental Science & Engineering in China*, 5, 99-110.

Tatarazako, N. & Oda, S. (2007). The water flea *Daphnia magna* (Crustacea, Cladocera) as a test species for screening and evaluation of chemicals with endocrine disrupting effects on crustaceans. *Ecotoxicology*, 16, 197-203.

Taylor, C. W. (2002). Controlling calcium entry. *Cell*, 111, 767-769.

Taylor, N. (2010). *Novel approaches to toxicity testing in Daphnia magna*. PhD, University of Birmingham.

Taylor, N. S., Weber, R. J. M., Southam, A. D., Payne, T. G., Hrydziuszko, O., Arvanitis, T. N. & Viant, M. R. (2009). A new approach to toxicity testing in *Daphnia magna*: application of high throughput FT-ICR mass spectrometry metabolomics. *Metabolomics*, 5, 44-58.

Taylor, N. S., Weber, R. J. M., White, T. A. & Viant, M. R. (2010). Discriminating between Different Acute Chemical Toxicities via Changes in the Daphnid Metabolome. *Toxicological Sciences*, 118, 307-317.

Tejamaya, M., Roemer, I., Merrifield, R. C. & Lead, J. R. (2012). Stability of Citrate, PVP, and PEG Coated Silver Nanoparticles in Ecotoxicology Media. *Environmental*

Science & Technology, 46, 7011-7017.

Tentschert, J., Draude, F., Jungnickel, H., Haase, A., Manton, A., Galla, S., Thunemann, A. F., Taubert, A., Luch, A. & Arlinghaus, H. F. (2013). TOF-SIMS analysis of cell membrane changes in functional impaired human macrophages upon nanosilver treatment. *Surface and Interface Analysis*, 45, 483-485.

Thomas, M. C., Mitchell, T. W. & Blanksby, S. J. (2006). Ozonolysis of phospholipid double bonds during electrospray ionization: A new tool for structure determination. *Journal of the American Chemical Society*, 128, 58-59.

Tieleman, D. P. & Marrink, S. J. (2006). Lipids out of equilibrium: Energetics of desorption and pore mediated flip-flop. *Journal of the American Chemical Society*, 128, 12462-12467.

Timbrell, J. (2000). *Principles of biochemical toxicology*, Taylor & Francis.

Tyurin, V. A., Tyurina, Y. Y., Feng, W., Mnuskin, A., Jiang, J., Tang, M., Zhang, X., Zhao, Q., Kochanek, P. M., Clark, R. S., Bayir, H. & Kagan, V. E. (2008). Mass-spectrometric characterization of phospholipids and their primary peroxidation products in rat cortical neurons during staurosporine-induced apoptosis. *Journal of Neurochemistry*, 107, 1614-1633.

Tyurin, V. A., Tyurina, Y. Y., Jung, M. Y., Tungekar, M. A., Wasserloos, K. J., Bayir, H., Greenberger, J. S., Kochanek, P. M., Shvedova, A. A., Pitt, B. & Kagan, V. E. (2009). Mass-spectrometric analysis of hydroperoxy- and hydroxy-derivatives of cardiolipin and phosphatidylserine in cells and tissues induced by pro-apoptotic and pro-inflammatory stimuli. *Journal of Chromatography.B, Analytical Technologies in the Biomedical and Life Sciences*.

UC Davis (2006) *FAAT* [Online] Available from:
<http://pubs.acs.org/doi/suppl/10.1021/ac0604179> [Accessed: 13th January 2014]

University of Helsinki (2006) *LIMSA* [Online] Available from:
<http://www.helsinki.fi/science/lipids/software.html> [Accessed: 13th January 2014]

University of Kansas (2011) *LipidomeDB* [Online] Available from:
<http://lipidome.bcf.ku.edu:9000/Lipidomics/> [Accessed: 13th January 2014]

USEPA. *ECOTOX database* [Online]. Available: <http://cfpub.epa.gov/ecotox/> [Accessed: 13th January 2014]

Valledor, L., Furuhashi, T., Hanak, A.-M. & Weckwerth, W. (2013). Systemic Cold Stress Adaptation of *Chlamydomonas reinhardtii*. *Molecular & Cellular Proteomics : MCP*, 12, 2032-47.

Vance, D. E. & Vance, J. E. (2008). Biochemistry of Lipids, Lipoproteins and Membranes (5th Edn.) Preface. *Biochemistry of Lipids, Lipoproteins and Membranes, 5th Edition*, V-VI.

Viant, M. R. (2008). Recent developments in environmental metabolomics. *Molecular bioSystems*, 4, 980-986.

Vieira, L. R., Gravato, C., Soares, A. M., Morgado, F. & Guilhermino, L. (2009). Acute effects of copper and mercury on the estuarine fish *Pomatoschistus microps*: Linking biomarkers to behaviour. *Chemosphere*.

Washington University (2013) *LipidQA* [Online] Available from: <http://lipidqa.dom.wustl.edu/> [Accessed: 13th January 2014]

Watanabe, H., Takahashi, E., Nakamura, Y., Oda, S., Tatarazako, N. & Iguchi, T. (2007). Development of a *Daphnia magna* DNA microarray for evaluating the toxicity of environmental chemicals. *Environmental Toxicology and Chemistry*, 26, 669-676.

Weber, R. J. M. & Viant, M. R. (2010). MI-Pack: Increased confidence of metabolite identification in mass spectra by integrating accurate masses and metabolic pathways. *Chemometrics and Intelligent Laboratory Systems*, 104, 75-82.

Weber, R. J. M., Southam, A. D., Sommer, U. & Viant, M. R. (2011). Characterization of Isotopic Abundance Measurements in High Resolution FT-ICR and Orbitrap Mass Spectra for Improved Confidence of Metabolite Identification. *Analytical Chemistry*, 83, 3737-3743.

WOK: Web of Knowledge (2014) *Web of knowledge search. Topic: lipidomics* [Online] Available from: <http://apps.webofknowledge.com> [Accessed: 13th January 2014]

Wu, H., Southam, A. D., Hines, A. & Viant, M. R. (2008). High-throughput tissue extraction protocol for NMR- and MS-based metabolomics. *Analytical Biochemistry*, 372, 204-212.

Yamada, N., Murakami, N., Morimoto, T. & Sakakibara, J. (1993). Auto-growth inhibitory substance from the fresh-water cyanobacterium *Phormidium tenue*. *Chemical & Pharmaceutical Bulletin*, 41, 1863-1865.

Yan, X., Xu, J., Chen, J., Chen, D., Xu, S., Luo, Q. & Wang, Y. (2012). Lipidomics focusing on serum polar lipids reveals species dependent stress resistance of fish under tropical storm. *Metabolomics*, 8, 299-309.

Yang, D., Fan, X., Kind, T., Fiehn, O. & Guo, R. (2013). Analysis of Polar Lipids in *Chlamydomonas reinhardtii* Using Nanoelectrospray Direct Infusion Method and Gas Chromatography and Mass Spectrometric Detection. *Acta Chimica Sinica*, 71, 663-669.

Yoon, K.-Y., Byeon, J. H., Park, J.-H. & Hwang, J. (2007). Susceptibility constants of *Escherichia coli* and *Bacillus subtilis* to silver and copper nanoparticles. *Science of the Total Environment*, 373, 572-575.

Zhao, C. M. & Wang, W. X. (2012). Importance of surface coatings and soluble silver in silver nanoparticles toxicity to *Daphnia magna*. *Nanotoxicology*, 6, 361-370.

Zhao, C.-M. & Wang, W.-X. (2011). Comparison of acute and chronic toxicity of silver

nanoparticles and silver nitrate to *Daphnia magna*. *Environmental Toxicology and Chemistry*, 30, 885-892.

A - Appendix

AI - Tables showing mass spectra from oxidised PE species

AI-I - Tables showing mass spectra of oxidised PE(14:0,0:0) in negative and positive ion mode

| Observed | | Identification | | | | |
|-----------|-----------|------------------|----------|------------------|------------|--------------|
| m/z | Intensity | Formula | Ion Form | Theoretical Mass | Mass Error | ID |
| 424.24716 | 1895131.5 | C19H40NO7P | [M-H]- | 424.24696 | -0.471 | PE(14:0,0:0) |
| 425.25049 | 364706.7 | C18(13C)H40NO7P | [M-H]- | 425.25032 | -0.400 | M(13C) |
| 478.29411 | 40930.5 | - | - | - | - | Unknown |
| 468.27344 | 31619.6 | C21H44NO8P | [M-H]- | 468.27318 | -0.566 | M+C2H4O |
| 426.25424 | 21594.0 | C17(13C2)H40NO7P | [M-H]- | 426.25367 | -1.337 | M(13C2) |

| Observed | | Identification | | | | |
|-----------|-----------|-----------------|------------|------------------|------------|--------------|
| m/z | Intensity | Formula | Ion Form | Theoretical Mass | Mass Error | ID |
| 448.24342 | 8104498.0 | C19H40NO7P | [M+Na]+ | 448.24346 | 0.089 | PE(14:0,0:0) |
| 449.24677 | 1638026.0 | C18(13C)H40NO7P | [M+Na]+ | 449.24682 | 0.111 | M(13C) |
| 470.22542 | 711664.6 | C19H40NO7P | [M+2Na-H]+ | 470.2254 | -0.043 | PE(14:0,0:0) |
| 471.22871 | 131907.7 | C18(13C)H40NO7P | [M+2Na-H]+ | 471.22876 | 0.095 | M(13C) |

AI-II - Tables showing mass spectra of oxidised PE(18:1,0:0) in negative and positive ion mode

| Observed | | Identification | | | | |
|-----------|-----------|------------------|-------------|------------------|------------|--------------|
| m/z | Intensity | Formula | Ion Form | Theoretical Mass | Mass Error | ID |
| 478.29405 | 3336271.0 | C23H46NO7P | [M-H]- | 478.29391 | -0.293 | PE(18:1,0:0) |
| 479.29749 | 829183.1 | C22(13C)H46NO7P | [M-H]- | 479.29727 | -0.459 | M(13C) |
| 494.28917 | 113866.3 | C23H46NO8P | [M-H]- | 494.28883 | -0.688 | M+O |
| 510.28403 | 102893.9 | C23H46NO9P | [M-H]- | 510.28374 | -0.568 | M+O2 |
| 536.25277 | 102015.5 | C23H46NO7P | [M+NaCl-H]- | 536.25253 | -0.442 | PE(18:1,0:0) |
| 480.30100 | 65897.5 | C21(13C2)H46NO7P | [M-H]- | 480.30062 | -0.791 | M(13C2) |

| Observed | | Identification | | | | |
|-----------|-----------|-----------------|------------|------------------|------------|--------------|
| m/z | Intensity | Formula | Ion Form | Theoretical Mass | Mass Error | ID |
| 502.29053 | 8833670.0 | C23H46NO7P | [M+Na]+ | 502.29041 | -0.239 | PE(18:1,0:0) |
| 502.30428 | 3800377.0 | - | - | - | - | Shoulder |
| 537.39502 | 2944052.0 | - | - | - | - | Blank peak |
| 503.29394 | 2094465.4 | C22(13C)H46NO7P | [M+Na]+ | 503.29377 | -0.348 | M(13C) |
| 537.40829 | 1655688.5 | - | - | - | - | Shoulder |
| 503.30795 | 986487.4 | - | - | - | - | Shoulder |
| 538.39841 | 915027.6 | - | - | - | - | Blank peak |
| 538.41150 | 524191.2 | - | - | - | - | Shoulder |
| 480.30860 | 496492.3 | C23H46NO7P | [M+H]+ | 480.30847 | -0.281 | PE(18:1,0:0) |
| 532.43966 | 279151.1 | - | - | - | - | Blank peak |
| 502.27453 | 252720.0 | - | - | - | - | Shoulder |
| 534.28047 | 238138.7 | C23H46NO9P | [M+Na]+ | 534.28024 | -0.430 | M+O2 |
| 518.28556 | 215779.8 | C23H46NO8P | [M+Na]+ | 518.28533 | -0.453 | M+O |
| 553.39014 | 210937.0 | - | - | - | - | Blank peak |
| 504.29772 | 192320.0 | - | - | - | - | Shoulder |
| 504.31170 | 178930.8 | - | - | - | - | Shoulder |
| 524.27250 | 171855.8 | C23H46NO7P | [M+2Na-H]+ | 524.27236 | -0.277 | PE(18:1,0:0) |
| 553.36891 | 155723.8 | - | - | - | - | Shoulder |
| 539.41477 | 152663.0 | - | - | - | - | Blank peak |
| 502.31337 | 134422.1 | - | - | - | - | Shoulder |
| 480.32355 | 127982.0 | - | - | - | - | Shoulder |
| 539.40196 | 126840.3 | - | - | - | - | Shoulder |
| 518.26455 | 121910.0 | C23H46NO7P | [M+K]+ | 518.26447 | -0.158 | PE(18:1,0:0) |
| 481.26212 | 115846.5 | - | - | - | - | Shoulder |
| 534.29985 | 115815.3 | - | - | - | - | Shoulder |
| 481.31193 | 112387.9 | C22(13C)H46NO7P | [M+H]+ | 481.31182 | -0.229 | M(13C) |
| 539.39070 | 110433.8 | - | - | - | - | Shoulder |
| 524.29125 | 107938.6 | - | - | - | - | Shoulder |
| 553.39754 | 106449.0 | - | - | - | - | Shoulder |
| 518.30013 | 102646.3 | - | - | - | - | Shoulder |

AI-III - Tables showing mass spectra of oxidised PE(14:0,14:0) in negative and positive ion mode

| Observed | | Identification | | | | |
|-----------|-----------|------------------|-----------|------------------|------------|---------------|
| m/z | Intensity | Formula | Ion Form | Theoretical Mass | Mass Error | ID |
| 634.44588 | 1124409.4 | C33H66NO8P | [M-H]- | 634.44532 | -0.883 | PE(14:0,14:0) |
| 635.44912 | 348028.5 | C32(13C)H66NO8P | [M-H]- | 635.44868 | -0.692 | M(13C) |
| 636.45218 | 70245.3 | C31(13C2)H66NO8P | [M-H]- | 636.45204 | -0.220 | M(13C2) |
| 670.42238 | 30887.2 | C33H66NO8P | [M+35Cl]- | 670.42200 | -0.567 | PE(14:0,14:0) |
| 678.47185 | 17461.5 | C35H70NO9P | [M-H]- | 678.47154 | -0.464 | M+C2H4O |

| Observed | | Identification | | | | |
|-----------|-----------|------------------|------------|------------------|------------|---------------|
| m/z | Intensity | Formula | Ion Form | Theoretical Mass | Mass Error | ID |
| 658.44166 | 3207376.0 | C33H66NO8P | [M+Na]+ | 658.44183 | 0.258 | PE(14:0,14:0) |
| 659.44508 | 1157601.5 | C32(13C)H66NO8P | [M+Na]+ | 659.44518 | 0.152 | M(13C) |
| 680.42370 | 378441.3 | C33H66NO8P | [M+2Na-H]+ | 680.42487 | 1.720 | PE(14:0,14:0) |
| 660.44821 | 206536.6 | C31(13C2)H66NO8P | [M+Na]+ | 660.44853 | 0.485 | M(13C2) |
| 681.42719 | 122541.8 | C32(13C)H66NO8P | [M+2Na-H]+ | 681.42822 | 1.512 | M(13C) |
| 714.55603 | 89728.5 | - | - | - | - | Unknown |
| 685.43567 | 87728.9 | - | - | - | - | Blank peak |
| 728.83081 | 75845.9 | - | - | - | - | Blank peak |

AI-IV - Tables showing mass spectra of oxidised PE(P-18,18:1) in negative and positive ion mode

| Observed | | Identification | | | | |
|-----------|-----------|------------------|-------------|------------------|------------|--------------|
| m/z | Intensity | Formula | Ion Form | Theoretical Mass | Mass Error | ID |
| 728.56082 | 859593.9 | C44H86NO7P | [M-H]- | 728.55996 | -1.180 | PE(P18,18:1) |
| 729.56457 | 283273.5 | C43(13C)H86NO7P | [M-H]- | 729.56332 | -1.720 | M(13C) |
| 756.55583 | 102284.2 | C45H86NO8P | [M-H]- | 756.55488 | -1.262 | M+CO |
| 764.53779 | 98855.1 | C44H86NO7P | [M+35Cl]- | 764.53664 | -1.507 | PE(P18,18:1) |
| 730.56774 | 78700.2 | C42(13C2)H86NO7P | [M-H]- | 730.56667 | -1.465 | M(13C2) |
| 765.54119 | 44171.1 | C43(13C)H86NO7P | [M+35Cl]- | 765.53999 | -1.564 | M(13C) |
| 757.55937 | 42745.3 | C44(13C)H86NO8P | [M-H]- | 757.55919 | -0.244 | M+CO(13C) |
| 766.53374 | 35128.5 | C44H86NO7P | [M+37Cl]- | 766.53369 | -0.068 | PE(P18,18:1) |
| 767.53730 | 14780.1 | C43(13C)H86NO7P | [M+37Cl]- | 767.53704 | -0.335 | M(13C) |
| 731.57002 | 12278.3 | C41(13C3)H86NO7P | [M-H]- | 731.57003 | 0.007 | M(13C3) |
| 786.51948 | 11799.8 | C44H86NO7P | [M+NaCl-H]- | 786.51858 | -1.140 | PE(P18,18:1) |
| 758.56184 | 9378.1 | C43(13C2)H86NO8P | [M-H]- | 758.56254 | 0.923 | M+CO(13C2) |

| Observed | | Identification | | | | |
|-----------|-----------|------------------|------------|------------------|------------|--------------|
| m/z | Intensity | Formula | Ion Form | Theoretical Mass | Mass Error | ID |
| 752.55602 | 2046361.8 | C44H86NO7P | [M+Na]+ | 752.55646 | 0.585 | PE(P18,18:1) |
| 753.55944 | 910765.1 | C43(13C)H86NO7P | [M+Na]+ | 753.55982 | 0.498 | M(13C) |
| 795.33431 | 232693.2 | - | - | - | - | Blank Peak |
| 754.56270 | 207559.0 | C42(13C2)H86NO7P | [M+Na]+ | 754.56317 | 0.623 | M(13C2) |
| 811.30828 | 131179.6 | - | - | - | - | Blank Peak |
| 796.33773 | 107471.7 | - | - | - | - | Blank Peak |
| 730.57441 | 80046.6 | C44H86NO7P | [M+H]+ | 730.57452 | 0.144 | PE(P18,18:1) |
| 774.53783 | 78654.2 | C44H86NO7P | [M+2Na-H]+ | 774.53841 | 0.742 | PE(P18,18:1) |
| 758.66863 | 76411.0 | - | - | - | - | Blank Peak |
| 812.31156 | 61232.8 | - | - | - | - | Blank Peak |
| 728.83228 | 52043.2 | - | - | - | - | Blank Peak |
| 768.52988 | 51009.1 | C44H86NO7P | [M+K]+ | 768.52996 | 0.101 | PE(P18,18:1) |
| 752.52073 | 47328.2 | - | - | - | - | Shoulder |
| 759.67177 | 30048.3 | - | - | - | - | Blank Peak |
| 731.57791 | 29626.0 | C43(13C)H86NO7P | [M+H]+ | 731.57787 | -0.055 | M(13C) |
| 755.56560 | 29525.4 | C41(13C3)H86NO7P | [M+Na]+ | 755.56653 | 1.224 | M(13C3) |
| 786.69969 | 26636.4 | - | - | - | - | Blank Peak |
| 727.46026 | 26063.2 | - | - | - | - | Unknown |
| 775.54067 | 25964.7 | C43(13C)H86NO7P | [M+2Na-H]+ | 775.54176 | 1.405 | M(13C) |

AI-V - Tables showing mass spectra of oxidised PE(18:1,18:1) in negative and positive ion mode

| Observed | | Identification | | | | |
|-----------|-----------|------------------|----------|------------------|------------|---------------|
| m/z | Intensity | Formula | Ion Form | Theoretical Mass | Mass Error | ID |
| 742.53973 | 5487501.0 | C41H78NO8P | [M-H]- | 742.53923 | -0.673 | PE(18:1,18:1) |
| 743.54349 | 2294502.5 | C40(13C)H78NO8P | [M-H]- | 743.54258 | -1.224 | M(13C) |
| 774.53027 | 1332754.5 | C41H78NO10P | [M-H]- | 774.52906 | -1.562 | M+O2 |
| 775.53366 | 590645.1 | C40(13C)H78NO10P | [M-H]- | 775.53241 | -1.612 | M+O2(13C) |
| 744.54682 | 520032.5 | C49(13C2)H78NO8P | [M-H]- | 744.54594 | -1.182 | M(13C2) |
| 806.52026 | 448276.9 | C41H78NO12P | [M-H]- | 806.51889 | -1.699 | M+O4 |
| 814.56177 | 314967.8 | - | - | | | Unknown |
| 758.53557 | 300841.2 | C41H78NO9P | [M-H]- | 758.53414 | -1.885 | M+O |
| 770.53556 | 297027.6 | C42H78NO9P | [M-H]- | 770.53415 | -1.836 | M+CO |
| 807.52365 | 199529.0 | C40(13C)H78NO12P | [M-H]- | 807.52224 | -1.746 | M+O4(13C) |
| 790.52557 | 197080.7 | C41H78NO11P | [M-H]- | 790.52397 | -2.024 | M+O3 |
| 756.51990 | 196801.6 | C41H76NO9P | [M-H]- | 756.51849 | -1.864 | (M+O2)-H2O |

| Observed | | Identification | | | | |
|-----------|-----------|---------------------|------------------------|------------------|------------|---------------------|
| m/z | Intensity | Formula | Ion Form | Theoretical Mass | Mass Error | ID |
| 766.53566 | 3469006.8 | C41H78NO8P | [M+Na] ⁺ | 766.53572 | 0.078 | PE(18:1,18:1) |
| 767.53911 | 1509734.5 | C40(13C)H78NO8P | [M+Na] ⁺ | 767.53908 | -0.039 | M(13C) |
| 798.52554 | 763339.8 | C41H78NO10P | [M+Na] ⁺ | 798.52556 | 0.025 | M+O2 |
| 795.33497 | 615778.9 | - | - | - | - | Blank peak |
| 744.55391 | 436273.7 | C41H78NO8P | [M+H] ⁺ | 744.55378 | -0.175 | PE(18:1,18:1) |
| 768.54243 | 347056.0 | C39(13C2)H78NO8P | [M+Na] ⁺ | 768.54244 | 0.013 | M(13C2) |
| 782.53076 | 346083.1 | C41H78NO9P | [M+Na] ⁺ | 782.53064 | -0.153 | M+O |
| 799.52888 | 338753.2 | C40(13C)H78NO10P | [M+Na] ⁺ | 799.52891 | 0.031 | M+O2(13C) |
| 830.51533 | 308243.6 | C41H78NO12P | [M+Na] ⁺ | 830.51538 | 0.060 | M+O4 |
| 796.33851 | 291053.0 | - | - | - | - | Blank peak |
| 745.55726 | 188746.0 | C40(13C)H78NO8P | [M+H] ⁺ | 745.55714 | -0.168 | M(13C) |
| 814.52073 | 175788.1 | C41H78NO11P | [M+Na] ⁺ | 814.52047 | -0.325 | M+O3 |
| 783.53407 | 152717.9 | C40(13C)H78NO9P | [M+Na] ⁺ | 783.534 | -0.096 | M+O(13C) |
| 812.50474 | 144232.1 | C41H76NO11P | [M+Na] ⁺ | 812.50482 | 0.092 | (M+O4)-H2O |
| 831.51858 | 132468.9 | C40(13C)H78NO12P | [M+Na] ⁺ | 831.51874 | 0.186 | M+O4(C13) |
| 780.51494 | 130184.8 | C41H76NO9P | [M+Na] ⁺ | 780.515 | 0.070 | (M+O2)-H2O |
| 758.66913 | 121014.1 | - | - | - | - | Blank peak |
| 811.30901 | 99248.4 | - | - | - | - | Blank peak |
| 815.52392 | 77694.1 | C40(13C)H78NO11P | [M+Na] ⁺ | 815.52382 | -0.123 | M+O3(13C) |
| 800.53183 | 76100.1 | C3940(13C2)H78NO10P | [M+Na] ⁺ | 800.53226 | 0.537 | M+O2(13C2) |
| 797.34143 | 73510.4 | - | - | - | - | Blank peak |
| 776.54376 | 70607.8 | C41H78NO10P | [M+H] ⁺ | 776.54361 | -0.193 | M+O2 |
| 813.50827 | 63022.0 | C40(13C)H76NO11P | [M+Na] ⁺ | 813.50817 | -0.123 | (M+O4)- H2O(13C) |
| 759.67256 | 59498.4 | - | - | - | - | Blank peak |
| 786.70046 | 55797.3 | - | - | - | - | Blank peak |
| 769.54530 | 55405.1 | C38(13C3)H78NO8P | [M+Na] ⁺ | 769.5458 | 0.643 | M(13C3) |
| 781.51821 | 55169.7 | C40(13C)H76NO9P | [M+Na] ⁺ | 781.51835 | 0.179 | (M+O2)- H2O(13C) |
| 788.51770 | 53575.4 | C41H78NO8P | [M+2Na-H] ⁺ | 788.51767 | -0.044 | PE(18:1,18:1) |
| 828.49969 | 48591.8 | - | - | - | - | Unknown |
| 772.58510 | 44375.7 | - | - | - | - | Unknown |
| 832.52194 | 41267.7 | C39(13C2)H78NO12P | [M+Na] ⁺ | 832.52209 | 0.180 | M+O4(13C2) |
| 746.56056 | 40673.6 | C39(13C2)H78NO8P | [M+H] ⁺ | 746.56049 | -0.094 | M(13C2) |

AI-VI - Tables showing mass spectra of oxidised PE(16:0,20:4) in negative and positive ion mode

| Observed | | Identification | | | | |
|-----------|-----------|------------------|----------|------------------|------------|---------------|
| m/z | Intensity | Formula | Ion Form | Theoretical Mass | Mass Error | ID |
| 738.50880 | 843962.1 | C41H74NO8P | [M-H]- | 738.50793 | -1.178 | PE(16:0,20:4) |
| 739.51219 | 382935.1 | C40(13C)H74NO8P | [M-H]- | 739.51129 | -1.224 | M(13C) |
| 766.50362 | 160127.2 | C42H74NO9P | [M-H]- | 766.50285 | -1.011 | M+CO |
| 740.51540 | 84438.4 | C39(13C2)H74NO8P | [M-H]- | 740.51464 | -1.026 | M(13C2) |
| 767.50701 | 72953.2 | C41(13C)H74NO9P | [M-H]- | 767.5062 | -1.055 | M+CO(13C) |
| 786.49389 | 63193.1 | C41H74NO11P | [M-H]- | 786.49268 | -1.545 | M+O3 |
| 802.48886 | 55972.9 | C41H74NO12P | [M-H]- | 802.48759 | -1.583 | M+O4 |
| 754.50362 | 45435.3 | C41H74NO9P | [M-H]- | 754.50285 | -1.027 | M+O |
| 770.49839 | 30471.3 | C41H74NO10P | [M-H]- | 770.49776 | -0.818 | M+O2 |
| 784.47768 | 24623.9 | C41H72NO11P | [M-H]- | 784.47703 | -0.835 | (M+O4)-H2O |
| 787.49710 | 22996.7 | C40(13C)H74NO11P | [M-H]- | 787.49603 | -1.359 | M+O3(13C) |
| 780.51891 | 20791.3 | - | - | - | - | Unknown |
| 804.50418 | 20494.0 | - | - | - | - | Unknown |
| 803.49217 | 19962.5 | C40(13C)H74NO12P | [M-H]- | 803.49095 | -1.525 | M+O4(13C) |
| 755.50683 | 17097.5 | C40(13C)H74NO9P | [M-H]- | 755.5062 | -0.834 | M+O(13C) |
| 768.48325 | 16582.2 | C41H72NO10P | [M-H]- | 768.48211 | -1.483 | (M+O3)-H2O |
| 800.47208 | 15697.1 | C41H72NO12P | [M-H]- | 800.47194 | -0.175 | (M+O5)-H2O |
| 768.51009 | 13932.9 | C40(13C2)H74NO9P | [M-H]- | 768.50956 | -0.696 | M+CO(13C2) |
| 788.49756 | 13501.5 | - | - | - | - | Unknown |

| Observed | | Identification | | | | |
|-----------|-----------|------------------|---------------------|------------------|------------|---------------|
| m/z | Intensity | Formula | Ion Form | Theoretical Mass | Mass Error | ID |
| 762.50400 | 1432521.0 | C41H74NO8P | [M+Na] ⁺ | 762.50443 | 0.564 | PE(16:0,20:4) |
| 763.50754 | 634503.4 | C40(13C)H74NO8P | [M+Na] ⁺ | 763.50779 | 0.321 | M(13C) |
| 795.33426 | 302879.5 | - | - | - | - | Blank peak |
| 811.30834 | 232301.3 | - | - | - | - | Blank peak |
| 810.48844 | 181081.9 | C41H74NO11P | [M+Na] ⁺ | 810.48918 | 0.907 | M+O3 |
| 796.33771 | 144109.3 | - | - | - | - | Blank peak |
| 764.51059 | 138853.1 | C40(13C2)H74NO9P | [M+Na] ⁺ | 764.51114 | 0.719 | M+CO(13C2) |
| 778.47747 | 131470.3 | C41H74NO8P | [M+K] ⁺ | 778.47794 | 0.601 | PE(16:0,20:4) |
| 778.49896 | 124540.0 | C41H74NO9P | [M+Na] ⁺ | 778.49935 | 0.495 | M+O |
| 758.66854 | 106162.3 | - | - | - | - | Blank peak |
| 812.31156 | 103404.0 | - | - | - | - | Blank peak |
| 794.49363 | 91411.2 | C41H74NO10P | [M+Na] ⁺ | 794.49426 | 0.793 | M+O2 |
| 826.48338 | 87694.0 | C41H74NO12P | [M+Na] ⁺ | 826.48409 | 0.859 | M+O4 |
| 811.49198 | 79690.4 | C40(13C)H74NO11P | [M+Na] ⁺ | 811.49253 | 0.678 | M+O3(13C) |
| 808.47297 | 59286.0 | C41H72NO11P | [M+Na] ⁺ | 808.47353 | 0.686 | (M+O4)-H2O |
| 779.50209 | 54650.1 | C40(13C)H74NO9P | [M+Na] ⁺ | 779.5027 | 0.783 | M+O(13C) |
| 740.52168 | 54330.7 | C41H74NO8P | [M+H] ⁺ | 740.52249 | 1.087 | PE(16:0,20:4) |
| 779.48068 | 52604.2 | C40(13C)H74NO8P | [M+K] ⁺ | 779.48129 | 0.786 | M(13C) |
| 776.48263 | 44350.2 | C41H72NO9P | [M+Na] ⁺ | 776.4837 | 1.372 | (M+O2)-H2O |
| 759.67201 | 43908.5 | - | - | - | - | Blank peak |
| 786.69989 | 35682.6 | - | - | - | - | Blank peak |
| 828.49976 | 34528.1 | - | - | - | - | - |
| 795.49662 | 34414.9 | C41(13C)H74NO9P | [M+Na] ⁺ | 795.49762 | 1.251 | M+O2(13C) |
| 827.48623 | 32520.4 | C40(13C)H74NO12P | [M+Na] ⁺ | 827.48745 | 1.468 | M+O4(13C) |
| 792.47835 | 30196.3 | C41H72NO10P | [M+Na] ⁺ | 792.47861 | 0.328 | (M+O3)-H2O |
| 762.46778 | 24287.5 | - | - | - | - | - |
| 771.48595 | 23929.3 | - | - | - | - | - |
| 797.34085 | 21735.8 | - | - | - | - | Blank peak |
| 809.47573 | 21066.9 | C41H72NO11P | [M+Na] ⁺ | 809.47688 | 1.421 | (M+O4)-H2O |
| 743.43409 | 19608.3 | - | - | - | - | - |

All - Manually annotated fragmentation patterns from oxidised PE products

All-I - Fragmentation patterns from PE(14:0,0:0) and oxidised products thereof in negative ion mode

| Parent (m/z) | 424.25 | | | |
|--------------|--------------|--------------------|----------------|-------------------------|
| Adduct | -H | | | |
| ID | PE(14:0,0:0) | | | |
| Formula | C19H39NO7P | | | |
| | Observed | | Identification | |
| Fragment m/z | Neutral loss | Relative Intensity | Formula | Annotation |
| 227.30 | 196.95 | 100 | C14H27O2 | Myristic Acid |
| 196.15 | 228.10 | 3 | C5H11NO5P | -Myristic acid |
| 214.14 | 210.11 | 2 | C5H13NO6P | -Myristic acid (ketene) |

| Parent (m/z) | 468.27 | | | |
|--------------|---------------------|--------------------|----------------|-------------------------|
| Adduct | -H | | | |
| ID | PE(14:0,0:0) +C2H4O | | | |
| Formula | C21H43NO8P | | | |
| | Observed | | Identification | |
| Fragment m/z | Neutral loss | Relative Intensity | Formula | Annotation |
| 227.29 | 240.98 | 100 | C14H27O2 | Myristic Acid |
| 436.32 | 31.95 | 34 | | |
| 240.12 | 228.15 | 2 | C7H15NO6P | -Myristic acid |
| 381.28 | 86.99 | 2 | | |
| 258.17 | 210.10 | 2 | C7H17NO7P | -Myristic acid (ketene) |
| 271.28 | 196.99 | 2 | | |

| Parent (m/z) | 478.29 | | | |
|--------------|--------------|--------------------|----------------|---------------|
| Adduct | | | | |
| ID | Unknown | | | |
| Formula | | | | |
| | Observed | | Identification | |
| Fragment m/z | Neutral loss | Relative Intensity | Formula | Annotation |
| 281.35 | 196.94 | 100 | | |
| 227.31 | 250.98 | 1 | C14H27O2 | Myristic Acid |
| 196.13 | 282.16 | 1 | C5H11NO5P | Unknown |
| 214.16 | 264.13 | 1 | C5H13NO6P | Unknown |

All-II - Fragmentation patterns from PE(14:0,0:0) and oxidised products thereof in positive ion mode

| Parent (m/z) | 448.24 | | | |
|--------------|--------------|--------------------|----------------|------------------|
| Adduct | +Na | | | |
| ID | PE(14:0,0:0) | | | |
| Formula | C19H40NO7PNa | | | |
| | Observed | | Identification | |
| Fragment m/z | Neutral loss | Relative Intensity | Formula | Annotation |
| 405.23 | 43.01 | 100 | C17H35O7PNa | -Aziridine |
| 387.22 | 61.02 | 85 | C17H33O6PNa | -Aziridine & H2O |
| 430.20 | 18.04 | 14 | C19H38NO6PNa | -H2O |
| 164.02 | 284.22 | 2 | | |

| Parent (m/z) | 470.22 | | | |
|--------------|--------------|--------------------|----------------|------------------|
| Adduct | | | | |
| ID | Unknown | | | |
| Formula | | | | |
| | Observed | | Identification | |
| Fragment m/z | Neutral loss | Relative Intensity | Formula | Annotation |
| 409.22 | 61.00 | 100 | | -Aziridine & H2O |
| 167.98 | 302.24 | 6 | | |

All-III - Fragmentation patterns from PE(18:1,0:0) and oxidised products thereof in negative ion mode

| Parent (m/z) | 478.29 | | | |
|--------------|--------------|--------------------|----------------|----------------------|
| Adduct | [-H] | | | |
| ID | PE(18:1,0:0) | | | |
| Formula | C23H45NO7P | | | |
| | Observed | | Identification | |
| Fragment m/z | Neutral loss | Relative Intensity | Formula | Annotation |
| 281.35 | 196.94 | 100 | C18H33O2 | Oleic acid anion |
| 196.15 | 282.14 | 2 | C5H11NO5P | -Oleic acid |
| 214.15 | 264.14 | 1 | C5H13NO6P | -Oleic acid (ketene) |

| Parent (m/z) | 494.29 | | | |
|--------------|----------------|--------------------|----------------|----------------------------|
| Adduct | [-H] | | | |
| ID | PE(18:1,0:0)+O | | | |
| Formula | C23H45NO8P | | | |
| | Observed | | Identification | |
| Fragment m/z | Neutral loss | Relative Intensity | Formula | Annotation |
| 297.34 | 196.95 | 100 | C18H33O3 | Oleic acid +O anion |
| 279.35 | 214.94 | 3 | C18H31O2 | (Oleic acid +O) -H2O anion |
| 296.37 | 197.92 | 2 | | |
| 196.15 | 298.14 | 1 | C5H11NO5P | -Oleic acid +O |
| 214.14 | 280.15 | 1 | C5H13NO6P | -(Oleic acid +O) (ketene) |
| 295.37 | 198.92 | 1 | C18H31O3 | Oleic acid +O2 -H2O anion |

| Parent (m/z) | 510.28 | | | |
|--------------|------------------|--------------------|----------------|----------------------------|
| Adduct | [-H] | | | |
| ID | PE(18:1,0:0) +O2 | | | |
| Formula | C23H45NO9P | | | |
| | Observed | | Identification | |
| Fragment m/z | Neutral loss | Relative Intensity | Formula | Annotation |
| 313.31 | 196.97 | 100 | C18H33O4 | Oleic acid +O2 anion |
| 295.33 | 214.95 | 77 | C18H31O3 | Oleic acid +O2 -H2O anion |
| 492.30 | 17.98 | 22 | C23H43NO8P | -H2O |
| 196.13 | 314.15 | 3 | C5H11NO5P | -Oleic acid +O2 |
| 214.14 | 296.14 | 3 | C5H13NO6P | -(Oleic acid +O2) (ketene) |
| 449.33 | 60.95 | 2 | | |
| 251.34 | 258.94 | 1 | | |
| 452.38 | 57.90 | 1 | | |
| 171.15 | 339.13 | 1 | | |

| Parent (m/z) | 536.25 | | | |
|--------------|----------------|--------------------|----------------|-------------------------|
| Adduct | [-H] | | | |
| ID | PE(18:1,0:0) | | | |
| | [NaCl] | | | |
| Formula | C23H45NO7PNaCl | | | |
| | Observed | | Identification | |
| Fragment m/z | Neutral loss | Relative Intensity | Formula | Annotation |
| 478.36 | 57.89 | 100 | C23H45NO7P | -[NaCl] |
| 281.37 | 254.88 | 18 | C18H33O2 | Oleic acid anion |
| 475.30 | 60.95 | 3 | | |
| 339.32 | 196.93 | 3 | C18H33O2NaCl | Oleic acid anion [NaCl] |

All-IV - Fragmentation patterns from PE(18:1,0:0) and oxidised products thereof in positive ion mode

| Parent (m/z) | 480.31 | | | |
|--------------|--------------|--------------------|----------------|------------------|
| Adduct | [+H] | | | |
| ID | PE(18:1,0:0) | | | |
| Formula | C23H47NO7P | | | |
| | Observed | | Identification | |
| Fragment m/z | Neutral loss | Relative Intensity | Formula | Annotation |
| 339.33 | 140.98 | 100 | C21H39O3 | -Head group |
| 462.21 | 18.10 | 88 | C23H45NO6P | -H2O |
| 419.13 | 61.18 | 7 | C21H40O6P | - Aziridine &H2O |
| 420.26 | 60.05 | 3 | | |
| 437.33 | 42.98 | 3 | C21H42O7P | -Aziridine |
| 436.30 | 44.01 | 2 | | |
| 481.28 | -0.97 | 2 | | |
| 480.40 | -0.09 | 1 | | |
| 393.25 | 87.06 | 1 | | |
| 265.27 | 215.04 | 1 | | |

| Parent (m/z) | 502.29 | | | |
|--------------|--------------|--------------------|----------------|---------------------|
| Adduct | [+Na] | | | |
| ID | PE(18:1,0:0) | | | |
| Formula | C23H46NO7PNa | | | |
| | Observed | | Identification | |
| Fragment m/z | Neutral loss | Relative Intensity | Formula | Annotation |
| 459.28 | 43.01 | 100 | C21H41O7PNa | -Aziridine |
| 441.28 | 61.01 | 71 | C21H39O6PNa | - Aziridine &H2O |
| 484.24 | 18.05 | 11 | C23H44NO6PNa | -H2O |
| 164.03 | 338.26 | 1 | C2H8NO4PNa | Unknown (141 + Na?) |

| Parent (m/z) | 518.28 | | | |
|--------------|------------------------|--------------------|----------------|----------------------|
| Adduct | [+Na] | | | |
| ID | PE(18:1,0:0) +O & [K]+ | | | |
| Formula | C23H46NO8PNa | | | |
| | Observed | | Identification | |
| Fragment m/z | Neutral loss | Relative Intensity | Formula | Annotation |
| 475.25 | 43.03 | 100 | C21H41O8PNa | -Aziridine |
| 457.28 | 61.00 | 58 | C21H39O7PNa | - Aziridine &H2O |
| 500.26 | 18.02 | 35 | C23H44NO7PNa | -H2O |
| 395.33 | 122.95 | 7 | C21H40O5Na | -Head group |
| 439.28 | 79.00 | 7 | C21H37O6PNa | - Aziridine & 2(H2O) |
| 377.31 | 140.97 | 4 | C21H38O4Na | -Head group |

| Parent (m/z) | 524.27 | | | |
|--------------|---------------|--------------------|----------------|-----------------------|
| Adduct | [2Na-H] | | | |
| ID | PE(18:1,0:0) | | | |
| Formula | C23H45NO7PNa2 | | | |
| | Observed | | Identification | |
| Fragment m/z | Neutral loss | Relative Intensity | Formula | Annotation |
| 463.26 | 61.01 | 100 | C21H38O6PNa2 | - Aziridine &H2O |
| 167.99 | 356.28 | 4 | C2H5NO3PNa2 | Unknown (123+2Na-H??) |
| 481.27 | 43.00 | 2 | C21H40O7PNa2 | -Aziridine |

| Parent (m/z) | 534.28 | | | |
|--------------|------------------|--------------------|----------------|----------------------|
| Adduct | [+Na] | | | |
| ID | PE(18:1,0:0) +O2 | | | |
| Formula | C23H46NO9PNa | | | |
| | Observed | | Identification | |
| Fragment m/z | Neutral loss | Relative Intensity | Formula | Annotation |
| 473.24 | 61.04 | 100 | C21H39O8PNa | - Aziridine & H2O |
| 491.23 | 43.05 | 70 | C21H41O9PNa | -Aziridine |
| 418.17 | 116.11 | 42 | | |
| 404.16 | 130.12 | 35 | | |
| 516.24 | 18.04 | 32 | C23H44NO8PNa | -H2O |
| 455.24 | 79.04 | 27 | C21H37O7PNa | - Aziridine & 2(H2O) |
| 500.26 | 34.02 | 15 | C23H44NO7PNa | -H2O2 |
| 349.12 | 185.16 | 12 | | |
| 331.14 | 203.14 | 11 | | |
| 393.29 | 140.99 | 11 | C21H38O5Na | -Head group |
| 345.14 | 189.14 | 10 | | |
| 375.26 | 159.02 | 9 | C21H36O4Na | -Head group & H2O |
| 411.30 | 122.98 | 8 | C21H40O6Na | -Head group |
| 292.10 | 242.18 | 8 | | |
| 317.11 | 217.17 | 7 | | |
| 363.12 | 171.16 | 6 | | |
| 400.19 | 134.09 | 5 | | |
| 279.02 | 255.26 | 4 | | |
| 533.40 | 0.88 | 4 | | |
| 164.03 | 370.25 | 4 | C2H8NO4PNa | Unknown (141 + Na?) |

All-V - Fragmentation patterns from PE(14:0,14:0) and oxidised products thereof in negative ion mode

| Parent (m/z) | 634.44 | | | |
|--------------|---------------|--------------------|----------------|-------------------------|
| Adduct | [-H] | | | |
| ID | PE(14:0,14:0) | | | |
| Formula | C33H65NO8P | | | |
| | Observed | | Identification | |
| Fragment m/z | Neutral loss | Relative Intensity | Formula | Annotation |
| 227.29 | 407.15 | 100 | C14H27O2 | Myristic acid anion |
| 424.31 | 210.13 | 15 | C19H39NO7P | -Myristic acid (ketene) |
| 406.32 | 228.12 | 2 | C19H37NO6P | -Myristic acid |

| Parent (m/z) | 678.47 | | | |
|--------------|----------------------|--------------------|----------------|-------------------------|
| Adduct | [-H] | | | |
| ID | PE(14:0,14:0) +C2H4O | | | |
| Formula | C35H69NO9P | | | |
| | Observed | | Identification | |
| Fragment m/z | Neutral loss | Relative Intensity | Formula | Annotation |
| 227.30 | 451.17 | 100 | C14H27O2 | Myristic acid anion |
| 468.38 | 210.09 | 20 | C21H43NO8P | -Myristic acid (ketene) |
| 436.31 | 242.16 | 3 | | |
| 241.27 | 437.20 | 2 | | |
| 450.06 | 228.41 | 2 | C21H41NO7P | -Myristic acid |
| 646.42 | 32.05 | 2 | | |
| 257.27 | 421.20 | 2 | | |
| 450.39 | 228.08 | 2 | | |
| 390.34 | 288.13 | 1 | | |
| 660.69 | 17.78 | 1 | | |
| 271.29 | 407.18 | 1 | | |
| 255.35 | 423.12 | 1 | | |
| 471.39 | 207.08 | 1 | | |
| 472.28 | 206.19 | 1 | | |

All-VI - Fragmentation patterns from PE(14:0,14:0) and oxidised products thereof in positive ion mode

| Parent (m/z) | 658.44 | | | |
|--------------|---------------|--------------------|----------------|----------------------------|
| Adduct | [+Na] | | | |
| ID | PE(14:0,14:0) | | | |
| Formula | C33H66NO8PNa | | | |
| | Observed | | Identification | |
| Fragment m/z | Neutral loss | Relative Intensity | Formula | Annotation |
| 615.33 | 43.11 | 100 | C31H61O8PNa | -Aziridine |
| 517.43 | 141.01 | 13 | C31H58O4Na | -Head group (PE) |
| 495.46 | 162.98 | 5 | C31H59O4 | -Sodiated headgroup |
| 535.45 | 122.99 | 3 | C31H60O5Na | -Head Group (PE) |
| 387.22 | 271.22 | 2 | C17H33O6PNa | -Myristic acid & Aziridine |
| 430.23 | 228.21 | 1 | C19H38NO6PNa | -Myristic acid |

| Parent (m/z) | 680.42 | | | |
|--------------|---------------|--------------------|----------------|--------------------------------------|
| Adduct | [+2Na-H] | | | |
| ID | PE(14:0,14:0) | | | |
| Formula | C33H65NO8PNa2 | | | |
| | Observed | | Identification | |
| Fragment m/z | Neutral loss | Relative Intensity | Formula | Annotation |
| 452.27 | 228.15 | 100 | C19H37NO6PNa2 | -Myristic acid |
| 387.22 | 293.20 | 56 | C17H33O6PNa | -(Myristic acid & Aziridine & Na) +H |
| 637.41 | 43.01 | 38 | C31H60O8PNa2 | -Aziridine |
| 409.23 | 271.19 | 11 | C17H32O6PNa2 | -Myristic acid & Aziridine |
| 430.22 | 250.20 | 6 | C19H38NO6PNa | -(Myristic acid & Na) +H |
| 273.22 | 407.20 | 3 | | |

| Parent (m/z) | 714.56 | | | |
|--------------|--------------|--------------------|----------------|----------------------|
| Adduct | | | | |
| ID | Unknown | | | |
| Formula | | | | |
| | Observed | | Identification | |
| Fragment m/z | Neutral loss | Relative Intensity | Formula | Annotation |
| 696.63 | 17.93 | 100 | | -H ₂ O |
| 678.44 | 36.12 | 74 | | -2(H ₂ O) |
| 714.57 | -0.01 | 16 | | |
| 656.72 | 57.84 | 12 | | |
| 450.24 | 264.32 | 9 | | |
| 653.19 | 61.37 | 7 | | |
| 670.71 | 43.85 | 6 | | -Aziridine |
| 705.73 | 8.83 | 5 | | |
| 685.71 | 28.85 | 5 | | |
| 682.35 | 32.21 | 4 | | |
| 428.39 | 286.17 | 3 | | |
| 682.65 | 31.91 | 3 | | |
| 464.29 | 250.27 | 3 | | -Myristic acid & Na |
| 715.42 | -0.86 | 3 | | |
| 486.25 | 228.31 | 2 | | -Myristic acid |
| 671.44 | 43.12 | 2 | | |
| 698.25 | 16.31 | 2 | | |
| 687.72 | 26.84 | 2 | | |
| 616.67 | 97.89 | 2 | | |
| 671.71 | 42.85 | 2 | | |
| 640.55 | 74.01 | 1 | | |
| 686.60 | 27.96 | 1 | | |
| 679.30 | 35.26 | 1 | | |
| 594.39 | 120.17 | 1 | | |
| 683.78 | 30.78 | 1 | | |
| 612.76 | 101.80 | 1 | | |
| 554.81 | 159.75 | 1 | | |
| 654.69 | 59.87 | 1 | | |
| 430.10 | 284.46 | 1 | | |
| 639.35 | 75.21 | 1 | | |

All-VII - Fragmentation patterns from PE(P18,18:1) and oxidised products thereof in negative ion mode

| Parent (m/z) | 728.56 | | | |
|--------------|--------------|--------------------|----------------|----------------------|
| Adduct | [-H] | | | |
| ID | PE(P18,18:1) | | | |
| Formula | C41H79NO7P | | | |
| | Observed | | Identification | |
| Fragment m/z | Neutral loss | Relative Intensity | Formula | Annotation |
| 281.36 | 447.20 | 100 | C18H33O2 | Oleic acid anion |
| 464.43 | 264.13 | 25 | C23H47NO6P | -Oleic acid (ketene) |
| 446.41 | 282.15 | 6 | C23H45NO5P | -Oleic acid |

| Parent (m/z) | 756.55 | | | |
|--------------|-----------------|--------------------|----------------|----------------------|
| Adduct | [-H] | | | |
| ID | PE(P18,18:1)+CO | | | |
| Formula | C42H79NO8P | | | |
| | Observed | | Identification | |
| Fragment m/z | Neutral loss | Relative Intensity | Formula | Annotation |
| 281.36 | 475.19 | 100 | C18H33O2 | Oleic acid anion |
| 492.41 | 264.14 | 22 | C24H47NO7P | -Oleic acid (ketene) |
| 403.37 | 353.18 | 14 | | |
| 474.40 | 282.15 | 5 | C24H45NO6P | -Oleic acid |
| 267.39 | 489.16 | 2 | | |

| Parent (m/z) | 786.52 | | | |
|--------------|---------------------|--------------------|----------------|-----------------------------|
| Adduct | [-H] | | | |
| ID | PE(P18,18:1)+[NaCl] | | | |
| Formula | C41H79NO7PNaCl | | | |
| | Observed | | Identification | |
| Fragment m/z | Neutral loss | Relative Intensity | Formula | Annotation |
| 728.54 | 57.98 | 100 | C41H79NO7P | -NaCl |
| 281.35 | 505.17 | 55 | C18H33O2 | Oleic acid anion |
| 464.41 | 322.11 | 8 | C23H47NO6P | -Oleic acid (ketene) & NaCl |
| 754.57 | 31.95 | 4 | | |
| 522.48 | 264.04 | 3 | C23H47NO6PNaCl | -Oleic acid (ketene) |
| 339.34 | 447.18 | 2 | | |
| 446.41 | 340.11 | 1 | C23H45NO5P | -Oleic acid & NaCl |
| 403.52 | 383.00 | 1 | | |

All-VIII - Fragmentation patterns from PE(P18,18:1) and oxidised products thereof in positive ion mode

| Parent (m/z) | 730.58 | | | |
|--------------|--------------|--------------------|----------------|------------------|
| Adduct | [+H] | | | |
| ID | PE(P18,18:1) | | | |
| Formula | C41H81NO7P | | | |
| | Observed | | Identification | |
| Fragment m/z | Neutral loss | Relative Intensity | Formula | Annotation |
| 392.29 | 338.29 | 100 | | |
| 339.34 | 391.24 | 16 | | |
| 712.47 | 18.11 | 13 | C41H79NO6P | -H2O |
| 294.37 | 436.21 | 12 | | |
| 730.70 | -0.12 | 6 | C41H81NO7P | Parent |
| 662.25 | 68.33 | 5 | | |
| 694.36 | 36.22 | 4 | C41H77NO5P | -2(H2O) |
| 524.26 | 206.32 | 4 | | |
| 656.51 | 74.07 | 4 | | |
| 730.19 | 0.39 | 2 | C41H81NO7P | Parent |
| 686.28 | 44.30 | 2 | | |
| 687.40 | 43.18 | 2 | C39H76O7P | -Aziridine |
| 658.93 | 71.65 | 2 | | |
| 644.42 | 86.16 | 2 | | |
| 692.44 | 38.14 | 2 | | |
| 669.46 | 61.12 | 1 | C39H74O6P | - Aziridine &H2O |
| 698.53 | 32.05 | 1 | | |
| 658.52 | 72.06 | 1 | | |
| 700.66 | 29.92 | 1 | | |
| 503.33 | 227.25 | 1 | | |
| 671.62 | 58.96 | 1 | | |
| 684.31 | 46.27 | 1 | | |
| 449.43 | 281.15 | 1 | | |
| 459.35 | 271.23 | 1 | | |
| 589.44 | 141.14 | 1 | C39H73O3 | -Head group (PE) |

| Parent (m/z) | 752.55 | | | |
|--------------|--------------|--------------------|----------------|----------------------|
| Adduct | [+Na] | | | |
| ID | PE(P18,18:1) | | | |
| Formula | C41H80NO7PNa | | | |
| | Observed | | Identification | |
| Fragment m/z | Neutral loss | Relative Intensity | Formula | Annotation |
| 709.45 | 43.10 | 100 | C39H75O7PNa | -Aziridine |
| 414.31 | 338.24 | 11 | | |
| 441.29 | 311.26 | 5 | C21H39O6PNa | -P18 & aziridine |
| 459.27 | 293.28 | 3 | | |
| 589.46 | 163.09 | 3 | C39H73O3 | -Sodiated head group |
| 611.50 | 141.05 | 2 | C39H72O3Na | -Head group (PE) |
| 629.54 | 123.01 | 1 | C39H74O4Na | -Head group (PE) |

| Parent (m/z) | 768.52 | | | |
|--------------|--------------|--------------------|----------------|------------------|
| Adduct | [+K] | | | |
| ID | PE(P18,18:1) | | | |
| Formula | C41H80NO7PK | | | |
| | Observed | | Identification | |
| Fragment m/z | Neutral loss | Relative Intensity | Formula | Annotation |
| 732.53 | 35.99 | 100 | C41H76NO5PK | - 2(H2O) |
| 725.39 | 43.13 | 100 | C39H75O7PK | -Aziridine |
| 430.23 | 338.29 | 19 | | |
| 627.47 | 141.05 | 17 | C39H72O3K | -Head group (PE) |
| 750.46 | 18.06 | 15 | C41H78NO7PNa | -H2O |
| 645.48 | 123.04 | 7 | C39H74O4K | -Head group (PE) |
| 475.27 | 293.25 | 7 | | |
| 707.27 | 61.25 | 5 | C39H73O6PK | - Aziridine &H2O |
| 457.23 | 311.29 | 4 | C21H39O6PK | -P18 & aziridine |
| 768.77 | -0.25 | 3 | C41H80NO7PK | Parent |
| 736.35 | 32.17 | 3 | | |
| 696.53 | 71.99 | 2 | | |
| 321.19 | 447.33 | 2 | | |
| 768.36 | 0.16 | 2 | C41H80NO7PK | Parent |
| 414.29 | 354.23 | 1 | | |
| 444.31 | 324.21 | 1 | | |
| 500.30 | 268.22 | 1 | | |
| 486.19 | 282.33 | 1 | | |
| 730.32 | 38.20 | 1 | | |

| Parent (m/z) | 774.54 | | | |
|--------------|---------------|--------------------|----------------|------------------|
| Adduct | [2Na-H] | | | |
| ID | PE(P18,18:1) | | | |
| Formula | C41H79NO7PNa2 | | | |
| | Observed | | Identification | |
| Fragment m/z | Neutral loss | Relative Intensity | Formula | Annotation |
| 731.54 | 43.00 | 100 | C39H74O7PNa2 | -Aziridine |
| 427.32 | 347.22 | 8 | | |
| 449.30 | 325.24 | 4 | | |
| 506.31 | 268.23 | 2 | C23H43NO6PNa2 | -P18 |
| 327.27 | 447.27 | 2 | | |
| 463.26 | 311.28 | 1 | C21H38O6PNa2 | -P18 & aziridine |
| 662.23 | 112.31 | 1 | | |

All-IX - Fragmentation patterns from PE(16:0,18:1) and oxidised products thereof in negative ion mode

| Parent m/z | 716.52 | | | |
|--------------|---------------|--------------------|----------------|-------------------------|
| Ion form | [M-H]- | | | |
| ID | PE(16:0,18:1) | | | |
| Formula | C39H75NO8P | | | |
| | Observed | | Identification | |
| Fragment m/z | Neutral loss | Relative Intensity | Formula | Annotation |
| 281.35 | 435.17 | 100 | C18H33O2 | Oleic acid anion |
| 255.34 | 461.18 | 48 | C16H31O2 | Palmitic acid anion |
| 452.37 | 264.15 | 13 | C21H43NO7P | -Oleic acid (ketene) |
| 478.36 | 238.16 | 5 | C23H45NO7P | -Palmitic acid (ketene) |
| 434.39 | 282.13 | 2 | C21H41NO6P | -Oleic acid |
| 460.36 | 256.16 | 1 | C23H43NO6P | -Palmitic acid |

| Parent (m/z) | 730.50 | | | |
|--------------|----------------------|--------------------|----------------|-------------------------------------|
| Adduct | [-H] | | | |
| ID | PE(16:0,18:1)+O2-H2O | | | |
| Formula | C39H73NO9P | | | |
| | Observed | | Identification | |
| Fragment m/z | Neutral loss | Relative Intensity | Formula | Annotation |
| 295.34 | 435.16 | 100 | C18H31O3 | Oleic acid + O2 -H2O anion |
| 255.33 | 475.17 | 46 | C16H31O2 | Palmitic acid anion |
| 452.35 | 278.15 | 14 | C21H43NO 7P | -(Oleic acid + O2 -H2O) (ketene) |
| 281.38 | 449.12 | 13 | C18H33O2 | Oleic acid anion |
| 492.32 | 238.18 | 4 | C23H43NO 8P | -Palmitic acid (ketene) |
| 474.41 | 256.09 | 3 | C23H41NO 7P | -Palmitic acid |
| 269.35 | 461.15 | 2 | | |
| 598.00 | 132.50 | 2 | | |
| 282.35 | 448.15 | 2 | | |
| 434.36 | 296.14 | 1 | C21H41NO 6P | -(Oleic acid + O2 -H2O) |

| Parent m/z | 732.51 | | | |
|--------------|-----------------|--------------------|----------------|------------------------------------|
| Ion form | [M-H]- | | | |
| ID | PE(16:0,18:1)+O | | | |
| Formula | C39H75NO9P | | | |
| | Observed | | Identification | |
| Fragment m/z | Neutral loss | Relative Intensity | Formula | Annotation |
| 297.34 | 435.17 | 100 | C18H33O3 | Oleic acid anion +O |
| 255.33 | 477.18 | 45 | C16H31O2 | Palmitic acid anion |
| 452.38 | 280.13 | 12 | C21H43NO7P | -(Oleic acid anion +O) (ketene) |
| 494.37 | 238.14 | 6 | C23H45NO8P | - Palmitic acid (ketene) |
| 279.34 | 453.17 | 5 | C18H31O2 | Oleic acid anion +O -H2O |
| 281.35 | 451.16 | 3 | C18H33O2 | Oleic acid anion |
| 295.33 | 437.18 | 2 | - | Unknown |
| 476.28 | 256.23 | 2 | C23H43NO7P | -Palmitic acid |
| 296.39 | 436.12 | 2 | - | Unknown |
| 256.38 | 476.13 | 1 | - | Unknown |
| 271.30 | 461.21 | 1 | C16H31O3 | Palmitic acid anion +O |

| Parent (m/z) | 744.51 | | | |
|--------------|-------------------|--------------------|----------------|-------------------------|
| Adduct | [-H] | | | |
| ID | PE(16:0,18:1)+ CO | | | |
| Formula | C40H75NO9P | | | |
| | Observed | | Identification | |
| Fragment m/z | Neutral loss | Relative Intensity | Formula | Annotation |
| 281.37 | 463.14 | 100 | C18H33O2 | Oleic acid anion |
| 255.33 | 489.18 | 45 | C16H31O2 | Palmitic acid anion |
| 480.39 | 264.12 | 11 | C22H43NO8P | -Oleic acid (ketene) |
| 391.27 | 353.24 | 5 | | |
| 506.37 | 238.14 | 4 | C24H45NO8P | -Palmitic acid (ketene) |
| 417.32 | 327.19 | 4 | | |
| 462.37 | 282.14 | 2 | C22H41NO7P | -Oleic acid |
| 309.32 | 435.19 | 2 | C19H33O3 | Oleic acid anion + CO |
| 488.32 | 256.19 | 2 | C24H43NO7P | -Palmitic acid |
| 295.34 | 449.17 | 2 | | |
| 291.30 | 453.21 | 1 | | |

| Parent (m/z) | 746.49 | | | |
|--------------|----------------------|--------------------|----------------|----------------------------------|
| Adduct | [-H] | | | |
| ID | PE(16:0,18:1)+O3-H2O | | | |
| Formula | C39H73NO10P | | | |
| | Observed | | Identification | |
| Fragment m/z | Neutral loss | Relative Intensity | Formula | Annotation |
| 311.34 | 435.15 | 100 | C18H31O4 | Oleic acid + O3 -H2O anion |
| 255.35 | 491.14 | 82 | C16H31O2 | Palmitic acid anion |
| 293.32 | 453.17 | 29 | C18H29O3 | Oleic acid + O3 -2(H2O) anion |
| 281.37 | 465.12 | 29 | C18H33O2 | Oleic acid anion |
| 452.38 | 294.11 | 26 | C21H43NO7P | -(Oleic acid + O3 -H2O) (ketene) |
| 282.35 | 464.14 | 21 | | |
| 297.35 | 449.14 | 17 | C18H33O3 | Oleic acid + O anion |
| 283.34 | 463.15 | 10 | | |
| 508.33 | 238.16 | 10 | C23H43NO9P | -Palmitic acid (ketene) |
| 490.37 | 256.12 | 8 | C23H41NO8P | -Palmitic acid |
| 256.31 | 490.18 | 7 | | |
| 295.42 | 451.07 | 6 | C18H31O3 | Oleic acid + O2 -H2O anion |
| 269.42 | 477.07 | 5 | | |
| 728.45 | 18.04 | 5 | C39H71NO9P | -H2O |
| 285.29 | 461.20 | 3 | | |
| 482.44 | 264.05 | 2 | C21H41NO9P | -Oleic acid (ketene) |
| 481.51 | 264.98 | 2 | | |
| 688.57 | 57.92 | 2 | | |
| 257.47 | 489.02 | 2 | | |
| 466.31 | 280.18 | 2 | | |
| 434.36 | 312.13 | 1 | C21H41NO6P | -(Oleic acid + O3 -H2O) |
| 271.25 | 475.24 | 1 | | |
| 716.58 | 29.91 | 1 | | |
| 391.31 | 355.18 | 1 | | |
| 271.53 | 474.96 | 1 | | |
| 507.49 | 239.00 | 1 | | |
| 313.31 | 433.18 | 1 | | |
| 737.14 | 9.35 | 1 | | |

| Parent m/z | 748.51 | | | |
|--------------|------------------|--------------------|----------------|-----------------------------|
| Ion form | [M-H]- | | | |
| ID | PE(16:0,18:1)+O2 | | | |
| Formula | C39H75NO10P | | | |
| | Observed | | Identification | |
| Fragment m/z | Neutral loss | Relative Intensity | Formula | Annotation |
| 313.34 | 435.17 | 100 | C18H33O4 | Oleic acid + O2 anion |
| 255.33 | 493.18 | 76 | C16H31O2 | Palmitic acid anion |
| 295.32 | 453.19 | 53 | C18H31O3 | Oleic acid + O2 -H2O anion |
| 730.52 | 17.99 | 33 | C39H73NO9P | -H2O |
| 452.36 | 296.15 | 20 | C21H43NO7P | -(Oleic acid + O2) (ketene) |
| 297.32 | 451.19 | 12 | C18H33O3 | Oleic acid + O anion* |
| 510.36 | 238.15 | 8 | C23H45NO9P | - Palmitic acid (ketene) |
| 492.35 | 256.16 | 8 | C23H43NO8P | -Palmitic acid |
| 271.33 | 477.18 | 6 | C16H31O3 | Palmitic acid anion +O* |
| 281.36 | 467.15 | 5 | C18H33O2 | Oleic acid anion* |
| 312.36 | 436.15 | 3 | - | Unknown |
| 311.32 | 437.19 | 2 | - | Unknown |
| 256.36 | 492.15 | 2 | - | Unknown |
| 269.37 | 479.14 | 2 | - | Unknown |
| 293.28 | 455.23 | 2 | - | Unknown |
| 434.39 | 314.12 | 2 | C21H41NO6P | -(Oleic acid + 2O) |
| 287.39 | 461.12 | 1 | - | Unknown |
| 468.35 | 280.16 | 1 | - | Unknown |
| 257.39 | 491.12 | 1 | - | Unknown |
| 716.61 | 31.90 | 1 | C39H75NO8P | -O2 |

| Parent (m/z) | 760.50 | | | |
|--------------|-------------------|--------------------|----------------|----------------------------|
| Adduct | [-H] | | | |
| ID | PE(16:0,18:1)+CO2 | | | |
| Formula | C40H75NO10P | | | |
| | Observed | | Identification | |
| Fragment m/z | Neutral loss | Relative Intensity | Formula | Annotation |
| 297.34 | 463.16 | 100 | C18H33O3 | Oleic acid + O anion |
| 255.35 | 505.15 | 48 | C16H31O2 | Palmitic acid anion |
| 281.34 | 479.16 | 32 | C18H33O2 | Oleic acid anion |
| 480.39 | 280.11 | 10 | C22H43NO8P | -(Oleic acid + O) (ketene) |
| 295.37 | 465.13 | 10 | C18H31O3 | Oleic acid + O2 -H2O anion |
| 522.35 | 238.15 | 6 | C24H45NO9P | -Palmitic acid (ketene) |
| 496.45 | 264.05 | 5 | C22H43NO9P | -Oleic acid (ketene) |
| 433.44 | 327.06 | 5 | | |
| 742.48 | 18.02 | 4 | C40H73NO9P | -H2O |
| 504.45 | 256.05 | 4 | C24H43NO8P | -Palmitic acid |
| 296.35 | 464.15 | 4 | | |
| 325.39 | 435.11 | 3 | | |
| 311.35 | 449.15 | 3 | C18H31O4 | Oleic acid + O3 -H2O anion |
| 279.37 | 481.13 | 3 | | |
| 391.30 | 369.20 | 3 | | |
| 452.39 | 308.11 | 2 | | |
| 256.35 | 504.15 | 2 | | |
| 285.29 | 475.21 | 2 | | |
| 462.44 | 298.06 | 2 | | |
| 716.55 | 43.95 | 2 | | |
| 282.37 | 478.13 | 2 | | |
| 269.32 | 491.18 | 1 | | |
| 271.32 | 489.18 | 1 | C16H31O3 | Palmitic acid anion +O |
| 289.26 | 471.24 | 1 | | |
| 702.60 | 57.90 | 1 | | |
| 689.41 | 71.09 | 1 | | |

| Parent (m/z) | 762.49 | | | |
|--------------|----------------------|--------------------|----------------|-----------------------------------|
| Adduct | [-H] | | | |
| ID | PE(16:0,18:1)+O4-H2O | | | |
| Formula | C39H73NO11P | | | |
| | Observed | | Identification | |
| Fragment m/z | Neutral loss | Relative Intensity | Formula | Annotation |
| 255.33 | 507.16 | 100 | C16H31O2 | Palmitic acid anion |
| 327.31 | 435.18 | 96 | C18H31O5 | Oleic acid + O4 -H2O anion |
| 309.27 | 453.22 | 50 | C18H29O4 | Oleic acid + O4 -2(H2O) anion |
| 506.35 | 256.14 | 44 | C23H41NO9P | -Palmitic acid |
| 744.50 | 17.99 | 40 | C39H71NO10P | -H2O |
| 452.36 | 310.13 | 34 | C21H43NO7P | - (Oleic acid + O4 -H2O) (ketene) |
| 297.32 | 465.17 | 29 | C18H33O3 | Oleic acid + O anion |
| 285.32 | 477.17 | 15 | | |
| 524.32 | 238.17 | 14 | C23H43NO10P | -Palmitic acid (ketene) |
| 298.35 | 464.14 | 13 | | |
| 291.33 | 471.16 | 12 | | |
| 295.34 | 467.15 | 12 | | |
| 313.35 | 449.14 | 11 | C18H33O4 | Oleic acid + O2 anion |
| 311.28 | 451.21 | 9 | C18H31O4 | Oleic acid + O3 -H2O anion |
| 299.36 | 463.13 | 9 | | |
| 281.29 | 481.20 | 8 | C18H33O2 | Oleic acid anion |
| 269.40 | 493.09 | 6 | | |
| 271.31 | 491.18 | 5 | C16H31O3 | Palmitic acid anion +O????? |
| 463.25 | 299.24 | 5 | | |
| 265.28 | 497.21 | 5 | | |
| 391.33 | 371.16 | 4 | | |
| 370.57 | 391.92 | 4 | | |
| 282.25 | 480.24 | 4 | | |
| 247.33 | 515.16 | 4 | | |
| 256.39 | 506.10 | 4 | | |
| 323.20 | 439.29 | 3 | | |
| 482.16 | 280.33 | 3 | | |
| 434.22 | 328.27 | 3 | | |
| 478.52 | 283.97 | 3 | | |
| 283.36 | 479.13 | 2 | | |

| Parent (m/z) | 764.50 | | | |
|--------------|------------------|--------------------|----------------|---------------------------------|
| Adduct | [-H] | | | |
| ID | PE(16:0,18:1)+O3 | | | |
| Formula | C39H75NO11P | | | |
| | Observed | | Identification | |
| Fragment m/z | Neutral loss | Relative Intensity | Formula | Annotation |
| 746.51 | 17.99 | 100 | C39H73NO10P | -H2O |
| 329.33 | 435.17 | 75 | C18H33O5 | Oleic acid + O3 anion |
| 255.32 | 509.18 | 64 | C16H31O2 | Palmitic acid anion |
| 311.33 | 453.17 | 54 | C18H31O4 | Oleic acid + O3 -H2O anion |
| 452.42 | 312.08 | 23 | C23H43NO9P | -Oleic acid + O3 anion (ketene) |
| 313.33 | 451.17 | 14 | C18H33O4 | Oleic acid + O2 anion |
| 297.35 | 467.15 | 14 | C18H33O3 | Oleic acid + O anion |
| 293.31 | 471.19 | 14 | C18H29O3 | Oleic acid + O3 -2(H2O) anion |
| 508.38 | 256.12 | 13 | C23H43NO9P | -Palmitic acid |
| 644.33 | 120.17 | 6 | | |
| 328.37 | 436.13 | 6 | | |
| 271.31 | 493.19 | 6 | C16H31O3 | Palmitic acid anion +O |
| 295.33 | 469.17 | 6 | C18H31O3 | Oleic acid + O2 -H2O anion |
| 327.34 | 437.16 | 6 | | |
| 269.29 | 495.21 | 5 | | |
| 526.45 | 238.05 | 5 | C23H45NO10P | -Palmitic acid (ketene) |
| 622.56 | 141.94 | 4 | | |
| 606.39 | 158.11 | 4 | | |
| 256.40 | 508.10 | 4 | | |
| 309.25 | 455.25 | 4 | | |
| 644.58 | 119.92 | 3 | | |
| 620.43 | 144.07 | 3 | | |
| 468.43 | 296.07 | 3 | | |
| 287.44 | 477.06 | 3 | C16H31O4 | Palmitic acid anion +O2 |
| 732.51 | 31.99 | 3 | | |
| 285.32 | 479.18 | 3 | | |
| 592.49 | 172.01 | 3 | | |
| 526.65 | 237.85 | 3 | | |
| 281.29 | 483.21 | 2 | | |
| 310.27 | 454.23 | 2 | | |

| Parent (m/z) | 776.50 | | | |
|--------------|-------------------|--------------------|----------------|-----------------------------|
| Adduct | [-H] | | | |
| ID | PE(16:0,18:1)+CO3 | | | |
| Formula | C40H75NO11P | | | |
| | Observed | | Identification | |
| Fragment m/z | Neutral loss | Relative Intensity | Formula | Annotation |
| 716.49 | 60.01 | 100 | | |
| 313.33 | 463.17 | 63 | C18H33O4 | Oleic acid + O2 anion |
| 295.36 | 481.14 | 27 | C18H31O3 | Oleic acid + O2 -H2O anion |
| 718.65 | 57.85 | 24 | | |
| 255.39 | 521.11 | 23 | C16H31O2 | Palmitic acid anion |
| 281.23 | 495.27 | 23 | C18H33O2 | Oleic acid anion |
| 758.35 | 18.15 | 22 | C40H73NO10P | -H2O |
| 758.64 | 17.86 | 15 | | |
| 520.24 | 256.26 | 15 | C24H43NO9P | -Palmitic acid |
| 449.30 | 327.20 | 13 | | |
| 341.40 | 435.10 | 13 | C19H33O5 | Oleic acid + CO3 anion |
| 297.36 | 479.14 | 10 | C18H33O3 | Oleic acid + O anion |
| 281.52 | 494.98 | 9 | | |
| 480.28 | 296.22 | 9 | | |
| 740.57 | 35.93 | 8 | C40H71NO9P | -2(H2O) |
| 538.33 | 238.17 | 7 | C24H45NO10P | -Palmitic acid (ketene) |
| 449.49 | 327.01 | 7 | | |
| 323.14 | 453.36 | 6 | C19H31O4 | Oleic acid + CO3 -H2O anion |
| 520.53 | 255.97 | 5 | | |
| 776.40 | 0.10 | 5 | | |
| 327.42 | 449.08 | 5 | | |
| 480.50 | 296.00 | 5 | | |
| 311.43 | 465.07 | 4 | C18H31O4 | Oleic acid + O3 -H2O anion |
| 294.09 | 482.41 | 4 | | |
| 645.27 | 131.23 | 4 | | |
| 293.23 | 483.27 | 4 | | |
| 620.21 | 156.29 | 3 | | |
| 620.49 | 156.01 | 3 | | |
| 732.80 | 43.70 | 3 | | |
| 462.08 | 314.42 | 3 | | |

| Parent (m/z) | 780.50 | | | |
|--------------|------------------|--------------------|----------------|-------------------------------|
| Adduct | [-H] | | | |
| ID | PE(16:0,18:1)+O4 | | | |
| Formula | C39H75NO12P | | | |
| | Observed | | Identification | |
| Fragment m/z | Neutral loss | Relative Intensity | Formula | Annotation |
| 762.49 | 18.01 | 100 | C39H73NO11P | -H2O |
| 255.34 | 525.16 | 60 | C16H31O2 | Palmitic acid anion |
| 345.30 | 435.20 | 28 | C18H33O6 | Oleic acid + O4 anion |
| 327.23 | 453.27 | 25 | C18H31O5 | Oleic acid + O4 -H2O anion |
| 622.44 | 158.06 | 22 | | |
| 524.34 | 256.16 | 19 | C23H43NO10P | -Palmitic acid |
| 295.35 | 485.15 | 13 | C18H31O3 | Oleic acid + O2 -H2O anion |
| 313.28 | 467.22 | 12 | C18H33O4 | Oleic acid + O2 anion |
| 281.28 | 499.22 | 11 | C18H33O2 | Oleic acid anion |
| 297.29 | 483.21 | 11 | C18H33O3 | Oleic acid + O anion |
| 269.36 | 511.14 | 10 | | |
| 722.62 | 57.88 | 10 | | |
| 452.30 | 328.20 | 9 | | |
| 744.63 | 35.87 | 7 | C39H71NO10P | -2(H2O) |
| 281.50 | 499.00 | 7 | | |
| 608.28 | 172.22 | 7 | | |
| 652.34 | 128.16 | 5 | | |
| 285.27 | 495.23 | 5 | | |
| 309.40 | 471.10 | 4 | C18H29O4 | Oleic acid + O4 -2(H2O) anion |
| 780.76 | -0.26 | 4 | | |
| 591.20 | 189.30 | 4 | | |
| 592.27 | 188.23 | 4 | | |
| 610.71 | 169.79 | 4 | | |
| 609.51 | 170.99 | 4 | | |
| 542.35 | 238.15 | 4 | C23H45NO11P | -Palmitic acid (ketene) |
| 537.37 | 243.13 | 4 | | |
| 311.52 | 468.98 | 4 | | |
| 623.35 | 157.15 | 3 | | |
| 744.07 | 36.43 | 3 | | |
| 326.51 | 453.99 | 3 | | |

All-X - Fragmentation patterns from PE(16:0,18:1) and oxidised products thereof in positive ion mode

Parent m/z 740.52
 Ion form [M+Na]
 ID PE(16:0,18:1)
 Formula C39H76NO8PNa

| Observed | | | Identification | |
|--------------|--------------|--------------------|----------------|-----------------------------|
| Fragment m/z | Neutral loss | Relative Intensity | Formula | Annotation |
| 697.37 | 43.15 | 100 | C37H71O8PNa | - Aziridine |
| 599.49 | 141.03 | 20 | C37H68O4Na | - Head group(PE) |
| 577.51 | 163.01 | 5 | C37H69O4 | - Sodiated head group |
| 617.52 | 123.00 | 3 | C37H70O5Na | -Head group (PE) |
| 441.31 | 299.21 | 2 | C21H39O6PNa | - Palmitic acid & aziridine |

Parent (m/z) 754.50
 Adduct [+Na]
 ID PE(16:0,18:1)+O2-H2O
 Formula C39H74NO9PNa

| Observed | | | Identification | |
|--------------|--------------|--------------------|----------------|------------------|
| Fragment m/z | Neutral loss | Relative Intensity | Formula | Annotation |
| 711.42 | 43.08 | 100 | C37H69O9PNa | - Aziridine |
| 613.50 | 141.00 | 42 | C37H66O5Na | - Head group(PE) |
| 631.52 | 122.98 | 12 | C37H68O6Na | -Head group (PE) |
| 736.50 | 18.00 | 10 | C39H72NO8PNa | -H2O |
| 754.52 | -0.02 | 3 | C39H74NO9PNa | Parent |

| Parent m/z | 756.51 | | | |
|--------------|-----------------|--------------------|----------------|------------------------|
| Ion form | [M+Na] | | | |
| ID | PE(16:0,18:1)+O | | | |
| Formula | C39H76NO9PNa | | | |
| | Observed | | Identification | |
| Fragment m/z | Neutral loss | Relative Intensity | Formula | Annotation |
| 713.42 | 43.09 | 100 | C37H71O9PNa | - Aziridine |
| 738.39 | 18.12 | 57 | C39H74NO8PNa | -H2O |
| 615.52 | 140.99 | 41 | C37H68O5Na | - Head group(PE) |
| 712.44 | 44.07 | 15 | | |
| 695.39 | 61.12 | 14 | C37H69O8PNa | - Aziridine & H2O |
| 633.52 | 122.99 | 10 | C37H70O6Na | - Head group(PE) |
| 614.52 | 141.99 | 6 | | |
| 597.46 | 159.05 | 2 | C37H66O4Na | - Head group(PE) & H2O |

| Parent (m/z) | 770.49 | | | |
|--------------|----------------------|--------------------|----------------|-------------------|
| Adduct | [+Na] | | | |
| ID | PE(16:0,18:1)+O3-H2O | | | |
| Formula | C39H74NO10PNa | | | |
| | Observed | | Identification | |
| Fragment m/z | Neutral loss | Relative Intensity | Formula | Annotation |
| 727.41 | 43.08 | 100 | C37H69O10PNa | - Aziridine |
| 629.49 | 141.00 | 52 | C37H66O6Na | - Head group(PE) |
| 752.44 | 18.05 | 16 | C39H72NO9PNa | -H2O |
| 647.52 | 122.97 | 15 | C37H68O7Na | -Head group (PE) |
| 734.48 | 36.01 | 3 | C39H70NO8PNa | -2(H2O) |
| 770.64 | -0.15 | 2 | C39H74NO10PNa | Parent |
| 709.42 | 61.07 | 2 | C37H67O9PNa | - Aziridine & H2O |

| Parent m/z | 772.51 | | | |
|--------------|------------------|--------------------|----------------|------------------------|
| Ion form | [M+Na] | | | |
| ID | PE(16:0,18:1)+O2 | | | |
| Formula | C39H76NO10PNa | | | |
| | Observed | | Identification | |
| Fragment m/z | Neutral loss | Relative Intensity | Formula | Annotation |
| 729.41 | 43.10 | 100 | C37H71O10PNa | - Aziridine |
| 631.51 | 141.00 | 55 | C37H68O6Na | - Head group(PE) |
| 754.42 | 18.09 | 39 | C39H74NO9PNa | -H2O |
| 711.42 | 61.09 | 33 | C37H69O9PNa | - Aziridine & H2O |
| 613.49 | 159.02 | 22 | C37H66O5Na | - Head group(PE) & H2O |
| 649.49 | 123.02 | 19 | C37H70O7Na | - Head group(PE) |
| 656.35 | 116.16 | 18 | - | Unknown |
| 738.42 | 34.09 | 17 | C39H74NO8PNa | - H2O2 |
| 642.36 | 130.15 | 15 | - | Unknown |
| 415.28 | 357.23 | 8 | - | Unknown |
| 638.40 | 134.11 | 7 | - | Unknown |
| 612.39 | 160.12 | 6 | - | Unknown |
| 736.48 | 36.03 | 6 | C39H72NO8PNa | -2(H2O) |
| 695.39 | 77.12 | 5 | - | Unknown |
| 624.40 | 148.11 | 5 | - | Unknown |
| 598.36 | 174.15 | 4 | - | Unknown |
| 361.30 | 411.21 | 3 | - | Unknown |
| 458.26 | 314.25 | 3 | - | Unknown |
| 530.27 | 242.24 | 2 | - | Unknown |
| 587.29 | 185.22 | 2 | - | Unknown |
| 772.51 | 0.00 | 2 | C39H76NO10PNa | Parent |
| 291.25 | 481.26 | 2 | - | Unknown |
| 332.13 | 440.38 | 2 | - | Unknown |
| 626.57 | 145.94 | 2 | - | Unknown |
| 693.37 | 79.14 | 2 | - | Unknown |
| 346.14 | 426.37 | 2 | - | Unknown |
| 489.39 | 283.12 | 2 | - | Unknown |
| 475.35 | 297.16 | 2 | - | Unknown |
| 503.42 | 269.09 | 2 | - | Unknown |
| 652.38 | 120.13 | 2 | - | Unknown |

| Parent (m/z) | 786.49 | | | |
|--------------|----------------------|--------------------|----------------|------------------------|
| Adduct | [+Na] | | | |
| ID | PE(16:0,18:1)+O4-H2O | | | |
| Formula | C39H74NO11PNa | | | |
| | Observed | | Identification | |
| Fragment m/z | Neutral loss | Relative Intensity | Formula | Annotation |
| 743.41 | 43.08 | 100 | C37H69O11PNa | - Aziridine |
| 645.48 | 141.01 | 49 | C37H66O7Na | - Head group(PE) |
| 768.42 | 18.07 | 41 | C39H72NO10PNa | -H2O |
| 786.46 | 0.03 | 20 | C39H74NO11PNa | Parent |
| 663.50 | 122.99 | 19 | C37H68O8Na | -Head group (PE) |
| 725.44 | 61.05 | 16 | C37H67O10PNa | - Aziridine & H2O |
| 785.60 | 0.89 | 12 | | |
| 627.52 | 158.97 | 9 | C37H64O6Na | - Head group(PE) & H2O |
| 754.48 | 32.01 | 6 | | |
| 750.53 | 35.96 | 5 | C39H70NO9PNa | -2(H2O) |
| 530.40 | 256.09 | 4 | | |
| 666.36 | 120.13 | 3 | | |
| 741.48 | 45.01 | 3 | | |
| 612.39 | 174.10 | 3 | | |
| 742.45 | 44.04 | 3 | | |
| 503.40 | 283.09 | 3 | | |
| 698.52 | 87.97 | 2 | | |
| 658.51 | 127.98 | 2 | | |
| 473.39 | 313.10 | 2 | | |
| 305.27 | 481.22 | 2 | | |
| 787.54 | -1.05 | 2 | | |
| 707.38 | 79.11 | 2 | | |
| 666.67 | 119.82 | 1 | | |
| 554.90 | 231.59 | 1 | | |
| 672.44 | 114.05 | 1 | | |
| 385.39 | 401.10 | 1 | | |
| 598.45 | 188.04 | 1 | | |
| 375.35 | 411.14 | 1 | | |
| 661.38 | 125.11 | 1 | | |
| 682.45 | 104.04 | 1 | | |

| Parent (m/z) | 788.51 | | | |
|--------------|------------------|--------------------|----------------|------------------------|
| Adduct | [+Na] | | | |
| ID | PE(16:0,18:1)+O3 | | | |
| Formula | C39H76NO11PNa | | | |
| | Observed | | Identification | |
| Fragment m/z | Neutral loss | Relative Intensity | Formula | Annotation |
| 745.41 | 43.10 | 100 | C37H71O11PNa | - Aziridine |
| 647.51 | 141.00 | 60 | C37H68O7Na | - Head group(PE) |
| 770.41 | 18.10 | 52 | C39H74NO10PNa | -H2O |
| 788.54 | -0.03 | 44 | C39H76NO11PNa | Parent |
| 532.14 | 256.37 | 27 | | |
| 727.35 | 61.16 | 19 | C37H69O10PNa | - Aziridine & H2O |
| 532.44 | 256.07 | 17 | | |
| 752.46 | 36.05 | 15 | | -2(H2O) |
| 665.63 | 122.88 | 12 | C37H70O8Na | -Head group (PE) |
| 629.60 | 158.91 | 10 | C37H66O6Na | - Head group(PE) & H2O |
| 789.57 | -1.06 | 9 | | |
| 507.34 | 281.17 | 6 | | |
| 458.27 | 330.24 | 6 | | |
| 437.38 | 351.13 | 6 | | |
| 506.29 | 282.22 | 6 | | |
| 676.47 | 112.04 | 5 | | |
| 672.40 | 116.11 | 5 | | |
| 611.61 | 176.90 | 5 | | |
| 676.19 | 112.32 | 5 | | |
| 628.36 | 160.15 | 5 | | |
| 415.26 | 373.25 | 5 | | |
| 475.39 | 313.12 | 5 | | |
| 758.57 | 29.94 | 5 | | |
| 779.71 | 8.80 | 4 | | |
| 616.35 | 172.16 | 4 | | |
| 353.26 | 435.25 | 4 | | |
| 588.33 | 200.18 | 4 | | |
| 682.43 | 106.08 | 4 | | |
| 654.50 | 134.01 | 4 | | |
| 665.00 | 123.51 | 4 | | |

All-XI - Fragmentation patterns from PE(18:1,18:1) and oxidised products thereof in negative ion mode

| Parent (m/z) | 742.54 | | | |
|--------------|---------------|--------------------|----------------|----------------------|
| Adduct | [-H] | | | |
| ID | PE(18:1,18:1) | | | |
| Formula | C41H77NO8P | | | |
| | Observed | | Identification | |
| Fragment m/z | Neutral loss | Relative Intensity | Formula | Annotation |
| 281.33 | 461.21 | 100 | C18H33O2 | Oleic acid anion |
| 478.34 | 264.20 | 12 | C23H45NO7P | -Oleic acid (ketene) |
| 460.35 | 282.19 | 2 | C23H43NO6P | -Oleic acid |

| Parent (m/z) | 756.51 | | | |
|--------------|-------------------------|--------------------|----------------|----------------------------|
| Adduct | [-H] | | | |
| ID | PE(18:1,18:1) + O2 -H2O | | | |
| Formula | C41H75NO9P | | | |
| | Observed | | Identification | |
| Fragment m/z | Neutral loss | Relative Intensity | Formula | Annotation |
| 281.33 | 475.18 | 100 | C18H33O2 | Oleic acid anion |
| 295.33 | 461.18 | 70 | C18H31O3 | Oleic acid + O2 -H2O anion |
| 478.38 | 278.13 | 12 | | |
| 492.35 | 264.16 | 11 | C23H43NO8P | -Oleic acid (ketene) |
| 474.33 | 282.18 | 5 | C23H41NO7P | -Oleic acid |
| 297.31 | 459.20 | 4 | C18H33O3 | Oleic acid + O anion |
| 623.98 | 132.53 | 2 | | |
| 282.31 | 474.20 | 2 | C17(C13)H33O2 | Oleic acid anion (C13) |
| 476.34 | 280.17 | 1 | | |
| 620.72 | 135.79 | 1 | | |
| 460.44 | 296.07 | 1 | C23H43NO6P | -Oleic acid + O2 -H2O |
| 279.38 | 477.13 | 1 | C18H31O2 | Oleic acid + O -H2O anion |

| Parent (m/z) | 758.53 | | | |
|--------------|-----------------|--------------------|----------------|----------------------------|
| Adduct | [-H] | | | |
| ID | PE(18:1,18:1)+O | | | |
| Formula | C41H77NO9P | | | |
| | Observed | | Identification | |
| Fragment m/z | Neutral loss | Relative Intensity | Formula | Annotation |
| 281.35 | 477.18 | 100 | C18H33O2 | Oleic acid anion |
| 297.32 | 461.21 | 85 | C18H33O3 | Oleic acid + O anion |
| 494.36 | 264.17 | 13 | C23H45NO8P | -Oleic acid (ketene) |
| 478.36 | 280.17 | 12 | | -Oleic acid + O (ketene) |
| 476.34 | 282.19 | 3 | C23H43NO7P | -Oleic acid |
| 282.33 | 476.20 | 3 | C17(C13)H33O2 | Oleic acid anion (C13) |
| 295.34 | 463.19 | 3 | C18H31O3 | Oleic acid + O2 -H2O anion |
| 279.33 | 479.20 | 3 | C18H31O2 | Oleic acid + O -H2O anion |
| 296.29 | 462.24 | 2 | | |
| 283.34 | 475.19 | 2 | C16(C13)2H33O2 | Oleic acid anion (C13*2) |
| 417.29 | 341.24 | 1 | | |

| Parent (m/z) | 770.53 | | | |
|--------------|------------------|--------------------|----------------|----------------------------|
| Adduct | [-H] | | | |
| ID | PE(18:1,18:1)+CO | | | |
| Formula | C42H77NO9P | | | |
| | Observed | | Identification | |
| Fragment m/z | Neutral loss | Relative Intensity | Formula | Annotation |
| 281.34 | 489.19 | 100 | C18H33O2 | Oleic acid anion |
| 506.36 | 264.17 | 12 | C24H45NO8P | -Oleic acid (ketene) |
| 417.30 | 353.23 | 7 | | |
| 295.34 | 475.19 | 4 | C18H31O3 | Oleic acid + O2 -H2O anion |
| 488.35 | 282.18 | 3 | C24H43NO7P | -Oleic acid |

| Parent (m/z) | 774.53 | | | |
|--------------|------------------|--------------------|----------------|----------------------------|
| Adduct | [-H] | | | |
| ID | PE(18:1,18:1)+O2 | | | |
| Formula | C41H77NO10P | | | |
| | Observed | | Identification | |
| Fragment m/z | Neutral loss | Relative Intensity | Formula | Annotation |
| 281.35 | 493.18 | 100 | C18H33O2 | Oleic acid anion |
| 756.50 | 18.03 | 83 | C41H75NO9P | -H2O |
| 295.31 | 479.22 | 74 | C18H31O3 | Oleic acid + O2 -H2O anion |
| 297.35 | 477.18 | 33 | C18H33O3 | Oleic acid + O anion |
| 313.32 | 461.21 | 24 | C18H33O4 | Oleic acid + O2 anion |
| 492.31 | 282.22 | 11 | C23H43NO8P | -Oleic acid |
| 478.53 | 296.00 | 6 | C23H45NO7P | -Oleic acid (ketene) + O2 |
| 742.54 | 31.99 | 5 | C41H77NO8P | -O2 |
| 510.33 | 264.20 | 4 | C23H45NO9P | -Oleic acid (ketene) |
| 494.34 | 280.19 | 4 | | |
| 282.37 | 492.16 | 3 | C17(C13)H33O2 | Oleic acid anion (C13) |
| 474.31 | 300.22 | 2 | | |
| 279.32 | 495.21 | 2 | | |
| 460.38 | 314.15 | 2 | C23H43NO6P | -Oleic acid + O2 |
| 283.35 | 491.18 | 1 | C16(C13)2H33O2 | Oleic acid anion (C13 x 2) |
| 293.30 | 481.23 | 1 | | |
| 311.34 | 463.19 | 1 | | |
| 312.31 | 462.22 | 1 | | |

| Parent (m/z) | 790.52 | | | | |
|--------------|------------------|--------------------|----------------|----------------------------|--|
| Adduct | [-H] | | | | |
| ID | PE(18:1,18:1)+O3 | | | | |
| Formula | C41H77NO11P | | | | |
| | Observed | | Identification | | |
| Fragment m/z | Neutral loss | Relative Intensity | Formula | Annotation | |
| 674.40 | 116.12 | 100 | | | |
| 297.34 | 493.18 | 71 | C18H33O3 | Oleic acid + O anion | |
| 772.59 | 17.93 | 44 | C41H75NO10P | -H2O | |
| 558.71 | 231.81 | 42 | | | |
| 281.28 | 509.24 | 38 | C18H33O2 | Oleic acid anion | |
| 295.39 | 495.13 | 30 | C18H31O3 | Oleic acid + O2 -H2O anion | |
| 732.60 | 57.92 | 22 | | | |
| 672.52 | 118.00 | 18 | | | |
| 556.79 | 233.73 | 16 | | | |
| 313.21 | 477.31 | 13 | C18H33O4 | Oleic acid + O2 anion | |
| 556.38 | 234.14 | 12 | | | |
| 281.57 | 508.95 | 11 | | Artefact? | |
| 770.96 | 19.56 | 11 | | | |
| 329.46 | 461.06 | 9 | C18H33O5 | Oleic acid + O3 anion | |
| 526.37 | 264.15 | 9 | C23H45NO10P | -Oleic acid (ketene) | |
| 508.16 | 282.36 | 9 | C23H43NO9P | -Oleic acid | |
| 492.52 | 298.00 | 8 | C23H43NO8P | - Oleic acid + O | |
| 510.22 | 280.30 | 8 | | | |
| 576.43 | 214.09 | 8 | | | |
| 706.12 | 84.40 | 6 | | | |
| 494.40 | 296.12 | 6 | | | |
| 463.24 | 327.28 | 6 | | | |
| 508.49 | 282.03 | 6 | | | |
| 313.62 | 476.90 | 6 | | | |
| 562.34 | 228.18 | 6 | | | |
| 732.24 | 58.28 | 6 | | | |
| 498.76 | 291.76 | 6 | | | |
| 616.59 | 173.93 | 6 | | | |
| 648.40 | 142.12 | 5 | | | |
| 328.88 | 461.64 | 5 | | | |

| Parent (m/z) | 806.51 | | | |
|--------------|------------------|--------------------|----------------|----------------------------|
| Adduct | [-H] | | | |
| ID | PE(18:1,18:1)+O4 | | | |
| Formula | C41H77NO12P | | | |
| | Observed | | Identification | |
| Fragment m/z | Neutral loss | Relative Intensity | Formula | Annotation |
| 295.32 | 511.19 | 100 | C18H31O3 | Oleic acid + O2 -H2O anion |
| 492.31 | 314.20 | 11 | C23H43NO8P | -Oleic acid + O2 |
| 281.34 | 525.17 | 9 | C18H33O2 | Oleic acid anion |
| 770.47 | 36.04 | 7 | C41H73NO10P | -2(H2O)? |
| 297.31 | 509.20 | 6 | C18H33O3 | Oleic acid + O anion |
| 690.46 | 116.05 | 4 | | |
| 327.37 | 479.14 | 4 | C18H31O5 | Oleic acid + O4 -H2O anion |
| 672.47 | 134.04 | 3 | | |
| 313.31 | 493.20 | 2 | C18H33O4 | Oleic acid + O2 anion |
| 311.36 | 495.15 | 2 | C18H31O4 | Oleic acid + O3 -H2O anion |
| 658.38 | 148.13 | 2 | | |
| 524.34 | 282.17 | 2 | C23H43NO10P | -Oleic acid |
| 474.29 | 332.22 | 2 | | |
| 732.46 | 74.05 | 1 | | |
| 748.46 | 58.05 | 1 | | |
| 329.40 | 477.11 | 1 | C18H33O5 | Oleic acid + O3 anion |

| Parent (m/z) | 814.56 | | | |
|--------------|--------------|--------------------|----------------|----------------------|
| Adduct | | | | |
| ID | Unknown | | | |
| Formula | | | | |
| | Observed | | Identification | |
| Fragment m/z | Neutral loss | Relative Intensity | Formula | Annotation |
| 281.35 | 533.21 | 100 | C18H33O2 | Oleic acid anion |
| 768.48 | 46.08 | 13 | | |
| 550.36 | 264.20 | 12 | | -Oleic acid (ketene) |
| 532.34 | 282.22 | 3 | | -Oleic acid |
| 417.28 | 397.28 | 3 | | |

All-XII - Fragmentation patterns from PE(18:1,18:1) and oxidised products thereof in positive ion mode

| Parent (m/z) | 744.55 | | | |
|--------------|---------------|--------------------|----------------|-------------------------------|
| Adduct | [+H] | | | |
| ID | PE(18:1,18:1) | | | |
| Formula | C41H79NO8P | | | |
| | Observed | | Identification | |
| Fragment m/z | Neutral loss | Relative Intensity | Formula | Annotation |
| 744.48 | 0.07 | 100 | C41H79NO8P | Parent |
| 708.43 | 36.12 | 64 | C41H75NO6P | -2(H ₂ O) |
| 603.53 | 141.02 | 41 | C39H71O4 | - Head group(PE) |
| 726.50 | 18.05 | 32 | C41H77NO7P | -H ₂ O |
| 712.31 | 32.24 | 30 | | |
| 700.54 | 44.01 | 17 | | |
| 745.41 | -0.86 | 15 | | |
| 672.41 | 72.14 | 13 | | |
| 524.30 | 220.25 | 13 | | |
| 712.70 | 31.85 | 11 | | |
| 462.21 | 282.34 | 10 | C23H45NO6P | - Oleic acid |
| 683.43 | 61.12 | 10 | C39H72O7P | - Aziridine &H ₂ O |
| 463.24 | 281.31 | 9 | | |
| 616.56 | 127.99 | 8 | | |
| 684.43 | 60.12 | 8 | | |
| 701.15 | 43.40 | 8 | | |
| 706.54 | 38.01 | 8 | | |
| 682.42 | 62.13 | 8 | | |
| 686.50 | 58.05 | 7 | | |
| 642.46 | 102.09 | 6 | | |
| 460.35 | 284.20 | 6 | | |
| 714.57 | 29.98 | 6 | | |
| 701.47 | 43.08 | 6 | C39H74O8P | - Aziridine |
| 665.20 | 79.35 | 5 | | |
| 588.34 | 156.21 | 5 | | |
| 698.57 | 45.98 | 5 | | |
| 620.49 | 124.06 | 4 | | |
| 475.16 | 269.39 | 4 | | |
| 474.44 | 270.11 | 4 | | |
| 722.23 | 22.32 | 4 | | |

| Parent (m/z) | 766.53 | | | |
|--------------|---------------|--------------------|----------------|--------------------------|
| Adduct | [+Na] | | | |
| ID | PE(18:1,18:1) | | | |
| Formula | C41H78NO8PNa | | | |
| | Observed | | Identification | |
| Fragment m/z | Neutral loss | Relative Intensity | Formula | Annotation |
| 723.39 | 43.14 | 100 | C39H73O8PNa | - Aziridine |
| 625.49 | 141.04 | 26 | C39H70O4Na | - Head group(PE) |
| 603.52 | 163.01 | 4 | C39H71O4 | - Sodiated head group |
| 643.53 | 123.00 | 3 | C39H72O5Na | -Head group (PE) |
| 441.29 | 325.24 | 3 | C21H39O6PNa | - Oleic acid & aziridine |
| 484.27 | 282.26 | 1 | C23H44NO6PNa | - Oleic acid |

| Parent (m/z) | 780.51 | | | |
|--------------|------------------------|--------------------|----------------|------------------|
| Adduct | [+Na] | | | |
| ID | PE(18:1,18:1)+O2 - H2O | | | |
| Formula | C41H76NO9PNa | | | |
| | Observed | | Identification | |
| Fragment m/z | Neutral loss | Relative Intensity | Formula | Annotation |
| 737.42 | 43.09 | 100 | C39H71O9PNa | - Aziridine |
| 639.49 | 141.02 | 68 | C39H68O5Na | - Head group(PE) |
| 762.51 | 18.00 | 14 | C41H74NO8PNa | -H2O |
| 657.52 | 122.99 | 11 | C39H70O6Na | -Head group (PE) |
| 780.52 | -0.01 | 2 | C41H76NO9PNa | Parent |
| 744.42 | 36.09 | 2 | C41H72NO7PNa | -2(H2O) |
| 441.33 | 339.18 | 1 | | |
| 638.42 | 142.09 | 1 | | |

| Parent (m/z) | 782.53 | | | |
|--------------|-----------------|--------------------|----------------|------------------------|
| Adduct | [+Na] | | | |
| ID | PE(18:1,18:1)+O | | | |
| Formula | C41H78NO9PNa | | | |
| | Observed | | Identification | |
| Fragment m/z | Neutral loss | Relative Intensity | Formula | Annotation |
| 739.40 | 43.13 | 100 | C39H73O9PNa | - Aziridine |
| 641.51 | 141.02 | 63 | C39H70O5Na | - Head group(PE) |
| 764.44 | 18.09 | 52 | C41H76NO8PNa | -H2O |
| 721.39 | 61.14 | 16 | C39H71O8PNa | - Aziridine & H2O |
| 659.55 | 122.98 | 11 | C39H72O6Na | - Head group(PE) |
| 623.49 | 159.04 | 3 | C39H68O4Na | - Head group(PE) & H2O |

| Parent (m/z) | 798.53 | | | |
|--------------|------------------|--------------------|----------------|------------------------|
| Adduct | [+Na] | | | |
| ID | PE(18:1,18:1)+O2 | | | |
| Formula | C41H78NO10PNa | | | |
| | Observed | | Identification | |
| Fragment m/z | Neutral loss | Relative Intensity | Formula | Annotation |
| 780.43 | 18.10 | 100 | C41H76NO9PNa | -H2O |
| 755.38 | 43.15 | 99 | C39H73O10PNa | - Aziridine |
| 657.51 | 141.02 | 82 | C39H70O6Na | - Head group(PE) |
| 639.47 | 159.06 | 70 | C39H68O5Na | - Head group(PE) & H2O |
| 737.41 | 61.12 | 63 | C39H71O9PNa | - Aziridine &H2O |
| 682.36 | 116.17 | 49 | | |
| 764.45 | 34.08 | 41 | C41H76NO8PNa | -H2O2 |
| 668.36 | 130.17 | 38 | | |
| 664.40 | 134.13 | 23 | | |
| 361.30 | 437.23 | 22 | | |
| 675.46 | 123.07 | 21 | C39H72O7Na | -Head group (PE) |
| 638.40 | 160.13 | 18 | | |
| 441.30 | 357.23 | 17 | | |
| 613.30 | 185.23 | 16 | | |
| 650.37 | 148.16 | 15 | | |
| 797.52 | 1.01 | 12 | | |
| 721.40 | 77.13 | 12 | | |
| 624.39 | 174.14 | 12 | | |
| 762.47 | 36.06 | 11 | C41H74NO8PNa | -2(H2O) |
| 627.35 | 171.18 | 11 | | |
| 754.43 | 44.10 | 10 | | |
| 652.41 | 146.12 | 10 | | |
| 656.47 | 142.06 | 9 | | |
| 489.41 | 309.12 | 8 | | |
| 529.37 | 269.16 | 7 | | |
| 543.25 | 255.28 | 7 | | |
| 503.43 | 295.10 | 7 | | |
| 779.44 | 19.09 | 6 | | |
| 515.40 | 283.13 | 6 | | |
| 763.42 | 35.11 | 5 | | |

| Parent (m/z) | 812.50 | | | | |
|--------------|------------------------|--------------------|----------------|------------------------|--|
| Adduct | [+Na] | | | | |
| ID | PE(18:1,18:1)+O4 - H2O | | | | |
| Formula | C41H76NO11PNa | | | | |
| | Observed | | Identification | | |
| Fragment m/z | Neutral loss | Relative Intensity | Formula | Annotation | |
| 794.42 | 18.08 | 100 | C41H74NO10PNa | -H2O | |
| 776.49 | 36.01 | 39 | C41H72NO9PNa | -2(H2O) | |
| 671.48 | 141.02 | 28 | C39H68O7Na | - Head group(PE) | |
| 769.39 | 43.11 | 27 | C39H71O11PNa | - Aziridine | |
| 751.38 | 61.12 | 19 | C39H69O10PNa | - Aziridine &H2O | |
| 653.51 | 158.99 | 18 | C39H66O6Na | - Head group(PE) & H2O | |
| 689.48 | 123.02 | 10 | C39H70O8Na | -Head group (PE) | |
| 778.39 | 34.11 | 10 | C41H74NO9PNa | -H2O2 | |
| 775.52 | 36.98 | 5 | | | |
| 678.40 | 134.10 | 5 | | | |
| 652.38 | 160.12 | 4 | | | |
| 664.37 | 148.13 | 3 | | | |
| 638.33 | 174.17 | 3 | | | |
| 666.36 | 146.14 | 2 | | | |
| 543.40 | 269.10 | 2 | | | |
| 529.36 | 283.14 | 2 | | | |
| 780.42 | 32.08 | 2 | | | |
| 359.30 | 453.20 | 2 | | | |
| 375.29 | 437.21 | 2 | | | |
| 627.33 | 185.17 | 2 | | | |
| 735.41 | 77.09 | 2 | | | |
| 455.37 | 357.13 | 2 | | | |
| 812.49 | 0.01 | 1 | | | |
| 613.35 | 199.15 | 1 | | | |
| 669.44 | 143.06 | 1 | | | |
| 758.44 | 54.06 | 1 | | | |
| 774.53 | 37.97 | 1 | | | |
| 696.47 | 116.03 | 1 | | | |
| 641.45 | 171.05 | 1 | | | |

| Parent (m/z) | 814.52 | | | |
|--------------|------------------|--------------------|----------------|------------------------|
| Adduct | [+Na] | | | |
| ID | PE(18:1,18:1)+O3 | | | |
| Formula | C41H78NO11PNa | | | |
| | Observed | | Identification | |
| Fragment m/z | Neutral loss | Relative Intensity | Formula | Annotation |
| 796.39 | 18.13 | 100 | C41H76NO10PNa | -H2O |
| 771.40 | 43.12 | 54 | C39H73O11PNa | - Aziridine |
| 673.49 | 141.03 | 39 | C39H70O7Na | - Head group(PE) |
| 655.46 | 159.06 | 33 | C39H68O6Na | - Head group(PE) & H2O |
| 753.39 | 61.13 | 31 | C39H71O10PNa | - Aziridine & H2O |
| 776.53 | 37.99 | 26 | | |
| 778.47 | 36.05 | 24 | C41H74NO9PNa | -2(H2O) |
| 780.45 | 34.07 | 18 | C41H76NO9PNa | -H2O2 |
| 691.46 | 123.06 | 18 | C39H72O8Na | -Head group (PE) |
| 680.38 | 134.14 | 12 | | |
| 637.48 | 177.04 | 11 | | |
| 735.39 | 79.13 | 10 | C39H69O9PNa | - Aziridine & 2(H2O) |
| 377.30 | 437.22 | 8 | | |
| 666.34 | 148.18 | 8 | | |
| 654.33 | 160.19 | 7 | | |
| 814.54 | -0.02 | 5 | | |
| 668.30 | 146.22 | 4 | | |
| 679.46 | 135.06 | 3 | | |
| 698.43 | 116.09 | 3 | | |
| 611.35 | 203.17 | 3 | | |
| 361.22 | 453.30 | 3 | | |
| 650.38 | 164.14 | 3 | | |
| 737.37 | 77.15 | 3 | | |
| 457.18 | 357.34 | 3 | | |
| 782.42 | 32.10 | 2 | | |
| 779.50 | 35.02 | 2 | | |
| 762.39 | 52.13 | 2 | | |
| 613.31 | 201.21 | 2 | | |
| 622.50 | 192.02 | 2 | | |
| 545.44 | 269.08 | 2 | | |

| Parent (m/z) | 830.51 | | | |
|--------------|------------------|--------------------|----------------|------------------------|
| Adduct | [+Na] | | | |
| ID | PE(18:1,18:1)+O4 | | | |
| Formula | C41H78NO12PNa | | | |
| | Observed | | Identification | |
| Fragment m/z | Neutral loss | Relative Intensity | Formula | Annotation |
| 830.50 | 0.01 | 100 | C41H78NO12PNa | Parent |
| 812.52 | 17.99 | 30 | C41H76NO11PNa | -H2O |
| 787.39 | 43.12 | 27 | C39H73O12PNa | - Aziridine |
| 696.34 | 134.17 | 24 | | |
| 794.46 | 36.05 | 21 | C41H74NO10PNa | -2(H2O) |
| 671.45 | 159.06 | 20 | C39H68O7Na | - Head group(PE) & H2O |
| 653.48 | 177.03 | 19 | | |
| 548.31 | 282.20 | 16 | C23H44NO10PNa | - Oleic acid |
| 682.32 | 148.19 | 13 | | |
| 796.54 | 33.97 | 11 | C41H76NO10PNa | -H2O2 |
| 769.38 | 61.13 | 11 | C39H71O11PNa | - Aziridine & H2O |
| 707.49 | 123.02 | 9 | C39H72O9Na | -Head group (PE) |
| 547.29 | 283.22 | 9 | | |
| 689.27 | 141.24 | 8 | C39H70O8Na | - Head group(PE) |
| 751.43 | 79.08 | 8 | C39H69O10PNa | - Aziridine & 2(H2O) |
| 689.69 | 140.82 | 7 | | |
| 678.42 | 152.09 | 6 | | |
| 664.40 | 166.11 | 6 | | |
| 627.41 | 203.10 | 5 | | |
| 377.31 | 453.20 | 5 | | |
| 786.44 | 44.07 | 5 | | |
| 361.37 | 469.14 | 5 | | |
| 700.34 | 130.17 | 4 | | |
| 534.26 | 296.25 | 4 | | |
| 455.26 | 375.25 | 4 | | |
| 670.33 | 160.18 | 4 | | |
| 637.60 | 192.91 | 3 | | |
| 515.30 | 315.21 | 3 | | |
| 543.43 | 287.08 | 3 | | |
| 778.50 | 52.01 | 3 | | |

All-XIII - Fragmentation patterns from PE(16:0,20:4) and oxidised products thereof in negative ion mode

| Parent (m/z) | 738.50 | | | |
|--------------|---------------|--------------------|----------------|----------------------------|
| Adduct | [-H] | | | |
| ID | PE(16:0,20:4) | | | |
| Formula | C41H73NO8P | | | |
| | Observed | | Identification | |
| Fragment m/z | Neutral loss | Relative Intensity | Formula | Annotation |
| 303.31 | 435.19 | 100 | C20H31O2 | Arachidonic acid anion |
| 255.35 | 483.15 | 53 | C16H31O2 | Palmitic acid anion |
| 452.35 | 286.15 | 24 | C21H43NO7P | -Arachidonic acid (ketene) |
| 259.38 | 479.12 | 10 | | |
| 500.34 | 238.16 | 5 | C25H43NO7P | -Palmitic acid (ketene) |
| 434.36 | 304.14 | 2 | C21H41NO6P | -Arachidonic acid |
| 482.32 | 256.18 | 2 | C25H41NO6P | -Palmitic acid |

| Parent (m/z) | 740.53 | | | |
|--------------|---------------|--------------------|----------------|---------------------|
| Adduct | [+H] | | | |
| ID | PE(16:0,20:4) | | | |
| Formula | C41H75NO8P | | | |
| | Observed | | Identification | |
| Fragment m/z | Neutral loss | Relative Intensity | Formula | Annotation |
| 697.35 | 43.18 | 100 | C39H70O8P | - Aziridine |
| 599.55 | 140.98 | 38 | C39H67O4 | - Head group(PE) |
| 740.64 | -0.11 | 23 | C41H75NO8P | Parent |
| 485.29 | 255.24 | 21 | | - Palmitic acid? |
| 722.26 | 18.27 | 19 | | -H2O? |
| 641.44 | 99.09 | 18 | | |
| 437.21 | 303.32 | 13 | | - Arachidonic acid? |
| 722.63 | 17.90 | 10 | | -H2O? |
| 696.49 | 44.04 | 7 | | |
| 704.51 | 36.02 | 6 | C41H71NO6P | -2(H2O) |
| 484.31 | 256.22 | 5 | | |
| 682.84 | 57.69 | 5 | | |
| 463.32 | 277.21 | 5 | | |
| 708.56 | 31.97 | 5 | | |
| 700.55 | 39.98 | 4 | | |
| 642.48 | 98.05 | 4 | | |
| 479.33 | 261.20 | 4 | | |
| 617.50 | 123.03 | 3 | C39H69O5 | -Head group (PE) |
| 601.52 | 139.01 | 3 | | |
| 617.20 | 123.33 | 3 | | |
| 577.40 | 163.13 | 3 | | |
| 313.21 | 427.32 | 3 | | |
| 711.61 | 28.92 | 3 | | |
| 700.75 | 39.78 | 3 | | |
| 682.33 | 58.20 | 3 | | |
| 679.28 | 61.25 | 3 | | |
| 666.20 | 74.33 | 3 | | |
| 507.23 | 233.30 | 3 | | |
| 704.10 | 36.43 | 2 | | |
| 684.25 | 56.28 | 2 | | |

| Parent (m/z) | 754.50 | | | |
|--------------|-------------------|--------------------|----------------|-------------------------------------|
| Adduct | [-H] | | | |
| ID | PE(16:0;20:4) + O | | | |
| Formula | C41H73NO9P | | | |
| | Observed | | Identification | |
| Fragment m/z | Neutral loss | Relative Intensity | Formula | Annotation |
| 255.33 | 499.17 | 100 | C16H31O2 | Palmitic acid anion |
| 319.29 | 435.21 | 97 | C20H31O3 | Arachidonic acid + O anion |
| 452.37 | 302.13 | 46 | C21H43NO7P | -(Arachidonic acid + O) (ketene) |
| 301.43 | 453.07 | 14 | C20H29O2 | Arachidonic acid + O -H2O anion |
| 498.35 | 256.15 | 9 | C25H41NO7P | -Palmitic acid |
| 516.37 | 238.13 | 8 | C25H43NO8P | -Palmitic acid (ketene) |
| 303.32 | 451.18 | 7 | C20H31O2 | Arachidonic acid anion |
| 736.51 | 17.99 | 6 | C41H71NO8P | -H2O |
| 696.65 | 57.85 | 5 | | |
| 257.46 | 497.04 | 5 | | |
| 391.30 | 363.20 | 5 | | |
| 392.35 | 362.15 | 4 | | |
| 271.36 | 483.14 | 3 | C16H31O3 | Palmitic acid anion +O |
| 434.44 | 320.06 | 2 | C21H41NO6P | -(Arachidonic acid + O) |
| 626.52 | 127.98 | 2 | | |
| 718.10 | 36.40 | 2 | C41H69NO7P | -2(H2O) |
| 722.45 | 32.05 | 2 | | |
| 634.34 | 120.16 | 2 | | |
| 710.53 | 43.97 | 2 | | |
| 256.52 | 497.98 | 2 | | |
| 318.28 | 436.22 | 2 | | |
| 259.33 | 495.17 | 2 | | |
| 304.43 | 450.07 | 2 | | |
| 714.96 | 39.54 | 2 | | |
| 256.18 | 498.32 | 2 | | |
| 737.07 | 17.43 | 2 | | |
| 489.73 | 264.77 | 1 | | |
| 467.59 | 286.91 | 1 | | |
| 467.91 | 286.59 | 1 | | |
| 275.40 | 479.10 | 1 | | |

| Parent (m/z) | 766.50 | | | |
|--------------|---------------|--------------------|----------------|----------------------------|
| Adduct | | | | |
| ID | Parent + (CO) | | | |
| Formula | C42H73NO9P | | | |
| | Observed | | Identification | |
| Fragment m/z | Neutral loss | Relative Intensity | Formula | Annotation |
| 303.30 | 463.20 | 100 | C20H31O2 | Arachidonic acid anion |
| 255.32 | 511.18 | 55 | C16H31O2 | Palmitic acid anion |
| 480.35 | 286.15 | 22 | C22H43NO8P | -Arachidonic acid (ketene) |
| 259.33 | 507.17 | 10 | | |
| 510.34 | 256.16 | 10 | C26H41NO7P | -Palmitic acid |
| 391.39 | 375.11 | 4 | | |
| 462.34 | 304.16 | 3 | C22H41NO7P | -Arachidonic acid |
| 439.39 | 327.11 | 3 | | |
| 528.50 | 238.00 | 2 | C26H43NO8P | -Palmitic acid (ketene) |
| 748.51 | 17.99 | 1 | C42H71NO8P | -H2O |
| 356.30 | 410.20 | 1 | | |

| Parent (m/z) | 770.49 | | | |
|--------------|--------------------|--------------------|----------------|-----------------------------------|
| Adduct | [-H] | | | |
| ID | PE(16:0;20:4) + O2 | | | |
| Formula | C41H73NO10P | | | |
| | Observed | | Identification | |
| Fragment m/z | Neutral loss | Relative Intensity | Formula | Annotation |
| 255.31 | 515.18 | 100 | C16H31O2 | Palmitic acid anion |
| 335.28 | 435.21 | 58 | C20H31O4 | Arachidonic acid + O2 anion |
| 452.34 | 318.15 | 46 | C21H43NO7P | -(Arachidonic acid + O2) (ketene) |
| 317.31 | 453.18 | 17 | C20H29O3 | Arachidonic acid + O2 - H2O anion |
| 532.38 | 238.11 | 13 | C25H43NO9P | -Palmitic acid (ketene) |
| 281.36 | 489.13 | 12 | | |
| 752.52 | 17.97 | 10 | C41H71NO9P | -H2O |
| 273.35 | 497.14 | 8 | | |
| 514.47 | 256.02 | 5 | C25H41NO8P | -Palmitic acid |
| 303.33 | 467.16 | 5 | C20H31O2 | Arachidonic acid anion |
| 391.39 | 379.10 | 5 | | |
| 734.39 | 36.10 | 4 | C41H69NO8P | -2(H2O) |
| 257.30 | 513.19 | 4 | | |
| 256.44 | 514.05 | 3 | | |
| 738.66 | 31.83 | 3 | | |
| 656.32 | 114.17 | 3 | | |
| 434.44 | 336.05 | 2 | | |
| 295.32 | 475.17 | 2 | | |
| 287.36 | 483.13 | 2 | | |
| 283.30 | 487.19 | 2 | | |
| 304.34 | 466.15 | 2 | | |
| 291.45 | 479.04 | 2 | | |
| 299.30 | 471.19 | 2 | | |
| 305.34 | 465.15 | 2 | | |
| 289.30 | 481.19 | 1 | | |
| 501.83 | 268.66 | 1 | | |
| 235.37 | 535.12 | 1 | | |
| 334.40 | 436.09 | 1 | | |
| 732.30 | 38.19 | 1 | | |
| 506.45 | 264.04 | 1 | | |

| Parent (m/z) | 780.51 | | | |
|--------------|--------------|--------------------|--|-----------------------------|
| Adduct | | | | |
| ID | Unknown | | | |
| Formula | | | | |
| | Observed | Identification | | |
| Fragment m/z | Neutral loss | Relative Intensity | Formula | Annotation |
| 303.32 | 477.19 | 100 | C ₂₀ H ₃₁ O ₂ | Arachidonic acid anion |
| 255.34 | 525.17 | 81 | C ₁₆ H ₃₁ O ₂ | Palmitic acid anion |
| 494.35 | 286.16 | 33 | | - Arachidonic acid (ketene) |
| 259.39 | 521.12 | 14 | | |
| 524.32 | 256.19 | 11 | | -Palmitic acid |
| 762.35 | 18.16 | 10 | | -H ₂ O |
| 542.42 | 238.09 | 8 | | -Palmitic acid (ketene) |
| 744.40 | 36.11 | 7 | | -2(H ₂ O) |
| 391.33 | 389.18 | 5 | | |
| 762.71 | 17.80 | 5 | | |
| 452.31 | 328.20 | 4 | | |
| 476.41 | 304.10 | 4 | | - Arachidonic acid |
| 317.38 | 463.13 | 4 | | |
| 388.39 | 392.12 | 3 | | |
| 439.39 | 341.12 | 3 | | |
| 748.29 | 32.22 | 2 | | |
| 761.48 | 19.03 | 2 | | |
| 669.38 | 111.13 | 2 | | |
| 736.44 | 44.07 | 2 | | |
| 345.45 | 435.06 | 2 | | |
| 660.48 | 120.03 | 1 | | |
| 480.44 | 300.07 | 1 | | |
| 636.52 | 143.99 | 1 | | |
| 299.23 | 481.28 | 1 | | |
| 697.74 | 82.77 | 1 | | |
| 505.95 | 274.56 | 1 | | |
| 743.85 | 36.66 | 1 | | |
| 541.54 | 238.97 | 1 | | |
| 680.16 | 100.35 | 1 | | |

| Parent (m/z) | 784.47 | | | |
|--------------|----------------------|--------------------|----------------|---|
| Adduct | [-H] | | | |
| ID | PE(16:0;20:4)+O4-H2O | | | |
| Formula | C41H71NO11P | | | |
| | Observed | | Identification | |
| Fragment m/z | Neutral loss | Relative Intensity | Formula | Annotation |
| 255.31 | 529.16 | 100 | C16H31O2 | Palmitic acid anion |
| 766.43 | 18.04 | 53 | C41H69NO10P | -H2O |
| 452.33 | 332.14 | 41 | C21H43NO7P | -(Arachidonic acid + O4 - H2O) (ketene) |
| 349.32 | 435.15 | 29 | C20H29O5 | Arachidonic acid + O4 - H2O anion |
| 331.29 | 453.18 | 23 | C20H27O4 | Arachidonic acid + O4 - 2(H2O) anion |
| 528.35 | 256.12 | 17 | C25H39NO9P | -Palmitic acid |
| 391.31 | 393.16 | 13 | | |
| 546.35 | 238.12 | 11 | C25H41NO10P | -Palmitic acid (ketene) |
| 256.38 | 528.09 | 11 | | |
| 313.29 | 471.18 | 9 | C20H25O3 | Arachidonic acid + O4 - 3(H2O) anion |
| 303.26 | 481.21 | 9 | C20H31O2 | Arachidonic acid anion |
| 304.36 | 480.11 | 8 | | |
| 287.31 | 497.16 | 7 | | |
| 765.46 | 19.01 | 7 | | |
| 269.32 | 515.15 | 5 | | |
| 303.51 | 480.96 | 5 | | |
| 319.32 | 465.15 | 4 | | |
| 305.30 | 479.17 | 4 | | |
| 748.16 | 36.31 | 4 | C41H67NO9P | -2(H2O) |
| 497.33 | 287.14 | 3 | | |
| 588.50 | 195.97 | 3 | | |
| 684.45 | 100.02 | 3 | | |
| 295.33 | 489.14 | 3 | | |
| 434.45 | 350.02 | 3 | | |
| 496.51 | 287.96 | 3 | | |
| 748.44 | 36.03 | 3 | | |
| 303.96 | 480.51 | 3 | | |
| 259.43 | 525.04 | 3 | | |
| 392.42 | 392.05 | 3 | | |
| 320.50 | 463.97 | 2 | | |

| Parent (m/z) | 786.49 | | | |
|--------------|--------------------|--------------------|----------------|--------------------------------------|
| Adduct | [-H] | | | |
| ID | PE(16:0;20:4) + O3 | | | |
| Formula | C41H73NO11P | | | |
| | Observed | | Identification | |
| Fragment m/z | Neutral loss | Relative Intensity | Formula | Annotation |
| 255.33 | 531.16 | 100 | C16H31O2 | Palmitic acid anion |
| 768.47 | 18.02 | 82 | C41H71NO10P | -H2O |
| 351.31 | 435.18 | 55 | C20H31O5 | Arachidonic acid + O3 anion |
| 452.38 | 334.11 | 51 | C21H43NO7P | -(Arachidonic acid + O3) (ketene) |
| 315.29 | 471.20 | 25 | C20H27O3 | Arachidonic acid + O3 - 2(H2O) anion |
| 333.30 | 453.19 | 19 | C20H29O4 | Arachidonic acid + O3 - H2O anion |
| 530.30 | 256.19 | 12 | C25H41NO9P | -Palmitic acid |
| 548.35 | 238.14 | 12 | C25H43NO10P | -Palmitic acid (ketene) |
| 271.32 | 515.17 | 10 | C16H31O3 | Palmitic acid anion +O |
| 297.32 | 489.17 | 4 | C20H25O2 | Arachidonic acid + O3 - 3(H2O) anion |
| 512.36 | 274.13 | 4 | | |
| 289.29 | 497.20 | 4 | | |
| 750.67 | 35.82 | 3 | C41H69NO9P | -2(H2O) |
| 295.35 | 491.14 | 3 | | |
| 434.32 | 352.17 | 3 | C21H41NO6P | -(Arachidonic acid + O3) |
| 256.35 | 530.14 | 3 | | |
| 281.36 | 505.13 | 2 | | |
| 303.35 | 483.14 | 2 | C20H31O2 | Arachidonic acid anion |
| 283.38 | 503.11 | 2 | | |
| 487.34 | 299.15 | 2 | | |
| 391.38 | 395.11 | 1 | | |
| 742.68 | 43.81 | 1 | | |
| 332.36 | 454.13 | 1 | | |

| Parent (m/z) | 800.46 | | | | |
|--------------|----------------------|--------------------|-------------|---|--|
| Adduct | [-H] | | | | |
| ID | PE(16:0;20:4)+O5-H2O | | | | |
| Formula | C41H71NO12P | | | | |
| | Observed | | | Identification | |
| Fragment m/z | Neutral loss | Relative Intensity | Formula | Annotation | |
| 782.45 | 18.01 | 100 | C41H69NO11P | -H2O | |
| 255.33 | 545.13 | 83 | C16H31O2 | Palmitic acid anion | |
| 452.36 | 348.10 | 44 | C21H43NO7P | -(Arachidonic acid + O5 - H2O) (ketene) | |
| 544.31 | 256.15 | 35 | C25H39NO10P | -Palmitic acid | |
| 365.30 | 435.16 | 21 | C20H29O6 | Arachidonic acid + O5 - H2O | |
| 347.31 | 453.15 | 18 | C20H27O5 | Arachidonic acid + O5 - 2(H2O) | |
| 329.29 | 471.17 | 14 | C20H25O4 | Arachidonic acid + O5 - 3(H2O) | |
| 781.53 | 18.93 | 14 | | | |
| 562.45 | 238.01 | 8 | C25H41NO11P | -Palmitic acid (ketene) | |
| 391.46 | 409.00 | 8 | | | |
| 764.54 | 35.92 | 7 | C41H67NO10P | -2(H2O) | |
| 526.32 | 274.14 | 7 | | | |
| 285.27 | 515.19 | 7 | | | |
| 256.35 | 544.11 | 6 | | | |
| 700.34 | 100.12 | 5 | | | |
| 764.12 | 36.34 | 5 | | | |
| 602.61 | 197.85 | 5 | | | |
| 434.35 | 366.11 | 4 | | | |
| 543.44 | 257.02 | 4 | | | |
| 756.61 | 43.85 | 4 | | | |
| 640.47 | 159.99 | 3 | | | |
| 281.36 | 519.10 | 3 | | | |
| 335.32 | 465.14 | 3 | | | |
| 566.52 | 233.94 | 3 | | | |
| 336.42 | 464.04 | 3 | | | |
| 488.30 | 312.16 | 3 | | | |
| 303.39 | 497.07 | 3 | | | |
| 618.25 | 182.21 | 3 | | | |
| 767.49 | 32.97 | 3 | | | |
| 295.34 | 505.12 | 3 | | | |

| Parent (m/z) | 802.48 | | | |
|--------------|--------------------|--------------------|----------------|--------------------------------------|
| Adduct | [-H] | | | |
| ID | PE(16:0;20:4) + O4 | | | |
| Formula | C41H73NO12P | | | |
| | Observed | | Identification | |
| Fragment m/z | Neutral loss | Relative Intensity | Formula | Annotation |
| 784.50 | 17.98 | 100 | C41H71NO11P | -H2O |
| 367.29 | 435.19 | 73 | C20H31O6 | Arachidonic acid + O4 anion |
| 255.33 | 547.15 | 68 | C16H31O2 | Palmitic acid anion |
| 546.33 | 256.15 | 53 | C25H41NO10P | -Palmitic acid |
| 452.36 | 350.12 | 50 | C21H43NO7P | -(Arachidonic acid + O4) (ketene) |
| 349.29 | 453.19 | 16 | C20H29O5 | Arachidonic acid + O4 - H2O anion |
| 305.29 | 497.19 | 15 | | |
| 503.26 | 299.22 | 14 | | |
| 331.28 | 471.20 | 12 | C20H27O4 | Arachidonic acid + O4 - 2(H2O) anion |
| 564.33 | 238.15 | 11 | C25H43NO11P | -Palmitic acid (ketene) |
| 740.43 | 62.05 | 9 | | |
| 676.44 | 126.04 | 9 | | |
| 528.29 | 274.19 | 8 | | |
| 245.29 | 557.19 | 8 | | |
| 289.31 | 513.17 | 7 | | |
| 391.31 | 411.17 | 6 | | |
| 287.29 | 515.19 | 6 | | |
| 766.48 | 36.00 | 5 | C41H69NO10P | -2(H2O) |
| 410.32 | 392.16 | 5 | | |
| 636.44 | 166.04 | 4 | | |
| 742.66 | 59.82 | 4 | | |
| 313.27 | 489.21 | 4 | C20H25O3 | Arachidonic acid + O3 - 3(H2O) anion |
| 576.32 | 226.16 | 4 | | |
| 261.32 | 541.16 | 3 | | |
| 434.36 | 368.12 | 3 | | |
| 269.32 | 533.16 | 2 | | |
| 759.49 | 42.99 | 2 | | |
| 758.36 | 44.12 | 2 | | |
| 256.31 | 546.17 | 2 | | |
| 658.55 | 143.93 | 2 | | |

| Parent (m/z) | 804.50 | | | |
|--------------|--------------|--------------------|----------------|--------------------------------------|
| Adduct | | | | |
| ID | Unknown | | | |
| Formula | | | | |
| | Observed | | Identification | |
| Fragment m/z | Neutral loss | Relative Intensity | Formula | Annotation |
| 369.31 | 435.19 | 100 | | Arachidonic acid + 66 |
| 255.35 | 549.15 | 54 | C16H31O2 | Palmitic acid anion |
| 786.43 | 18.07 | 28 | | -H2O |
| 452.38 | 352.12 | 27 | | -(Arachidonic acid + 66) (ketene) |
| 548.33 | 256.17 | 13 | | -Palmitic acid |
| 566.38 | 238.12 | 7 | | -Palmitic acid (ketene) |
| 368.32 | 436.18 | 5 | | |
| 256.29 | 548.21 | 4 | | |
| 367.28 | 437.22 | 4 | | |
| 768.36 | 36.14 | 4 | | -2(H2O) |
| 351.31 | 453.19 | 3 | | Arachidonic acid + 66 - H2O |
| 453.34 | 351.16 | 3 | | |
| 505.32 | 299.18 | 3 | | |
| 434.34 | 370.16 | 2 | | -(Arachidonic acid + 66) |
| 772.49 | 32.01 | 2 | | |
| 760.45 | 44.05 | 2 | | |
| 766.34 | 38.16 | 2 | | |
| 785.56 | 18.94 | 2 | | |
| 547.28 | 257.22 | 1 | | |
| 325.35 | 479.15 | 1 | | |
| 454.45 | 350.05 | 1 | | |
| 547.55 | 256.95 | 1 | | |
| 307.27 | 497.23 | 1 | | |
| 530.28 | 274.22 | 1 | | |
| 684.57 | 119.93 | 1 | | |
| 245.27 | 559.23 | 1 | | |
| 690.71 | 113.79 | 1 | | |
| 676.40 | 128.10 | 1 | | |

All-XIV - Fragmentation patterns from PE(16:0,20:4) and oxidised products thereof in positive ion mode

| Parent (m/z) | 762.50 | | | |
|--------------|---------------|--------------------|----------------|-----------------------------|
| Adduct | [+Na] | | | |
| ID | PE(16:0,20:4) | | | |
| Formula | C41H74NO8PNa | | | |
| | Observed | | Identification | |
| Fragment m/z | Neutral loss | Relative Intensity | Formula | Annotation |
| 719.38 | 43.12 | 100 | C39H69O8PNa | - Aziridine |
| 621.49 | 141.01 | 51 | C39H66O4Na | - Head group(PE) |
| 639.50 | 123.00 | 4 | C39H68O5Na | -Head group (PE) |
| 463.29 | 299.21 | 1 | C23H37O6PNa | - Palmitic acid & aziridine |
| 599.49 | 163.01 | 1 | C39H67O4 | - Sodiated head group |

| Parent (m/z) | 776.48 | | | |
|--------------|--------------------------|--------------------|----------------|------------------|
| Adduct | [+Na] | | | |
| ID | PE(16:0,20:4) + O2 - H2O | | | |
| Formula | C41H72NO9PNa | | | |
| | Observed | | Identification | |
| Fragment m/z | Neutral loss | Relative Intensity | Formula | Annotation |
| 733.37 | 43.11 | 100 | C39H67O9PNa | - Aziridine |
| 635.49 | 140.99 | 42 | C39H64O5Na | - Head group(PE) |
| 520.24 | 256.24 | 18 | | |
| 758.59 | 17.89 | 16 | C41H70NO8PNa | -H2O? |
| 653.55 | 122.93 | 9 | C39H66O6Na | -Head group (PE) |
| 601.31 | 175.17 | 6 | | |
| 776.69 | -0.21 | 4 | | |
| 455.19 | 321.29 | 3 | | |
| 437.12 | 339.36 | 2 | | |
| 480.24 | 296.24 | 2 | | |
| 732.37 | 44.11 | 2 | | |
| 656.27 | 120.21 | 2 | | |
| 341.28 | 435.20 | 2 | | |
| 477.27 | 299.21 | 1 | | |
| 576.41 | 200.07 | 1 | | |
| 437.44 | 339.04 | 1 | | |
| 678.45 | 98.03 | 1 | | |
| 747.03 | 29.45 | 1 | | |
| 548.37 | 228.11 | 1 | | |

| Parent (m/z) | 828.50 | | | |
|--------------|--------------|--------------------|----------------|------------------------|
| Adduct | | | | |
| ID | Unknown | | | |
| Formula | | | | |
| | Observed | | Identification | |
| Fragment m/z | Neutral loss | Relative Intensity | Formula | Annotation |
| 785.41 | 43.09 | 100 | | - Aziridine |
| 687.46 | 141.04 | 54 | | - Head group(PE) |
| 572.28 | 256.22 | 35 | | |
| 810.44 | 18.06 | 34 | | -H2O |
| 705.49 | 123.01 | 20 | | -Head group (PE) |
| 767.58 | 60.92 | 12 | | - Aziridine & H2O |
| 792.42 | 36.08 | 5 | | -2(H2O) |
| 784.57 | 43.93 | 3 | | |
| 393.19 | 435.31 | 3 | | |
| 437.19 | 391.31 | 3 | | |
| 731.37 | 97.13 | 3 | | |
| 770.82 | 57.68 | 2 | | |
| 508.36 | 320.14 | 2 | | |
| 774.34 | 54.16 | 2 | | -3(H2O) |
| 524.30 | 304.20 | 2 | | |
| 437.43 | 391.07 | 2 | | |
| 507.32 | 321.18 | 2 | | |
| 365.16 | 463.34 | 2 | | |
| 669.74 | 158.76 | 2 | | |
| 550.40 | 278.10 | 2 | | |
| 749.11 | 79.39 | 2 | | - Aziridine & 2(H2O) |
| 743.35 | 85.15 | 1 | | |
| 728.40 | 100.10 | 1 | | |
| 415.22 | 413.28 | 1 | | |
| 480.37 | 348.13 | 1 | | |
| 669.30 | 159.20 | 1 | | - Head group(PE) & H2O |
| 792.80 | 35.70 | 1 | | |
| 828.51 | -0.01 | 1 | | |
| 529.33 | 299.17 | 1 | | |
| 433.23 | 395.27 | 1 | | |

| Parent (m/z) | 778.47 | | | | |
|--------------|--------------------------|--------------------|--------------|------------------------|--|
| Adduct | [+Na] | | | | |
| ID | PE(16:0,20:4) + O & [K]+ | | | | |
| Formula | C41H74NO9PNa | | | | |
| | Observed | | | Identification | |
| Fragment m/z | Neutral loss | Relative Intensity | Formula | Annotation | |
| 735.39 | 43.08 | 100 | C39H69O9PNa | - Aziridine | |
| 637.46 | 141.01 | 35 | C39H66O5Na | - Head group(PE) | |
| 760.40 | 18.07 | 13 | C41H72NO8PNa | -H2O | |
| 655.51 | 122.96 | 9 | C39H68O6Na | -Head group (PE) | |
| 717.38 | 61.09 | 6 | C39H67O8PNa | - Aziridine & H2O | |
| 778.63 | -0.16 | 5 | C41H74NO9PNa | Parent | |
| 619.52 | 158.95 | 2 | C39H64O4Na | - Head group(PE) & H2O | |

| Parent (m/z) | 792.48 | | | |
|--------------|--------------------------|--------------------|----------------|-------------------|
| Adduct | [+Na] | | | |
| ID | PE(16:0,20:4) + O3 - H2O | | | |
| Formula | C41H72NO10PNa | | | |
| | Observed | | Identification | |
| Fragment m/z | Neutral loss | Relative Intensity | Formula | Annotation |
| 749.40 | 43.08 | 100 | C39H67O10PNa | - Aziridine |
| 651.43 | 141.05 | 44 | C39H64O6Na | - Head group(PE) |
| 774.58 | 17.90 | 29 | C41H70NO9PNa | -H2O |
| 791.64 | 0.84 | 27 | | |
| 536.24 | 256.24 | 25 | | |
| 669.44 | 123.04 | 16 | C39H66O7Na | -Head group (PE) |
| 731.49 | 60.99 | 13 | C39H65O9PNa | - Aziridine & H2O |
| 792.52 | -0.04 | 10 | | |
| 760.43 | 32.05 | 8 | | |
| 756.42 | 36.06 | 4 | C41H68NO8PNa | -2(H2O) |
| 690.67 | 101.81 | 4 | | |
| 762.79 | 29.69 | 4 | | |
| 777.56 | 14.92 | 4 | | |
| 507.35 | 285.13 | 4 | | |
| 734.63 | 57.85 | 3 | | |
| 792.85 | -0.37 | 3 | | |
| 480.38 | 312.10 | 3 | | |
| 748.39 | 44.09 | 3 | | |
| 437.50 | 354.98 | 3 | | |
| 736.66 | 55.82 | 3 | | |
| 718.72 | 73.76 | 3 | | |
| 508.50 | 283.98 | 2 | | |
| 672.36 | 120.12 | 2 | | |
| 493.31 | 299.17 | 2 | | |
| 471.22 | 321.26 | 2 | | |
| 733.93 | 58.55 | 2 | | |
| 692.46 | 100.02 | 2 | | |
| 617.22 | 175.26 | 2 | | |
| 668.97 | 123.51 | 2 | | |
| 723.96 | 68.52 | 2 | | |

| Parent (m/z) | 808.47 | | | |
|--------------|--------------------------|--------------------|----------------|------------------------|
| Adduct | [+Na] | | | |
| ID | PE(16:0,20:4) + O4 - H2O | | | |
| Formula | C41H72NO11PNa | | | |
| | Observed | | Identification | |
| Fragment m/z | Neutral loss | Relative Intensity | Formula | Annotation |
| 765.39 | 43.08 | 100 | C39H67O11PNa | - Aziridine |
| 667.47 | 141.00 | 43 | C39H64O7Na | - Head group(PE) |
| 790.40 | 18.07 | 33 | C41H70NO10PNa | -H2O |
| 685.48 | 122.99 | 16 | C39H66O8Na | -Head group (PE) |
| 807.60 | 0.87 | 16 | | |
| 764.42 | 44.05 | 10 | | |
| 747.38 | 61.09 | 10 | C39H65O10PNa | - Aziridine & H2O |
| 772.39 | 36.08 | 10 | C41H68NO9PNa | -2(H2O) |
| 552.31 | 256.16 | 5 | | |
| 808.68 | -0.21 | 5 | | |
| 649.46 | 159.01 | 4 | C39H62O6Na | - Head group(PE) & H2O |
| 551.37 | 257.10 | 3 | | |
| 729.43 | 79.04 | 3 | C39H63O9PNa | - Aziridine & 2(H2O) |
| 776.45 | 32.02 | 1 | | |
| 710.44 | 98.03 | 1 | | |
| 437.40 | 371.07 | 1 | | |
| 626.42 | 182.05 | 1 | | |

| Parent (m/z) | 810.49 | | | |
|--------------|--------------------|--------------------|----------------|------------------------|
| Adduct | [+Na] | | | |
| ID | PE(16:0,20:4) + O3 | | | |
| Formula | C41H74NO11PNa | | | |
| | Observed | | Identification | |
| Fragment m/z | Neutral loss | Relative Intensity | Formula | Annotation |
| 767.40 | 43.09 | 100 | C39H69O11PNa | - Aziridine |
| 669.49 | 141.00 | 49 | C39H66O7Na | - Head group(PE) |
| 687.49 | 123.00 | 18 | C39H68O8Na | -Head group (PE) |
| 792.39 | 18.10 | 14 | C41H72NO10PNa | -H2O |
| 749.36 | 61.13 | 14 | C39H67O10PNa | - Aziridine & H2O |
| 774.39 | 36.10 | 7 | C41H70NO9PNa | -2(H2O) |
| 766.38 | 44.11 | 3 | | |
| 651.47 | 159.02 | 3 | C39H64O6Na | - Head group(PE) & H2O |
| 731.39 | 79.10 | 3 | C39H65O9PNa | - Aziridine & 2(H2O) |
| 633.44 | 177.05 | 2 | | |
| 668.44 | 142.05 | 1 | | |
| 554.25 | 256.24 | 1 | | |

| Parent (m/z) | 826.48 | | | |
|--------------|--------------------|--------------------|----------------|------------------------|
| Adduct | [+Na] | | | |
| ID | PE(16:0,20:4) + O4 | | | |
| Formula | C41H74NO12PNa | | | |
| | Observed | | Identification | |
| Fragment m/z | Neutral loss | Relative Intensity | Formula | Annotation |
| 783.41 | 43.07 | 100 | C39H69O12PNa | - Aziridine |
| 685.47 | 141.01 | 42 | C39H66O8Na | - Head group(PE) |
| 808.45 | 18.03 | 34 | C41H72NO11PNa | -H2O |
| 570.26 | 256.22 | 29 | | |
| 703.51 | 122.97 | 22 | C39H68O9Na | -Head group (PE) |
| 765.38 | 61.10 | 13 | C39H67O11PNa | - Aziridine & H2O |
| 790.46 | 36.02 | 9 | C41H70NO10PNa | -2(H2O) |
| 522.28 | 304.20 | 7 | | |
| 463.29 | 363.19 | 6 | | |
| 415.25 | 411.23 | 5 | | |
| 826.84 | -0.36 | 4 | | |
| 772.43 | 54.05 | 4 | C41H68NO9PNa | -3(H2O) |
| 741.68 | 84.80 | 3 | | |
| 437.20 | 389.28 | 3 | | |
| 616.79 | 209.69 | 2 | | |
| 825.89 | 0.59 | 2 | | |
| 667.44 | 159.04 | 2 | C39H64O7Na | - Head group(PE) & H2O |
| 728.49 | 97.99 | 2 | | |
| 747.26 | 79.22 | 2 | C39H65O10PNa | - Aziridine & 2(H2O) |
| 729.39 | 97.09 | 2 | C39H63O9PNa | - Aziridine & 3(H2O) |
| 800.40 | 26.08 | 2 | | |
| 391.32 | 435.16 | 1 | | |
| 747.58 | 78.90 | 1 | | |
| 434.27 | 392.21 | 1 | | |
| 437.54 | 388.94 | 1 | | |
| 508.34 | 318.14 | 1 | | |
| 814.33 | 12.15 | 1 | | |

All - Baseline lipidome of *D. magna*

* Indicates confirmation of structure based on bulk fragmentation conducted by Dr. A Southam. For more information see chapter 4.

Where masses are missing they relate to the same mass as the mass in the above row

| Theoretical mass (m/z) | | Identification | | |
|------------------------|-----------|----------------|-----------|-----------------------|
| Ion Form | Neutral | Ion form | Headgroup | Annotation |
| 436.28335 | 437.29063 | [M-H]- | PE | LPE(P-16:0e) |
| 450.26262 | 451.26989 | [M-H]- | PE | LPE(16:1) |
| 452.27827 | 393.26441 | [M-H]- | PE | LPE(16:0) |
| 466.33030 | 467.33758 | [M-H]- | PE | LPE(O-18:0) |
| 474.26262 | 475.26989 | [M-H]- | PE | LPE(18:3) |
| 476.27827 | 477.28554 | [M-H]- | PE | LPE(18:2) |
| 478.29392 | 479.30119 | [M-H]- | PE | LPE(18:1) |
| 479.31432 | 480.32159 | [M-H]- | PA | LPA(21:0,0:0) |
| 480.30957 | 481.31684 | [M-H]- | PE | LPE(18:0) |
| 492.34595 | 493.35323 | [M-H]- | PE | LPE(P-20:0) |
| 495.30923 | 496.31651 | [M-H]- | PG | LPG(P-18:0) |
| 498.26262 | 499.26989 | [M-H]- | PE | LPE(20:5) |
| 500.27827 | 501.28554 | [M-H]- | PE | LPE(20:4) |
| 502.29392 | 503.30119 | [M-H]- | PE | LPE(20:3) |
| 504.30957 | 505.31684 | [M-H]- | PE | LPE(20:2) |
| 509.32488 | 450.31103 | [M+Ac]- | PA | LPA(P-20:0,0:0) |
| 554.34635 | 495.33249 | [M+Ac]- | PC | LPC(16:0)* |
| | | [M+Ac]- | PE | LPE(19:0) |
| 562.31505 | 503.30119 | [M+Ac]- | PE | LPE(20:3) |
| 564.33070 | 505.31684 | [M+Ac]- | PE | LPE(20:2) |
| | | [M+Ac]- | PC | LPC(17:2) |
| 576.33070 | 517.31684 | [M+Ac]- | PC | LPC(18:3)* |
| | | [M-H]- | PS | LPS(22:2)* |
| 578.34635 | 519.33249 | [M+Ac]- | PC | LPC(18:2)* |
| | | [M-H]- | PS | LPS(22:1) |
| 580.36200 | 521.34814 | [M+Ac]- | PC | LPC(18:1)* |
| | | [M-H]- | PS | LPS(22:0) |
| 684.46098 | 685.46826 | [M-H]- | PE | PE(32:3) |
| 686.47663 | 687.48391 | [M-H]- | PE | PE(32:2) |
| 688.49228 | 689.49956 | [M-H]- | PE | PE(32:1) |
| 694.48172 | 695.48899 | [M-H]- | PE | PE(P-34:4) |
| 696.46098 | 697.46826 | [M-H]- | PE | PE(33:4) |
| 696.49737 | 697.50464 | [M-H]- | PE | PE(P-34:3)/PE(O-34:4) |
| 697.40861 | 638.39476 | [M+Ac]- | PA | PA(32:5) |
| 698.51302 | 699.52029 | [M-H]- | PE | PE(P-34:2)/PE(O-34:3) |
| 700.52867 | 701.53594 | [M-H]- | PE | PE(P-34:1)/PE(O-34:2) |
| 709.48138 | 710.48866 | [M-H]- | PA | PA(37:4) |
| 710.47663 | 711.48391 | [M-H]- | PE | PE(34:4) |
| 712.49228 | 713.49956 | [M-H]- | PE | PE(34:3) |
| 714.50793 | 715.51521 | [M-H]- | PE | PE(34:2) |
| 716.52358 | 717.53086 | [M-H]- | PE | PE(34:1) |

| | | | | |
|-----------|-----------|---------|----|-----------------------|
| 717.47121 | 658.45736 | [M+Ac]- | PA | PA(33:2) |
| | | [M-H]- | PG | PG(32:2) |
| 718.53923 | 719.54651 | [M-H]- | PE | PE(34:0) |
| 719.48686 | 660.47301 | [M+Ac]- | PA | PA(33:1) |
| | | [M-H]- | PG | PG(32:1) |
| 720.49737 | 721.50464 | [M-H]- | PE | PE(P-36:5) |
| 721.48138 | 722.48866 | [M-H]- | PA | PA(38:5) |
| 721.50251 | 662.48866 | [M+Ac]- | PA | PA(33:0) |
| | | [M-H]- | PG | PG(32:0) |
| 722.51302 | 723.52029 | [M-H]- | PE | PE(P-36:4)/PE(O-36:5) |
| 723.49703 | 724.50431 | [M-H]- | PA | PA(38:4) |
| 724.49228 | 725.49956 | [M-H]- | PE | PE(35:4) |
| 724.52867 | 725.53594 | [M-H]- | PE | PE(P-36:3)/PE(O-36:4) |
| 726.50793 | 727.51521 | [M-H]- | PE | PE(35:3) |
| 726.54432 | 727.55159 | [M-H]- | PE | PE(P-36:2)/PE(O-36:3) |
| 728.52358 | 729.53086 | [M-H]- | PE | PE(35:2) |
| 728.55997 | 729.56724 | [M-H]- | PE | PE(P-36:1)/PE(O-36:2) |
| 730.53923 | 731.54651 | [M-H]- | PE | PE(35:1) |
| 730.57562 | 731.58289 | [M-H]- | PE | PE(P-36:0)/PE(O-36:1) |
| 733.50251 | 674.48866 | [M+Ac]- | PA | PA(34:1) |
| | | [M-H]- | PG | PG(33:1) |
| 734.47663 | 735.48391 | [M-H]- | PE | PE(36:6) |
| 735.48178 | 676.46792 | [M+Ac]- | PG | PG(P-30:1) |
| 736.47703 | 677.46317 | [M+Ac]- | PS | PS(P-29:0) |
| 736.49228 | 737.49956 | [M-H]- | PE | PE(36:5) |
| 736.51341 | 677.49956 | [M+Ac]- | PC | PC(28:0) |
| | | [M+Ac]- | PE | PE(31:0) |
| 737.49743 | 678.48357 | [M+Ac]- | PG | PG(P-30:0)/PG(O-30:1) |
| 738.49268 | 679.47882 | [M+Ac]- | PS | PS(O-29:0) |
| 738.50793 | 739.51521 | [M-H]- | PE | PE(36:4) |
| 739.51308 | 680.49922 | [M+Ac]- | PG | PG(O-30:0) |
| 740.52358 | 741.53086 | [M-H]- | PE | PE(36:3) |
| 741.47121 | 682.45736 | [M+Ac]- | PA | PA(35:4) |
| | | [M-H]- | PG | PG(34:4) |
| 741.54398 | 742.55126 | [M-H]- | PA | PA(39:2) |
| 742.53923 | 683.52538 | [M-H]- | PE | PE(36:2) |
| 743.48686 | 684.47301 | [M+Ac]- | PA | PA(35:3) |
| | | [M-H]- | PG | PG(34:3) |
| 744.55488 | 745.56216 | [M-H]- | PE | PE(36:1) |
| 745.50251 | 686.48866 | [M-H]- | PA | LBPA(34:2) |
| | | [M-H]- | PG | PG(34:2) |
| | | [M+Ac]- | PA | PA(35:2) |
| 747.51816 | 688.50431 | [M-H]- | PA | LBPA(34:1) |
| | | [M-H]- | PG | PG(34:1) |
| | | [M+Ac]- | PA | PA(35:1) |
| 748.49228 | 749.49956 | [M-H]- | PE | PE(37:6) |
| 749.53381 | 690.51996 | [M+Ac]- | PA | PA(35:0) |
| | | [M-H]- | PG | PG(34:0) |

| | | | | |
|-----------|-----------|---------|----|-----------------------|
| 750.50793 | 751.51521 | [M-H]- | PE | PE(37:5) |
| 750.54432 | 751.55159 | [M-H]- | PE | PE(P-38:4)/PE(O-38:5) |
| 751.51308 | 692.49922 | [M+Ac]- | PG | PG(P-31:0)/PG(O-31:1) |
| 752.52358 | 753.53086 | [M-H]- | PE | PE(37:4) |
| 752.55997 | 753.56724 | [M-H]- | PE | PE(P-38:3)/PE(O-38:4) |
| 754.50285 | 695.48899 | [M+Ac]- | PE | PE(P-34:4) |
| 754.53923 | 755.54651 | [M-H]- | PE | PE(37:3) |
| 754.57562 | 755.58289 | [M-H]- | PE | PE(P-38:2)/PE(O-38:3) |
| 756.48211 | 697.46826 | [M+Ac]- | PE | PE(33:4) |
| | | [M+Ac]- | PC | PC(30:4) |
| | | [M-H]- | PS | PS(34:3) |
| 756.51850 | 697.50464 | [M-H]- | PS | PS(P-35:2) |
| | | [M+Ac]- | PE | PE(P-34:3)/PE(O-34:4) |
| 756.55488 | 757.56216 | [M-H]- | PE | PE(37:2) |
| 756.59127 | 757.59854 | [M-H]- | PE | PE(P-38:1)/PE(O-38:2) |
| 758.47663 | 759.48391 | [M-H]- | PE | PE(38:8) |
| 758.57053 | 759.57781 | [M-H]- | PE | PE(37:1) |
| 758.60692 | 759.61419 | [M-H]- | PE | PE(P-38:0)/PE(O-38:1) |
| 760.49228 | 761.49956 | [M-H]- | PE | PE(38:7) |
| 762.50793 | 763.51521 | [M-H]- | PE | PE(38:6) |
| 763.51308 | 704.49922 | [M+Ac]- | PG | PG(P-32:1) |
| 764.50833 | 705.49447 | [M+Ac]- | PS | PS(P-31:0)/PS(O-31:1) |
| 764.52358 | 765.53086 | [M-H]- | PE | PE(38:5) |
| 765.47121 | 706.45736 | [M+Ac]- | PA | PA(37:6) |
| | | [M-H]- | PG | PG(36:6) |
| 765.52873 | 706.51487 | [M+Ac]- | PG | PG(32:0)/PG(O-32:1) |
| 766.53923 | 767.54651 | [M-H]- | PE | PE(38:4) |
| 767.48686 | 708.47301 | [M+Ac]- | PA | PA(37:5) |
| | | [M-H]- | PG | PG(36:5) |
| 767.50799 | 708.49414 | [M+Ac]- | PG | PG(31:0) |
| | | [M-H]- | PI | PI(O-30:0) |
| 767.54438 | 708.53052 | [M+Ac]- | PG | PG(O-32:0) |
| 768.55488 | 769.56216 | [M-H]- | PE | PE(38:3) |
| 769.50251 | 710.48866 | [M+Ac]- | PA | PA(37:4) |
| | | [M-H]- | PG | PG(36:4) |
| 770.49776 | 711.48391 | [M+Ac]- | PE | PE(34:4) |
| | | [M+Ac]- | PC | PC(31:4) |
| | | [M-H]- | PS | PS(35:3)* |
| 771.51816 | 712.50431 | [M+Ac]- | PA | PA(37:3) |
| | | [M-H]- | PG | PG(36:3) |
| 772.51341 | 713.49956 | [M+Ac]- | PE | PE(34:3) |
| | | [M+Ac]- | PC | PC(31:3) |
| | | [M-H]- | PS | PS(35:2)* |
| 772.54980 | 713.53594 | [M+Ac]- | PC | PC(O-34:3)* |
| | | [M-H]- | PS | PS(P-36:1)/PS(O-36:2) |
| | | [M+Ac]- | PE | PE(P-35:2) |
| 773.53381 | 714.51996 | [M-H]- | PA | LBPA(36:2) |
| | | [M-H]- | PG | PG(36:2) |

| | | | | |
|-----------|-----------|---------|----|-----------------------|
| | | [M+Ac]- | PA | PA(37:2) |
| 776.54471 | 717.53086 | [M+Ac]- | PE | PE(34:1) |
| | | [M+Ac]- | PC | PC(31:1)* |
| | | [M-H]- | PS | PS(35:0) |
| 778.50285 | 779.51012 | [M-H]- | PE | PE(38:6)-OH |
| 780.48211 | 721.46826 | [M-H]- | PS | PS(36:5)* |
| | | [M+Ac]- | PE | PE(35:6) |
| 780.55488 | 781.56216 | [M-H]- | PE | PE(39:4) |
| 781.48726 | 782.49453 | [M-H]- | PI | PI(30:0) |
| 782.49776 | 723.48391 | [M+Ac]- | PC | PC(32:5)* |
| | | [M+Ac]- | PE | PE(35:5) |
| | | [M-H]- | PS | PS(36:4)* |
| 786.52906 | 727.51521 | [M+Ac]- | PE | PE(35:3) |
| | | [M+Ac]- | PC | PC(32:3)* |
| | | [M-H]- | PS | PS(36:2)* |
| 787.51308 | 728.49922 | [M+Ac]- | PG | PG(P-34:3)/PG(O-34:4) |
| 788.52358 | 729.50973 | [M-H]- | PE | PE(40:7) |
| 788.54471 | 729.53086 | [M+Ac]- | PE | PE(35:2) |
| | | [M+Ac]- | PC | PC(32:2)* |
| | | [M-H]- | PS | PS(36:1)* |
| 789.52873 | 730.51487 | [M+Ac]- | PG | PG(P-34:2)/PG(O-34:3) |
| 790.53923 | 731.52538 | [M-H]- | PE | PE(40:6) |
| 790.56036 | 731.54651 | [M+Ac]- | PE | PE(35:1) |
| | | [M+Ac]- | PC | PC(32:1)* |
| | | [M-H]- | PS | PS(36:0) |
| 791.54438 | 732.53052 | [M+Ac]- | PG | PG(P-34:1)/PG(O-34:2) |
| 791.61715 | 732.60329 | [M+Ac]- | PA | PA(O-39:0) |
| | | [M-H]- | PG | PG(O-38:0) |
| 792.55488 | 793.56216 | [M-H]- | PE | PE(40:5) |
| 792.57601 | 733.56216 | [M+Ac]- | PE | PE(35:0) |
| | | [M+Ac]- | PC | PC(32:0)* |
| 793.56003 | 734.54617 | [M+Ac]- | PG | PG(P-34:0)/PG(O-34:1) |
| 794.57053 | 795.57781 | [M-H]- | PE | PE(40:4) |
| 796.51341 | 737.49956 | [M+Ac]- | PC | PC(33:5)* |
| | | [M-H]- | PS | PS(37:4)* |
| | | [M+Ac]- | PE | PE(36:5) |
| 796.54980 | 737.53594 | [M-H]- | PS | PS(P-38:3)/PS(O-38:4) |
| | | [M+Ac]- | PC | PC(P-34:4) |
| 796.58618 | 797.59346 | [M-H]- | PE | PE(40:3) |
| 798.52906 | 739.51521 | [M+Ac]- | PE | PE(36:4) |
| | | [M+Ac]- | PC | PC(33:4) |
| | | [M-H]- | PS | PS(37:3) |
| 798.56545 | 739.55159 | [M+Ac]- | PC | PC(P-34:3)/PC(O-34:4) |
| | | [M-H]- | PS | PS(P-38:2)/PS(O-38:3) |
| 798.60183 | 799.60911 | [M-H]- | PE | PE(40:2) |
| 800.54471 | 741.53086 | [M+Ac]- | PE | PE(36:3) |
| | | [M+Ac]- | PC | PC(33:3)* |
| | | [M-H]- | PS | PS(37:2) |

| | | | | |
|-----------|-----------|---------|----|------------------------|
| 800.58110 | 741.56724 | [M+Ac]- | PC | PC(P-34:2)/PC(O-34:3)* |
| | | [M-H]- | PS | PS(P-38:1)/PS(O-38:2) |
| | | [M+Ac]- | PE | PE(P-37:2) |
| 802.46646 | 803.47374 | [M-H]- | PS | PS(38:8) |
| 802.56036 | 743.54651 | [M+Ac]- | PE | PE(36:2) |
| | | [M+Ac]- | PC | PC(33:2)* |
| | | [M-H]- | PS | PS(37:1) |
| 802.59675 | 743.58289 | [M+Ac]- | PC | PC(P-34:1)/PC(O-34:2)* |
| | | [M-H]- | PS | PS(P-38:0)/PS(O-38:1) |
| | | [M+Ac]- | PE | PE(P-37:1)/PE(O-37:2) |
| 803.47161 | 804.47888 | [M-H]- | PI | PI(32:3) |
| 804.57601 | 745.56216 | [M+Ac]- | PE | PE(36:1) |
| | | [M+Ac]- | PC | PC(33:1)* |
| | | [M-H]- | PS | PS(37:0) |
| 804.61240 | 745.59854 | [M+Ac]- | PC | PC(P-34:0)/PC(O-34:1)* |
| | | [M-H]- | PS | PS(O-38:0) |
| | | [M+Ac]- | PE | PE(P-37:0)/PE(O-37:1) |
| 806.53415 | 747.52029 | [M-H]- | PE | PE(40:6) |
| | | [M+Ac]- | PE | PE(O-38:7) |
| 808.51341 | 749.49956 | [M+Ac]- | PE | PE(37:6) |
| | | [M+Ac]- | PC | PC(34:6)* |
| | | [M-H]- | PS | PS(38:5)* |
| 808.54980 | 749.53594 | [M+Ac]- | PE | PE(P-38:5)/PE(O-38:6) |
| 810.52906 | 751.51521 | [M+Ac]- | PE | PE(37:5) |
| | | [M+Ac]- | PC | PC(34:5)* |
| | | [M-H]- | PS | PS(38:4)* |
| 810.56545 | 751.55159 | [M+Ac]- | PE | PE(P-38:4)/PE(O-38:5) |
| 810.63822 | 811.64549 | [M-H]- | PE | PE(P-42:2) |
| 812.54471 | 753.53086 | [M+Ac]- | PE | PE(37:4) |
| | | [M+Ac]- | PC | PC(34:4)* |
| | | [M-H]- | PS | PS(38:3)* |
| 812.58110 | 753.56724 | [M+Ac]- | PC | PC(O-35:4) |
| | | [M+Ac]- | PE | PE(P-38:3)/PE(O-38:4) |
| 812.65387 | 813.66114 | [M-H]- | PE | PE(P-42:1)/PE(O-42:2) |
| 814.56036 | 755.54651 | [M+Ac]- | PE | PE(37:3) |
| | | [M+Ac]- | PC | PC(34:3)* |
| | | [M-H]- | PS | PS(38:2) |
| 814.66952 | 815.67679 | [M-H]- | PE | PE(P-42:0)/PE(O-42:1) |
| 816.57601 | 757.56216 | [M+Ac]- | PE | PE(37:2) |
| | | [M+Ac]- | PC | PC(34:2)* |
| | | [M-H]- | PS | PS(38:1)* |
| 817.56003 | 758.54617 | [M+Ac]- | PG | PG(P-36:2)/PG(O-36:3) |
| 818.49776 | 759.48391 | [M+Ac]- | PE | PE(38:8) |
| | | [M-H]- | PS | PS(39:7) |
| 818.59166 | 759.57781 | [M+Ac]- | PE | PE(37:1) |
| | | [M+Ac]- | PC | PC(34:1)* |
| | | [M-H]- | PS | PS(38:0) |
| 822.52906 | 763.51521 | [M+Ac]- | PE | PE(38:6) |

| | | | | |
|-----------|-----------|---------|----|------------------------|
| | | [M+Ac]- | PC | PC(35:6)* |
| | | [M-H]- | PS | PS(39:5) |
| 824.54471 | 765.53086 | [M+Ac]- | PE | PE(38:5) |
| | | [M+Ac]- | PC | PC(35:5)* |
| | | [M-H]- | PS | PS(39:4) |
| 824.61748 | 825.62476 | [M-H]- | PE | PE(42:3) |
| 825.45596 | 826.46323 | [M-H]- | PI | PI(34:6) |
| 826.46646 | 827.47374 | [M-H]- | PS | PS(40:10)* |
| 826.56036 | 767.54651 | [M+Ac]- | PE | PE(38:4) |
| | | [M+Ac]- | PC | PC(35:4)* |
| | | [M-H]- | PS | PS(39:3) |
| 827.47161 | 828.47888 | [M-H]- | PI | PI(34:5) |
| 828.57601 | 769.56216 | [M+Ac]- | PE | PE(38:3) |
| | | [M+Ac]- | PC | PC(35:3)* |
| | | [M-H]- | PS | PS(39:2) |
| 829.48726 | 830.49453 | [M-H]- | PI | PI(34:4) |
| 830.59166 | 771.57781 | [M+Ac]- | PE | PE(38:2) |
| | | [M+Ac]- | PC | PC(35:2)* |
| | | [M-H]- | PS | PS(39:1) |
| 832.57093 | 773.55707 | [M+Ac]- | PS | PS(P-36:1)/PS(O-36:2) |
| 832.60731 | 773.59346 | [M+Ac]- | PE | PE(38:1) |
| | | [M+Ac]- | PC | PC(35:1)* |
| | | [M-H]- | PS | PS(39:0) |
| 832.64370 | 773.62984 | [M+Ac]- | PC | PC(P-36:0)/PC(O-36:1)* |
| | | [M-H]- | PS | PS(O-40:0)* |
| | | [M+Ac]- | PE | PE(P-39:0)/PE(O-39:1) |
| 834.56545 | 775.55159 | [M+Ac]- | PE | PE(P-40:6) |
| 836.54471 | 777.53086 | [M+Ac]- | PE | PE(39:6) |
| | | [M+Ac]- | PC | PC(36:6)* |
| | | [M-H]- | PS | PS(40:5) |
| 838.53923 | 839.54651 | [M-H]- | PE | PE(44:10) |
| 838.56036 | 779.54651 | [M+Ac]- | PE | PE(39:5) |
| | | [M+Ac]- | PC | PC(36:5)* |
| | | [M-H]- | PS | PS(40:4) |
| 839.54438 | 780.53052 | [M+Ac]- | PG | PG(P-38:5)/PG(O-38:6) |
| 840.57601 | 781.56216 | [M+Ac]- | PE | PE(39:4) |
| | | [M+Ac]- | PC | PC(36:4)* |
| | | [M-H]- | PS | PS(40:3) |
| 841.52364 | 782.50979 | [M+Ac]- | PG | PG(37:5) |
| | | [M-H]- | PI | PI(P-36:4)/PI(O-36:5) |
| 842.49776 | 783.48391 | [M+Ac]- | PE | PE(40:10) |
| 842.59166 | 783.57781 | [M+Ac]- | PE | PE(39:3) |
| | | [M+Ac]- | PC | PC(36:3)* |
| | | [M-H]- | PS | PS(40:2) |
| 843.50291 | 844.51018 | [M-H]- | PI | PI(35:4) |
| 844.60731 | 785.59346 | [M+Ac]- | PE | PE(39:2) |
| | | [M+Ac]- | PC | PC(36:2)* |
| | | [M-H]- | PS | PS(40:1) |

| | | | | |
|-----------|-----------|---------|----|-----------------------|
| 845.59133 | 786.57747 | [M+Ac]- | PG | PG(P-38:2)/PG(O-38:3) |
| 847.53421 | 848.54148 | [M-H]- | PI | PI(35:2) |
| 850.56036 | 791.54651 | [M+Ac]- | PE | PE(40:6) |
| | | [M+Ac]- | PC | PC(37:6)* |
| | | [M-H]- | PS | PS(41:5) |
| 852.53963 | 793.52577 | [M+Ac]- | PS | PS(P-38:5)/PS(O-38:6) |
| 852.57601 | 793.56216 | [M+Ac]- | PE | PE(40:5) |
| | | [M+Ac]- | PC | PC(37:5)* |
| | | [M-H]- | PS | PS(41:4) |
| 853.48726 | 854.49453 | [M-H]- | PI | PI(36:6) |
| 854.55528 | 795.54142 | [M+Ac]- | PS | PS(P-38:4)/PS(O-38:5) |
| 854.59166 | 795.57781 | [M+Ac]- | PE | PE(40:4) |
| | | [M+Ac]- | PC | PC(37:4)* |
| | | [M-H]- | PS | PS(41:3) |
| 855.50291 | 856.51018 | [M-H]- | PI | PI(36:5) |
| 855.56042 | 796.54657 | [M+Ac]- | PI | PI(O-32:0) |
| 856.57093 | 797.55707 | [M+Ac]- | PC | PC(36:4)-OH |
| | | [M+Ac]- | PS | PS(P-38:3)/PS(O-38:4) |
| 856.60731 | 797.59346 | [M+Ac]- | PE | PE(40:3) |
| | | [M+Ac]- | PC | PC(37:3)* |
| | | [M-H]- | PS | PS(41:2) |
| 857.51856 | 858.52583 | [M-H]- | PI | PI(36:4) |
| 858.58658 | 799.57272 | [M+Ac]- | PS | PS(P-38:2)/PS(O-38:3) |
| 858.62296 | 799.60911 | [M+Ac]- | PE | PE(40:2) |
| | | [M+Ac]- | PC | PC(37:2)* |
| | | [M-H]- | PS | PS(41:1) |
| 863.56551 | 864.57278 | [M-H]- | PI | PI(36:1) |
| 864.57601 | 805.56216 | [M+Ac]- | PE | PE(41:6) |
| | | [M+Ac]- | PC | PC(38:6)* |
| | | [M-H]- | PS | PS(42:5) |
| 865.58116 | 866.58843 | [M-H]- | PI | PI(36:0) |
| 866.55528 | 807.54142 | [M+Ac]- | PE | PE(40:6)-OH |
| 866.59166 | 807.57781 | [M+Ac]- | PE | PE(41:5) |
| | | [M+Ac]- | PC | PC(38:5)* |
| | | [M-H]- | PS | PS(42:4) |
| 867.56042 | 808.54657 | [M+Ac]- | PI | PI(P-33:0)/PI(O-33:1) |
| 868.60731 | 809.59346 | [M+Ac]- | PE | PE(41:4) |
| | | [M+Ac]- | PC | PC(38:4)* |
| | | [M-H]- | PS | PS(42:3) |
| 869.51856 | 870.52583 | [M-H]- | PI | PI(37:5) |
| 869.57607 | 810.56222 | [M+Ac]- | PI | PI(O-33:0) |
| 870.62296 | 811.60911 | [M+Ac]- | PE | PE(41:3) |
| | | [M+Ac]- | PC | PC(38:3)* |
| | | [M-H]- | PS | PS(42:2) |
| 871.53421 | 872.54148 | [M-H]- | PI | PI(37:4) |
| 872.63861 | 813.62476 | [M+Ac]- | PE | PE(41:2) |
| | | [M+Ac]- | PC | PC(38:2) |
| | | [M-H]- | PS | PS(42:1) |

| | | | | |
|-----------|-----------|---------|----|-----------------------|
| 874.58149 | 815.56764 | [M+Ac]- | PS | PS(38:2) |
| 877.58116 | 878.58843 | [M-H]- | PI | PI(37:1) |
| 878.59166 | 819.57781 | [M+Ac]- | PE | PE(42:6) |
| | | [M+Ac]- | PC | PC(39:6) |
| 879.50291 | 880.51018 | [M-H]- | PI | PI(38:7) |
| 879.59681 | 880.60408 | [M-H]- | PI | PI(37:0) |
| 880.57093 | 821.55707 | [M+Ac]- | PS | PS(P-40:5)/PS(O-40:6) |
| 880.60731 | 821.59346 | [M+Ac]- | PE | PE(42:5) |
| | | [M+Ac]- | PC | PC(39:5) |
| | | [M-H]- | PS | PS(43:4) |
| 881.51856 | 882.52583 | [M-H]- | PI | PI(38:6) |
| 882.58658 | 823.57272 | [M+Ac]- | PE | PE(38:4)15ke |
| | | [M+Ac]- | PS | PS(P-40:4)/PS(O-40:5) |
| 882.62296 | 823.60911 | [M+Ac]- | PE | PE(42:4) |
| | | [M+Ac]- | PC | PC(39:4) |
| 883.53421 | 884.54148 | [M-H]- | PI | PI(38:5) |
| 884.63861 | 825.62476 | [M+Ac]- | PE | PE(42:3) |
| | | [M+Ac]- | PC | PC(39:3)* |
| | | [M-H]- | PS | PS(43:2) |
| 885.54986 | 886.55713 | [M-H]- | PI | PI(38:4) |
| 889.58116 | 890.58843 | [M-H]- | PI | PI(38:2) |
| 890.51889 | 831.50504 | [M+Ac]- | PS | PS(40:8) |
| 891.59681 | 892.60408 | [M-H]- | PI | PI(38:1) |
| 894.55019 | 835.53634 | [M+Ac]- | PS | PS(40:6) |
| 894.62296 | 835.60911 | [M+Ac]- | PC | PC(40:5)* |
| | | [M-H]- | PS | PS(44:4) |
| 896.63861 | 837.62476 | [M+Ac]- | PE | PE(43:5) |
| | | [M+Ac]- | PC | PC(40:4)* |
| | | [M-H]- | PS | PS(44:3) |
| 898.58149 | 839.56764 | [M+Ac]- | PS | PS(40:4) |
| 898.65426 | 839.64041 | [M+Ac]- | PC | PC(40:3)* |
| | | [M-H]- | PS | PS(44:2) |
| 900.59714 | 841.58329 | [M+Ac]- | PS | PS(40:3) |
| 901.54477 | 842.53092 | [M+Ac]- | PI | PI(P-36:4)/PI(O-36:5) |
| 903.56042 | 844.54657 | [M+Ac]- | PI | PI(P-36:3)/PI(O-36:4) |
| 908.56584 | 849.55199 | [M+Ac]- | PS | PS(41:6) |
| 908.60223 | 849.58837 | [M+Ac]- | PS | PS(O-42:6) |
| 910.58149 | 851.56764 | [M+Ac]- | PS | PS(41:5) |
| 919.62811 | 920.63538 | [M-H]- | PI | PI(40:1) |
| 920.56584 | 861.55199 | [M+Ac]- | PS | PS(42:7) |
| 922.58149 | 863.56764 | [M+Ac]- | PS | PS(42:6) |
| 924.59714 | 865.58329 | [M+Ac]- | PS | PS(42:5) |
| 926.61279 | 867.59894 | [M+Ac]- | PS | PS(42:4) |
| 926.68556 | 867.67171 | [M+Ac]- | PC | PC(42:3) |
| 929.57607 | 870.56222 | [M+Ac]- | PI | PI(P-38:4)/PI(O-38:5) |
| 938.68556 | 879.67171 | [M+Ac]- | PC | PC(43:4) |
| 939.52404 | 880.51018 | [M+Ac]- | PI | PI(38:7) |
| 945.64376 | 946.65103 | [M-H]- | PI | PI(42:2) |

| | | | | |
|-----------|-----------|---------|----|----------|
| 946.58149 | 887.56764 | [M+Ac]- | PS | PS(44:8) |
| 950.61279 | 891.59894 | [M+Ac]- | PS | PS(44:6) |
| 965.53969 | 906.52583 | [M+Ac]- | PI | PI(40:8) |

AIV - Baseline lipidome of *C. reinhardtii*

| Theoretical mass (m/z) | | Identification | | |
|------------------------|-----------|----------------|-----------|-------------|
| Ion Form | Neutral | Ion form | Headgroup | Annotation |
| 353.17347 | 354.18074 | [M-H]- | PA | LPA(12:0) |
| 367.15273 | 368.16001 | [M-H]- | PA | PA(12:0) |
| 379.18912 | 380.19639 | [M-H]- | PA | LPA(14:1) |
| 393.20477 | 394.21204 | [M-H]- | PA | LPA(15:1) |
| 403.12941 | 368.16001 | [M+Cl]- | PA | PA(12:0) |
| 407.22042 | 408.22769 | [M-H]- | PA | LPA(16:1) |
| 441.18951 | 442.19679 | [M-H]- | PG | LPA(19:1) |
| 449.26737 | 450.27464 | [M-H]- | PA | LPA(19:0) |
| 451.28302 | 452.29029 | [M-H]- | PA | LPA(19:0) |
| 453.22590 | 394.21204 | [M+Ac]- | PA | LPA(15:1) |
| | 454.23317 | [M-H]- | PG | LPG(14:1) |
| 465.18144 | 430.21204 | [M+Cl]- | PA | LPA(18:4) |
| 465.29867 | 466.30594 | [M-H]- | PA | LPA(20:0) |
| 467.27793 | 468.28521 | [M-H]- | PG | LPG(P-16:0) |
| 472.24697 | 473.25424 | [M-H]- | PE | LPE(18:4) |
| 474.26262 | 475.26989 | [M-H]- | PE | LPE(18:3) |
| 476.27827 | 477.28554 | [M-H]- | PE | LPE(18:2) |
| 478.29392 | 479.30119 | [M-H]- | PC | LPC(15:1) |
| | | [M-H]- | PE | LPE(18:1) |
| 479.24155 | 420.22769 | [M+Ac]- | PA | LPA(17:2) |
| 479.31432 | 480.32159 | [M-H]- | PA | LPA(21:0) |
| 481.25720 | 422.24334 | [M+Ac]- | PA | LPA(17:1) |
| | 482.26447 | [M-H]- | PG | LPG(16:1) |
| 481.29358 | 422.27973 | [M+Ac]- | PA | LPA(P-18:0) |
| 483.23646 | 424.22261 | [M+Ac]- | PA | PA(16:0) |
| 483.27285 | 424.25899 | [M+Ac]- | PA | LPA(17:0) |
| | 484.28012 | [M-H]- | PG | LPG(16:0) |
| 485.26737 | 486.27464 | [M-H]- | PA | LPA(22:4) |
| 487.24109 | 450.27464 | [M+(37Cl)]- | PA | LPA(19:1) |
| 491.24155 | 432.22769 | [M+Ac]- | PA | LPA(18:3) |
| 491.31432 | 492.32159 | [M-H]- | PA | LPA(22:1) |
| 493.25720 | 434.24334 | [M+Ac]- | PA | LPA(18:2) |
| | 494.26447 | [M-H]- | PG | LPG(17:2) |
| 495.30923 | 496.31651 | [M-H]- | PG | LPG(P-18:0) |
| 497.25211 | 498.25939 | [M-H]- | PG | PG(16:0) |
| 500.27827 | 501.28554 | [M-H]- | PE | LPE(20:4) |

| | | | | |
|-----------|-----------|-------------|----|-------------|
| 505.25720 | 446.24334 | [M+Ac]- | PA | LPA(19:3) |
| | 506.26447 | [M-H]- | PG | LPG(18:3) |
| 506.32522 | 507.33249 | [M-H]- | PC | LPC(17:1) |
| | | [M-H]- | PE | LPE(20:1) |
| 507.27285 | 508.28012 | [M-H]- | PG | LPG(18:2) |
| 509.32488 | 450.31103 | [M+Ac]- | PA | LPA(P-20:0) |
| 513.24703 | 454.23317 | [M+Ac]- | PG | LPG(14:1) |
| 541.24194 | 542.24922 | [M-H]- | PI | LPI(14:1) |
| 546.28375 | 547.29102 | [M-H]- | PS | LPS(20:3) |
| 641.29437 | 582.28052 | [M+Ac]- | PI | LPI(17:2) |
| 651.27872 | 592.26487 | [M+Ac]- | PI | LPI(18:4) |
| 655.31002 | 596.29617 | [M+Ac]- | PI | LPI(18:2) |
| 663.36121 | 626.39476 | [M+(37Cl)]- | PA | PA(31:4) |
| 675.36121 | 638.39476 | [M+(37Cl)]- | PA | PA(32:5) |
| 677.41878 | 678.42606 | [M-H]- | PA | PA(35:6) |
| 679.43443 | 680.44171 | [M-H]- | PA | PA(35:5) |
| 681.32567 | 622.31182 | [M+Ac]- | PI | LPI(20:3) |
| 681.45008 | 682.45736 | [M-H]- | PA | PA(35:4) |
| 683.46573 | 684.47301 | [M-H]- | PA | PA(35:3) |
| 685.48138 | 686.48866 | [M-H]- | PA | PA(35:2) |
| 687.49703 | 688.50431 | [M-H]- | PA | PA(35:1) |
| 689.37686 | 652.41041 | [M+(37Cl)]- | PA | PA(33:5) |
| 701.37686 | 664.41041 | [M+(37Cl)]- | PA | PA(34:6) |
| 703.43443 | 704.44171 | [M-H]- | PA | PA(37:7) |
| 705.45008 | 706.45736 | [M-H]- | PA | PA(37:6) |
| 707.34132 | 648.32747 | [M+Ac]- | PI | LPI(22:4) |
| 707.46573 | 708.47301 | [M-H]- | PA | PA(37:5) |
| 709.48138 | 710.48866 | [M-H]- | PA | PA(37:4) |
| 711.49703 | 712.50431 | [M-H]- | PA | PA(37:3) |
| 713.51268 | 714.51996 | [M-H]- | PA | PA(37:2) |
| 718.61200 | 719.61928 | [M-H]- | PE | PE(O-36:0) |
| 719.48686 | 660.47301 | [M+Ac]- | PA | PA(33:1) |
| | 720.49414 | [M-H]- | PG | PG(32:1) |
| 721.50251 | 662.48866 | [M+Ac]- | PA | PA(33:0) |
| | 722.50979 | [M-H]- | PG | PG(32:0) |
| 733.50251 | 674.48866 | [M+Ac]- | PA | PA(34:1) |
| | 734.50979 | [M-H]- | PG | PG(33:1) |
| 734.47663 | 735.48391 | [M-H]- | PE | PE(36:6) |
| 736.49228 | 737.49956 | [M-H]- | PC | PC(33:5) |
| | | [M-H]- | PE | PE(36:5) |
| 738.50793 | 739.51521 | [M-H]- | PC | PC(33:4) |
| | | [M-H]- | PE | PE(36:4) |
| 739.51308 | 680.49922 | [M+Ac]- | PG | PG(O-30:0) |

| | | | | |
|-----------|-----------|-------------|------|------------|
| 740.52358 | 741.53086 | [M-H]- | PC | PC(33:3) |
| | | [M-H]- | PE | PE(36:3) |
| 741.45008 | 742.45736 | [M-H]- | PA | PA(40:9) |
| 741.47121 | 682.45736 | [M+Ac]- | PA | PA(35:4) |
| | 742.47849 | [M-H]- | PG | PG(34:4) |
| 742.53923 | 743.54651 | [M-H]- | PC | PC(33:2) |
| | | [M-H]- | PE | PE(36:2) |
| 743.48686 | 684.47301 | [M+Ac]- | PA | PA(35:3) |
| | 744.49414 | [M-H]- | PG | PG(34:3) |
| 745.50251 | 686.48866 | [M+Ac]- | PA | PA(35:2) |
| | 746.50979 | [M-H]- | PA | LBPA(34:2) |
| | | [M-H]- | PG | PG(34:2) |
| 747.51816 | 688.50431 | [M+Ac]- | PA | PA(35:1) |
| | 748.52544 | [M-H]- | PA | LBPA(34:1) |
| | | [M-H]- | PG | PG(34:1) |
| 749.52574 | 714.55634 | [M+Cl]- | PA | PA(O-38:2) |
| 750.52906 | 691.51521 | [M+Ac]- | PC | PC(29:0) |
| | | [M+Ac]- | PE | PE(32:0) |
| 763.51308 | 704.49922 | [M+Ac]- | PG | PG(P-32:1) |
| 765.52873 | 706.51487 | [M+Ac]- | PG | PG(O-32:1) |
| 773.53381 | 714.51996 | [M+Ac]- | PA | PA(37:2) |
| | 774.54109 | [M-H]- | PA | LBPA(36:2) |
| | | [M-H]- | PG | PG(36:2) |
| 781.50251 | 722.48866 | [M+Ac]- | PA | PA(38:5) |
| | 782.50979 | [M-H]- | PG | PG(37:5) |
| 783.46335 | 746.49690 | [M+(37Cl)]- | MGDG | MGDG(34:6) |
| 791.49848 | 792.50575 | [M-H]- | SQDG | SQDG(32:1) |
| 793.48726 | 794.49453 | [M-H]- | PI | PI(31:1) |
| 793.49697 | 756.53052 | [M+(37Cl)]- | PG | PG(O-36:4) |
| 793.51413 | 794.52140 | [M-H]- | SQDG | SQDG(32:0) |
| 793.51557 | 758.54617 | [M+Cl]- | PG | PG(O-36:3) |
| 794.49222 | 757.52577 | [M+(37Cl)]- | PS | PS(P-35:2) |
| 794.51889 | 735.50504 | [M+Ac]- | PS | PS(32:0) |
| 795.49484 | 760.52544 | [M+Cl]- | PG | PG(35:2) |
| 796.52647 | 761.55707 | [M+Cl]- | PS | PS(O-35:1) |
| 803.44241 | 768.47301 | [M+Cl]- | PA | PA(42:10) |
| 803.44494 | 766.47849 | [M+(37Cl)]- | PG | PG(36:6) |
| 807.53122 | 772.56182 | [M+Cl]- | PG | PG(P-37:2) |
| 813.57335 | 754.55950 | [M+Ac]- | MGDG | MGDG(34:2) |
| 815.44494 | 778.47849 | [M+(37Cl)]- | PG | PG(37:7) |
| 815.47161 | 816.47888 | [M-H]- | PI | PI(33:4) |
| 815.49992 | 780.53052 | [M+Cl]- | PG | PG(O-38:6) |
| 815.52595 | 778.55950 | [M+(37Cl)]- | MGDG | MGDG(36:4) |

| | | | | |
|-----------|-----------|-------------|------|------------|
| 816.50324 | 757.48939 | [M+Ac]- | PS | PS(34:3) |
| 817.50251 | 818.50979 | [M-H]- | PA | LBPA(40:8) |
| | | [M-H]- | PG | PG(40:8) |
| 818.51889 | 759.50504 | [M+Ac]- | PS | PS(34:2) |
| 819.51262 | 782.54617 | [M+(37Cl)]- | PG | PG(O-38:5) |
| 819.53122 | 784.56182 | [M+Cl]- | PG | PG(O-38:4) |
| 820.53454 | 761.52069 | [M+Ac]- | PS | PS(34:1) |
| 827.49274 | 768.47888 | [M+Ac]- | PI | PI(29:0) |
| 827.50799 | 768.49414 | [M+Ac]- | PG | PG(36:5) |
| 829.52364 | 770.50979 | [M+Ac]- | PG | PG(36:4) |
| 831.50291 | 832.51018 | [M-H]- | PI | PI(34:3) |
| 831.52640 | 772.51255 | [M+Ac]- | MGDG | MGDG(36:7) |
| 832.50787 | 795.54142 | [M+(37Cl)]- | PS | PS(P-38:4) |
| 833.51856 | 834.52583 | [M-H]- | PI | PI(34:2) |
| 834.52352 | 797.55707 | [M+(37Cl)]- | PC | PC(36:4) |
| | | [M+(37Cl)]- | PS | PS(P-38:3) |
| 835.50501 | 800.53561 | [M+Cl]- | PA | PA(44:8) |
| 835.53421 | 836.54148 | [M-H]- | PI | PI(34:1) |
| 836.53917 | 799.57272 | [M+(37Cl)]- | PS | PS(P-38:2) |
| 837.54179 | 802.57239 | [M+Cl]- | PG | PG(38:2) |
| 841.60465 | 782.59080 | [M+Ac]- | MGDG | MGDG(36:2) |
| 894.52906 | 835.51521 | [M+Ac]- | PE | PE(44:11) |
| 914.51889 | 855.50504 | [M+Ac]- | PS | PS(42:10) |
| 914.59166 | 855.57781 | [M+Ac]- | PC | PC(42:9) |
| 936.57601 | 877.56216 | [M+Ac]- | PC | PC(44:12) |
| 989.54793 | 930.53408 | [M+Ac]- | DGDG | DGDG(36:9) |